Mechanisms Underlying Chronic Pelvic Pain Associated with Endometriosis

By

Jessica Maddern

Thesis
Submitted to Flinders University
for the degree of

Doctor of Philosophy

College of Medicine and Public Health
Flinders University
Adelaide, South Australia

August 12th, 2022

CONTENTS

LIST OF FIGURES AND TABLES

SUMMARY

Endometriosis is a chronic and debilitating gynaecological condition which affects 10% of reproductive aged women. Chronic pelvic pain (CPP) is a cardinal symptom of endometriosis, with many patients experiencing widespread pain, or being co-diagnosed with visceral comorbidities associated with chronic pain. Unfortunately, little progress has been made in understanding the mechanisms that contribute to CPP in endometriosis, and as such, therapeutic treatments are lacking. Unfortunately, a major limiting factor in the development of treatments for CPP in endometriosis is the lack of translatable research originating from effective pre-clinical animal models. To this end, the work presented in this thesis focuses on pain in endometriosis with the primary aim to advance pre-clinical models of endometriosis and specifically utilize them for the study of CPP mechanisms.

This thesis starts by exploring the current literature surrounding endometriosis, covering disease pathogenesis and diagnosis, current treatments, and details currently suggested mechanisms of CPP development in endometriosis. By doing this, we highlight the unmet clinical need in successful treatment of CPP in endometriosis and emphasize the importance of pre-clinical models in elucidating mechanisms to identify key therapeutic targets.

From here, we present our original contribution to the field, aimed at investigating the mechanisms of CPP development in endometriosis. In Chapters 2 and 3, we establish two pre-clinical models of endometriosis in mice. Specifically, we further characterise the chronic development of endometriosis and use multiple *in vivo* approaches to investigate the development of widespread CPP. By presenting indications of both spontaneous and evoked 'pain like' behaviours across visceral organs commonly associated with endometriosis comorbidities, including the bladder, colon, and vagina, we position these pre-clinical models of endometriosis for the study of CPP mechanisms associated with this disease.

To investigate how CPP develops in these models, we first must understand how pain is signalled from visceral organs affected by endometriosis in normal/healthy animals. Chapter 4 aims to bridge this knowledge gap by investigating how normal and nociceptive stimuli are sensed by sensory nerves within the female reproductive tract. Making use of pharmacological modulators and specialised *in vivo*, *ex vivo* and *in vitro* techniques, we study the function of voltage gated sodium channels (Na_V) expressed in vaginal-innervating sensory neurons and demonstrate the role they play in regulating vaginal nociception.

Building on this new knowledge in pain signalling in healthy animals, we use our mouse model of endometriosis and CPP to link these concepts in Chapter 5. In this chapter, we successfully utilise our endometriosis mouse model to explore alterations in vaginal sensory signalling.

Specifically, we investigate a role of the Na_V channel subtype, Na_V 1.7, in the development of enhanced vaginal pain in endometriosis.

Finally, in Chapter 6, we employ live-cell calcium imaging to explore a direct role of the peritoneal fluid in aberrant pain associated with endometriosis. Bridging the gap between our pre-clinical model and the clinic, we utilise peritoneal fluid samples collected from both mice and women with endometriosis and CPP.

Published peer-reviewed papers have been included in this thesis, in which Jessica Maddern is primary author. An author contribution statement is listed at the beginning of each relevant chapter.

DECLARATION

I certify that this thesis does not incorporate without acknowledgment any material previously submitted for a degree or diploma in any university; and that to the best of my knowledge and belief it does not contain any material previously published or written by another person except where due reference is made in the text.

Signed.....

Date.....

ACKNOWLEDGEMENTS

First and foremost, I would like to thank my supervisors, Prof. Stuart Brierley, Dr. Joel Castro and Dr. Luke Grundy. Taking me on this journey with such a significant project, their continued support and encouragement throughout a rollercoaster 3 years contributed greatly to my success in this endeavour. The work being done in this lab is important, and I am grateful and honoured to be a part of it. I would also like to thank Flinders University, The Hospital Research Foundation, The Australian Government Research Training Program, The South Australian Department of Environment and Water and the Visceral Pain Research Group for their financial support contributing to my achievements. In addition, I would like to thank collaborators Prof. Irena Vetter and Prof. Glenn King for pharmacological modulators of $Na_V1.7$, A/Prof Martin Healey, Dr. Sarah Holdsworth-Carson and Prof. Peter Rogers for providing patient samples and A/Prof Wendy Imlach for $Na_V1.8$-Cre mice used to generate $Na_V1.8$xGCaMP6s mice utilised in this thesis.

Teamwork makes the dream work, and the support of the Visceral Pain Research Group is a testament to that. I would especially like to thank Dr. Gudrun Schober, Tracey 'treats' O'Donnell, Dr. Ashlee Caldwell and Dr. Andrea Harrington for their friendship and kindness above and beyond that which is expected from colleagues. My collectable art has grown substantially, and the support and professionalism displayed by these women will never be taken for granted.

Most importantly, I need to thank my family for their support and encouragement throughout the last 3 years. My husband, Josh, and my two children William and Charlotte, you've made the hard times easier, let me be selfish when I've needed and managed to learn more about endometriosis than any other family out there. My goal became our goal, and this is a testament to our awesomeness. I would also like to extend gratitude to my parents, Jayne and Alan, the unwavering support and endless snack deliveries are hidden throughout this thesis. I don't think anyone out there could be prouder of my achievements than my family, and that is a warm and fuzzy feeling.

Finally, I'd like to congratulate myself. You did this. You grew. You should be proud.

"Just keep swimming" - *Dory*

PUBLICATIONS AND ACHIEVEMENTS

PUBLICATIONS GENERATED DURING CANDIDATURE – related to this thesis

Maddern, J*., L. Grundy*, J. Castro and S. M. Brierley (2020). "Pain in Endometriosis." Frontiers in Cellular Neuroscience 14(335). Oct;14:590823. *Contributed equally. (Featured in Chapter 1)

Castro, J*., **J. Maddern***, A. Erickson, A. Caldwell, L. Grundy, A. M. Harrington, and S. M. Brierley (2020). "Pharmacological modulation of voltage-gated sodium (NaV) channels alters nociception arising from the female reproductive tract." Pain. Jan;162(1):227-242. *Contributed equally. (Featured in Chapter 4)

Castro, J*., **J. Maddern***, L. Grundy, J. Manavis, A. M. Harrington, G. Schober and S. M. Brierley (2021). "A mouse model of endometriosis that displays vaginal, colon, cutaneous, and bladder sensory comorbidities." FASEB J. 35(4):e21430. *Contributed equally. (Featured in Chapter 2)

J. Maddern, L. Grundy, A. Harrington, G. Schober, J. Castro* and S. M. Brierley* (2021). "A syngeneic inoculation mouse model of endometriosis that develops multiple comorbid visceral and cutaneous pain like behaviours." Pain. Dec;Epub ahead of print. (Featured in Chapter 3)

CONFERENCE AND SOCIETY INCLUSIONS

Australian Pain Society (APS) - 40th Annual Scientific Meeting – May 2020 – Inclusion in APS special edition newsletter (Volume 40, Issue 4, May 2020) in lieu of meeting (cancelled due to COVID-19)

Australian Pain Society (APS) Newsletter – Basic Pain Research Special Interest Group – Dec 2020 – Journal watch review article (Volume 40, Issue 11, Dec 2020)

14th World Congress of Endometriosis – March 2021 – Audio poster presentation (online only due to COVID-19)

SCHOLARSHIPS AND AWARDS

The Australian Government Research Training Program – Tuition fee offset

The Hospital Research Foundation – Postgraduate Scholarship - $96,000

Department of Environment and Water – Minister's Humane Research Scholarship - $25,000

Flinders Health and Medical Research Institute – HDR Student Small Research Grant - $4,698

14th World Congress on Endometriosis – Best Scientific Poster Award

ADDITIONAL PUBLICATIONS GENERATED DURING CANDIDATURE

Harrington, A. M., S. G. Caraballo, **J. E. Maddern**, L. Grundy, J. Castro and S. M. Brierley (2019). "Colonic afferent input and dorsal horn neuron activation differs between the thoracolumbar and lumbosacral spinal cord." American Journal of Physiology-Gastrointestinal and Liver Physiology 317(3): G285-g303.

Castro, J., A. M. Harrington, T. Lieu, S. Garcia-Caraballo, **J. Maddern**, G. Schober, T. O'Donnell, L. Grundy, A. L. Lumsden, P. Miller, A. Ghetti, M. S. Steinhoff, D. P. Poole, X. Dong, L. Chang, N. W. Bunnett and S. M. Brierley (2019). "Activation of pruritogenic TGR5, MrgprA3, and MrgprC11 on colon-innervating afferents induces visceral hypersensitivity." JCI Insight 4(20): e131712.

Jiang, Y., J. Castro, L. V. Blomster, A. J. Agwa, **J. Maddern**, G. Schober, V. Herzig, C. Y. Chow, F. C. Cardoso, P. Demétrio De Souza França, J. Gonzales, C. I. Schroeder, S. Esche, T. Reiner, S. M. Brierley and G. F. King (2021). "Pharmacological Inhibition of the Voltage-Gated Sodium Channel Na($_V$)1.7 Alleviates Chronic Visceral Pain in a Rodent Model of Irritable Bowel Syndrome." ACS Pharmacology and Translational Science 4(4): 1362-1378.

Castro, J., S. Garcia-Caraballo, **J. Maddern**, G. Schober, A. Lumsden, A. Harrington, S. Schmiel, B. Lindstrom, J. Adams and S. M. Brierley (2022). "Olorinab (APD371), a peripherally acting, highly selective, full agonist of the cannabinoid receptor 2, reduces colitis-induced acute and chronic visceral hypersensitivity in rodents." Pain 163(1): e72-e86.

Bayrer J.R*, Castro J*, Venkataraman A, Touhara K.K, Rossen N.D, Morrie R.D, Hendry A, **Maddern J**, Braverman KN, Schober G, Brizuela M, Bueno Silva C, Ingraham H.A, Brierley S.M*, Julius D*. (2022). Gut Enterochromaffin Cells are Critical Drivers of Visceral Pain and Anxiety. BioRxiv. preprint doi: https://doi.org/10.1101/2022.04.04.486775. Posted April 5, 2022. * Contributed equally.

ABBREVIATIONS

ANOVA Analysis of variance

ASIC3 Acid-sensing ion channel 3

AUC Area under the curve

β-NGF Beta-nerve growth factor precursor

Ca_V Voltage gated calcium channel

CB_1R Cannabinoid receptor type 1

CD3 Cluster of differentiation 3

CNS Central nervous system

CRD Colorectal distension

CPP Chronic pelvic pain

BPS Bladder pain syndrome

DAB Diaminobenzidine tetrahydrochloride

DAMPs Damage-associated molecular patterns

DDH Deep dorsal horn

DGC Dorsal grey commissure

DRG Dorsal root ganglia

EMG Electromyography

ER-α Estrogen receptor

EvF Electronic von Frey

GC-C Guanylate cyclase-C

GEE Generalised estimating equations

GM-CSF Granulocyte-macrophage colony-stimulating factor

GnRH Gonadotropin-releasing hormone

H&E Haematoxylin and eosin

IBS Irritable bowel syndrome

IBD Inflammatory bowel disease

IC/BPS Interstitial cystitis/bladder pain syndrome

IL-β Interleukin 1β

IL-6 Interleukin 6

IL-13 Interleukin 13

IL-17 Interleukin 17

IL-33 Interleukin 33

IMG Inferior mesenteric ganglion

IVC Individually ventilated cages

LS Lumbosacral

LSD Least significant difference

LSN Lateral spinal nucleus

MCP-1 Monocyte chemoattractant protein 1

MPG Major pelvic ganglion

MRGPR Mas-related G-protein coupled receptor

Na_V Voltage gated sodium channel

NGF Nerve growth factor

Ninj1 Nerve injury-induced protein 1

NK Natural killer

Ns Not significant

NSAIDs Nonsteroidal anti-inflammatory drugs

OAB Overactive bladder syndrome

P2X3 P2X purinoceptor 3

PAR Protease-activated receptor

PBMC Peripheral blood mononuclear cell

PDK Pyruvate dehydrogenase kinase

PFA Paraformaldehyde

PF Peritoneal fluid

PGE_2 Prostaglandins

PGP9.5 Protein gene product 9.5

QRT-PCR Quantitative reverse transcription-polymerase chain reaction

RANTES Regulated on activation, normal T cell expressed and secreted (also known as C-C chemokine ligand 5 (CCL5)

ROS Reactive oxygen species

RT-PCR Reverse transcription-polymerase chain reaction

SDH Superficial dorsal horn

SEM Standard error of the mean

SPN Sacral parasympathetic nucleus

TGFβ Transforming growth factor β

THC Δ9-tetrahydrocannabinol

TL Thoracolumbar

TNFα Tumour necrosis factor

TrkA Tyrosine kinase A

TRPA Transient receptor potential ankyrin

TRPV Transient receptor potential vailloid

TTX Tetrodotoxin

VD Vaginal distension

VEGF Vascular endothelial growth factor

VFH Von Frey hair

VMR Visceromotor response

CHAPTER 1: REVIEW OF LITERATURE

1.1 Statement of Authorship

With permission from all authors, this chapter includes an earlier version of work found in the following publication:

Publication: **Maddern, J***., L. Grundy*, J. Castro and S. M. Brierley (2020). "Pain in Endometriosis." Frontiers in Cellular Neuroscience 14(335).

*Contributed equally to this work.

Students' contribution to publication:

Jessica Maddern: Planning, literature review, generation of figures and writing manuscript

Estimated overall percentage contribution: 50%

Co-author contributions:

Dr L. Grundy: Conceptualized and edited manuscript. Provided supervision and expert advice

Dr J. Castro: Reviewed manuscript and provided supervision and expert advice.

Prof. S. Brierley: Provided supervision and expert advice. Reviewed and edited manuscript and figures for submission. Corresponding author.

1.2 Overview

Endometriosis is a chronic and debilitating condition affecting ~10% of women worldwide. Endometriosis is characterized by infertility and chronic pelvic pain (CPP), yet treatment options remain limited. In many respects this is related to an underlying lack of knowledge of the aetiology and mechanisms contributing to endometriosis-induced pain. Whilst many studies focus on retrograde menstruation, and the formation and development of lesions in the pathogenesis of endometriosis, the mechanisms underlying CPP remain poorly described. In this introductory chapter, we review literature surrounding recent clinical and experimental evidence of the mechanisms contributing to CPP in endometriosis. In particular, we consider the mechanisms occurring in the periphery including the roles of inflammation, neurogenic inflammation, neuroangiogenesis and peripheral sensitization, as well as exploring central sensitization. As endometriosis patients are also known to have co-morbidities such as irritable bowel syndrome and interstitial cystitis/bladder pain syndrome, we highlight how common nerve pathways innervating the colon, bladder and female reproductive tract can contribute to these visceral comorbidities via cross-organ sensitization. Finally, we highlight the need for pre-clinical models of endometriosis to facilitate the much-needed research into mechanisms of chronic pelvic pain in endometriosis.

1.3 Chronic Pain

The human body facilitates complex physiological functions whilst we remain unaware of the intricate mechanisms taking place to sustain healthy life. Throughout life, we experience various occurrences of acute pain. Acute pain sensation is a protective mechanism which occurs in response to external stimuli, such as a cut on your hand or touching a hot surface. Acute pain can also be internally driven, such as with abdominal pain or a migraine. Simply put, whatever the underlying cause, the transmission of pain, or nociception, originates from sensory afferents located peripherally within the skin, tissue, and our internal organs. Ion channels and receptors within these peripheral sensory afferents are tuned to detect a variety of noxious stimuli, translating mechanical, thermal, and chemical stimulation from the local environment into nociceptive signals when necessary. Nociceptive signals are then transmitted to the dorsal horn of the spinal cord, where they are transferred to second order neurons and transmitted through the central nervous system (CNS) for complex sensory processing and modulation, ultimately leading to pain sensation [1].

Unfortunately, whilst acute pain generally resolves after the initial insult, persistent or chronic pain can remain even after resolution of the original stimulus. Defined as early as 1953, chronic pain is recognized as pain which persists past the normal time of healing and, as such, is no longer protective but rather pathological [2, 3]. The present classification from the International Association for the Study of Pain (IASP) defines chronic pain as “persistent or recurrent pain lasting longer than 3 months” [4, 5]. The revised classification recognizes that chronic pain can still manifest though normal healing may not have occurred and identifies that the time taken to induce chronic pain is relative to the origin of pain and cannot universally be defined [6]. With this in mind, chronic pain is generally accepted as pain lasting for more than 3 months and is not amenable to routine methods of pain control [6].

It is estimated that 20% of people worldwide endure chronic pain [4], with an additional 1 in 10 adults diagnosed with chronic pain every year [6, 7]. Patient prevalence, reaching up to 34% in some countries [7-10], imposes significant socio-economic constraints, with total costs of chronic pain exceeding $600 billion annually in the USA alone [11, 12]. Adding to this, patients who suffer from chronic pain are more likely to experience psychological disorders, including depression, anxiety, and fatigue [10]. Unfortunately, despite research progress in understanding chronic pain mechanisms, treatments available rarely eradicate the symptoms of chronic pain and are often linked with adverse side effects as well as a concerning risk of misuse and addiction [12, 13]. Taken together, the direct socioeconomic impacts of chronic pain, the detrimental psychological implications, and the lack of effective treatment options severely impacts a patient’s quality of life. As such, chronic pain remains a high priority for healthcare worldwide [12, 14].

Population based research consistently demonstrates that females are not only more likely to experience chronic pain than males [15-19] but are also more likely to experience multiple coexisting chronic pain conditions [20]. Women are more likely to suffer from chronic widespread pain and neuropathic pain as well as chronic pain comorbidities including fibromyalgia, migraine headaches, irritable bowel syndrome (IBS), interstitial cystitis/bladder pain syndrome (IC/BPS) and chronic pelvic pain (CPP) [15, 18, 19]. Affecting between 14-24% of reproductive-aged women [21], CPP is defined as non-cyclical pain in the lower abdomen or pelvis, of at least 6 months in duration [21, 22]. CPP accounts for up to 10% of gynaecological visits [23] and, as one of the most common clinical signs of endometriosis, results in the majority of these women being diagnosed with endometriosis upon laparoscopy [24, 25].

Endometriosis is a common gynaecological condition that can encompass chronic pain disorders such as CPP, as well as comorbidities associated with chronic pain, including IBS and IC [26, 27]. Endometriosis imparts a financial and socioeconomic burden similar to major chronic diseases such as diabetes, Crohn's disease and rheumatoid arthritis [28]. Unfortunately, as a complex disease, limited progress has been made in understanding endometriosis progression. As such, successful treatments for the many women that continue to suffer daily from endometriosis are lacking. The substantial impact endometriosis has on women is contributing to a continued research priority appeal, calling on researchers to advance understanding of this multifaceted disease and ultimately enable vital progress towards improving the quality of life for millions of patients worldwide [29].

1.4 Pain in Endometriosis

1.4.1 Introduction

Endometriosis is a chronic and debilitating condition characterized by chronic pelvic pain (CPP) and infertility. Endometriosis has a large clinical burden, affecting approximately 1 in 10 women globally [28, 30, 31]. As such, endometriosis is associated with significant societal and economic burden that costs the US economy alone, $22 billion annually in lost productivity and direct healthcare costs [28, 30, 31]. Despite this burden, the aetiology and pathogenesis of endometriosis remains poorly defined, whilst efficacious therapeutic interventions remain limited.

Endometriosis is diagnosed surgically by the presence of endometrial lesions outside of the uterus. However, surgical intervention and diagnosis are usually preceded by bouts of chronic abdominal pain and/or CPP, leading patients to present to their consulting physician. More than 60% of women diagnosed with endometriosis report CPP, with endometriosis patients 13 times more likely to experience abdominal pain than healthy subjects [32]. Despite this disease homogeneity, the mechanisms by which endometriosis induces a chronic pain state remain poorly understood [32]. Surgical removal of endometrial lesions can be successful in alleviating pain in some endometriosis patients, supporting a role of these lesions in chronic pain. However, disparity exists in the correlation between pain severity and lesion score [33]. Moreover, chronic pain frequently returns in patients within 12 months of lesion removal, even in the absence of lesion regeneration [34, 35]. As such, there is a clear disconnect between the traditional theory that endometriosis associated pain is solely dependent on lesions, and the reality experienced by endometriosis patients throughout the world. This disconnect is further highlighted by the observation that endometriosis patients frequently suffer from a number of clinical comorbidities, largely unrelated to lesion location [36, 37]. Endometriosis is commonly co-diagnosed with bladder and colon disorders that are characterized by sensory dysfunction, such as interstitial cystitis/bladder pain syndrome (IC/BPS), and irritable bowel syndrome (IBS) [38]. These comorbidities are suggestive of a more complex pathophysiology for endometriosis induced pain that cannot be explained by endometrial lesions alone. Growing evidence now indicates that a chronic remodelling of the nervous system occurs in shared sensory neural pathways to induce a state of protracted peripheral and central sensitization and chronic pain in endometriosis patients.

1.4.2 Pathogenesis

As an estrogen dependent disorder, endometriosis predominantly effects women of reproductive years, aged 15-50 [39]. Endometriosis is a chronic inflammatory condition, characterized by the migration of uterine endometrial cells into the pelvic cavity, where they form lesions at multiple sites across multiple organs. Retrograde menstruation is the generally accepted

mechanism underlying the pathogenesis of endometriosis [39, 40]. This mechanism was originally proposed in 1927, whereby endometrial fragments migrate from the fallopian tubes into the peritoneal cavity during menstruation **(Figure** 1.1**)**. However, retrograde menstruation naturally occurs in 90% of women, but only 10% of women develop endometriosis [41]. Interestingly, more recent data shows the prevalence of retrograde menstruation is no different in women with or without endometriosis, suggesting a more complex aetiology than retrograde menstruation alone [42, 43]. Patients with endometriosis typically have more frequent and higher volumes of menstrual flow, shorter menstrual cycle intervals and increased endometrial fragments within the peritoneal cavity [44, 45]. Once the endometrial debris becomes ectopic, adhesion needs to occur in order to initiate the development of endometrial lesions and the induction of endometriosis. While the mechanisms underlying this process remain unclear, it is considered that immune dysfunction and the subsequent inability to effectively clear these fragments enables the endometrial lesions to form in the peritoneal cavity [39].

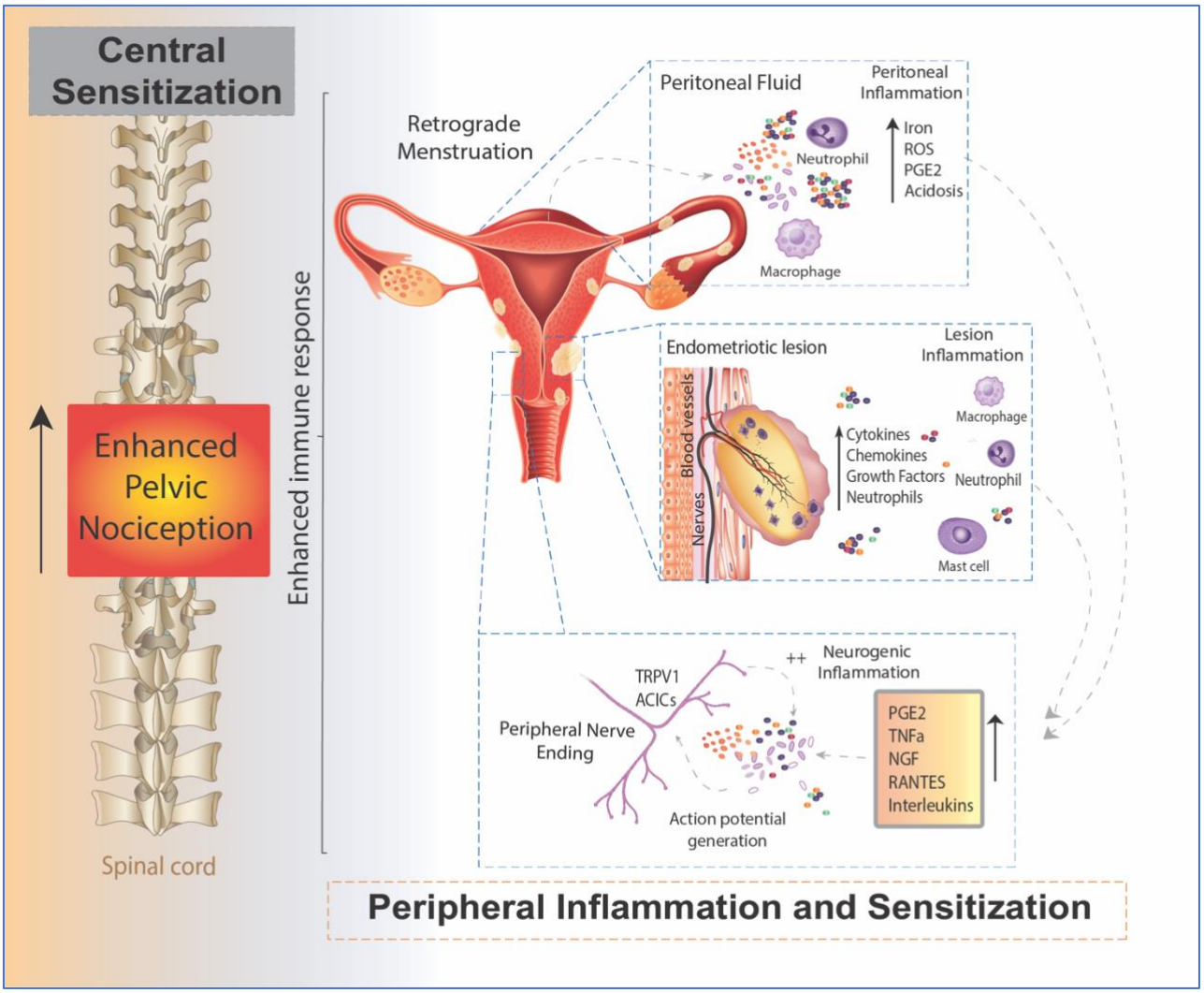

Figure 1.1: Schematic overview of an enhanced immune response leading to chronic pelvic pain in endometriosis.

Endometrial fragments in the peritoneum, originating from the uterus during retrograde menstruation, lead to the production and build-up of iron, reactive oxygen species (ROS), prostaglandin E_2 (PGE_2) and acidosis in the peritoneal fluid (peritoneal inflammation). This immune response is also seen at lesions sites throughout the peritoneal cavity, where the increased production of cytokines, chemokines, growth factors and neutrophils also contribute to an enhanced inflammatory environment present in the peritoneal cavity of women with endometriosis (lesion inflammation). Of these inflammatory mediators, PGE_2, tumour necrosis factor α (TNFα), nerve growth factor (NGF), RANTES and interleukins (IL) IL-8 and IL-1β are able to directly activate sensory nerve endings and activate a positive feedback loop, further increasing proinflammatory modulator production (neurogenic inflammation). The enhanced stimulation and activation of peripheral nerve endings in the peritoneal cavity (peripheral sensitization) increases the painful stimuli transmitted to the spinal cord, initiating, and maintaining chronic pelvic pain (central sensitization). RANTES, regulated on activation, normal T cell expressed and secreted; TRPV1, transient receptor potential subfamily V1.

Normal menstruation requires the initiation of an innate immune response to provide cyclical breakdown and clearing of endometrial cells from the uterus in a highly regulated process [46]. Similarly, in women who don't develop endometriosis, ectopic endometrial debris is cleared from the peritoneum by an innate immune response facilitated by the peritoneal fluid (PF). This immune response is characterized by increased local neutrophils, macrophages, natural killer (NK) cells and dendritic cells locally within the PF [42, 47]. Dysregulation in this innate immune response in response to ectopic endometrial tissue has been implicated in endometriosis pathophysiology. Numerous studies have shown increased peritoneal macrophages in response to the infiltration of circulating monocytes in the peritoneal cavity [48-50], which facilitate the growth of endometrium-like tissue [51-53]. In women without endometriosis, tight regulation and control of immune cells clears the way for the next menstrual cycle. However, in women with endometriosis the chronic inflammatory milieu has been linked to the generation of pain [54].

Although retrograde menstruation is the oldest and most widely accepted mechanism, other theories have been proposed in the pathogenesis of endometriosis. Amongst these, metaplasia of specialized cells in the peritoneal tissue into endometrial like cells (Coelomic metaplasia), hormonal imbalance, progesterone resistance, immune dysfunction and inflammation, are all able to facilitate lesion growth along with a genetic component that provides bias towards first degree relatives and twins [55]. Understanding the pathogenesis of endometriosis and how each of these mechanisms may intertwine is an important area for research. Elucidating risk factors and mechanisms will enable a more widespread understanding of the development of endometriosis and ultimately treatment and prevention of ectopic lesion formation and growth.

1.4.3 Clinical diagnosis

The most common symptoms of endometriosis include dysmenorrhea, dyspareunia, back pain, and chronic lower abdominal pain or pain that is associated with bladder filling and defecation

[26, 27, 38, 56-58]. As these symptoms mimic those of other diseases or conditions, the clinical diagnosis of endometriosis is complex [59]. Despite multiple studies aimed at identifying biomarkers in the blood or urine to facilitate non-invasive biological testing and clinical diagnosis of endometriosis, no biomarkers have been identified as yet [60, 61]. Clinical examination via palpation of the abdominal and pelvic area, in conjunction with patient history are early stages of the endometriosis diagnosis process but are only steppingstones to further investigation [62]. Non-surgical clinical examination cannot definitively diagnose endometriosis with ultrasound, the most common non-invasive investigation, correctly identifying only ~10% of cases [63]. Recent advances in medical imaging suggests potential for transvaginal ultrasound and MRI as diagnostic tools for some types of endometriosis, however, the identification of superficial peritoneal lesions is not yet possible as the size of the lesions is below the threshold for detection [60, 64, 65]. Accordingly, endometriosis can only be diagnosed and classified via surgical laparoscopy or laparotomy to confirm the presence of endometrial lesions [59]. Endometrial lesions are described as superficial peritoneal lesions, ovarian cysts (endometriomas), deep endometriosis and the less common extrapelvic lesions, based on their location [66]. Due to the surgically invasive nature of this diagnostic testing, as well as the limited understanding of endometriosis pathology, progression, and risk factors, there is often frequent misdiagnosis and a consequential delay in determining the correct diagnosis. Multiple studies investigating the time between the onset of pain and the diagnosis of endometriosis report a significant delay, with an average of eight years in the UK and up to 12 years in many countries including the USA [30, 67-69]. Such delays in diagnosis are likely to aid in the progressive chronicity of the disease.

Once surgically confirmed, the stage and extent of endometriosis is categorized via a standardized worldwide classification system into one of four grades, determined by the severity of lesions/adhesions [70, 71]. Although this is the standard and accepted method for classification, there is only a weak correlation between the graded severity of morphological characteristics and the intensity and character of pain symptoms [36, 72]. As diagnosis and classification of endometriosis evolves, it has become clear that it is a chronic and systemic disease with inadequate understanding, and diagnosed stage is not indicative of patient suffering [73, 74]. The location of ectopic lesions can vary dramatically between patients and are found predominantly on the peritoneum, but also adhered to organs, including ovaries, vagina, fallopian tubes, bladder, colon, and small intestine [75, 76]. Whilst pain is often experienced from the reproductive organs, pain can also originate from visceral organs in close proximity, such as the bowel and bladder. Accordingly, patients with endometriosis exhibit significant comorbidity with chronic abdominal pain and CPP disorders such as IC/BPS (70-80% of endometriosis patients) [57, 58] and IBS (50-70% of endometriosis patients) [26, 27]. Although lesions can be removed or ablated as an initial treatment for endometriosis associated CPP, additional treatments or further surgery are often required. Whilst surgery, hormonal, and non-hormonal pharmaceutical agents (discussed in greater detail below) are

used to try and resolve CPP **(Table** 1.1**)**, complete eradication of endometriosis associated pain is rarely possible.

Table 1.1: Current approaches for CPP in endometriosis

Class	Type	Mechanism	Side effects
Hormonal	GnRH agonists Aromatase inhibitors Contraceptive Pill	Modulation of hormone signalling and prevention of menstruation	Hypoestrogenic – decreased bone density, mood changes and breast atrophy Not viable with pregnancy
Non-Hormonal	NSAIDS Opioids	Targets inflammation	Often ineffective Exhibit toxicity Tolerance, dependence, constipation, and addiction
Surgical	Lesion excision or ablation Partial or complete Hysterectomy	Target lesions or uterus as site of endometriosis	Invasive surgery with significant complication rates Early menopause Not always viable with pregnancy (hysterectomy)

Abbreviations: GnRH, Gonadotropin-releasing hormone; NSAIDs, Nonsteroidal anti-inflammatory drugs.

1.4.4 Mechanisms underlying endometriosis induced pain

The majority of research into the mechanisms underlying pain in endometriosis has focused on the endometrial lesions and adhesions as the primary source of endometriosis associated pain. Although lesion specific pain is apparent, and undoubtably essential for the induction of endometriosis induced pain, lesion removal does not provide pain relief in all cases, with reports suggesting 20-28% of patients do not have pain relief following surgery [35, 77]. Furthermore, only a marginal association exists between endometriosis stage (defined by lesion morphology) and the severity of pelvic symptoms [72], suggesting additional complex mechanisms are involved. More recent understanding of the mechanisms underlying the development of a chronic pain state in endometriosis implicates cyclical bleeding from lesions and subsequent inflammation at both lesion sites and in the peritoneal cavity. These proinflammatory responses then result in sensory nerve activation and altered activation of nociceptive pathways **(Table** 1.2**)** [78-80].

Table 1.2: Pain mechanisms in endometriosis

	Site	Mechanism	Key players in pain
Inflammation	Peritoneal fluid and endometrial lesions	Retrograde menstruation and cyclical bleeding at lesion sites	Activation of an innate immune response increases inflammatory and nociceptive cytokines/chemokines (TNFα interleukins IL-8 and IL-1β) [81], ROS, growth factors (NGF and VEGF) [82], neutrophils and prostaglandins (PGE_2) [83], [84]
Neurogenic inflammation	Sensory nerves	Build-up of pro-nociceptive environment can act directly on sensory nerve fibres	Degraded tissue by-products including ROS, PGE_2 and acidification can activate sensory nerves [85], [86]. Positive feedback loop maintains inflammation by releasing further proinflammatory modulators including SP and CGRP [87].
Peripheral Sensitization	Peripheral sensory nerves	Neuroplasticity of peripheral sensory nerves	Persistent inflammation can cause structural and synaptic changes occur to shift the neuronal function into a more sensitized state [88]. The abundance of inflammatory molecules in the peritoneal fluid, including glycodelin, ROS, TNFα, NGF and PGE_2 may contribute to this [89].
Central Sensitization	Central nervous system (CNS)	Long term changes in CNS signalling	Persistent nociceptive barrage leads to a long-lasting central sensitization of sensory afferents, evoking long term changes in pain processing or 'memory' [90, 91].
Cross-organ Sensitization	Sensitized afferents across multiple organs	Sensitized afferents from one organ induce sensitization of the afferents innervating another organ	Visceral afferents converge into similar areas of the spinal cord providing opportunity for the sensitization of neighbouring cells due to spatial location [92]

Abbreviations: TNFα, tumour necrosis factor α; IL, interleukin; ROS, reactive oxygen species; NGF, nerve growth factor; VEGF, vascular endothelial growth factor; PGE_2, prostaglandin E_2; SP, substance P; CGRP, calcitonin gene-related peptide.

1.4.4.1 Inflammation

In the uterus, the natural breakdown and elimination of endometrial tissue during menstruation is a highly regulated response to falling levels of estrogen and progesterone, acting to remove menstrual debris from the uterus, to make way for another cycle of endometrial regeneration [93]. Carried out by the innate immune system, this process recruits a large number of immune cells, including neutrophils, macrophages and natural killer (NK) cells to facilitate menstrual breakdown. The endometrial lining undergoes apoptosis and necrosis and is finally shed [93]. The programmed cell death during menstruation releases numerous cellular products, including iron, reactive oxygen

species (ROS), prostaglandins and a family of damage-associated molecular patterns (DAMPs) amongst others [54]. In endometriosis, when retrograde menstruation occurs, endometrial fragments adhere and form lesions within the peritoneum, where they remain endometrial in nature, expressing estrogen receptors and undergoing cyclical inflammatory and menstrual events [94, 95]. Cyclical bleeding in response to sex hormones, which naturally occurs in the uterus during menstruation, can also be seen within the peritoneal cavity at the site of endometrial lesions [48]. As such, menstrual by-products also arise from extra-uterine lesions and are released into the peritoneal cavity where they initiate further immune response **(Table** 1.2**, Figure** 1.1**)** [54]. Not only does the attempted breakdown of existing endometrial lesions and residual retrograde menstruation in the peritoneal cavity activate an immune response, but the amplified inflammatory milieu leads to a build-up of iron, ROS, prostaglandin E2 (PGE_2) and acidosis [85]. This immune response is evident at lesion sites, with increased inflammatory cytokines/chemokines, growth factors, neutrophils and prostaglandins found within the peritoneal cavity of endometriosis patients [81-84]. Of these mediators, PGE_2, tumour necrosis factor-α (TNFα), nerve growth factor (NGF), Regulated on Activation Normal T cell Expressed and Secreted (RANTES, also known as C-C chemokine ligand 5: CCL5), and interleukin (IL) IL-8 and IL-1β are all elevated within the PF of endometriosis patients who reported CPP [81, 96-98]. Crucially these mediators are all able to directly activate sensory nerve endings, suggesting inflammatory mechanisms may be important in endometriosis associated pain [99, 100]. A recent study showed that cytokine analysis of PF could differentiate women diagnosed and stratified laparoscopically with ovarian endometrioma, peritoneal endometriosis, or deep infiltrating endometriosis. This suggests that certain cytokine signatures could be driving different biological signalling events and immune responses in these patients [101].

In addition, ROS induce oxidative modification of proteins, with significantly higher levels of protein oxidative stress markers found within the peritoneal fluid of women with endometriosis [102]. Interestingly, the targeting of oxidized proteins with oral antioxidants, including vitamin E and vitamin C, significantly reduced reported chronic pain in women with endometriosis compared to placebo following 8 weeks of treatment [103]. This treatment approach also decreased inflammatory markers within the peritoneal fluid [103]. Oxidized proteins, and the subsequent activation of nociceptors, has been suggested to promote endometriosis associated pain although the underlying mechanism remains unclear [104, 105].

Overall, the resulting increase in extra-uterine debris, heightened by further retrograde menstruation, induces an enhanced inflammatory response within the peritoneum and PF which presents an opportunity for the interaction of these immune cells with sensory nerves to induce CPP [106]. Long term exposure to proinflammatory cytokines is proposed to activate and sensitize peripheral sensory nerves present in endometriotic lesions and surrounding visceral organs, initiating the transfer of nociceptive signals to the central nervous system (CNS) [54]. The activation

of peripheral sensory nerve fibres to generate and convey pain to the CNS is a vital step in the pain processing pathway and contributes to other forms of chronic visceral pain [88, 107-109]. Whilst this cyclical inflammation can exacerbate pain during menstruation, non-cyclical pain is also experienced by many women with endometriosis [72]. This disconnect suggests further mechanisms, independent of cyclical events, also contribute to CPP in endometriosis.

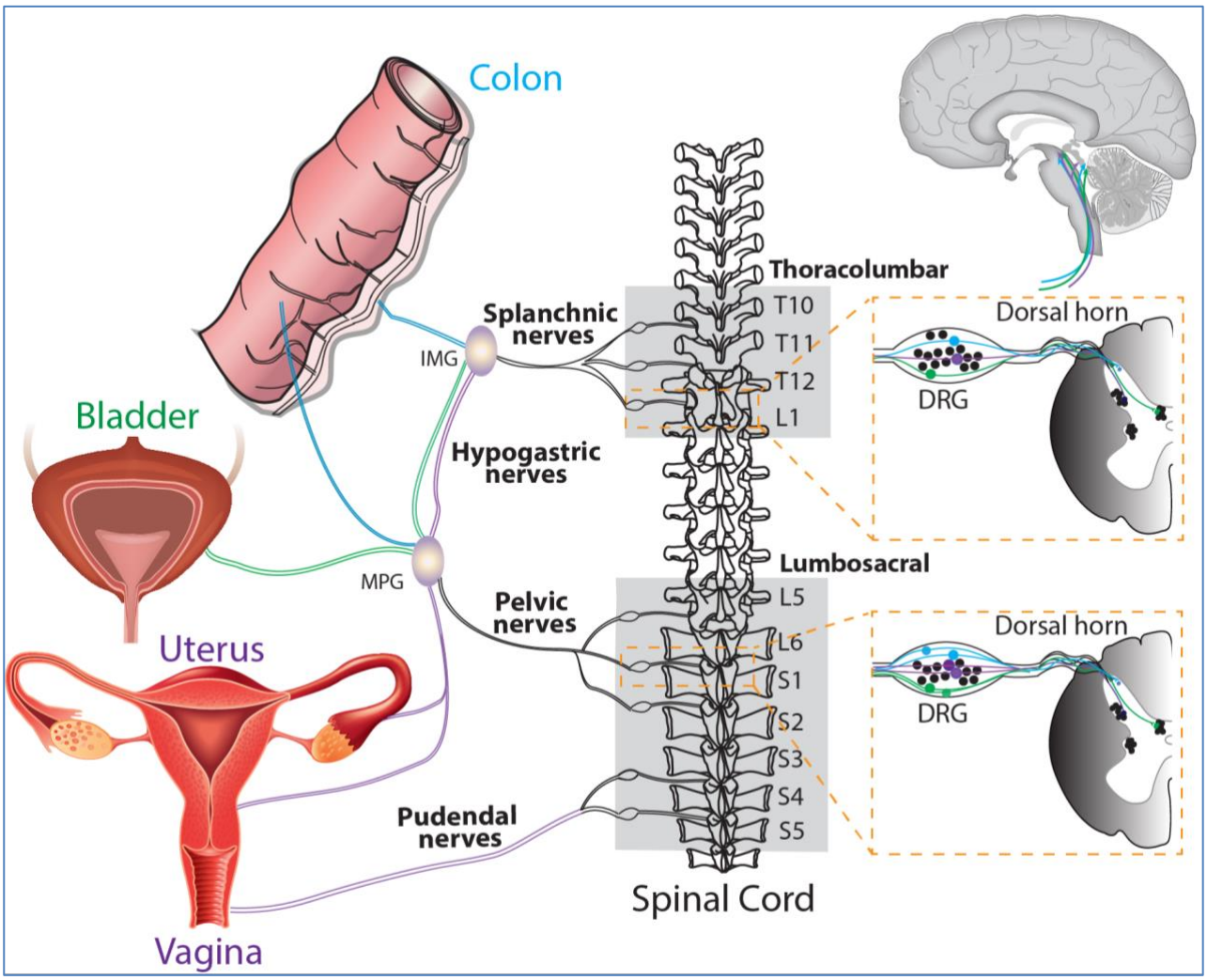

Figure 1.2: Schematic overview of the sensory innervation of the colon, bladder and uterus/vagina allowing for cross organ sensitization.

The colon is innervated by spinal afferents within the splanchnic and pelvic pathways. These spinal afferents can travel via the splanchnic or pelvic nerves (with some afferents traversing the hypogastric nerve) and have cell bodies located within the thoracolumbar and lumbosacral dorsal root ganglia (DRG). The bladder is also innervated by both splanchnic and pelvic pathways [108]. The central terminals of colon and bladder afferents terminate within the dorsal horn of the thoracolumbar and lumbosacral dorsal horn [110-112]. Afferents innervating the uterus and vagina also share the splanchnic and pelvic pathways, whilst the vagina is also innervated by the pudendal nerves, with cell bodies within the lumbosacral DRG and central terminals within the lumbosacral dorsal horn [107]. The central terminals of colon, bladder, uterus, and vaginal afferents synapse onto second order dorsal horn neurons in the spinal cord, which ultimately transmit signals to the brain. Accordingly, these different visceral organs share common nerve pathways to the DRG and spinal cord, allowing the potential for cross organ sensitization. TL, Thoracolumbar; LS, Lumbosacral; IMG, Inferior Mesenteric Ganglion; MPG, Major Pelvic Ganglion.

1.4.4.2 Neuroangiogenesis

Pain relies on the existence of sensory transduction pathways linking peripheral stimuli to the spinal cord for processing and ultimately to the brain for pain perception **(Figure** 1.2**).** However, endometrial fragments do not have an intrinsic sensory nerve supply connected to these pathways. For endometrial lesions to induce chronic pain, the development of new sensory nerves to convey these signals needs to occur. A number of studies have now shown that once endometrial fragments adhere to a peritoneal location and develop into endometrial lesions, they undergo a process of neuroangiogenesis [106]. This consists of the coordinated establishment of a blood supply through the generation of new blood vessels to support growth and survival (angiogenesis), together with the synchronized innervation by nerve fibres (neurogenesis) [113].

Neuroangiogenesis is regulated by estrogen and immune cells, including macrophages, which are an important source of vascular endothelial growth factor (VEGF) and nerve growth factor (NGF) [76], both of which are increased in endometriosis [114, 115]. Macrophages exacerbate local inflammation, facilitate growth of ectopic endometrial lesions, and are directly involved in angiogenesis, releasing chemokines and cytokines that further drive the growth of endometrial tissue [116-118]. In a surgically transplanted endometriosis mouse model, macrophage secretion of the angiogenic factors VEGF, TNFα and macrophage inflammatory proteins (MIP-1α and MIP-2) into the peritoneal fluid in early stages of endometriosis progression correlated with a peak in active angiogenesis in lesions [118]. Heightened angiogenesis, driving both the establishment and growth of endometrial lesions, is also evident in patients. Studies have identified increased angiogenic factors, including VEGF and TNFα, in the pelvic PF of patients with endometriosis [119]. These changes are further supported by a rich vascularization correlating with more active peritoneal endometrial lesions [120].

As angiogenic factors promote blood supply and support lesion growth and establishment, neurotrophic factors are essential for the development of both autonomic neurons and peripheral sensory afferents, of which the latter can transmit nociceptive stimuli [121, 122]. An increased density of small, unmyelinated nerve fibres (sensory afferents, sympathetic and parasympathetic efferents) have been found in endometrial lesions [87] as well as the endometrium of women with endometriosis [123]. The vast majority of these unmyelinated nerve fibres have been identified as C-fibre sensory afferents, unmyelinated nerves that typically function as nociceptors, implicating them strongly in the generation of CPP in endometriosis [124]. Directly highlighting their importance in CPP, early removal of lesions, before they established nerve fibre innervation, reversed hypersensitivity seen in an endometriosis mouse model [125]. Moreover, endometriosis associated menstrual pain was highest in women whose endometriotic lesions had increased nerve fibre innervation [126, 127].

An increase in neuroangiogenic markers has been linked to a dense nerve supply in lesions and the endometrium and is closely related to CPP symptoms in women suffering from endometriosis [128, 129]. Markers for both adrenergic and cholinergic neurons (neuropeptide Y), as well as unmyelinated C-fibres (substance P: SP, calcitonin gene-related peptide: CGRP) are significantly higher in the endometrium of patients with endometriosis [128]. The nerve injury-induced protein 1 (Ninj1), which promotes neurite outgrowth, has also been found to be expressed in ovarian and peritoneal endometriotic tissues [130]. Increased levels of neurotrophins and their receptors, including NGF and its receptor tyrosine kinase A (TrkA), are also seen in endometrial biopsies of women with endometriosis [131]. NGF promotes new nerve sprouting and acts directly on existing sensory nerve fibres to induce pain [132, 133]. These effects are exacerbated by increased levels of circulating estrogen in women with endometriosis, as estrogen can enhance NGF activation of TrkA [134]. This is important as its downstream target is the well-known nociceptive cation channel transient receptor potential subfamily V member 1 (TRPV1), which has been found to be upregulated in endometrial lesions and ectopic endometrial cells [135, 136]. An increase in the density of nerve endings throughout lesions and an enhanced excitability of nerves provides the basis for increased nociception at lesion sites.

Together with the establishment and growth of endometrial lesions, neuroangiogenesis aids irritation and invasion of existing nerves. Nerve density is increased in deep infiltrating endometriotic nodules when compared to healthy vaginal tissue, an observation also seen in peritoneal endometrial lesions relative to the normal peritoneum [87, 137, 138]. The close proximity of endometrial adhesions and lesions to pelvic nerves can cause their encapsulation or compression, which may contribute to CPP associated with endometriosis [139]. Hyperalgesia due to dense nerve supply and encapsulation is supported by multiple studies, which show the highest pain score from endometriosis patients correlates with a higher density of nerves and nerve encapsulations [126, 127, 140].

It has also been suggested that an imbalance between the activation of anti-nociceptive and pro-nociceptive ion channels on these lesion innervating neurons is a possible mechanism for pain pathophysiology [141]. Such imbalances also contribute to other visceral pain conditions [142]. An imbalance resulting in increased nociceptive input, with a decreased parasympathetic control at lesion sites could lead to a heightened pain response. Changes in this autonomic equilibrium occur in a number of chronic visceral pain disorders including fibromyalgia, gastroesophageal reflux disease and IBS [143], with decreased parasympathetic and increased sympathetic activity [144], favouring the transmission of painful stimuli. Sensory nerves had a significantly higher density in areas close to endometriotic lesions compared to sympathetic nerve fibres [141]. Interestingly, it has been shown that traditional hormone therapies that alleviate pain in endometriosis, including progestogens and oral contraceptives, significantly reduced nerve fibre density in ectopic

endometrium [131]. Although a novel finding, pain severity was not assessed, and further studies are needed to determine if the nerve fibre reduction in endometrial lesions in response to hormone therapy would show a clinical effect on lesion specific pain. Along these lines, estrogen receptor expression in endometrial samples has been shown to predict symptom severity and pain recurrence in endometriosis. In particular, a higher expression of ER-α increased the prospect of moderate to severe dysmenorrhea and deep dyspareunia [145]. Correspondingly, progestin therapy reduced ER-α expression, whereas androgen receptor, aromatase expression and progesterone receptor abundance were unaltered [145]. Unfortunately, hormone therapy is not conducive to reproductive plans, and therapeutic treatment of endometriosis associated CPP with hormonal treatment types is often not a long-term solution for many women.

1.4.4.3 Neurogenic inflammation

Adding to the already pro-nociceptive environment induced by endometrial lesions in the peritoneal cavity, build-up of degraded tissue by-products, including ROS, PGE_2 and acidification can directly act on or sensitize sensory nerve fibres through receptors on nociceptive afferent nerves located within lesions **(Table** 1.2**, Figure** 1.1**)** [85, 86, 146]. Compounding this nociceptive barrage, sensitized sensory nerve fibres maintain inflammation by a positive feedback loop called 'neurogenic inflammation'. Excitation of these nerve fibres results in their terminals releasing further pro-inflammatory modulators. This includes neuropeptides such as SP and CGRP, both of which are found close to endometrial lesions in women with endometriosis associated pain [123]. Moreover, activation of sensory afferent nerves initiates the recruitment of mast cells and subsequent release of pro-inflammatory cytokines, including TNFα, NGF, PGE_2 and a variety of interleukins, such as IL-1β, which contributes to a chronic state of neurogenic inflammation [89, 147]. This inflammation encourages further stimulation of locally circulating mast cells and macrophages that are found in elevated levels and in close proximity to nerve fibres in women with endometriosis [148]. A number of other chronic pain conditions, such as asthma, arthritis, IC/PBS, IBS, inflammatory bowel disease (IBD; including ulcerative colitis and Crohn's disease), display a chronic neurogenic inflammatory state that induces chronic pain [88, 147, 149, 150].

1.4.4.4 Peripheral sensitization

Neuroplasticity of peripheral sensory nerves, such that structural, synaptic or intrinsic changes occur to shift neuronal function into a more sensitized state, is an established process in the development of chronic visceral pain [88, 151]. Under normal circumstances, peripheral sensitization causes the threshold for neuronal activation to drop, inducing pain from a stimulus that does not normally provoke pain (allodynia) or heightens existing pain (hyperalgesia). This mechanism provides protection from further damage following the development of inflammation from an existing injury [152]. However, if inflammation persists, or a maladaptation to the original sensitizing stimulus occurs, nociceptors can become chronically hypersensitive even after

inflammation resolves and histology appears normal. This peripheral hypersensitivity of nociceptive fibres at lesion sites may play a role in allodynia and hyperalgesia experienced by endometriosis patients **(Figure** 1.1**)** [78].

As described above, there is an abundance of inflammatory molecules, including glycodelin, ROS, TNFα, NGF and PGE_2 in the PF of women with endometriosis, which may contribute to the induction of a more pro-nociceptive state **(Table** 1.2**)** [89, 153]. Interestingly, increased levels of TNFα and glycodelin correlate with central hyperexcitability in response to repeated electrical stimulation and altered pain response to nociceptive withdrawal reflex, as well as higher levels of menstrual pain experienced by endometriosis patients [96, 154]. Patients with the highest pain scores also had the highest levels of TNFα, which was independent of lesion score [155]. Further supporting a role in chronic pain conditions, TNFα activates nerve fibres innervating the colon, and has been shown to be elevated in samples from IBS patients, which correlates with patient clinical pain scores [156].

Hypersensitivity of sensory afferents innervating visceral organs has also been demonstrated in animal models of chronic diseases such as IBS and IC/BPS [151, 157-163]. Various membrane receptors and ion channels located on sensory afferents tightly regulate their sensitivity to detect a range of stimuli and can contribute to changes in pain sensation. Contributing to sensory afferent hypersensitivity, TRPV channels, voltage gated sodium channels (Na_V), voltage gated calcium channels (Ca_V), purinergic ion channels, cannabinoid receptors, as well as protease-activated receptors (PAR) have all been suggested to play a role in the generation of visceral hypersensitivity in other chronic conditions such as IBS [164]. For example, the nociceptive ion channel TRPV1 has been implicated in chronic pain conditions such as rheumatoid arthritis, osteo arthritis and IBS [135, 142, 165], acting as a molecular sensor to potentiate and integrate responses to pain inducing stimuli, such as acidosis, oxidative stress or inflammatory mediators [135, 166]. Supporting an involvement of TRPV1 in endometriosis associated pain, elevated expression of TRPV1 has been found in dorsal root ganglion (DRG) of rats with endometriosis [167] as well as locally on infiltrating adhesions in endometriosis patients and within the peritoneum [168], the increase correlating with pain intensity [136, 169]. This is not surprising, as a number of the processes responsible for TRPV1 upregulation and sensitization are found in endometriosis patients, including enhanced ROS concentrations and increased levels of neurotrophins such as NGF. Together these mechanisms have the ability to activate TRPV1 as well as increase its expression, further driving sensitization of peripheral nociceptors [135, 170, 171]. It has been proposed that chronic sensitization of peripheral sensory nerve fibres in turn induces sensitization of the CNS in endometriosis [141, 172]. Recent studies also show exposure to chronic stress early in life can increase the likelihood of CPP later in life, whilst bouts of acute stress can trigger or worsen symptoms [173-176].

1.4.4.5 Central sensitization

Chronic neuroinflammation and hyperexcitability of peripheral afferents has also been shown to induce long-term changes in CNS signalling, as well as increased sprouting of central terminals within the spinal cord dorsal horn in other painful visceral disorders, including IBS and IC/BPS [110, 111, 151]. These conditions contribute to the sensitization of CNS neurons in the spinal cord and brain that produces long lasting hyperexcitability in the absence of noxious stimuli [177-179]. The persistent nociceptive barrage from inflammatory endometriotic lesions and the PF is thought to lead to a long-lasting central sensitization of sensory afferents **(Figure** 1.1**)** [90]. This phenomenon has been seen in patients with chronic pain related to osteoarthritis, whiplash [180] and fibromyalgia [181] and is often considered the cause for 'unexplained' chronic pain [182].

Central sensitization can evoke long-term changes in pain processing, similar to the generation of 'memory'. Neonatal irritation of hollow organs or maternal separation are able to drive long-term visceral/somatic hypersensitivity and central sensitization [173, 175, 176]. Central sensitization is also often initiated and maintained by peripheral sensitization, resulting in pain persisting long after the peripheral insult or pathology or has resolved **(Table** 1.2**)** [91]. This may be particularly relevant in endometriosis as many women experience persistent pain despite treatment or removal of endometrial lesions [34, 183]. Furthermore, women with dysmenorrhea (menstrual pain) have increased CNS activation to noxious stimuli compared to women who don't experience menstrual pain, a phenomenon seen at various stages of the menstrual cycle [184]. Accordingly, central sensitization of pain pathways could help to explain why chronic pain persists in some patients following lesion removal or why diagnosed lesion scores do not correlate with pain intensity [183].

Neuroimaging has been used to identify chronic changes in the brains of women with CPP, both with and without endometriosis. A decreased volume of grey matter has been identified in areas of the brain related to pain processing, including the thalamus and insula, a brain region consistently activated during acute and chronic pain states [185]. These changes were seen in women with endometriosis that experience CPP but not in asymptomatic women, further supporting a role for CNS pain processing in CPP. Furthermore, proton magnetic resonance spectroscopy determined that women with endometriosis had increased levels of excitatory neurotransmitters in their anterior insula compared with healthy women [185]. Using an animal model of endometriosis, changes in gene expression in similar pain processing areas of the brain, including the amygdala, insula and hippocampus were also observed [183].

Not only does central sensitization alter the pain response from the direct area of insult, it can also alter pain from seemingly unrelated areas. Animal models of endometriosis experience allodynia and hyperalgesia to different noxious stimuli including heat and vaginal distension [115, 183, 186]. Similarly, a cohort of endometriosis patients experienced enhanced muscular pain

following saline injection into the hand when compared to healthy participants [90]. In these scenarios, both hyperalgesia and allodynia are apparent once a stimulus is applied, allowing the changes in sensitization to become apparent. Although increased pain responses have been demonstrated in both animal and human studies, the CNS pathway changes, together with the molecular mechanisms underlying central sensitization in endometriosis, are more difficult to determine.

Although changes in central pain processing have been reported in endometriosis, whether they exacerbate CPP following changes initiated by endometriosis, or whether these women are already sensitized and have a heightened response to endometrial disease, is unclear. As the delay between onset of pain and diagnosis and treatment of endometriosis is typically between eight to twelve years, there is ample opportunity for these lesions to induce the chronic changes needed to induce central sensitization. Although it is currently unknown if earlier diagnosis and removal of lesions could reverse or avoid these changes in patients, the removal of lesions in the early stages of progression in animal models reversed the pain experienced [115, 125], whilst removing them at later stages had no effect [125].

1.4.4.6 Cross organ sensitization

Women with endometriosis have a high comorbidity rate with other chronic pain syndromes associated with peripheral and central changes in pain processing, including , fibromyalgia, migraine headaches, IBS and IC/PBS [187]. The phenomenon of cross organ sensitization, described as the spreading of noxious inputs from a diseased visceral organ to a normal organ in close proximity, has been studied in other pathological conditions where comorbidities are common, including IBS, IBD, IC/BPS and other CPP disorders [109, 188-191].

Experimental evidence of functional cross organ sensitization in the pelvis has been observed in many combinations, including bladder/colon [110, 192], vagina/colon, bladder/uterus [92] and uterus/colon [191, 193]. For example, uterine inflammation produced signs of inflammation in the colon and the bladder [190], whilst bladder inflammation has been found to alter uterine contractility [194]. These alterations have been displayed in pre-clinical endometriosis models where abnormal endometrial tissue growth induced vaginal hyperalgesia in a rat, which was exacerbated by estradiol [186, 195]. It has also been demonstrated that endometriosis increased pain behaviours of rats with kidney stones, another comorbidity of women with endometriosis [196], and reduced the micturition threshold of rats, indicating increased urinary urgency and frequency, a clinical symptom of bladder disorders [107, 187].

Cross organ sensitization is thought to occur when sensitized afferents from one organ induce sensitization of the afferents innervating another organ **(Table** 1.2**, Figure** 1.2**)**. Visceral afferents converge into similar areas of the spinal cord providing opportunity for the sensitization of

neighbouring cells due to spatial location [92, 110]. The precise mechanisms responsible for cross-organ sensitization are unclear, however, overlap of peripheral afferent pathways within the DRG and spinal cord are crucial [25, 109, 151]. Following neuroangiogenesis, which includes the presence of CGRP, TRPV1, and transient receptor potential ankyrin 1 (TRPA1) expressing nerve fibres [197], the sensory nerves innervating endometriotic lesions may converge into the same spinal pathways from the afferents they originally sprouted from in the periphery. As such, they will share the same cell bodies in the DRG and the same central terminals within the spinal cord [198]. As the location of ectopic lesions appears to be random, this could help to explain why the experience of pain is heterogenous within an endometriosis population.

With retrograde menstruation the primary theory for development of endometriosis, pelvic lesions are often found around the reproductive tract, with extra-pelvic lesions found in close proximity, located frequently upon the gastrointestinal tract and urinary system [199]. Pain from these more distant lesions often mimics the pain from pelvic lesions and the extent of disease continues to be independent from symptom severity, regardless of lesion location. Conscious pain mapping of women with endometriosis confirmed half of participants localized their pain to lesion sites, but many women described generalized pain in the pelvis and bowel, indicating a widespread visceral hypersensitivity and pain independent of lesion location [36, 200]. Palpation of various lesion types during laparoscopy of women with endometriosis also saw pain extend into normal looking tissue [201], whilst referred pain was reported in half of women under conscious sedation during laparoscopy for CPP [202]. Lesion specific pain on visceral organs may be explained by neuroangiogenesis in lesions converging with existing neuronal pathways in the adhered organ, promoting cross organ sensitization due to shared nerve pathways.

Cross organ sensitization may also occur through shared innervation pathways of anatomically distinct organs. Recent studies have shown that a single peripheral neuronal cell body located within the DRG is able to generate multiple axons that innervate a number of abdominal organs simultaneously [203-205]. Often referred to as ‘dichotomizing afferents’, these nerve fibres converge from multiple visceral organs to a single cell body within the DRG and therefore terminate onto the same second order spinal neurons. Whilst the evolution of these dichotomizing afferents is embedded within the physiological coordination of sexual, defecatory and urinary function, sensitization of these pathways in pathological conditions can allow cross organ sensitization to occur. Retrograde tracing has revealed these neurons co-innervate a number of pelvic organs including the colon/bladder [110, 204], colon/vagina [92] and colon/uterus [205, 206].

The chronic generalized hypersensitivity across visceral organs may in part be a result of cross organ sensitization. The female reproductive tract is innervated by splanchnic, pelvic, and pudendal nerve pathways, presenting an opportunity for cross talk through shared neuronal pathways of other organs in close proximity, such as the bladder and bowel. Unfortunately, not much

is known about how the female reproductive tract senses pain. Whilst nerve development within lesions has been of interest, further understanding the path that new nerves take and the changes they facilitate is a necessary step in interpreting pain progression in endometriosis patients.

1.4.5 Current Treatments

Eighty percent of endometriosis patients suffer from CPP, with subfertility affecting 60% of these women. Although both symptoms are prevalent, their treatment is often independent, with reproductive plans complicating optimal treatment regimens. With up to 87% of women presenting with CPP found to have endometriosis [207], the treatment of CPP is an effective strategy to improve the quality of life in these patients, independent of subfertility. Overall, current therapeutic options provide pain relief for more than 6 months in only 40% to 70% of patients [208, 209]. As such, a greater understanding of the mechanisms underlying endometriosis induced pain is necessary to achieve greater clinical outcomes in the future.

As briefly mentioned above, traditional treatments focus on lesions as the cause of CPP associated with endometriosis **(Table** 1.2**)**. Modulation of hormonal signalling via gonadotropin-releasing hormone (GnRH) agonists, aromatase inhibitors and oral contraceptive pills is known to suppress pain symptoms via estrogen inhibition and prevention of menstruation, lesion formation and growth. However, their incompatibility with fertility makes them a short-term treatment option for many women, with conclusion of treatment seeing the return of menstruation and symptoms [209-211]. By reducing the availability of estrogen, the estrogen dependent disease is significantly diminished, and cyclical bleeding is abolished. Although initially effective, pain relief was noted in only 40%-70% of patients after 6 months [208]. Together with the hypoestrogenic side effects including loss of bone mineral density and secondary osteoporosis, mood changes and breast atrophy [212], the use of GnRH is approved for only 6 months. Furthermore, contraceptive pills are not viable with pregnancy, making them a short-term solution for many women, especially those with reproductive plans. Aromatase inhibitors inhibit extra-ovarian estrogen production, making them particularly relevant for post-menopausal women or in combination with GnRH agonists, however their reduction in pain is again offset by adverse side effects, including osteoporosis and bone fractures [211].

Non-hormonal pain reducing agents such as nonsteroidal anti-inflammatory drugs (NSAIDs) and strong analgesics (opioids) reduce inflammation and mask pain [213]. NSAIDs are used to target inflammation, although a review of their effectiveness in managing pain caused by endometriosis is inconclusive [213]. Unfortunately, it has also been noted that NSAIDs are often ineffective and exhibit toxicity [214]. Opioids therapy is also used to treat chronic pain associated with endometriosis and surgical intervention [215]. Whilst opioids provide pain management, their effectiveness in the

treatment of endometriosis is not reliably understood. Misuse and abuse is a growing problem amongst many chronic pain conditions, together with tolerance and addiction making opioids an undesirable treatment option [216]. Unfortunately, whilst these medications represent a relatively non-invasive treatment plan, they either lack efficacy, or result in tolerance, dependence, and addiction.

As the most invasive option, but often required due to the debilitating nature of chronic pain [216] and treatment of endometriosis associated subfertility, surgical treatment of endometriosis is based on the principal of removing all endometriotic lesions to alleviate symptoms. Whilst endometrial lesions within the peritoneum can be excised or ablated, they often grow back due to continuing retrograde menstruation and disease progression, and further surgery is needed in many cases [217]. Between 20-28% of patients are non-responsive to surgery [35, 77], whilst reoccurrence is as high as 40-50% at 5 years post-surgery [34]. The surgical removal of lesions can sometimes prove challenging depending on the stage and grade of endometriosis, which further complicates outcomes. Surgical removal of deep infiltrating endometrial lesions reduces endometrial CPP, but is associated with significant complication rates, requiring complex surgery to remove lesions, with resection of the bowel, damage to the bladder wall and stenting of the ureter often required [218]. The lowest rates of further surgery in pain management is following complete hysterectomy, with over 90% of patients remaining follow-up surgery free for up to 7 years, although the removal of the ovaries as well as the uterus is not as effective in younger women [34]. In addition, associated health risks due to early menopause and incompatibility with pregnancy make hysterectomy a non-viable treatment for many women of reproductive age [34].

Even with a combination of therapies, complete eradication of endometrial associated pain is rarely possible. While the current therapies aim to suppress pain and delay reoccurrence, the disease often manifests itself once treatments have stopped or lesions have reformed. While the complete eradication of lesions is not likely, further understanding of chronic pain associated with endometriosis and identification of possible targets for pain management may help improve the quality of life for those suffering with endometriosis.

1.4.6 Future therapies? Insights from animal models of endometriosis

Endometriosis is currently considered an inflammatory disease, with non-surgical treatment targeted at the prevention of menstruation and hormonal therapy to limit disease progression and inflammation. It is increasingly evident that this disease has a multifaceted nature with 40% of women experiencing non-cyclical pelvic pain, thus limiting endometriosis treatment to anti-inflammatory or hormonal control of menstruation seems to miss the mark. Currently the delay in diagnosis allows complex disease progression, increasing the opportunity for long term changes in pain processing

to occur. Although progress has been made in the diagnosis and classification of endometriosis, assistance in early diagnosis is still of importance. Recent research priorities for endometriosis include an emphasis on biomarkers and imaging for non-invasive diagnostic techniques [29]. Despite multiple studies aimed at identifying a reliable biomarker as a clinical diagnostic tool, a systematic review of the last 25 years concluded that no single biomarker was confirmed to be clinically useful [219]. Strikingly, it has also been noted that very little progress has been made in understanding chronic pain associated with endometriosis, and subsequent advancement in treatment is lacking [29].

Modulating pain at an ion channel level and the targeting of specific pain receptors at lesion sites or organs involved in cross organ sensitization may provide a novel and non-hormonal approach for endometriosis patients suffering from CPP [220]. Indeed, limiting neuroangiogenesis to prevent lesion innervation and growth, together with direct modulation of key targets on peripheral nerves, is an important direction for future CPP management in endometriosis. Supported by evidence from a mouse model of endometriosis, lesion removal at early time points reduces CPP [115, 125, 126]. But in many cases this approach is not possible, whether it be delayed diagnosis, incomplete lesion removal, or deep infiltrating lesions, it is clear complete lesion removal at an early time point is a difficult venture.

Animal models of endometriosis have demonstrated novel mechanisms for reducing CPP. This includes the use of estrogen EP_2 receptor antagonists to reduce primary hyperalgesia by 80% and secondary hyperalgesia by 40% in a mouse model of endometriosis [114]. Furthermore, bradykinin receptor 2 antagonists can block bradykinin induced endothelin-1 production, which is important as endothelin-1 causes neuronal sensitization [221]. Other studies have demonstrated a key role for GPR30, a G protein-coupled receptor for estrogen, in endometriosis associated pain, whereby intra-lesion GPR30 agonists produce persistent mechanical hyperalgesia, whilst GPR30 antagonists inhibit mechanical hyperalgesia [222].

Conversely, activation of cannabinoid receptor type 1 (CB_1R), which are expressed by the sensory and sympathetic neurons innervating endometrial lesions, decreases endometriosis associated hyperalgesia [223]. Moreover, antagonists of CB_1R increase endometriosis associated hyperalgesia, suggesting an endogenous cannabinoid tone [223]. More recent studies show that Δ9-tetrahydrocannabinol (THC) alleviates mechanical hypersensitivity and pain in a mouse model of surgically induced endometriosis. THC also restored cognitive function and inhibited the development of endometrial cysts [224]. These studies suggest CB_1R plays a crucial role in the growth of lesions and endometriosis associated pain.

Recent studies have also suggested the potential of repurposing treatments for other conditions. This includes repurposing dichloroacetate, a pyruvate dehydrogenase kinase (PDK)

inhibitor/ pyruvate dehydrogenase activator used for treating cancer. This is because dichloroacetate normalizes human peritoneal mesothelial cells metabolism, reduces lactate concentrations and endometrial stromal cell proliferation in a co-culture cell model. In a mouse model of endometriosis oral administration of dichloroacetate reduces lactate concentrations within PF and endometrial lesion size [225].

Animal models of other chronic pain conditions, such as IBS, have been used to successfully demonstrate the modulation of pain by targeting the periphery. For example, chronic treatment with a guanylate cyclase-C (GC-C) agonist reversed the neuroplastic changes that cause both colonic hypersensitivity and cross organ sensitization of the bladder in a mouse model of IBS [110]. More recently, the same agonist, whose direct target GC-C is expressed within the gastrointestinal tract, has been used to reduce vaginal hyperalgesia and allodynia in a rat model of endometriosis [92]. This gives rise to the idea that targeting pain in one area may in fact reduce pain from other organs and that chronic changes due to an area of insult in one organ may in fact modulate pain experienced in another. Using animal models of endometriosis provides an important medium to uncover the mechanisms associated with CPP in endometriosis and explore the use of therapeutic interventions for the treatment of endometriosis associated CPP.

Current literature provides evidence for an overall heterogeneity in endometriosis development and symptom prevalence, rather than a ‘one size fits all’ approach. This strongly suggests a personalized treatment approach based on aetiology and symptomatology. Shifting the paradigm of lesion specific and cyclical inflammatory pain will continue to open further areas to expand treatment opportunities. Utilizing animal models of endometriosis that closely recapitulate the human disease will provide an insightful opportunity to further study disease progression and chronic pain. With the development of animal models of endometriosis already providing quality insight into disease progression and current treatment mechanisms, the next step is to dig a little deeper, and elucidate disease specific changes and their targets at the lesion, DRG, spinal cord and brain levels.

1.5 Pre-clinical models of Endometriosis

As described throughout this review of literature, endometriosis is a multifaceted chronic disease with a complex and variable display of clinical symptoms, not always correlated to disease progression. With endometriosis affecting over 10% of women worldwide, unmatched with effective treatment strategies, there remains a clear need for relevant and translatable models of endometriosis to support research progression [29]. Pre-clinical models have advanced scientific knowledge into various areas of endometriosis development and progression and are paramount to pre-clinical testing of viable treatment options **(Table** 1.3**)** [29, 226, 227]. Unfortunately, despite a rise of over 150% in published endometriosis research over the last decade, pre-clinical studies have failed to translate to effective clinical outcomes once they reach clinical trials [228]. A major factor suggested to contribute to the translational block may come down to the reproducibility of animal models and their ability to replicate the spectrum of disease to that which is spontaneously developed in humans [229]. A key factor in the development of any pre-clinical model of chronic disease is to encompass its complex features, from disease aetiology to mechanisms of disease progression and symptom development [229]. This is no different when considering a model for endometriosis. Fortunately, development of pre-clinical models of endometriosis has improved in recent years, building on the utilisation of human tissue as well as animal models, sometimes in combination [228-230].

The development of endometriosis is multifactorial in nature, with complex mechanisms of chronic inflammation and chronic pain development contributing to disease pathogenesis [231]. As such, whole body systems with an intact nervous system are of fundamental benefit to pre-clinical models. Forming the basis of endometriosis development in animal models, translocation of eutopic endometrial tissue to ectopic locations has led to the growth of endometrial-like lesions and the successful production of animal models of endometriosis. Of these, non-human primates and murine models are discussed below.

1.5.1 Non-human primates

As the most genetically alike to humans, non-human primates, such as the baboon and rhesus monkey, have been used in the study of endometriosis **(Table** 1.3**)** [232]. As menstruating primates, they share physiological similarities to humans, with similar menstrual cycles and instances of spontaneous endometriosis [233, 234]. Following inoculation of menstrual endometrial tissue into the peritoneal cavity, baboons develop lesions like those seen in humans, retaining structural similarities such as endometrial glands and stroma as early as one month after inoculation [235, 236]. Similarities are also apparent in the inflammatory parameters of the peritoneal fluid (PF), with elevated cytokines including TNFα, transforming growth factor β (TGFβ), cluster of differentiation 3

(CD3) and human leukocyte antigen – DR isotope (HLA-DR) [237]. The angiogenic factor VEGF is also elevated in both human and baboon ectopic endometrium following endometriosis development [236]. With clear similarities in disease, the non-human primate models of endometriosis have provided useful insights into mechanisms of endometriosis development [232], although it has been noted that research has thus far failed to translate to clinically relevant treatments [228]. Although physiologically relevant to human disease, non-human primates are sensitive to captivity and expensive, which makes high throughput experiments difficult and ultimately limiting to research output.

Table 1.3: Animal models of endometriosis

Species	Advantages	Disadvantages	Examples of Endometriosis research
Non-human primates	• Genetically similar to humans with spontaneous endometriosis development [233, 234]. • Physiological relevant to human disease.	• Sensitive to captivity. • Expensive. • Limited genetic modifications.	• Development [232]. • Inflammation [236, 237].
Murine (rats and mice)	• Easily bred/sources. • Affordable. • Genetical modifications readily available. • Advanced knowledge of physiological body systems due to popular use in research. • Have been successfully used to study endometriosis.	• Do not naturally menstruate. • Intervention always required for endometriosis development. • Clinical translation has proven difficult.	• Development [226, 238-244]. • Inflammation [245]. • Infertility [244, 246, 247]. • Treatments [92, 225, 242, 248, 249]. • Pain [114, 115, 125, 126, 222].

1.5.2 Murine

More commonly, murine models of disease have been important in many areas of scientific discovery and development. Rats and mice are a popular choice for many pre-clinical models as they are easily bred and affordable, offer an array of genetic modification options, and advanced physiological knowledge of their body systems exists due to their extensive use in many fields **(Table** 1.3**)** [250]. Despite distinct advantages, laboratory mice and rats do not naturally menstruate or develop spontaneous endometriosis, therefore model development requires intervention. The earliest small animal model of endometriosis was developed by Vernon and Wilson in 1985, employing surgical transplantation of uterine tissue onto the mesenteric arteries of rats [251]. This model was the first to demonstrate the attachment and growth of endometriosis lesions within the peritoneal cavity and successfully aided in the development of treatments utilised today [242]. In an

extension of this surgical attachment model, a model reducing the invasive nature of induction by instead injecting fragments of uterine tissue into the peritoneal cavity to induce endometriosis has also been developed [197]. This model more closely recapitulates retrograde menstruation, although does not have the benefit of selective lesion placement. Due to success of this model and more recent technological innovations, variations have been incorporated to progress key areas of endometriosis research. Modifications include injecting fluorescently tagged uterine tissue to enable fluorescent imaging of lesion growth [243, 252], inoculating human tissue into immunocompromised mice for the establishment of human endometrial endometriosis [248, 253], and developing a menstruating mouse model to more closely mimic the human phenotype [252]. All variations of these models successfully report eutopic lesion development, resembling what is seen in women with endometriosis. Thanks to the development of these small animal models of endometriosis, research has progressed in many areas including endometriosis growth and development [226, 238-244], inflammation [245], infertility [244, 246, 247], treatment [92, 225, 242, 248, 249] and pain [114, 115, 125, 126, 222], to name a few. Despite contributions discussed throughout this chapter, it is recognised that research into pain mechanisms is still unfortunately lacking [254], and further refining these models to understand pain development is necessary to advance this research in endometriosis [250].

1.5.3 Animal Models and Pain

Animals cannot self-report pain like humans, however, measuring inferred pain from both spontaneous and evoked interactions provides insight into 'pain-like' behaviours [255]. Fortunately, rodent models are the most commonly used species for pain assessment experiments [255], and the combination of established behavioural techniques with the endometriosis model is conducive to pain research in endometriosis.

1.5.3.1 Evoked responses

Evoked behavioural studies allow researchers to assess changes in the response of an animal to an external factor, such as thermal or mechanical stimuli, initiating pain **(Figure 1.3)**. These techniques allow measurement of hypersensitivity to a set stimulus (i.e. mechanical allodynia and hyperalgesia) [255] and have been employed in a variety of studies to confirm pain development in pre-clinical models of chronic pain, including rodent models of endometriosis. Mechanical allodynia and hyperalgesia have been demonstrated using a variety of techniques in both rat and mouse models of endometriosis. For example, mechanical allodynia has been demonstrated in endometriosis mice by measuring abdominal and hind paw withdrawal thresholds to von Frey hair (vfh) filaments [256-258], with an earlier withdrawal reflex indicating the development of hypersensitivity to a mechanical stimulus. Various groups have also demonstrated the development of vaginal mechanical hypersensitivity (both allodynia and hyperalgesia) in rodent models of

endometriosis by measuring the escape response or visceromotor response (VMR) to vaginal distension [92, 115, 125, 186, 259].

The development of widespread visceral pain in rodent models of endometriosis has also been demonstrated, with colonic distension resulting in an increased abdominal withdrawal reflex compared to Sham [260]. In addition, endometriosis-induced cutaneous thermal hypersensitivity has been demonstrated using both the hot plate and tail flick test, with reduced reaction latency demonstrating a developed sensitivity to noxious thermal stimuli [183, 261, 262]. In a similar way, cold sensitivity has also been demonstrated using the acetone test [256].

Importantly, these evoked response measurements have served to successfully indicate changes in visceral and cutaneous sensitivity to nociceptive stimuli, allowing researchers to test potential therapeutics to target these 'pain-like' responses associated with endometriosis [256-259, 261, 262].

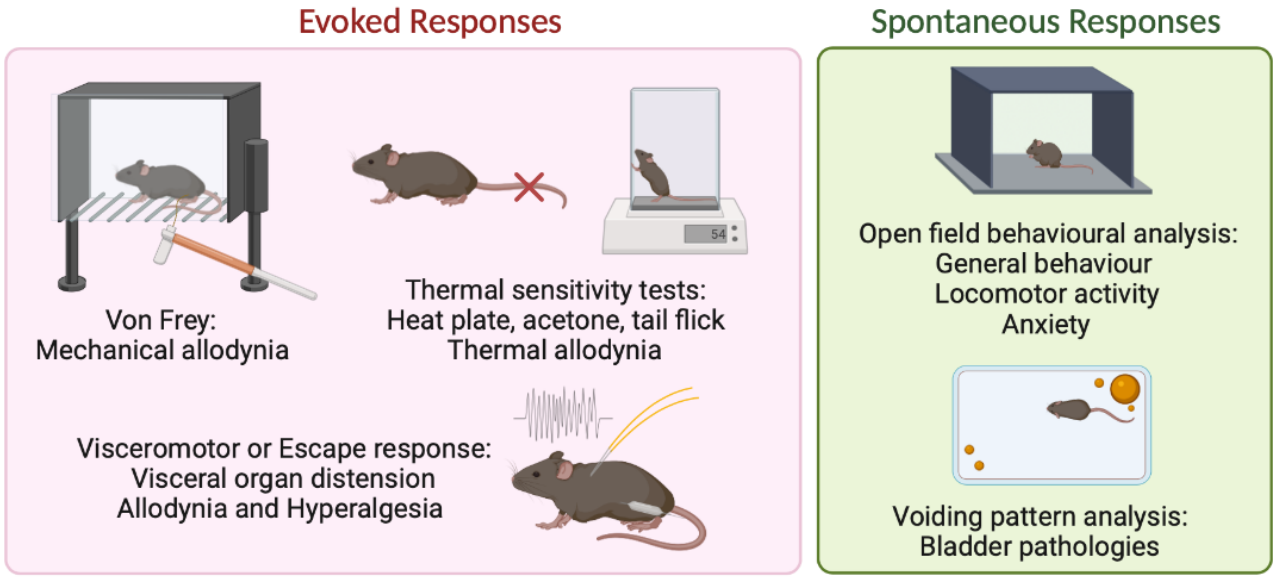

Figure 1.3: Experimental techniques used to measure alterations in evoked and spontaneous behavioural responses.

Evoked behavioural response techniques include von Frey analysis to measure mechanical allodynia, thermal sensitivity tests including the use of a heat plate, acetone administration or tail flick testing as an indication of the development of thermal allodynia. Visceromotor or escape measurements in response to visceral organ distension, such as the vagina and colon, gives an indication of the development of allodynia and hyperalgesia associated with visceral hypersensitivity. Spontaneous response techniques include open field behavioural analysis, allowing measurement of general behaviours, locomotor activity and can give an indication of the development of psychological conditions such as anxiety. Voiding pattern analysis gives an indication of the development of comorbid bladder pathologies. Figure created with BioRender.com.

1.5.3.2 Spontaneous responses

Spontaneous behavioural responses are assessed by monitoring spontaneous behaviours to a set of non-invasive parameters **(Figure 1.3)**. Changes in spontaneous behaviour can give an indication of pathophysiological changes and quality of life, which differ from those that are uncovered when considering evoked changes [263]. Although scarcely measured, spontaneous pain is suggested to be the best predictor of overall pain [255, 263]. While limited spontaneous measurements in endometriosis models have been reported, when included, endometriosis mice do demonstrate altered behavioural responses to non-evoked techniques. For example, increased abdominal licking and reduced tunnel entries have been observed in a mouse model of endometriosis [257] as well as the development of anxiety-related behaviour by 6 weeks of endometriosis development [183]. In these experiments, open field testing was used as a measure of general activity and anxiety related behaviours, recognising reduced time and distance spent within a central area, known as an aversive place, seen in endometriosis mice [183]. Spontaneous voiding pattern analysis can also present indications of bladder comorbidities associated with bladder pathologies, such as overactive bladder (OAB) and IC/PBS [110, 264], although this has not yet been utilised in pre-clinical models of endometriosis. While some behavioural changes are apparent using these techniques following endometriosis development, many studies don't address these parameters, and combining both evoked and spontaneous behavioural experiments would help provide a more complete profile of endometriosis related changes.

1.5.4 Clinically relevant animal models of endometriosis for the study of chronic pelvic pain: a present challenge

Small animal models of endometriosis show great promise as pre-clinical tools to investigate the mechanisms of CPP in endometriosis. As demonstrated using established behavioural techniques, there are some clear signs that these animal models recapitulate many pain attributes seen in women with endometriosis. Unfortunately, developing and characterising these animal models as models that recapitulate multiple pain symptoms associated with endometriosis is not apparent at an extensive level. With a preference for behavioural studies performed in rats current research in mice is underdeveloped. In addition, studies often employ only one or two behavioural techniques focused on an area of interest, rather than using multiple techniques to uncover altered pain responses in diverse and unrelated areas. This multifaceted approach is important for the study of pain mechanisms in a disease that can induce pain across multiple sites and organs. Evoked pain responses form the majority of pain related testing in endometriosis models, leaving non-evoked methods, which are suggested to be a better predictor of overall pain, lacking.

When considering the possible mechanisms of pain development and maintenance in endometriosis, it is crucial to consider the complex combination of disease progression with chronic

disease establishment. Currently, the timing of many behavioural studies is limiting, with studies completed during the early weeks of endometriosis induction preferentially reflecting early disease development. Although this is helpful to uncover early mechanisms, as a chronic disease with years of development preceding diagnosis in most cases, the mechanisms by which endometriosis can induce CPP may reflect a different phase of disease than during early development. As such, it is important to consider whether CPP remains during later stages of disease development in animal models of endometriosis.

Completing an extensive characterisation of pain across both spontaneous and evoked behaviours would allow us to address the combination of complex features and comorbidities experienced by women [254]. In addition, chronic progression of disease allows for complicated mechanistic progression, and looking at later time points may provide a more relevant indication of chronic pain mechanisms [250]. With an extensive list of possible mechanisms involved in chronic pain development [231], a reproducible pre-clinical model of endometriosis that exhibits multiple altered pain-like behaviours reflective of the human disease is fundamental to the progression of CPP in endometriosis research.

GENERAL HYPOTHESES AND AIMS

The importance of understanding mechanisms of chronic pelvic pain generation in endometriosis is apparent, with limited therapeutic treatments available for women that suffer from this debilitating disease. The need for pre-clinical models of endometriosis that recapitulate a wide spectrum of clinical symptomology is a vital step in advancing knowledge in this area. Ultimately, pre-clinical models will provide a platform to elucidate mechanisms of pain generation in endometriosis and importantly, offer a medium for pre-clinical testing of targeted treatment options.

To this end, the work presented in this thesis is directed towards the following key aims:

Aim 1: Develop and characterise two mouse models of endometriosis that experiences chronic pelvic pain across multiple visceral organs.

Aim 2: Elucidate the role of voltage gated sodium channels in sensation arising from the female reproductive tract and, using a mouse model of endometriosis, determine whether they may be involved in CPP developed in endometriosis.

Aim 3: Determine whether peritoneal fluid alone can directly activate sensory neurons and whether the aberrant peritoneal fluid from both mice and women with endometriosis may differentially activate sensory neurons.

CHAPTER 2: A MOUSE MODEL OF ENDOMETRIOSIS THAT DISPLAYS VAGINAL, COLON, CUTANEOUS AND BLADDER SENSORY CO-MORBIDITIES.

2.1 Statement of Authorship

With permission from all authors, this chapter includes an earlier version of work found in the following publication:

Publication: Castro, J*., **J. Maddern***, L. Grundy, J. Manavis, A. M. Harrington, G. Schober and S. M. Brierley (2021). "A mouse model of endometriosis that displays vaginal, colon, cutaneous, and bladder sensory comorbidities." FASEB J 35(4): e21430. *Contributed equally to this work.

Parts of this chapter were presented in poster format at the 14th World Congress of Endometriosis and in abstract format in the Australian Pain Society Newsletter – Special Edition (volume 40, issue 4, May 2020).

Students' contribution to publication:

J. Maddern: Involved in experimental design. Performed surgical procedures and endometriosis progression analysis. Designed and performed *in vivo* behavioural experiments, including data analysis, interpretation, and preparation of figures. Contributed to manuscript writing and editing.

Estimated overall percentage contribution: 50%

Co-author contributions:

Dr J. Castro*: Involved in experimental design and performed surgical procedures. Contributed to data analysis, figure preparation, writing and editing of the manuscript. Provided supervision and expert advice. Corresponding author.

Dr. L. Grundy and Dr. A. M. Harrington: Reviewed manuscript and provided expert advice.

J. Manavis: Designed and performed immunohistochemical staining of slides for analysis.

Dr. G Schober: Performed behavioural box experiments. Reviewed manuscript and provided expert advice.

Prof. S. Brierley: Provided expert advice, assisted with experimental design, supervision, and interpretation of data. Contributed with manuscript writing, editing and figure layout.

Acknowledgements: T. Patton, J. Abramovitch and C. Osborne from Crux Biolab for running Quantibody Mouse Array for cytokine analysis.

2.2 Overview

Animal models that recapitulate the features and symptoms experienced by women with endometriosis are essential for investigating the aetiology of endometriosis, as well as developing new treatments. This chapter describes a comprehensive characterization of a transplant mouse model of endometriosis, aimed at evaluating similar clinical features and symptoms to those experienced by women with endometriosis. In this study, we developed and characterized an autologous mouse model of endometriosis to examine a combination of disease features and symptoms including: (1) a 10-week time course of endometriotic lesion development; (2) the chronic inflammatory environment within the peritoneal fluid and development of neuroangiogenesis within lesions; (3) sensory hypersensitivity and altered evoked pain response to vaginal, colon, bladder, and skin stimulation; and (4) spontaneous animal behaviour.

2.3 Introduction

As a complex inflammatory disease, studies into the aetiology of endometriosis rely on pre-clinical animal models. The autologous transplant model of endometriosis, first reported by Vernon and Wilson in rats, successfully developed endometriotic lesion growth following autologous uterine horn tissue transplantation to the mesentery and utero-ovarian ligament [251]. Lesions grew rapidly over the first 30 days and were structurally similar to lesions collected from women with endometriosis, containing endometrial glands and stroma [251]. More recently, this model has been successfully achieved in mice, with lesion growth monitored up to 8 weeks post endometriosis induction [238]. The success of this model has led to adaptations, including uterine tissue transplantation to various sites throughout the abdomen, peritoneal wall and ovaries. This model has been used to study therapeutic effects on lesion growth and development [92, 265, 266], infertility [246, 251], and the replication of site specific endometriosis models [267].

The autologous transplant model has recapitulated many of the chronic features developed in patients with endometriosis. It is well documented that the peritoneal fluid (PF) of women with endometriosis facilitates a pro-inflammatory environment [81, 96-98]. The development of this pro-inflammatory environment is important in the study of pain, with the chronic inflammatory milieu being linked to the generation of pain in women [54]. Similar to humans, increased inflammatory cytokines have been found in the transplant mouse model of endometriosis during lesion development [118]. Moreover, establishment of blood vessels and sensory nerves (neuroangiogenesis), which is known to be another key player in the transmission of pain in women with endometriosis [78, 126-129], has been identified within transplanted lesions [115, 268]. Key neuroangiogenic factors, including vascular endothelial growth factor (VEGF) and nerve growth factor (NGF), have also been detected in mice with endometriosis, including within cultured PF [118] as well as endometrial lesions themselves [269].

Despite these advances, little progress has been made in understanding the aetiology of CPP associated with endometriosis [270, 271]. Preclinical models of endometriosis have shown that rats develop bladder and vaginal hypersensitivity up to 13 weeks following autologous transplantation of uterine horns onto the intestinal mesenteric cascade [92, 186, 259, 272]. Moreover, nociceptive sensitivity was found to be esterous cycle dependant in rats [92, 259, 273]. However, whether the transplant mouse model of endometriosis develops both spontaneous or evoked CPP, across multiple organs, has not yet been established. There is little to no information addressing the time course for lesion progression or the development of a chronic inflammatory environment in mice using the autologous transplantation model of endometriosis. Whether individual mice with endometriosis experience pain across multiple organs, such as the vagina, colon, bladder and skin, is also unknown. With comorbidities affecting most women with endometriosis, developing and characterising multifaceted co-morbid pain in a pre-clinical model

that recapitulates the complex disease heterogeneity, is a key first step to better understanding endometriosis associated CPP.

With this in mind, the aims of this study were: 1) To establish chronic lesion development in an autologous transplant mouse model of endometriosis, tracking lesion growth in the small intestinal mesentery and alongside the uterus over a 10 week period; 2) to determine whether the chronic inflammatory environment and established neuroangiogenesis seen in this pre-clinical endometriosis model mimics that seen in patients; and 3) to ascertain whether these mice experience widespread chronic hypersensitivity and altered pain responses, evident in both evoked and spontaneous pain like behaviours, across various organs, *in vivo*.

2.4 Materials and Methods

2.4.1 Animals

The Animal Ethics Committee of the South Australian Health and Medical Research Institute (SAHMRI) approved all experiments involving animals (ethics number SAM342). All animal experiments conformed to the relevant regulatory standards and the ARRIVE guidelines. Female C57BL/6J mice at 6 weeks of age were used and acquired from an in-house C57BL/6J breeding programme (Jax strain #000664; originally purchased from The Jackson Laboratory (breeding barn MP14; Bar Harbor, ME; USA) within SAHMRI's specific and opportunistic pathogen-free animal care facility. All female mice use in this study were virgin (never been mated) and housed in the absence of males from weening. Vaginal lavage or other cytology test to confirm cycle stage were not performed, but it has been reported that an extended absence of male pheromones leads to a state of anestrous (lee-boot effect) [274]. Mice were individually housed following surgery within individually ventilated cages (IVC) filled with coarse chip dust-free aspen bedding (PURA®; Cat# – ASPJMAEB-CA, Niederglatt, Switzerland). Animal cages were stored on IVC racks in housing rooms within a humidity and temperature-controlled environment, maintaining 22±1 °C and a 12 h light/12 h dark cycle. Mice had free access to LabDiet® JL Rat and Mouse/Auto6F chow (Cat# 5K52, St. Louis, MO; USA) and were provided with autoclaved reverse osmosis purified water.

2.4.2 Development of an autologous mouse model of surgically induced endometriosis

In this study, we used an adapted version of the previously established autologous mouse model of surgically induced endometriosis. This model was first developed in the rat [251] and later transferred to the mouse [275]. A schematic representation showing timelines for different

interventions is shown in **Figure 2.1**. In addition to uterine horn fragments being sutured onto the intestinal mesentery **(Figure 2.2A)**, as previously described [275], two uterine horn fragments were also sutured alongside the uterus of ovariectomised mice. A total of 182 mice were used in this study (N = 64 Sham mice and N = 118 Endo mice)

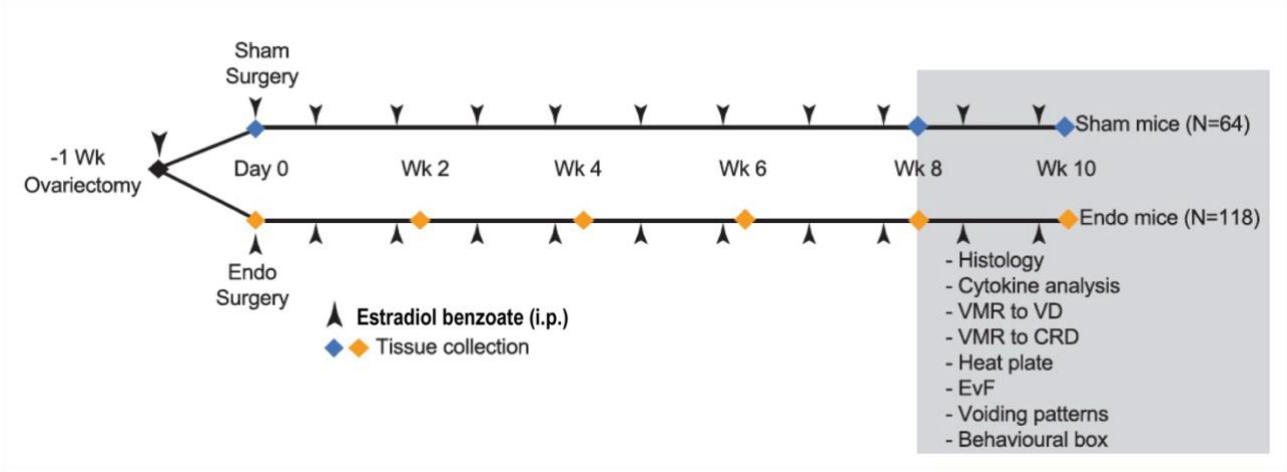

Figure 2.1: Schematic diagram showing timeline for different interventions performed in this study.

Schematic representation showing timelines for different interventions performed throughout this study. Mice were ovariectomised one-week (-1 wk) prior to auto-transplantation of uterine horns fragments (Endo surgery) or fat (Sham surgery), which constitutes day 0 of the model. The total number of mice used for this study was N = 64 Sham mice and N = 118 Endo mice. All mice were injected weekly with intraperitoneal (i.p.) estradiol benzoate to maintain steady levels of circulating estrogen (vertical ticks). Uterine horn fragments (orange diamonds) and fat tissue (blue diamonds) used for transplantation were collected at day 0 and used as baseline for lesion development. Endometriotic lesions developed in Endo mice were collected every 2 weeks throughout a 10-week period, whilst fat tissue transplanted on Sham mice was collected at week 8-10 post-surgery. Histological characterisation of endometriotic lesions (for Endo mice) or fat tissue (for Sham mice), was performed in mice with fully developed endometriosis (weeks 8-10 post-transplant, shaded box). Cytokine analysis and *in vivo* pain assessment studies, comparing Sham and Endo mice, were performed between weeks 8-10 post-transplant (shaded box).

2.4.2.1 Ovariectomy surgery

Seven days prior to surgical induction of endometriosis, female mice were ovariectomised in order to deplete endogenous steroid production. Briefly, at 6-8 weeks of age, mice were anesthetized under isoflurane (2.5%/0.5 L O_2) and given a low dose (0.05 mg/kg) of analgesic buprenorphine prior to the commencement of surgery. Following aseptic conditions, a small longitudinal paralumbar incision of the skin and dorsal abdominal muscle was performed to expose the ovaries on either side. Ovaries were exteriorised and oviduct/ovarian artery and vein/ovarian ligaments were severed using cauterisation. The reproductive tract was returned to the abdominal cavity and abdominal muscles sutured using sterile absorbable 6.0 suture material. The superficial skin layer was then

closed using 9 mm clips (AutoClip® System, FST). Ovariectomised mice were allowed to recover for a minimum of 5 days before removal of surgical clips. As endometriosis is an estrogen dependant disease, it is important to maintain steady levels of circulating estrogen and minimize any difference related to the stage of the estrous cycle [276]. All mice were given an intraperitoneal injection of 100 µg/kg estradiol benzoate (or Progynon-B) following ovariectomy [276, 277].

2.4.2.2 Endometriosis (Endo) and Sham surgeries

Seven days after ovariectomy and estradiol benzoate injection, mice were surgically induced with endometriosis. For this, mice were anesthetized under isoflurane and given a low dose (0.05 mg/kg) of analgesic buprenorphine prior to the commencement of surgery. Following aseptic conditions, a small midline abdominal incision was made to expose the abdominal cavity. Each uterine horn was exposed allowing the proximal and distal ends to be ligated with 6.0 Prolene sutures to occlude blood supply. Both uterine horns were tied off and cut as close as possible to the body of the uterus to ensure minimal eutopic endometrial tissue remained. Uterine horns were then excised and pinned out in a dissecting dish with ice-cold sterile phosphate buffered saline (PBS) containing penicillin (100 U/ml) and streptomycin (100 µg/ml) (Sigma-Aldrich, St. Louis, MO). Uterine horns were longitudinally opened, with 5 x 2 mm sections of uterine horn tissue removed using a 2 mm biopsy punch (Kai medical, KAI00010). Three circular fragments (2 mm diameter) of uterine horn tissue were sutured on alternate mesenteric cascade arteries (approximately 0.5 cm from the bowel) that supply the small intestine using 6.0 Prolene sutures (Figure 2.2A); the remaining 2 circular fragments (2 mm diameter) were sutured on either side of the uterus (similarly sized pieces of abdominal fat were sutured during Sham surgeries). Any remaining uterine horn tissue left in the dissecting dish after biopsy sections were removed was disposed of. This consisted of irregular pieces (have different sizes/shapes/weights to the ones auto transplanted). After ensuring that all of the organs were appropriately back to their anatomical position, the wound was closed, with muscle and skin sutured separately. In order to maintain steady levels of circulating estrogen and minimize any difference related to the stage of the estrous cycle, all mice were given an intraperitoneal injection of 100 µg/kg estradiol benzoate (or Progynon-B) immediately after surgery, and once a week for up to 10 weeks. Throughout the surgery and during the recovery period, animals were positioned on a heating mat to maintain body temperature. During recovery from surgery, animals were monitored daily for complications. No signs of distress or unusual pain behaviours were observed. Circular uterine horns fragments (2 mm), collected with a biopsy punch, from 5 separate ovariectomised and estradiol benzoate treated animals were used as controls to estimate lesions' size and weight at Day 0.

2.4.3 Characterization of endometriosis development

Endometrial cysts growing from the auto-transplanted uterine horns fragments were collected and measured every 2 weeks, from 2-10 weeks post-surgery to track endometriosis lesions development. A schematic representation showing timeline for different interventions is shown in **Figure 2.1**.

2.4.3.1 Collection of endometriotic lesions and peritoneal fluid

Lesions/fat tissue were located, counted, dissected, measured, and weighed post-mortem from a total of 33 mice. Up to 5 endometriosis lesions were collected from each mouse (3 x mesenteric and 2 x uterine lesions). Lesions that were damaged during dissection, or could not be cleanly separated from surrounding tissue, were not included in lesion growth analysis. Measurements at the largest point of the lesion were taken using callipers (Castroviejo callipers 8.5 cm / 3-1/4"). Lesions were then snap frozen in liquid nitrogen and stored at -80°C or stored at 4°C in 4% paraformaldehyde (PFA) for subsequent paraffin embedding. Overall, cyst anatomy, as well as identification of inflammation and neuroangiogenesis within the cysts, were performed as described below. In addition to collecting cysts/fat tissue from Endo and Sham mice respectively, we collected uterine horns from 5 mice, 7 days post-ovariectomy and estradiol benzoate injection (to ensure high circulating levels of estrogen). Biopsies punch fragments (2 mm) obtained from this tissue were used as baseline (Day 0) for the size and weight parameters assessed in **Figure** 3.2**C**.

In addition to endometriotic lesions, peritoneal fluid (PF) was taken on week 8-10 post-surgery to assess inflammation in mice with fully developed endometriosis versus Sham animals. To do this, mice were anesthetized under isoflurane (2.5%/0.5 L O_2) and a small incision was made on the midline and into the peritoneal cavity of each individual mouse. 200 µl of sterile saline was injected into the peritoneal cavity, and the abdomen was gently massaged to distribute the saline within the peritoneal cavity. A larger incision was made to expose the peritoneal cavity and approximately 100 µl of the resultant PF was immediately collected, snap frozen in liquid nitrogen and stored at -80^{o}C for future analysis. Care was taken not to disrupt any peritoneal organs. Samples that were contaminated with blood from surgical incision were excluded.

2.4.3.2 Characterization of endometriosis lesion anatomy

As endometriosis is diagnosed by the growth of endometrial tissue, containing endometrial glands and stroma, outside of the uterus [207], we used haematoxylin and eosin (H&E) staining to confirm lesions were endometrial in nature. For this, a subset of lesions (for Endo mice) or fat tissue (for Sham mice) were collected at 8-10 weeks post-surgery and fixed in 4% PFA for 24 hours, rinsed and transferred to 70% ethanol before being embedded in paraffin. Paraffin blocks were cut in 10 µm sections and subsequently stained with H&E by the University of Adelaide Histology Core Facility (Adelaide, South Australia). Slides were imaged using brightfield settings with an automated digital slide scanner (Pannoramic slide scanner, 3DHISTECH Ltd, Budapest, Hungary). Biopsies that did

not contain the morphology of endometrium were not included for any further neuroangiogenesis analysis.

2.4.3.3 Characterization of neuroangiogenesis developed within endometriosis lesions

To confirm endometrial lesions contained nerve growth, another set of sections were stained with Protein Gene Product 9.5 (PGP9.5), a neural/nerve sheath marker. We used a mouse monoclonal anti PGP9.5 antibody (clone 3A13, Novus Biologicals, USA, Code # NB600-1160) and followed a standard streptavidin-biotinylated immuno-peroxidase technique, as previously described [278]. In brief, paraffin sections were dewaxed using xylene and then rehydrated through alcohols. Sections were then treated with methanol/H_2O_2 for 30 min. Next, the sections were rinsed twice in PBS (pH 7.4) for a further 5 min each wash. Antigen retrieval was then performed using citrate buffer (pH 6.0). Slides were allowed to cool and washed twice in PBS (pH 7.4). Non-specific proteins were blocked using normal horse serum for 30 min. The monoclonal PGP9.5 antibody was applied at a dilution of 1:2000 at room temperature overnight. Negative control slides, minus the primary antibody, were also run in parallel. The following day, sections were washed twice with PBS before the addition of a biotinylated anti-mouse secondary (Vector Laboratories, USA, Cat # BA-2000) for 30 min at room temperature. Following two PBS washes, slides were incubated for 1h at room temperature with streptavidin-conjugated horseradish peroxidase (HRP) (Pierce, USA, Cat # 21127). Sections were visualised using diaminobenzidine tetrahydrochloride (DAB), washed, counterstained with haematoxylin, dehydrated, cleared, and mounted on glass slides. Biopsies that did not contain the morphology of endometrium were not included for any further neuroangiogenesis analysis. Blood vessels were visually identified in both H&E and PGP9.5 stained sections. Slides were imaged using brightfield settings with an automated digital slide scanner (Pannoramic slide scanner, 3DHISTECH Ltd, Budapest, Hungary).

2.4.3.4 Quantification of inflammation.

The presence of inflammatory cytokines within peritoneal fluid samples of mice with fully developed endometriosis (8-10 weeks after transplant of uterine horns) was quantified using multiplex cytokine analysis with a custom Mouse 11-plex Array. Peritoneal fluid from donor mice, 7 days post-ovariectomy and estradiol treatment, was used to determine baseline cytokine levels (baseline). Snap frozen peritoneal fluid samples were defrosted and used directly for cytokine quantification.

A custom Quantibody Mouse Array (RayBiotech, Georgia, USA) was used to detect 11 analytes (GM-CSF, IL-1β, IL-6, IL-13, IL-17α, IL-33, MCP-1, RANTES, TNFα, β-NGF and VEGF) simultaneously, according to manufacturer's instructions, by Crux Biolab (Melbourne, Australia). Slides were scanned (GenePix400B Array Scanner (Micromon Genomics, Monash University, Australia)) and analysed using Genepix Pro (v4.0.0.54) acquisition software.

2.4.3.5 Lesion growth and inflammatory markers analysis

Weekly lesion growth in mice with endometriosis was normalised to the size of the original fragments of uterine horns transplanted at Day 0. Data are presented as mean ± standard error of the mean (SEM), N represents the number of animals and n represent the number of individual lesions per group. Data were graphed using Prism 8 software (GraphPad Software, San Diego, CA, USA), and analysed using one-way analysis of variance (ANOVA) with Turkeys multiple comparisons. Differences were considered statistically significant at $*P < 0.05$, $**P < 0.01$, $***P < 0.001$, $****P < 0.0001$.

Inflammatory markers detected on the multiplex array were graphed using Prism 8 software (GraphPad Software, San Diego, CA, USA). Data are presented as mean ± SEM, and N represents the number of animals. Data was statistically analysed using unpaired two-tailed Student *t* test with two tails for 2 groups of equal variances; or using the Mann-Whitney non-parametric test for 2 groups with unequal variances (specifics contained within respective figure legends). Differences were considered statistically significant at $*P < 0.05$, $**P < 0.01$, $***P < 0.001$, $****P < 0.0001$.

2.4.4 In vivo assessment of chronic pelvic pain by quantification of visceromotor responses (VMR).

The visceromotor response (VMR) is a nociceptive brainstem reflex consisting of the contraction of the abdominal muscles in response to noxious distension of hollow organs such as the vagina [92, 195, 220] and the colorectum [110, 157, 159, 161, 279-281]. We recorded the VMR to vaginal distension (VD) or colorectal distension (CRD) as an objective measurement of vaginal and colonic sensitivity to pain, respectively, in fully conscious animals [92, 115, 186, 195, 220, 273, 282]. VMR of mice with fully developed endometriosis (weeks 8-10 after uterine horn fragment transplant) was compared with the VMR of Sham animals (weeks 8-10 after Sham fat transplant). A total of 45 mice were used for the VMR assays (N = 21 for VMR to VD and 24 for VMR to CRD). All mice were studied 3 days post-estradiol administration (as schematised in **Figure 2.1**).

2.4.4.1 Surgical implantation of electromyography (EMG) electrodes

The VMR was objectively assessed by recording the electrical activity (electromyography (EMG)) produced by abdominal muscle contractions in response to non-noxious and noxious vaginal or colorectal distensions. Three days prior to the VMR and under isoflurane anaesthesia, the bare endings of two teflon-coated stainless-steel wires (Advent Research Materials Ltd, Oxford, UK) were sutured into the right external oblique abdominal muscle of Sham or endometriosis mice and tunnelled subcutaneously to be exteriorized at the base of the neck for future access. At the end of the surgery, mice received prophylactic antibiotic (Baytril®; 5 mg/kg s.c.) and analgesic

(buprenorphine; 0.5 mg/10 kg s.c.) and were returned to their individual housing and allowed to recover as previously described [220].

2.4.4.2 Assessing visceromotor responses (VMR) to vaginal distension (VD) or colorectal distension (CRD)

On the day of VMR assessment, mice were temporarily anaesthetized using inhaled isoflurane and a saline enema administered via catheter to either the colorectum (100 μL) or vaginal cavity (50 μL) and a balloon was inserted into either the colorectum or vaginal cavity for VMR assessment, as previously described [157, 159]. Briefly, a lubricated balloon was gently introduced through the anus and inserted into the colorectum up to 0.25 cm past the anal verge (2.5 cm length latex balloon) for CRD or gently passed through the vagina and inserted up to 1 mm proximal to the vaginal verge (3 mm length latex balloon) for VD. The balloon catheter was secured to the base of the tail with surgical tape and connected to a barostat (Isobar 3, G&J Electronics, Willowdale, Canada) for graded and pressure-controlled balloon distension. Mice were gently restrained in a mouse restrainer with dorsal access and allowed to recover from anaesthesia for 10 minutes prior to initiation of the distension sequence. Distension sequences were pre-set and applied at 20-30-40-60-70 mm Hg (20 seconds duration) at 4 minute-intervals for CRD or 20-30-40-60-70 mm Hg (30 seconds duration) applied at 3 minute-intervals for VD. The EMG electrodes were relayed to a data acquisition system and the signal was recorded (NL100AK headstage), amplified (NL104), filtered (NL 125/126, Neurolog, Digitimer Ltd, bandpass 50–5000 Hz) and digitized (CED 1401, Cambridge Electronic Design, Cambridge, UK) to a PC for off-line analysis using Spike2 (Cambridge Electronic Design), as previously described [157].

2.4.4.3 Statistical analysis of VMR to VD and CRD data

The analogue EMG signal was rectified and integrated. To quantify the magnitude of the VMR at each distension pressure, the area under the curve (AUC) during the distension (20 seconds for CRD or 30 seconds for VD) was corrected for the baseline activity (AUC pre-distension, 20 seconds for CRD or 30 seconds for VD). Total area under the curve was quantified by adding the individual AUC at each distension pressure, as previously described [159, 220]. VMR data are presented as mean ± SEM, and N represents the number of animals. Analysis and figures were prepared in GraphPad Prism software (Version 8, San Diego, CA, USA). VMR data were statistically analysed by generalised estimating equations (GEE) followed by least significant difference (LSD) post hoc test when appropriate using SPSS 23.0. Differences were considered statistically significant at $*P < 0.05$, $**P < 0.01$, $***P < 0.001$, $****P < 0.0001$.

2.4.5 *In vivo* assessment of cutaneous sensitivity to thermal and mechanical stimuli.

The hot plate test is a popular test using thermal stimulation to measure acute thermal nociception by monitoring reflexive behaviours to thermal stimuli [283, 284]. The Electronic von Frey (EvF) test is used to assess mechanical allodynia to mechanical stimuli by measuring the withdrawal to a stimulus that is not normally painful [284]. Utilising these non-invasive tests, we determined any changes in the threshold or sensitivity to pain in mice with fully developed endometriosis (weeks 8-10 after uterine horn fragment transplant), compared to Sham animals (weeks 8-10 after fat transplant). A total of 50 mice were used (N = 31 for hot test plate and 19 for EvF). All mice were studied 3 days post-estradiol administration (as schematised in Figure 2.1).

2.4.5.1 Assessing cutaneous sensitivity to noxious thermal stimuli with hot plate latency.

Mice were moved to the testing room in their IVC and allowed to acclimatize for a minimum of 15 minutes. Mice were individually placed on a preheated hot plate (LE7406, Harvard Apparatus, Panlab, Spain), set at 54 ± 1°C, which is shown to be a noxious stimuli [284], and surrounded by a clear methacrylate protection casing. The time between being placed on the hot plate and their first sign of pain response, including hind paw licking, hind paw flicking, or jumping (whichever comes first), was recorded as their hot plate latency. Mice were allowed to recover in their cage for 24 hours, and the test was repeated. The average response latency of both tests was recorded as their final hot plate latency. Mice were returned to their home cage and were used for further behavioural measurements.

2.4.5.2 Assessing cutaneous sensitivity to mechanical stimuli with electronic von Frey (EvF) reflex.

Before EvF testing, mice were habituated to the enclosure made of clear Plexiglas (observation chamber approx. 230x240x146 mm, BSBIOPVF, Panlab, Spain) and placed on an elevated wire mesh stand, for 30 minutes each day, over 2 days. On the day of testing, at 8 weeks post-surgery and 3 days post-estradiol administration, mice were moved to the testing room in their IVC and allowed to acclimatize for a minimum of 15 minutes. Animals were individually placed into the testing arenas, with an aerated lid placed on top, and left undisturbed for 15 minutes. The EvF unit (hand-held force transducer, BSBIOEVF4s, Panlab, Spain) was fitted with a semi-flexible tip and zeroed. Once the animal was still and quiet, the force transducer was applied perpendicularly to the animal's hind paw or lower abdomen, from below. Force was gradually and linearly increased until a clear withdrawal response, such as hind paw retraction, hind paw licking, or abdominal retraction or licking was observed. The maximum force applied (in grams) that elicited the paw or abdominal withdrawal was noted as the withdrawal threshold. Each area was stimulated 5 times, with the average recorded as the experimental withdrawal threshold for each mouse. To ensure consistency and reduce bias, the same investigator carried out all measurements in a blinded fashion. At the end of testing, mice were returned to their home cage and returned to their IVC rack.

2.4.5.3 Statistical analysis of cutaneous sensitivity to thermal and mechanical stimuli

The average response, in seconds, was taken from both exposures to the heat plate and the average force in grams required to elicit a withdrawal response using EvF, was recorded for analysis. Data are presented as mean ± SEM, and N represents the number of animals. Data were statistically analysed using Prism 8 software (GraphPad Software, San Diego, CA, USA) and were analysed using unpaired two-tailed Student *t* test with two tails for two groups of equal variances; or the using the Mann-Whitney non-parametric test for two groups with unequal variances. Differences were considered statistically significant at $*P < 0.05$, $**P < 0.01$, $***P < 0.001$, $****P < 0.0001$.

2.4.6 *In vivo* assessment of bladder dysfunction by voiding pattern analysis.

Voiding pattern analysis is a micturition assessment tool that provides information about changes in spontaneous behavioural patterns related to urinary tract pathologies, including overactive bladder (OAB) and interstitial cystitis/painful bladder syndrome (IC/PBS) [110, 264]. Voiding pattern analysis was performed as previously described for assessing changes in bladder function [110]. Voiding pattern of mice with fully developed endometriosis (weeks 8-10 after uterine horn fragment transplant) was compared with the voiding pattern of Sham animals (weeks 8-10 after Sham fat transplant). A total of 22 mice were used in this study (N = 11 Sham mice and N = 11 Endo mice). To minimise the impact of estrogen on voiding function, all experiments were performed 3 days post-estradiol administration (as schematised in **Figure 2.1**).

2.4.6.1 Voiding pattern collection assay

Filter paper for voiding pattern analysis was collected from mice immediately prior to Sham or Endo induction surgery and at 8 weeks post-surgery. In order to minimise changes to their environment, bedding was removed from Endo and Sham mice home IVC and filter paper positioned on the bottom of their cage. Mice remained in their lined cages for 3 hours, between 9 AM and 12 PM, with free access to food and water. Filter paper was collected and stored for imaging and bedding was returned to IVCs.

2.4.6.2 Voiding pattern imaging and analysis

Filter paper was imaged using an ultraviolet trans-illuminator (Bio-Rad, California, USA) and digitised into binary images using ImageJ software (NIH, ImageJ, 2.0.0). The number and size of urine spots was determined using pre-set thresholds within ImageJ software, and for the purposes of this study, the number of small (100-1000 pixels), medium (1001-100 000 pixels) and large (>100 000 pixels) spots were quantified. The change in total spots from day 0 to week 8 was quantified for both Sham and Endo mice.

Data are presented as mean ± SEM, and N represents the number of animals. Data were graphed using Prism 8 software (GraphPad Software, San Diego, CA, USA) and, where appropriate, were analysed using unpaired two-tailed Student *t* test with two tails for two groups of equal variances; or the using the Mann-Whitney non-parametric test for two groups with unequal variances. Two-way ANOVA followed by Bonferroni's multiple comparison post-hoc test was used to compare between more than two groups. Differences were considered statistically significant at $*P < 0.05$, $**P < 0.01$, $***P < 0.001$, $****P < 0.0001$.

2.4.7 In vivo assessment of spontaneous behaviour and locomotor activity:

Studies recording the spontaneous behaviour of mice in a behavioural spectrometer have been used to assess whether mice exhibit chronic pain-like behaviours, *in vivo* [159, 284]. The behavioural spectrometer is used to record spontaneous behaviour (23 different parameters automatically calculated by the behavioural spectrometer) in freely moving mice. We used the behavioural spectrometer to determine any differences in spontaneous behaviour in the absence of a stimulus, in both Endo and Sham mice. Behaviour of mice with fully developed endometriosis (weeks 8-10 after uterine horn fragment transplant) was compared with the behaviour of Sham animals (weeks 8-10 after Sham fat transplant). All mice were studied 3 days post-estradiol administration to minimise estrogen variation between time points.

2.4.7.1 Assessing spontaneous behaviour of Sham and Endo mice

Behavioral studies were performed as previously described [159]. Briefly, mice were transferred in their home cage to a temperature-controlled test room (24 ± 1^{o}C) and allowed to acclimatize for at least 10 minutes prior to testing. All experiments were performed during the light phase, between 1 PM and 5 PM each day. Assessment of locomotor activity and spontaneous behaviour in mice was evaluated using a behavioural spectrometer (Behavior Sequencer, Behavioral Instruments, NJ and BiObserve, DE) [159, 285].

For testing, Sham or Endo mice were individually placed in the centre of the behavioural spectrometer, and their behaviour was filmed/tracked and evaluated/analyzed by a computerized video tracking software (Viewer^{3}, BiObserve, DE) for 20 minutes. Evaluation of the total distance traveled in the open field (in cm), average velocity of locomotion (in cm/sec), time spent in the central area (20 x 20 cm; in sec), wall distance (in cm) and the time spent (in sec) on different behavioral patterns including grooming, orienting, rearing, scratching, and forms of locomotion was obtained. An independent experimenter performed all sessions. Testing was conducted in an order counterbalanced for experimental group and returned to their home cage following behavioural monitoring. Reported measurements occurred over 20 minutes after placement within the behavioural spectrometer. Between mice, the apparatus was cleaned thoroughly with a disinfectant

(F10 SC veterinary solution) to remove smell and excrement from previous mice. A total of 32 mice were used in this study (N = 17 Sham mice and N = 15 Endo mice).

2.4.7.2 Statistical analysis of behavioural spectrometer data

Normality of the data was assessed using the Shapiro-Wilk test prior to statistical analysis. Data represent mean ± SEM and were analysed with unpaired two-tailed Student *t* tests, using Prism 8 software (GraphPad Software, San Diego, CA, USA). N represents the number of animals used. Differences were considered statistically significant at $*P < 0.05$, $**P < 0.01$, $***P < 0.001$, $****P < 0.0001$.

2.5 Results

2.5.1 Endometriotic lesion development in the autologous transplantation mouse model of endometriosis

In this study, we developed an autologous transplant model of endometriosis in mice and followed the growth of endometriotic lesions for 10 consecutive weeks, as schematically illustrated in **Figure 2.1**. We found that uterine tissue surgically transplanted onto the mesenteric arteries of the small intestine **(Figure 2.2A i)**, or alongside the uterus **(Figure 2.2A ii)**, developed into endometriotic lesions. Moreover, adhesions were commonly found at the site of lesion formation **(Figure 2.2A ii-iv)**. These adhesions were able to bind visceral organs together, including the small intestine with the caecum **(Figure 2.2A iii)** and the small intestine with the bladder/uterus **(Figure 2.2A iv)**. Sham surgery, where fat was surgically transplanted in place of uterine tissue, resulted in no endometrial lesion development 8-10 weeks after surgery **(Figure 2.2B i-ii)**. Moreover, no adhesions were found at the site of sutures in Sham mice. Additionally, using H&E staining, we found that the lesions developed on mice with endometriosis **(Figure 2.2C i)**, but not in Sham mice **(Figure 2.2C ii)**, displayed both endometrial glands and stroma. Furthermore, staining with cytokeratin revealed the presence of a well-defined pseudostratified glandular epithelium across the entire lumen of the gland, which is surrounded by cell-rich stroma **(Figure 2.2C iii)**. No cytokeratin staining was detected on tissue from Sham mice **(Figure 2.2C iv)**. Finally, we found that these endometrial lesions grew, increasing in size and weight over a period of 10 weeks, with significant growth seen from 6 weeks after transplantation **(Figure 2.2D i, ii)**. There was no difference in the body weight between mice with fully developed endometriosis and Sham mice (8-10 weeks after transplant) (Sham: 22.98 ± 0.42 g vs. Endo: 23.01 ± 0.44 g, ns, $P > 0.05$, unpaired *t* test).

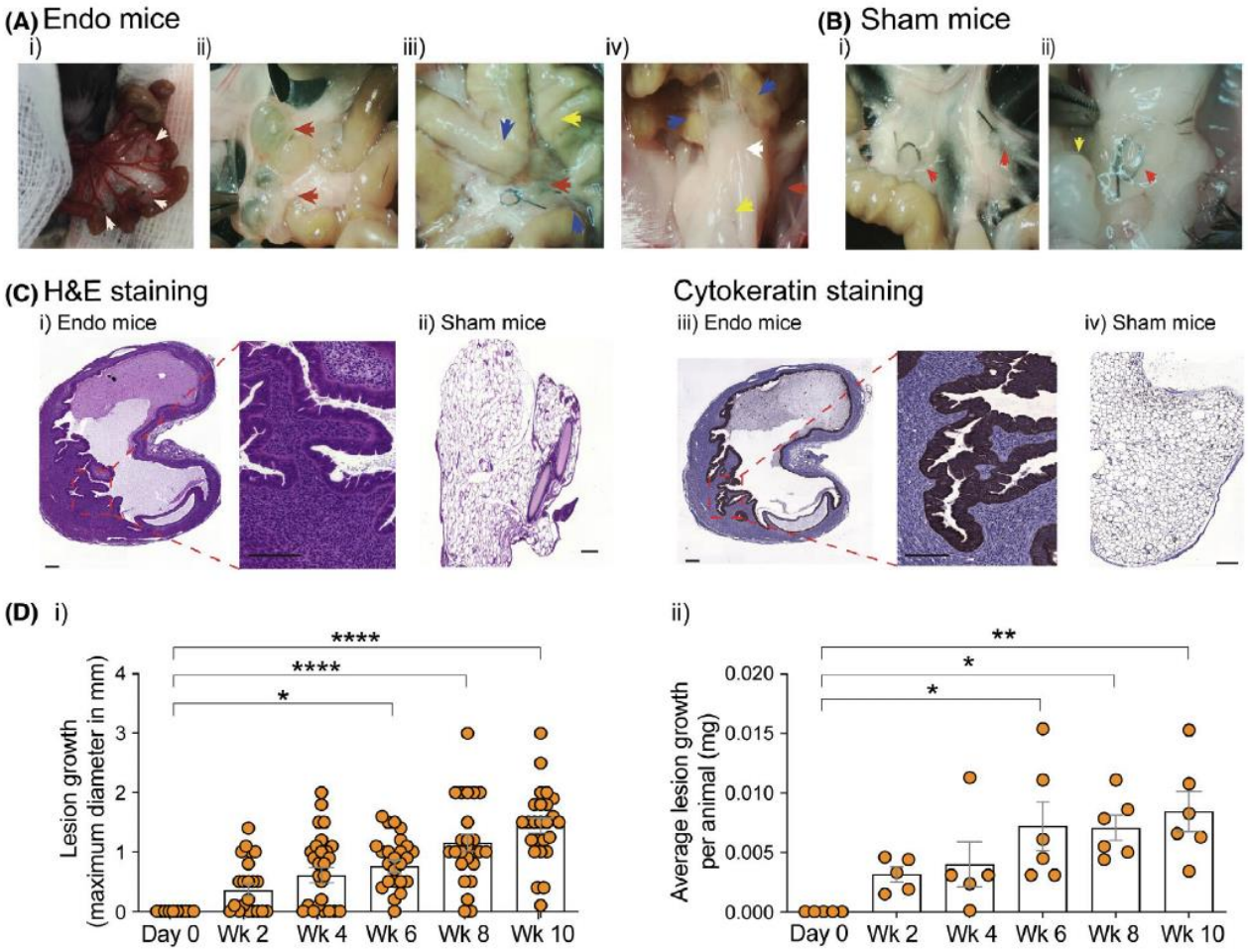

Figure 2.2: Transplantation of uterine horn fragments onto the small intestinal mesentery induces growth of endometriotic lesions *in vivo*.

(A) Representative images of endometriosis development induced by autologous transplant surgery of the mice' uterine horn fragments including **(i)** mesenteric arteries exteriorised and 3 uterine horn fragments transplanted during endometriosis surgery (white arrows); **(ii)** endometriotic lesions (red arrows) developed after 8-10 weeks post endometriosis induction; **(iii)** adhesions formed around a lesion (red arrows) resulting in fusion of the small intestine (blue arrows) with the caecum (yellow arrow). **(iv)** adhesions formed around a lesion (red arrows head) resulting in fusion of the small intestine (blue arrows) with the bladder (yellow arrows). **(B)** 8-10 weeks after fat tissue transplant, Sham mice do not develop lesions in either the **(i)** mesenteric cascade or **(ii)** adjacent to the uterus. **(C)** Histological representative images of lesions. Right panels **i)** and **iii)** show staining at higher magnification, all scale bars represent 200 mm. **(i)** H&E staining of an endometrial lesion collected at 8 weeks post endometriosis induction surgery show lesions contained both endometrial glands surrounded by cell-rich stroma. **(ii)** Transplant tissue collected from Sham mice do not display endometrial glands or stroma. **(iii)** Representative image of cytokeratin staining performed in another section from the same endometrial lesion shown in panel **(i)**, showing the presence of a well-defined pseudostratified glandular epithelium across the entire lumen of the gland, which is surrounded by cell-rich stroma. **(iv)** Transplant tissue collected from Sham mice do not display endometrial glands or stroma. **(D)** Grouped data showing growth of both **(i)** maximum individual mesenteric lesion diameter (mm) and **(ii)** average lesion weight per animal (mg) up to 10 weeks post endometriosis induction. Data represent mean ± SEM and normalised to growth from day 0. (*$P < 0.05$, **$P < 0.01$ ****$P < 0.0001$ one-way ANOVA with Tukey's multiple comparisons. Data was obtained from a total of 33 mice (N = 5 mice at weeks 0, 2 and 4 and N = 6 mice at weeks 6, 8 and 10 as indicated in panel **(D) ii)**. Additionally, panel **(D) i)** shows the maximum size of each individual lesion obtained from mice at each of the times points. A maximum of 5 lesions were harvested from each individual mouse, resulting in 10-29 lesions per time point. Wk: week.

2.5.2 Neuroangiogenesis and an inflammatory environment is evident in endometriotic lesions and peritoneal fluid

Sustained development and growth of endometriotic lesions, and the existence of an inflammatory environment, are suggested necessary features for the development and maintenance of CPP associated with endometriosis. Neuroangiogenesis is an important factor in this process, with the growth of both nerves and blood vessels known to be key contributors in the establishment of endometrial lesions. To investigate the possible presence of neurogenesis in our model, we performed immunohistochemical staining against PGP9.5 (a pan neuronal marker) **(Figure 2.3A)**. We found nerve fibres running throughout lesions collected from mice with fully developed endometriosis (weeks 8-10 after uterine horn fragments transplant) **(Figure 2.3A i)**, that were absent from lesions collected from Sham mice **(Figure 2.3A ii)**. Additionally, immunohistochemical staining for endothelial cells using CD31 identified blood vessels running throughout lesions collected from mice with fully developed endometriosis **(Figure 2.3B)**.

In addition to the identification of nerve fibres and blood vessels within the endometriosis lesions, which strongly indicate neuroangiogenesis is taking place within these lesions, we performed a multiplex-array to identify a subset of inflammatory mediators present in the peritoneal fluid of mice with fully developed endometriosis (8-10 weeks after uterine horn fragments transplant). Our results showed that the peritoneal fluid from animals with fully developed endometriosis, contained significatively elevated levels of the proinflammatory cytokines Interleukin 1 β (IL-β), Interleukin 33 (IL-33), Interleukin 17 (IL-17), and Interleukin 6 (IL-6) when compared to the peritoneal fluid of mice prior to endometriosis induction (Day 0) **(Figure 2.3C i-iv)**. Additionally, the angiogenic factor Vascular Endothelial Grow Factor (VEGF) was also found to be elevated within the peritoneal fluid of mice with fully developed endometriosis, compared to mice prior to endometriosis induction (Day 0) **(Figure 2.3C v)**. However, peritoneal fluid from mice with fully developed endometriosis did not exhibit significant differences in the levels of Tumour necrosis factor α (TNFα), Monocyte chemoattractant protein 1 (MCP-1), and Regulated on Activation, Normal T Cell Expressed and Secreted (RANTES), compared to mice prior to endometriosis induction (Day 0) **(Figure 2.3D i-iii)** Similarly, Beta-nerve growth factor precursor (β-NGF), Granulocyte-macrophage colony-stimulating factor (GM-CSF), and Interleukin-13 (IL-13); which despite being found close to the limit of detection for quantification, did not exhibit any significant changes in the peritoneal fluid of mice with fully developed endometriosis **(Figure 2.3D iv-vi)**.

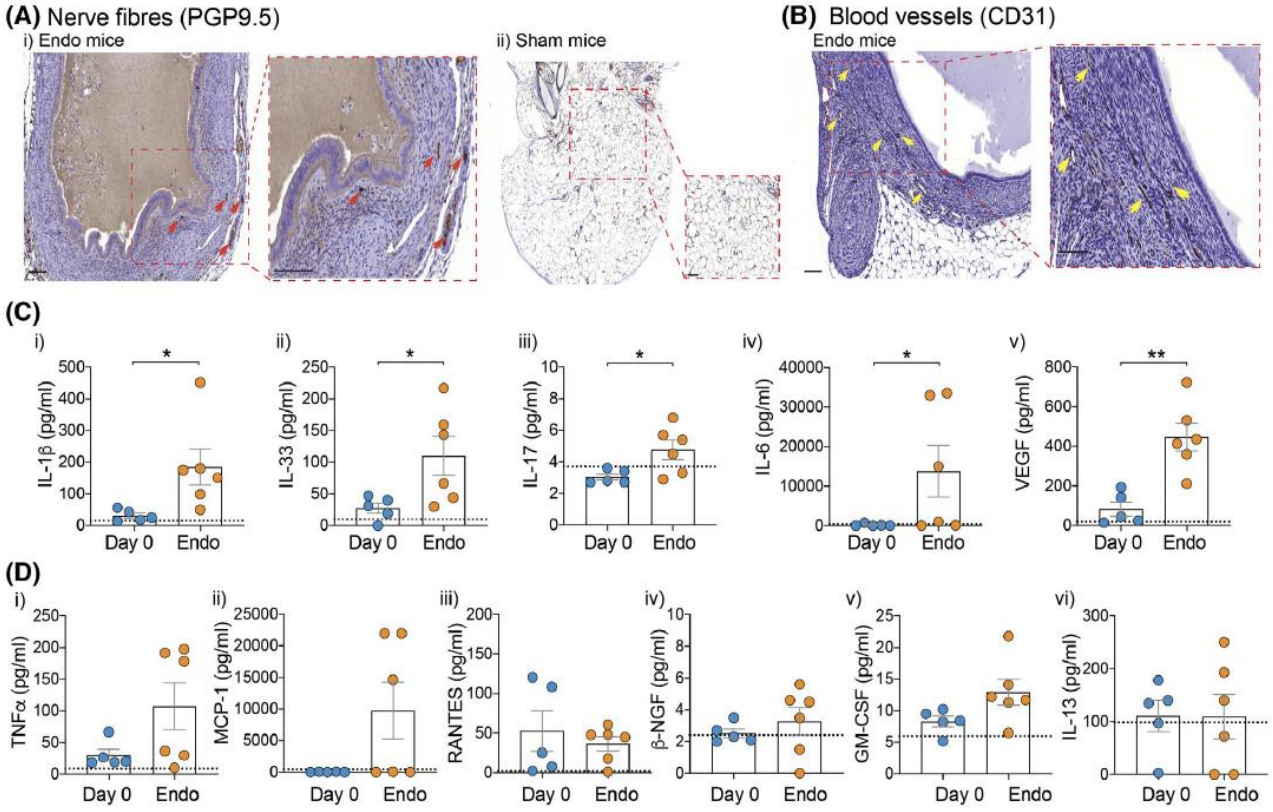

Figure 2.3: Neuroangiogenesis and inflammation in mice with endometriosis.

(A) i) Representative image taken from a paraffin embedded section of a fully developed endometriosis lesion (Endo mice, 8-10 weeks after uterine horn fragments transplant), showing immunohistochemical staining again PGP9.5. Nerve bundles that can be seen running in parallel or perpendicular to the plane of view are shown by red arrows. A zoomed area displayed in the right panel shows nerve bundles at higher magnification (red arrows). Scale bars represent 100 μm. **ii)** PGP9.5 staining shows no nerve fibre bundles within fat tissue sutured on Sham mice. Scale bar represents 100 μm. The right panel shows a magnified image confirming nerves fibres are not present in the tissue. Scale bar represent 100 μm. **(B)** Representative image taken from a paraffin embedded section of a fully developed endometriosis lesion showing immunohistochemical staining for endothelial cells using CD31. Blood vessels can be seen running in parallel or perpendicular to the plane of view are showed by yellow arrows. A zoomed area displayed in the right panel shows blood vessels at higher magnification (yellow arrows). Scale bars represent 100 μm. (C) The peritoneal fluid from mice with fully developed endometriosis (Endo mice) contained significatively higher levels of the cytokines: **i)** Interleukin 1β (IL-β), **ii)** Interleukin 33 (IL-33), **iii)** Interleukin 17 (IL-17), **iv)** Interleukin 6 (IL-6), and **v)** Vascular Endothelial Growth Factor (VEGF); compared to peritoneal fluid obtained at Day 0 of the endometriosis model. Data represent mean ± SEM. (*P <0.05, (**P <0.01, unpaired two-tailed Student t test, from N = 5-6 mice). Black dotted lines represent the lower limit of detection for each of the analytes. Each dot represents data from an individual animal. **(D)** No significant differences in the levels of the inflammatory cytokines: **i)** Tumour necrosis factor α (TNFα), **ii)** Monocyte chemoattractant protein 1 (MCP-1), **iii)** Regulated on Activation, Normal T Cell Expressed and Secreted (RANTES), **iv)** Beta-nerve growth factor precursor (β-NGF), **v)** Granulocyte-macrophage colony-stimulating factor (GM-CSF) and **vi)** Interleukin-13 (IL-13), were found in the peritoneal fluid of mice with fully developed endometriosis (8-10 weeks after uterine horn fragments transplant) compared to Day 0 of the endometriosis model (ns, P >0.05, unpaired, two-tailed Student t test for RANTES, β-NGF, GM-CSF and IL-13; and Mann-Whitney non-parametric test for TNFα and MCP-1. Data was obtained from N = 5 mice at day 0 and N = 6 mice 8-10 weeks after Endo induction). Black dotted lines represent the lower limit of detection for each of the analytes. Each dot represents data from an individual animal.

Having established that transplanted uterine horn fragments developed into mature endometriotic lesions, in a process accompanied by inflammation and apparent neuroangiogenesis, we investigated whether mice with fully developed endometriosis (8-10 weeks after uterine horn fragments transplant) experienced altered sensitivity to pain across various organs, *in vivo*.

2.5.3 Hypersensitivity to vaginal and colonic distension is enhanced in mice with endometriosis

First, we assessed whether mice with endometriosis displayed increased vaginal pain sensitivity in fully conscious animals. For this, we measured the visceromotor response (VMR) to increasing vaginal distension (VD) pressures by recording electromyography (EMG) activity from electrodes surgically implanted into the abdominal muscles of the mouse, as previously described [220]. In Sham mice (8-10 weeks after fat tissue transplant) vaginal distension evokes an increase in the VMR to VD, with the degree of VMR related to the VD pressure **(Figure** 2.4**A-B)**. We found that mice with fully developed endometriosis (Endo mice, 8-10 weeks after uterine horn fragment transplant) displayed significant hypersensitivity to VD *in vivo*, particularly at 30 mm Hg, 40 mm Hg and 60 mm Hg pressures of VD compared to Sham mice (8-10 weeks after fat transplant) **(Figure** 2.4**A-C)**.

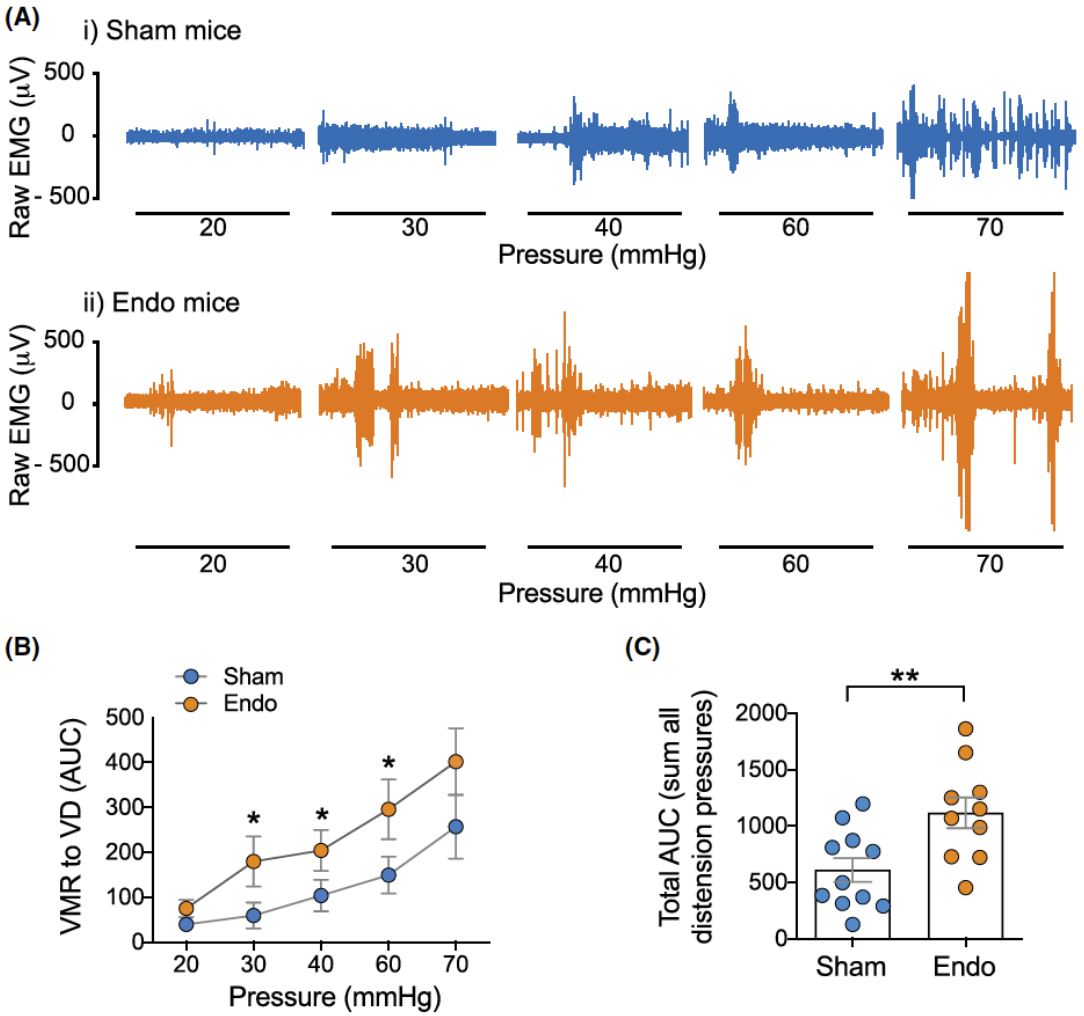

Figure 2.4: Endometriosis mice display enhanced abdominal pain evoked by vaginal distension *in vivo*.

(A) Representative electromyography (EMG) recordings at increasing vaginal distension (VD) pressures (mm Hg) in conscious **(i)** Sham mice (8-10 weeks after fat tissue transplant), or **(ii)** Endo mice (mice with fully developed endometriosis, 8-10 weeks after uterine horn fragments transplant). **(B)** Grouped data showing increased visceromotor responses (VMR) to VD from Sham mice compared with Endo mice (**P* <0.05 at 30, 40 and 60 mm Hg, generalised estimating equations followed by LSD post hoc test, from N = 10-11 mice). Data represent mean ± SEM. **(C)** Grouped data expressed as the total area under the curve (AUC) of the VMR to VD shows significantly increased responses Endo mice compared with Sham mice (***P* <0.01, unpaired, two-tailed Student *t* test, from N = 11 Sham mice and N = 10 Endo mice). Each dot represents the total AUC from an individual animal. Data represent mean ± SEM.

We next aimed to determine whether mice with fully developed endometriosis also have hypersensitivity evoked by colorectal distension (CRD). For this we measured VMR to increasing CRD pressures in conscious animals by recording EMG activity, as previously described [110, 157, 159]. Distension of the colorectum evokes an increase in the VMR in Sham mice, with the degree of VMR directly proportional to the extent of the CRD pressure **(Figure 2.5A-B)**. Interestingly, we found that mice with endometriosis exhibited a pronounced hypersensitivity to colonic distension, *in*

vivo **(Figure 2.5A-C)**, which occurred across a wide range of non-noxious and noxious distension pressures of CRD when compared to Sham mice **(Figure 2.5A-C)**.

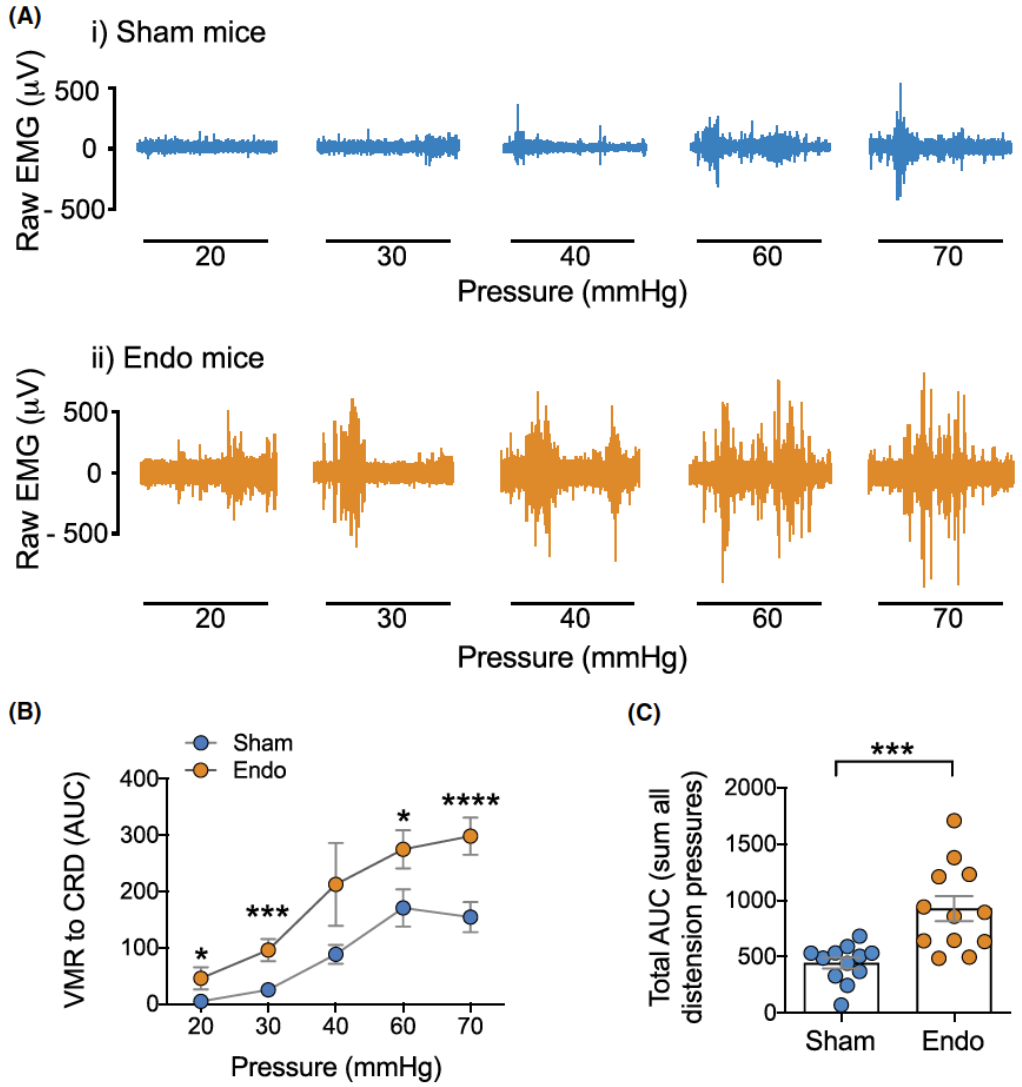

Figure 2.5: Endometriosis mice display enhanced abdominal pain evoked by colorectal distension *in vivo*.

(A) Representative electromyography (EMG) recordings at increasing colorectal distension (CRD) pressures (mm Hg) in conscious **(i)** Sham mice (8-10 weeks after fat tissue transplant), or **(ii)** Endo mice (mice with fully developed endometriosis, 8-10 weeks after uterine horn fragments transplant). **(B)** Grouped data showing increased visceromotor responses (VMR) to CRD from Sham mice compared with Endo mice at all distension pressures (**P* <0.05, ****P* <0.001 and *****P* <0.0001, generalised estimating equations followed by LSD post hoc test, from N = 12 mice). Data represent mean ± SEM. **(C)** Grouped data expressed as the total area under the curve (AUC) of the VMR to CRD shows significantly increased responses Endo mice compared with Sham mice (****P* <0.001, unpaired, two-tailed Student *t* test, from N = 12 Sham mice and N = 12 Endo mice). Each dot represents the total AUC from an individual animal. Data represent mean ± SEM.

2.5.4 Mice with endometriosis display altered bladder function

To investigate whether mice with endometriosis developed altered bladder function, indicating the development of overactive bladder (OAB) or interstitial cystitis/bladder pain syndrome (IC/BPS) phenotype, we examined and compared bladder-voiding patterns of mice before endometriosis induction (Day 0) with their developed voiding patterns 8-10 weeks after uterine horns fragments (Endo mice) or fat transplantation (Sham mice) **(Figure** 2.6**A-B)**.

Filter paper samples from Sham mice showed a similarly organised pattern of voiding at both Day 0 and at the Week 8-10 timepoints **(Figure** 2.6**A i-iii)**. In contrast, Endo mice displayed a disrupted voiding pattern 8-10 weeks following the induction of endometriosis **(Figure** 2.6**B i)**. This was characterised by an increase in the total number of urine spots, in particular an increase in the number of small urine spots **(Figure** 2.6**B ii-iii)**.

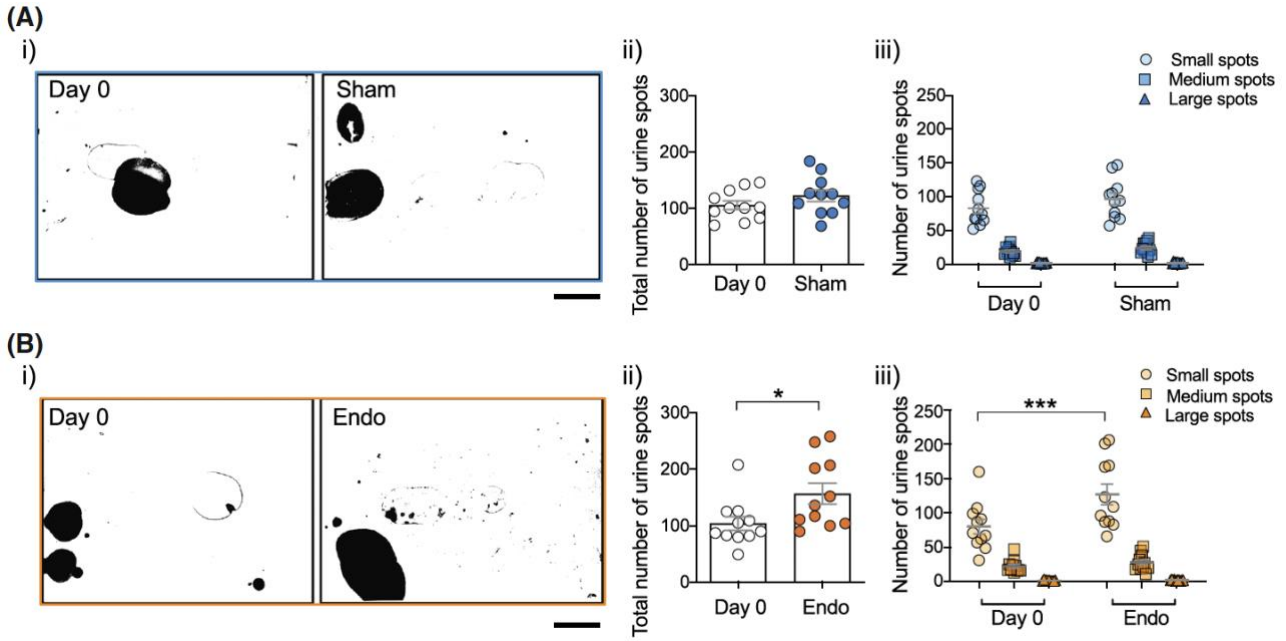

Figure 2.6: Endometriosis mice develop changes in bladder voiding patterns.

(A) (i) Representative images illustrating voiding patterns at Day 0 (prior to transplantation surgery) and at full time course of the Sham model (Sham, 8-10 weeks after fat tissue transplant). Scale bar represent 5cm. **(ii)** Group data of total urine spot counts showing no difference in voiding pattern developed in Sham mice, compared to Day 0 (ns, P > 0.05, unpaired two-tailed Student *t* test, from N = 11 mice). **(iii)** Group data showing no changes in the total number of small (100-1,000 pixels) medium (1,001-100,000 pixels) or large (>100,001 pixels) urine spots in fully developed Sham mice (Sham), when compared to Day 0 (ns, *P* >0.05, two-way ANOVA with Bonferroni's multiple comparisons, from N = 11 mice). **(B) (i)** Representative images illustrating voiding patterns at Day 0 (prior to transplantation surgery) and at the full development of endometriosis (Endo, 8-10 weeks after uterine horn fragments transplant). Scale bar represent 5cm. **(ii)** Group data from Endo mice of total urine spot count shows a significant increase in the total spots after fully development of endometriosis (Endo, 8-10 weeks after uterine horn fragments transplant), compare to mice prior to endometriosis induction surgery (Day 0) (**P* < 0.05, Mann-Whitney non-parametric test, from N = 11 mice). **(iii)** Group data from Endo mice showing a significant change in the total number of small

urine spots (100-1,000dpi), with no change in medium (1,001-100,000dpi) or large (> 100,001dpi) urine spots, between mice with fully developed endometriosis (Endo) and mice prior to endometriosis induction surgery (Day 0) (***P < 0.001, two-way ANOVA with Bonferroni's multiple comparisons, from N = 11 mice). Data represent mean ± SEM. Dots represent values from individual mice.

2.5.5 Mice with endometriosis develop enhanced cutaneous sensitivity to thermal and mechanical stimuli

To determine whether the development of endometriosis has an effect on cutaneous sensitivity evoked by thermal and mechanical stimuli, mice underwent hot plate and Electronic von Frey (EvF) testing.

We found that mice with fully developed endometriosis (Endo mice, 8-10 weeks after uterine horn fragments transplant) exhibited an enhanced sensitivity to thermal stimuli, indicated by a significantly reduced latency of response to the hot plate compared to their Sham counterparts (8-10 weeks after fat tissue transplant) **(Figure** 2.7**A)**. We also found that Endo mice developed a significantly enhanced sensitivity to mechanical stimulation of both their hind paw and abdomen, indicated by a significantly reduced force required to elicit a response compared with their Sham counterparts **(Figure** 2.7**B-C)**. The force required to elicit a response is termed the mechanical threshold, with a reduction in this threshold indicating enhanced sensitivity to mechanical stimuli.

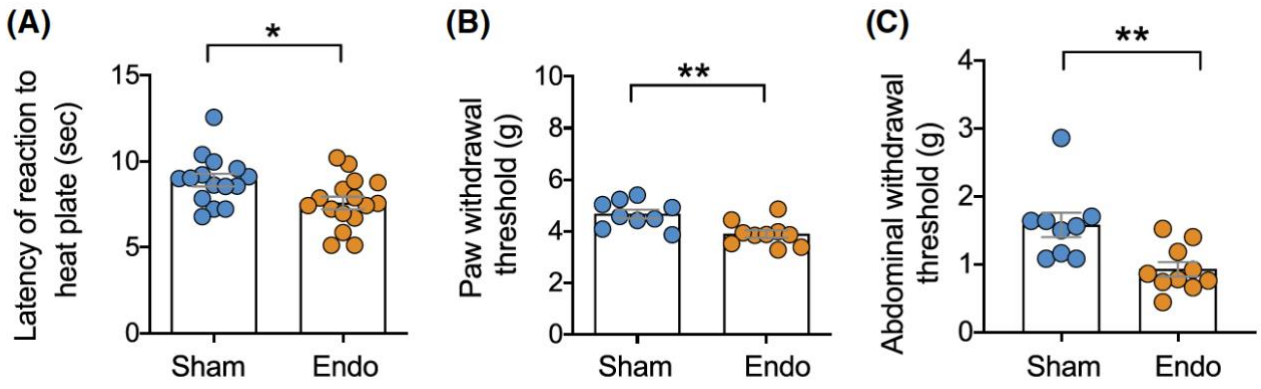

Figure 2.7: Endometriosis mice develop thermal and mechanical cutaneous hypersensitivity.

(A) Group data displaying the latency of reaction to the heat plate shows that Endo mice (8-10 weeks after uterine horn fragments transplant) display a significantly reduced response time to noxious thermal stimuli compared to Sham mice (8-10 weeks after fat tissue transplant) (*P < 0.05, unpaired, two-tailed Student *t test*, from N = 15 Sham mice and N = 16 Endo mice). **(B)** Mechanical withdrawal threshold induced by Electronic von Frey filament stimulation of the hind-paw showed a significant reduction in the withdrawal threshold in endometriosis mice compared with Sham-treated animals. (**P < 0.01, unpaired, two-tailed Student *t* test, from N = 9 Sham mice and N = 10 Endo mice). **(C)** Mechanical withdrawal threshold induced by Electronic von Frey filament stimulation of the abdomen showed a significant reduction in the withdrawal threshold in endometriosis mice compared with Sham-treated animals. (**P < 0.01, Mann-Whitney non-parametric test, from N = 9 Sham mice and N = 10 Endo mice). Data represent mean ± SEM. Dots represent values from individual mice.

2.5.6 The development of endometriosis has no effect on the spontaneous behaviour and locomotor activity of mice

To determine whether the development of endometriosis has an effect on mouse behaviour we recorded spontaneous animal behaviour of both Sham and Endo mice 8-10 weeks post-surgery of fat or uterine horn fragments respectively. For this we monitored the behaviour of mice over a 20 minute period using a behavioural spectrophotometer to automatically record track paths and 23 different spontaneous behaviours, as previously described [159].

Behavioural testing showed that mice from both Sham and Endo groups displayed no significant differences in the track patterns, including the total track length or time spent in the central field **(Figure** 2.8**A and 2.8B i-ii)**. Analysis of time engaged in both grooming or locomotive activities also showed no difference between Sham and Endo treated groups **(Figure** 2.8**B iii-iv)**, which was evident across all 23 individual behaviours measured **(Figure** 2.8**C i-iii)**.

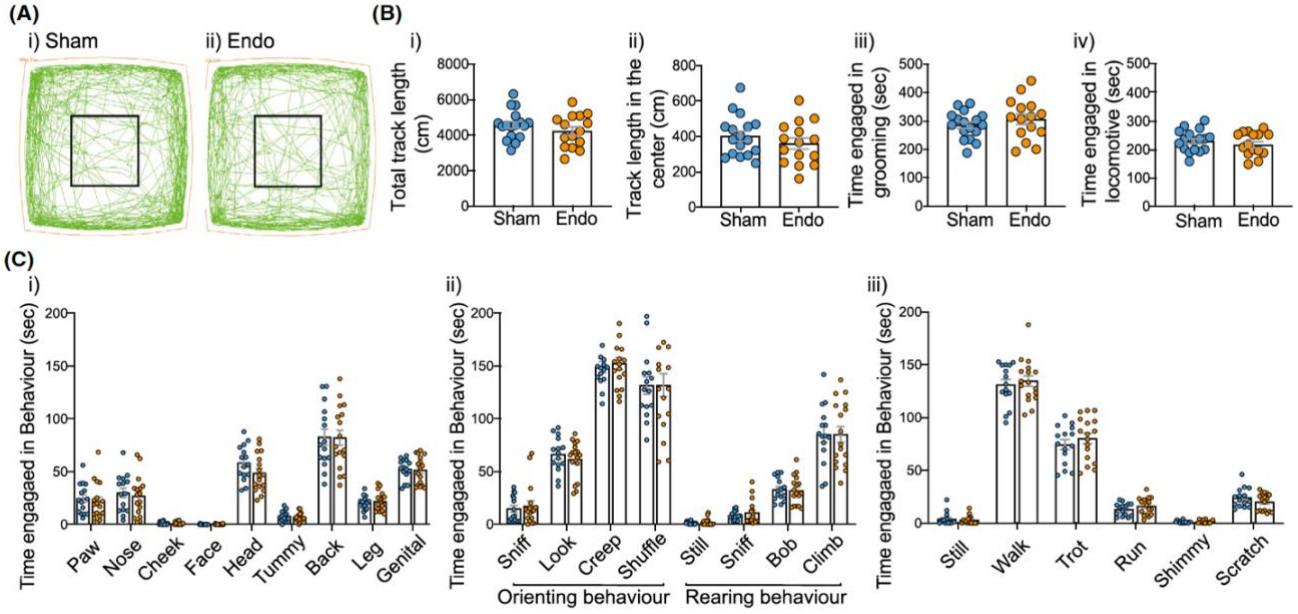

Figure 2.8: Endometriosis mice exhibit no changes in spontaneous behaviour.

(A) Representative track paths are shown for both a **(i)** Sham mouse (8-10 weeks after fat tissue transplant) and an **(ii)** Endo mouse (8-10 weeks after uterine horn fragments are transplanted). The square shows the center of the arena. **(B)** Group data show Sham and Endo mice do not develop changes in **(i)** the total track length (cm) or **(ii)** the centre track length (cm), **(iii)** time engaged in either grooming nor **(iv)** locomotive behaviours (ns, $P > 0.05$, unpaired, two-tailed Student *t* test, from N = 17 Sham and N = 15 Endo mice). Data represent mean ± SEM. Dots represent values from individual mice. **(C)** Endometriosis mice demonstrated no changes in the time engaged in 23 individual behaviours monitored over 20 minutes in the behavioural spectrometer. Behaviours included **(i)** 9 individual grooming behaviours, **(ii)** exploratory behaviours including individual orienteering and rearing, as well as **(iii)** individual locomotor behaviours. (ns, $P > 0.05$, unpaired, two-tailed Student *t* test, from N = 17 Sham and N = 15 Endo mice). Data represent mean ± SEM. Dots represent values from individual mice.

2.6 Discussion

Animal models that recapitulate the complex disease heterogeneity that arises in endometriosis are paramount to investigating the underlying aetiology of this painful disorder. In this study we established and comprehensively characterised a pre-clinical mouse model that recapitulates several features and comorbidities affecting women with endometriosis, including cyst-like endometriotic lesions, an inflammatory environment, and altered sensitivity to pain across multiple peripheral organs.

The animal model used in this study is an adaptation of the previously published model developed by Vernon and Wilson in rats [251]. We transplanted five uterine horns fragments into the abdominal cavity of a mouse, three alongside the arterial cascade of the small intestine mesentery and one on either side of the uterus and followed individual lesion development through a 10-week period. Importantly, as endometriosis is an estrogen dependant disease, all mice used to generate our model were ovariectomised and received weekly injections of estradiol to control estrogen levels. Maintaining a high circulating level of estrogen has been described to be involved in early-stage lesion development and inflammation as well playing an important role in CPP development and maintenance [99, 273, 276].

We found that a significant increase in lesion size only occurs from 6 weeks after fragment transplantation. Additionally, fully mature endometriotic lesions (8-10 weeks after uterine horn fragments transplantation) were cyst-like in nature and contained endometrial glands and stroma, similar to lesions collected from women with endometriosis [286]. Importantly, no lesion development occurred when fat was transplanted in place of uterine horn fragments in Sham mice, highlighting the specificity of our model with the growth of uterine tissue. In addition, similar to what has been described in humans [87, 106], we found that lesions were infiltrated with blood vessels and nerve fibres suggesting that active neuroangiogenesis is taking place in our endometriosis model. Reinforcing this observation, we found that the peritoneal fluid of mice with endometriosis contained elevated levels of the angiogenic factor Vascular Endothelial Growth Factor (VEGF). VEGF is a major promotor in the development of new blood vessels and is found elevated in the peritoneal fluid of women with endometriosis, where it is suggested to promote growth and inflammation of endometriosis lesions (69). Overall, the above described features have been identified within transplanted lesions in other animal models of endometriosis [115, 268] and are recognised to be key players in the transmission of pain in women with endometriosis [78, 126-129].

Further establishing the relevance of this model, our pre-clinical mouse model recapitulates the existence of a pro-inflammatory environment within the peritoneal fluid [81, 96-98] along with the formation of intraperitoneal lesions [72, 287]; both of which are closely linked to the generation of pain in women with endometriosis [54]. We found that the peritoneal fluid of mice with fully developed

endometriosis (Endo mice, 8-10 weeks after uterine horn fragments transplantation) exhibit elevated levels of several proinflammatory cytokines including IL-1β, IL-33, IL-17 and IL-6. Although TNFα and MCP-1 showed a trend toward being increased, the variability between mice prevented this from being definitive. TNFα and MCP-1 have both been implicated in early stages of endometriosis progression in mice [288], although their role in chronic disease is less defined and may explain the variability between mice at the time point examined in this study. Notably, we found that mice with fully developed endometriosis had also developed peritoneal adhesions binding visceral organs together, including the small intestine with the caecum, or the small intestine with the bladder and/or the uterus. Our findings are similar to those found in women with endometriosis, commonly complicating surgical diagnosis and removal of endometriosis lesions in patients [287, 289]. These peritoneal adhesions may be due to the local inflammatory environment [290] and have also been reported in other rodent models of endometriosis, particularly following surgery [291, 292]. Previous reports also showed that local inflammation is a fundamental mediator in adhesion formation, with IL-1β, IL-6 and VEGF identified amongst key players in their formation [293]. Whilst the persistent inflammatory environment has been suggested to play a role in CPP [54], the relationship between adhesion formation and the generation of pain in women with endometriosis remains inconclusive [72].

In addition to the comprehensive characterisation of the endometriotic lesions, the inflammatory environment and the formation of adhesions, the present study expands beyond previously published work by showing that mice with fully developed endometriosis exhibited CPP manifesting as an altered sensitivity to pain across multiple peripheral organs. As women with endometriosis are commonly co-diagnosed with other chronic visceral comorbidities such as interstitial cystitis/bladder pain syndrome (IC/BPS) and irritable bowel syndrome (IBS) [38, 187], as well as increased incidence of migraine headaches, fibromyalgia and altered pain sensitivity amongst others [90, 184], an animal model that recapitulates widespread chronic pain conditions is important to more closely recapitulate the underlying mechanisms of pain.

We first found that mice with endometriosis displayed elevated visceromotor response (VMR) to vaginal (VD) and colorectal (CRD) distensions compared to Sham mice, indicating an enhanced sensitivity to visceral stimuli. Visceromotor response in the mouse has been successfully utilised to identify altered pain sensitivity in both healthy and disease models, including CRD for IBS/IBD [294] and more recently, VD has been utilised in the mouse to further understand pain pathways in the female reproductive tract and to help identify possible treatments for endometriosis associated vaginal pain in the rat [92, 220, 259]. Interestingly, mice with endometriosis displayed both allodynia (pain responses at pressures that do not evoke VMRs on Sham animals, such as 30 mmHg), and hyperalgesia (exacerbated pain responses at pressures above 40 mmHg) to distensions of both colon and vagina. Vaginal hyperalgesia (dyspareunia) has previously been demonstrated in a rat

model of endometriosis [186], however, to our knowledge, this is the first study to demonstrate combined vaginal and colonic hypersensitivity in a mouse model of endometriosis. This finding is clinically relevant, as women with endometriosis often experience severe pelvic pain involving both the colon and the vagina [38, 220].

Women with endometriosis also suffer from other comorbidities including OAB and IC/BPS [38, 57]. In this study we showed that mice with fully developed endometriosis displayed altered bladder function, as evidenced by alterations in bladder voiding patterns. We found that Sham mice showed a distinctly organised pattern of voiding; whilst mice with endometriosis developed a disrupted, scattered voiding pattern, characterised by an increase in the number of small sized urine spots. This type of voiding pattern is indicative of the OAB/IC/BPS symptoms of urgency and frequency [264]. Previous reports have shown that following autologous transplantation of uterine horns, rats developed bladder hypersensitivity, however this model utilised micturition threshold of anesthetized rats, as well as turpentine induce inflammation, as a measure of hypersensitivity [272]. Our study is the first of its kind utilising a non-invasive technique to determine changes in spontaneous voiding patterns in fully conscious endometriosis mice, as an indication of the development of bladder hypersensitivity.

One of the plausible reasons of why women with endometriosis experience pain associated with multiple visceral organs is related with the formation of lesions on those particular visceral organs, accompanied with the development of an inflammatory environment and adhesion formation [231]. Another widely accepted mechanism involves a coordinated phenomenon named central sensitization, which is often considered the cause for ‘unexplained’ chronic pain [182]. Central sensitization has been demonstrated to occur in chronic visceral pain disorders such as IBS [111] and IC/PBS [151]. Sensitization occurring within the spinal cord and brain as a consequence of persistent hyperexcitability of peripheral afferents can facilitate long term abnormalities in pain processing in the absence of noxious stimuli. Central sensitization has been suggested to occur in women with endometriosis [231]. This phenomenon may explain why lesions and adhesions themselves don’t always correlate to pain intensity, but rather pain is widespread and experienced across multiple organs, even in the absence of lesions being present on those organs.

Interestingly, in addition to suffering from comorbidities associated with visceral organs, women with endometriosis also experienced alteration in cutaneous sensation [295, 296]. In this study we demonstrated that our mouse model of endometriosis indeed experiences enhanced sensitivity to cutaneous thermal and mechanical stimuli compared to Sham mice; which was evidenced by a reduction in the animal’s withdraw threshold to both types of stimuli. Investigation of whether this is caused by central sensitization and/or other mechanism(s) does not form part of this study, but certainly, the autologous transplantation mouse model of endometriosis described here represents a useful tool for future investigations on this topic.

Finally, we tested whether the development of endometriosis was able to alter the spontaneous behaviour of mice. Behavioural patterns have been used to quantify changes in pain like behaviours as well as indicators of spontaneous centrally mediated behavioural changes, such as reduced time spent in the centre field indicating the development of anxiety [183, 284]. Interestingly, we found both Endo and Sham mice displayed similar behaviour in all the parameters examined, including spontaneous, grooming, and locomotive behaviours. This suggests that the overall changes taking place during the formation and establishment of lesions together with CPP have no effect on animal spontaneous behavioural patterns and that changes may only be apparent following an evoked response, as seen in other *in vivo* methods used in this study. This was found in contrast to other studies where experimenters reported altered pain behaviours including spontaneous changes in abdominal directed grooming and exploration in early lesion development in mice [258]. In addition, alteration in anxiety like behaviour including reduced time and distance travelled in central areas was also observed in a transplant model of endometriosis, with significant differences between Sham and endo seen between 6 and 12 weeks post-surgery [183], although changes in locomotive behaviour such as distance travelled was only noted at 2, 6 and 12 weeks following surgery, indicating variation across time points. Whether mice in these studies adapted to continual exposure to behavioural studies to allow changes to be seen, or whether spontaneous behavioural changes are only apparent at various time points across lesion development remains to be seen. However, at 8-10 weeks post endometriosis induction, our mice experienced no altered spontaneous behaviours.

To date, little progress has been made in understanding the aetiology of CPP associated with endometriosis [270, 271]. With comorbidities affecting most women with endometriosis [38], developing a pre-clinical animal model that recapitulates the complex disease heterogeneity, with specific identification of altered sensitivity to pain across multiple peripheral organs including the vagina, colon, and bladder, is a vital first step. The comprehensive characterisation of the mouse model of endometriosis described in this study, with analysis of evoked and spontaneous behaviours, delivers a valuable framework to investigate the aetiology of endometriosis associated CPP. Moreover, by utilising these behavioural techniques, it provides a platform for the development of new therapies to manage the debilitating pelvic pain suffered by women with endometriosis.

CHAPTER 3: A SYNGENEIC INOCULATION MOUSE MODEL OF ENDOMETRIOSIS THAT DEVELOPS MULTIPLE COMORBID VISCERAL AND CUTANEOUS PAIN LIKE BEHAVIOURS

3.1 Statement of Authorship

With permission from all authors, this chapter includes an earlier version of work found in the following publication:

Publication: **J. Maddern**, L. Grundy, A. Harrington, G. Schober, J. Castro* and S. M. Brierley* (2021). "A syngeneic inoculation mouse model of endometriosis that develops multiple comorbid visceral and cutaneous pain like behaviours." Pain. Online ahead of print.

Parts of this chapter were presented in poster format at the 14th World Congress of Endometriosis and abstract form in the Australian Pain Society Newsletter – Special Edition (May 2020).

Students' contribution to publication:

J Maddern: Involved in experimental design and procedures. Performed surgical procedures and endometriosis progression analysis. Designed and performed *in vivo* behavioural experiments, including data analysis, interpretation, and preparation of figures. Drafted manuscript.

Estimated overall percentage contribution: 60%

Co-author contributions:

Dr. L Grundy: Designed, performed, analysed, and prepared figure for *ex vivo* bladder afferent recording experiments. Reviewed manuscript and provided supervision and expert advice.

Dr. A. Harrington: Reviewed manuscript and provided expert advice.

Dr. G Schober: Performed behavioural box experiments and reviewed manuscript.

Dr J. Castro: Involved in experimental design and procedures. Contributed to data analysis, figure preparation, writing and editing of the manuscript. Provided supervision and expert advice. Corresponding author.

Prof. S. Brierley: Provided expert advice, assisted with experimental design, supervision, and interpretation of data. Contributed with manuscript writing, editing and figure layout.

Acknowledgements: T. Patton, J. Abramovitch and C. Osborne from Crux Biolab for running Quantibody Mouse Array for cytokine analysis. Jim Manavis for H&E and PGP9.5 staining.

3.2 Overview

Throughout Chapter 2, the successful development of endometriosis and associated CPP was described in the autologous transplant model of endometriosis. Whilst this well-accepted pre-clinical model has the advantage of controlled lesion placement, the invasive nature of surgical induction does not mimic natural endometriosis formation and inflammation from surgically induced endometriosis may confound early CPP mechanisms. With this in mind, the aim of the study presented in this chapter was to characterise the syngeneic mouse model of endometriosis that mimics naturally occurring retrograde menstruation, thought to precede endometriosis development in patients. In this study, we: (1) characterised the development of endometriosis over 10 weeks following uterine tissue inoculation; (2) measured evoked *in vivo* and *ex vivo* hypersensitivity to mechanical stimuli across multiple visceral organs; and (3) assessed alterations in spontaneous behaviour.

3.3 Introduction

Endometriosis is pathologically confirmed by the identification of eutopic endometrial lesions throughout the peritoneal cavity, thought to be preceded by retrograde menstruation introducing ectopic endometrial cells into the peritoneal cavity. In the previous chapter, we demonstrated that uterine tissue surgically transplanted within the mesentery and alongside the uterus, developed into endometriosis lesions and induced a CPP-like phenotype, with hypersensitivity across various organs, *in vivo* [297]. Whilst this model has the advantage of controlled lesion placement, the invasive nature of surgical induction does not mimic natural endometriosis formation. In contrast, an animal model of endometriosis that mimics retrograde menstruation has been developed by utilising inoculation of donor endometrial tissue into the peritoneal cavity of a recipient mouse.

First described in 1999 by Somigliana *et al.*, using this inoculation method of endometriosis induction in mice, lesions were seen to develop within 3 weeks [277]. Endometrial lesions developed in similar locations to those found in women, including on the peritoneal wall, within visceral fat, on the uterine surface and within the intestinal mesenteric surfaces. Importantly, lesions contained distinctive structure to confirm endometriosis, with endometrial epithelium and stroma lining glands [277]. Since its development, this syngeneic model of endometriosis induction has continued to demonstrate reliable endometrial lesion development [197] and has been used to study both lesion growth and inflammation [252, 298]. More recently, studies have used this model to indicate the development of mechanically evoked pain, identified using von Frey filaments on the abdomen and hind paw, as well as indications of spontaneous abdominal pain, recognised by increased abdominal licking and contortions [197, 258]. Recent studies have also identified neuronal changes consistent with peripheral sensitization develop in this model, with sensitization of DRG neurons following endometriosis development, although direct afferent sensitivity was not measured [197]. While indications of CPP are apparent in the syngeneic inoculation model, slight differences in endometriosis induction and the lack of extensive characterisation of pain-like behaviours across multiple visceral organs make conclusions difficult across studies [254].

With comorbidities affecting many women with endometriosis, further characterising the CPP experienced across multiple visceral organs is fundamental groundwork for research into understanding mechanisms of widespread endometriosis associated CPP. In the present study, we aimed to complete an extensive characterisation of the less invasive syngeneic inoculation model of endometriosis. The aims of this study were: 1) to establish chronic lesion development in syngeneic inoculation mouse model of endometriosis, tracking lesion growth in the small intestinal mesentery and alongside the uterus over a 10 week period; 2) to determine whether the chronic inflammatory environment and established neuroangiogenesis seen in this pre-clinical endometriosis model mimics that seen in patients; and 3) to ascertain whether these mice experience widespread chronic hypersensitivity and altered pain responses, evident in both evoked and spontaneous pain like

behaviours, across various organs, *in vivo*. In addition, we examined whether endometriosis mice experienced neuronal hypersensitivity of bladder innervating sensory afferents, *ex vivo.*

3.4 Methods

3.4.1 Study design, timeline, and sequence of behavioural assays

The aim of this study was to characterise endometriosis development in a syngeneic mouse model of endometriosis. We wanted to identify the development of comorbidities in these mice, focusing on multiple indications of CPP at various sites. To do this, data was obtained from a total of 82 mice, including 26 Sham and 56 Endo mice. For endometriosis development measurements, a minimum of 5 mice were used per time point (total N = 31 Endo mice). For non-invasive/observational *in vivo* behavioural assays, including (1) voiding pattern analysis, (2) hot plate testing and (3) behavioural spectrometer recordings a set of N = 11 Sham and N = 10 Endo mice were used, in a longitudinal study design. These 3 behavioural assays were performed sequentially on each mouse following the order listed above (1-3), with a minimum of 24 hours between testing protocols. To determine pain sensitivity evoked by distension of the colorectum (CRD) and the vagina (VD) *in vivo*, a separate group of mice was used (N = 10 Sham and N = 10 Endo mice). These 2 behavioural assays were performed sequentially on each mouse, commencing with CRD. Finally, a dedicated group of mice were used for *ex vivo* electrophysiology experiments (N = 5 Sham and N = 5 Endo).

3.4.2 Animals

The Animal Ethics Committee of the South Australian Health and Medical Research Institute (SAHMRI) approved all experiments involving animals (ethics number SAM342). All animal experiments conformed to the relevant regulatory standards and the ARRIVE guidelines. Female C57BL/6J mice at 6 weeks of age were used and acquired from an in-house C57BL/6J breeding programme (Jax strain #000664; originally purchased from The Jackson Laboratory (breeding barn MP14; Bar Harbor, ME; USA) within SAHMRI's specific and opportunistic pathogen-free animal care facility, as described in Chapter 2. All female mice use in this study were virgin (never been mated) and housed in the absence of males from weening. Vaginal lavage or other cytology test to confirm cycle stage were not performed, but it has been reported that an extended absence of male pheromones leads to a state of anestrous (lee-boot effect) [274].

3.4.3 Development of a syngeneic inoculation mouse model of endometriosis

3.4.3.1 Ovariectomy surgery

Prior to surgical induction of endometriosis, female mice were ovariectomised in order to deplete endogenous steroid production, as described in Chapter 2 [297]. Ovariectomised mice were given an intraperitoneal injection (i.p.) of 100µg/kg estradiol benzoate (or Progynon-B) to maintain steady levels of circulating estrogen [276, 277].

3.4.3.2 Endometriosis (Endo) and Sham induction

Following ovariectomy recovery for a minimum of 5 days, endometriosis or Sham induction was performed **(Figure 3.1)**. Virgin (never been mated) naïve female mice aged 8-10 weeks of age, group housed and with no previous intervention, were used to harvest donor tissue. Under isoflurane, both donor uterine horns were removed and placed in a sterile glass petri dish containing approximately 1 mL of ice-cold PBS including penicillin (100 U/ml) and streptomycin (100 µg/ml) (Sigma). Excess fat and debris were cleaned from the uterine horn tissue, which was then transferred to a fresh dissecting dish containing 0.5mL of PBS (penicillin (100 U/ml) and streptomycin (100 µg/ml) and placed on ice. Uterine horns were then carefully cut into fine endometrial fragments containing both uterine muscle and eutopic endometrium using small dissecting scissors (14 mm length), resulting in minced endometrial tissue suspended in 0.5 mL µL PBS (penicillin (100 U/ml) and streptomycin (100 µg/ml) **(Figure 3.1A)**.

Recipient mice were anesthetized under isoflurane and given a low dose (0.05 mg/kg) of analgesic buprenorphine prior to the commencement of surgery. Following aseptic conditions, a small 0.5 cm laparotomic incision was made into the peritoneal space just below the umbilicus. Half (250 µL) of the donor endometrial fragment suspension was inoculated into the peritoneal cavity using a 1ml pipette. Light massaging of the abdominal cavity was performed to help disperse fragments, and the abdominal and superficial skin layer was closed using 6.0 Prolene sutures. Tissue from 1 donor mouse was used to induce endometriosis in 2 recipient mice. Sham surgeries were performed to assess which effects are the result of surgery versus effects attributable to endometriosis. In line with similar models [197, 299], Sham surgeries consisted of 250 µL of sterile PBS (penicillin: 100 U/ml) and streptomycin: 100 µg/ml) in the absence of any tissue, inoculated into the peritoneal cavity. Throughout the surgery and during the recovery period, animals were kept on a heating pad to maintain body temperature. After recovery from surgery, animals were monitored daily for postsurgical complications for 5 days. No signs of distress or unusual pain behaviours were observed.

To maintain steady levels of circulating estrogen and minimize any difference related to the stage of the estrous cycle, both Endo and Sham mice were given an i.p. injection of 100 µg/kg estradiol benzoate (or Progynon-B) immediately after surgery. All mice continued to receive 100

μg/kg estradiol benzoate i.p. once a week throughout endometriosis development, for up to 10 weeks as schematically shown in **Figure 3.1B**.

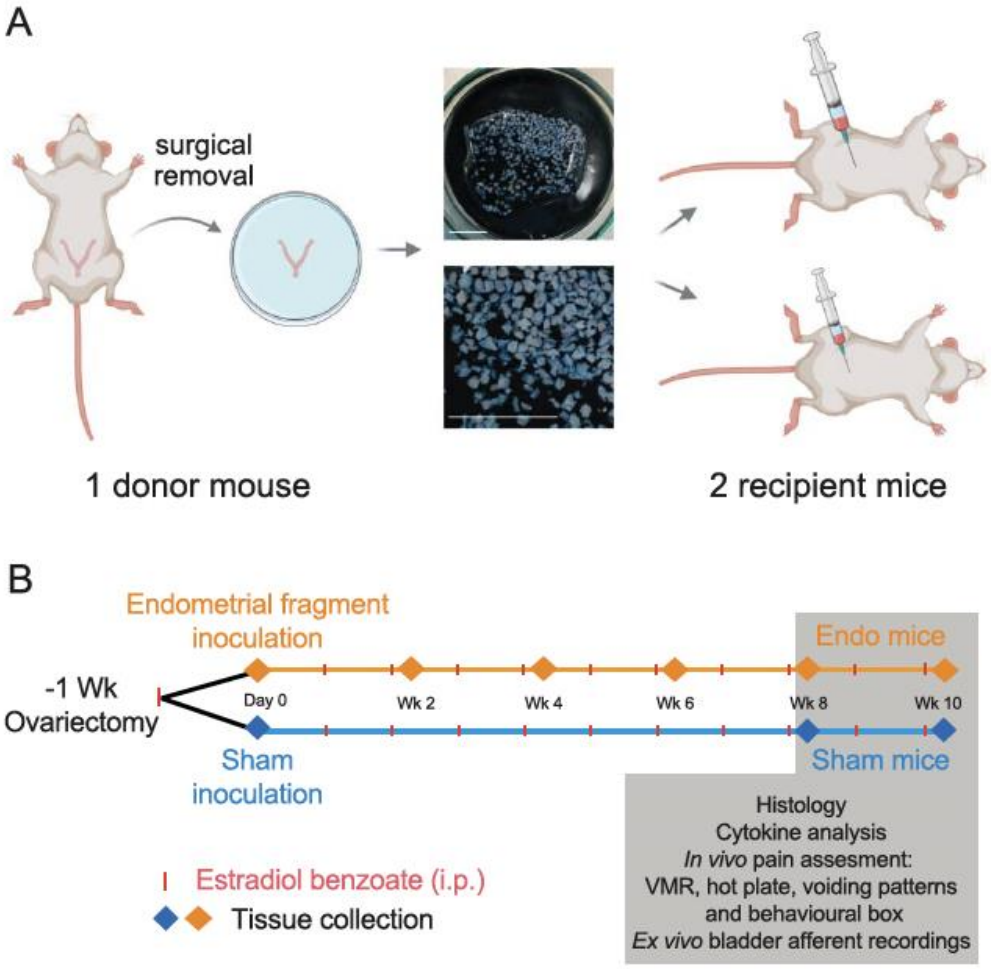

Figure 3.1: Schematic for the interventions performed and their timelines.

(A) Schematic diagram depicting the method of endometriosis induction. Uterine horns are surgically removed from 1 donor mouse and transferred to a dissecting dish for clearing of excess fat and connective tissue. Cleaned uterine horns are then transferred into 0.5 ml of PBS (penicillin (100 U/ml) and streptomycin (100 μg/ml)) and minced into small sections (measurement bars represent 1 cm). The resulting tissue from one donor mouse is then equally injected into 2 recipient mice through a small incision in the abdomen. **(B)** Schematic diagram indicating the timeline in which studies were completed. Seven days after ovariectomy surgery (day 0), mice underwent either endometrial fragment or Sham inoculation. Mice received a weekly i.p. injections of estradiol benzoate (red lines) throughout the study to maintain levels of circulating estrogen. Tissue collection for lesion growth analysis occurred every 2 weeks, between 2-10 weeks post-surgery. All *in vivo* and *ex vivo* experiments were completed between 8-10 weeks in both Sham and Endo mice. Created in part with BioRender.com.

3.4.4 Characterization of endometriosis development.

Endometrial cysts growing from the inoculated uterine horn fragments were collected every 2 weeks, from 2-10 weeks post Endo induction **(Figure 3.1B)** to track endometriosis development as described below. Baseline measurements of inoculated tissue size was calculated by averaging the size (in mm) of the minced uterine horn fragments from donor mice immediately before inoculation (Day 0, as illustrated in **Figure 3.1B**). Sham mice were inoculated with sterile PBS (in the absence of any other tissue type) and do not develop lesions throughout the length of the model. To determine whether endometriosis mice exhibit signs of a local inflammatory environment, we measured a subset of inflammatory cytokines within the peritoneal fluid and within endometriosis lesions collected from mice with fully developed endometriosis (week 8-10). We compared these cytokine levels with the cytokine levels present within the peritoneal fluid and minced uterine horn fragments collected from donor mice at day 0 the of model (baseline measurements), as illustrated in Figure 3.1B.

3.4.4.1 Collection of endometrial lesions and peritoneal fluid.

Lesions were located, dissected, counted, and weighed post-mortem. Measurements at the largest point of the lesion were taken using (Castroviejo callipers 8.5 cm / 3 $^{1}/_{4}$”) and normalised to the average size of a sample of minced uterine horn fragments (0.88 ± 0.09 mm) inoculated into the peritoneal cavity in the endometriosis mouse model to represent growth of lesions. The total weight of all located lesions per mouse (in milligrams) was recorded. Following measurements, lesions were snap frozen in liquid nitrogen and stored at -80°C for protein extraction or stored at 4°C in 4% paraformaldehyde (PFA) for subsequent paraffin embedding.

Peritoneal fluid samples were collected from mice at 8-10 weeks post endometriosis induction, as described in Chapter 2 [297]. Peritoneal fluid samples were snap frozen and stored at -80°C for future analysis. Careful attention was paid to not introduce any blood or disturb any of the peritoneal organs and any sample that was contaminated during collection was immediately discarded.

3.4.4.2 Characterisation of endometrial lesion anatomy

As endometriosis is diagnosed by the presence of viable endometrial like glands and stroma outside of the uterus [207], we used haematoxylin and eosin (H&E) staining to confirm lesion structure, as described in Chapter 2 [297]. Control uterine horn samples and a subset of endometriosis lesions collected at 8-10 weeks post endometriosis induction were histologically assessed to confirm the morphological presence of both epithelial glands and stromal cells [197, 207, 297]. Biopsies that did not contain the morphology of endometrium were not included for any further neuroangiogenesis analysis.

3.4.4.3 Characterisation of neuroangiogenesis development within endometriosis lesions.

To visually identify whether endometrial lesions contained both nerves and blood vessels, another set of sections (10 µm) were stained with Protein Gene Product 9.5 (PGP9.5; Mouse monoclonal anti PGP9.5, clone 3A13, Novus Biologicals, USA, Code # NB600-1160), a neural/nerve sheath marker, or CD31 (mouse anti Rat CD31, clone SZ31, Dianova GmbH, Germany, Code # DIA-310), a platelet endothelial cell adhesion molecule-1 marker widely used to identify endothelial cells, as described in Chapter 2 [297].

All slides were scanned at 40x using autofocus brightfield settings with an automated digital slide scanner by the South Australian Health and Medical Research Institute (SAHMRI) Histology Slide Scanning Service using a Pannoramic slide scanner (3DHISTECH Ltd, Budapest, Hungary). Slides were visualised, and representative images taken using QuPath (version 0.1.2).

3.4.4.4 Quantification of inflammatory markers.

Inflammatory markers within endometriotic lesions and peritoneal fluid samples were quantified using multiplex cytokine analysis with a custom Mouse 11-plex Array. Samples from mice at baseline (day 0) and 8 weeks post endometriosis induction were examined in parallel. Baseline tissue was collected from a separate group of mice at 7 days post ovariectomy/estradiol treatment (day 0) and included eutopic uterine horn sections and peritoneal fluid, this tissue was used as a baseline for all inflammatory parameters assessed.

Snap frozen lesions and uterine horn tissue at day 0 were processed for protein extraction and quantification before undergoing cytokine analysis. Briefly, 150 µl of Cell Lysis Buffer (EPX-99999-000) was added to each tissue sample. Tissue was homogenized using 5-mm Stainless Steel Beads (Qiagen, Hilden, Germany) in a TissueLyser for 4 minutes at 50 Hz. Samples were centrifuged at 4°C for 10 minutes at 10,000 g and supernatant was transferred to a new microcentrifuge tube and stored at -80°C. Tissue protein concentration was measured using BCA protein assay quantification (Pierce BCA Protein Assay Kit) to allow quantification of inflammatory markers as picograms per milligram (pg/mg) of protein per sample. Snap frozen peritoneal fluid samples were defrosted and 60 µl was used directly for cytokine quantification and was assessed as pg/mL of peritoneal fluid.

For both protein and peritoneal fluid samples, a custom Quantibody Mouse Array (RayBiotech, Norcross, GA) was used to detect 11 analytes (GM-CSF, IL-1β, IL-6, IL-13, IL-17α, IL-33, MCP-1, RANTES, TNFα, β-NGF and VEGF) simultaneously by Crux Biolab (Melbourne, Australia), according to manufacturer's instructions. Slides were scanned (GenePix400B Array Scanner (Micromon Genomics, Monash University, Australia)) and analysed using GenePix Pro (v4.0.0.54) acquisition software.

3.4.5 In vivo assessment of evoked pelvic pain by quantification of visceromotor responses (VMR).

The visceromotor response (VMR) to vaginal distension (VD) and colorectal distension (CRD) was recorded as an objective measurement of vaginal or colonic sensitivity to pain in fully conscious animals [92, 115, 186, 195, 273, 282, 297]. Where possible, VMR measurements to both VD and CRD were recorded in the same mouse, with a minimum 2-hour break between distension protocols.

3.4.5.1 Surgical implantation of electromyography (EMG) electrodes

The VMR was assessed by recording the electrical activity (EMG) produced by abdominal muscle contractions in response to non-noxious and noxious VD or CRD, as described in Chapter 2 [297]. Briefly, the bare endings of two Teflon-coated stainless-steel wires (Advent Research Materials Ltd, Oxford, UK) were sutured into the right external oblique abdominal muscle of Sham or Endo mice and tunnelled subcutaneously to be exteriorized at the base of the neck for VMR experiments following 3 days recovery.

3.4.5.2 Assessing visceromotor responses (VMR) to vaginal distension (VD) or colorectal distension (CRD)

On the day of VMR assessment, mice were briefly anaesthetized using inhaled isoflurane and a saline enema administered via catheter to either the colorectum (100 μL) or vaginal cavity (50 μL). and a balloon was inserted into either the colorectum or vaginal cavity for VMR assessment, as described in Chapter 2 [297]. Graded distensions were applied at 20-40-50-60-70-80 mm Hg (20 seconds duration) at 4 minute-intervals for CRD or 20-30-40-60-70-80 mm Hg (30 seconds duration) at 3 minute-intervals for VD. Following the final CRD distension mice were returned to their IVC for a minimum of 2 hours before the VD protocol, any mice with imperfect electrodes were excluded from further testing.

To quantify the magnitude of the VMR at each distension pressure, the area under the curve (AUC) during the distension was corrected for baseline activity (AUC pre-distension). The AUC was quantified by adding the individual AUC at each distension pressure and included total AUC (all distension pressures), non-noxious AUC (pressures between 20 and 40 mm Hg) and noxious AUC (pressures between 50 and 80 mm Hg).

3.4.6 *In vivo* assessment of evoked cutaneous sensitivity to thermal stimuli.

The hot plate test was used to measure changes in the threshold or sensitivity to pain evoked by heat in Endo mice compared to Sham controls [283, 284, 297].

3.4.6.1 Assessing cutaneous sensitivity to noxious thermal stimuli with hot plate test

The assessment of cutaneous sensitivity to noxious thermal stimuli was measured using the hot plate test, as described in Chapter 2 [297]. Hot plate testing was performed at 8 weeks post Sham or Endo induction, and 3 days post estradiol benzoate administration, using a hot plate temperature of 54 ± 0.1°C degrees, previously demonstrated to be a noxious stimuli [284]. The time (in seconds) between being placed on the hot plate and their first sign of response, including hind paw licking, hind paw flicking, or jumping (whichever comes first), was recorded as the response latency. The average latency of both tests was recorded as their final response latency.

3.4.7 *In vivo* assessment of spontaneous animal behaviour:

The behavioural spectrometer (Behavior Sequencer; Behavioral Instruments, NJ and BiObserve, Wilhelmstr, Germany) was used to assess 23 different parameters in freely active mice in an open filed, to assess whether Endo mice exhibit chronic pain-like behaviours or develop behavioural changes indicative of anxiety or depression, *in vivo* [159, 284, 297, 300].

3.4.7.1 Assessing spontaneous behaviour of Sham and endometriosis mice

For testing, individual naïve Sham or Endo mice were placed in the centre of the behavioural spectrometer, and their behaviour was filmed/tracked and evaluated/analyzed by computerized video tracking software (Viewer^3, BiObserve, DE) for 20 min, as described in Chapter 2. Evaluation of the total distance traveled in the open field, time spent in the central area (20 x 20 cm), wall distance, different behavioral patterns including grooming, orienting, rearing, scratching, and forms of locomotion was performed. An independent experimenter performed all sessions in an order counterbalanced for experimental group.

3.4.8 Assessment of bladder dysfunction

3.4.8.1 In vivo assessment of bladder dysfunction by spontaneous voiding pattern analysis

Voiding pattern analysis was performed for assessing changes in bladder function [110, 297].

3.4.8.1.1 Voiding pattern collection, imaging, and analysis

Filter paper for voiding pattern analysis was collected immediately prior to Sham or Endo induction and again at 8 weeks post induction, as described in Chapter 2. Filter paper was imaged using a Bio-Rad ultraviolet trans-illuminator and digitised into binary images using ImageJ software (NIH). The number and size of urine spots was determined using pre-set thresholds within ImageJ software and, for the purposes of this study, the number of small (100-1,000 pixels), medium (1,001-100,000 pixels) and large (>100,000 pixels) spots were quantified as well as the total number of

spots per animal. The number and size of urine spots quantified at day 0 (prior to induction surgery) was compared to spots quantified at 8 weeks post induction surgery for both Sham and Endo mice to determine any developed alterations in voiding patterns over 8 weeks.

3.4.8.2 Assessment of bladder dysfunction by ex vivo analysis of nerve fibres innervating the bladder

We use *ex vivo* bladder electrophysiology to record pelvic afferent nerve excitability in response to changes in bladder pressure to compare the sensitivity of bladder innervating pelvic afferents between Sham and Endo mice. Previous studies have indicated altered bladder afferent activity is a key component of disorders such as IC, with a switch from normosensitive afferents (healthy state) to hypersensitive afferents apparent in disease states [151, 301-304].

3.4.8.2.1 Ex vivo bladder preparation

Ex vivo pelvic nerve recording was performed as previously described [301, 305]. Briefly, mice were humanely killed via CO_2 inhalation and the bladder, urethra and ureters together with surrounding tissue carefully removed and placed a modified organ bath containing gassed Krebs bicarbonate solution (comprised of (in mmol/L) 118.4 NaCl, 24.9 $NaHCO_3$, 1.9 $CaCl_2$, 1.2 $MgSO_4$, 4.7 KCl, 1.2 KH_2PO_4, and 11.7 glucose). Ureters were tied and the bladder catheterised via the urethra and connected to a syringe pump to allow for a controlled bladder fill rate. A second catheter was then inserted and secured at the dome of the bladder and connected to a pressure transducer to enable intravesical pressure recording throughout graded distension. Pelvic nerves were isolated from other nerve fibres between the pelvic ganglia and spinal cord, where they were dissected into fine multiunit branches. From here, a single branch was placed within a sealed glass pipette containing a microelectrode and attached to a neurology headstage. Nerve activity was amplified (NL104), filtered (NL 125/126, band pass: 50–5,000 Hz, Neurolog, Digitimer), and digitized (CED 1401, Cambridge Electronic Design, Cambridge, UK) to a personal computer for offline analysis using Spike2 software (Cambridge Electronic Design). The number of action potentials crossing a pre-set threshold at two times the background electrical noise was determined per second to quantify the afferent response. Single unit analysis was performed offline to determine the activation threshold of single afferent units by matching individual spike waveforms, discriminated as single units based on distinguishable waveforms, amplitudes, and durations, through linear interpolation using Spike2 (version 5.21) software (Cambridge Electronic Design, Cambridge, UK).

3.4.8.2.2 Afferent recording experimental protocol

Bladder distensions were performed with intravesical infusion of saline (0.9% NaCl) at a rate of 100 µL/min to a maximum pressure of 60 mm Hg. The volume in the bladder was extrapolated from the known fill rate (100 µL/min) and the time taken (in seconds) to reach maximum pressure (60 mm Hg). Compliance was determined by plotting intravesical pressure against the calculated volume.

3.4.9 Statistical analysis

Data was graphed using Prism 9 software (GraphPad Software, San Diego, CA, USA) and represented as mean ± SEM, with N representing the number of animals per group. Normality of data was assessed using the Shapiro-Wilk test prior to statistical analysis. When comparing two groups, data were analysed using unpaired two-tailed Student *t* tests for groups of equal variances: or using the Mann-Whitney nonparametric test for groups with unequal variances. Data comparing more than two groups were analysed using an ordinary one-way analysis of variance (ANOVA) with Turkey's multiple comparisons (lesion growth analysis) or two-way ANOVA with Fisher's LSD or Sidak multiple comparisons post hoc tests (bladder afferent recordings). VMR distension data were analysed using generalised estimating equations (GEE) followed by least significant difference (LSD) post hoc test when appropriate, using SPSS 27.0. Differences were considered statistically significant at $*P < 0.05$, $**P < 0.01$, $***P < 0.001$ and $****P < 0.0001$.

3.5 Results

3.5.1 Endometrial lesion growth is seen in the syngeneic mouse model of endometriosis.

Development of endometriotic lesions outside of the uterus is the defining characteristic of endometriosis development. In this study, we found that minced eutopic uterine tissue inoculated into the peritoneal cavity of healthy mice **(Figure 3.1A)** developed into endometriosis lesions **(Figure** 3.2**A-D)**. Lesions were found throughout the peritoneal cavity, with half of all lesions found within abdominal fat and near peritoneal organs, including alongside the colon, kidneys, and uterine horns **(Figure** 3.2**A and B i-iv)**. The number of lesions found in each mouse was highest at 8-10 weeks of development, with a significant increase compared to both 2 and 4 weeks **(Figure** 3.2**C i)**. The total weight of lesions collected per mouse significantly increased in a similar fashion, with combined lesion weight per mouse the largest at 8-10 weeks of development **(Figure** 3.2**C ii)**. When looking at individual lesion growth normalised to the average individual inoculated tissue size, we found that progressive increase was reached between week 8-10, indicating significant lesion growth up to 10 weeks following inoculation **(Figure** 3.2**C iii)**. Mice that underwent Sham inoculation did not develop lesions. Histological staining with H&E of uterine horn (UH) tissue collected from healthy naïve mice at day 0 displayed typical morphology **(Figure** 3.2**D i)** [207]. Similarly, ectopic lesions collected from Endo mice contained the same structural identifiers as endometrial tissue in-situ, including endometrial glands and cell rich stroma **(Figure** 3.2**D ii)**. Staining with PGP9.5, a pan neuronal marker, identified multiple nerve fibres located throughout endometriosis lesions collected at 8 weeks **(Figure** 3.2**E)**. In addition, endothelial cell staining with CD31 identified blood vessels located throughout endometriosis lesions **(Figure** 3.2**F)**.

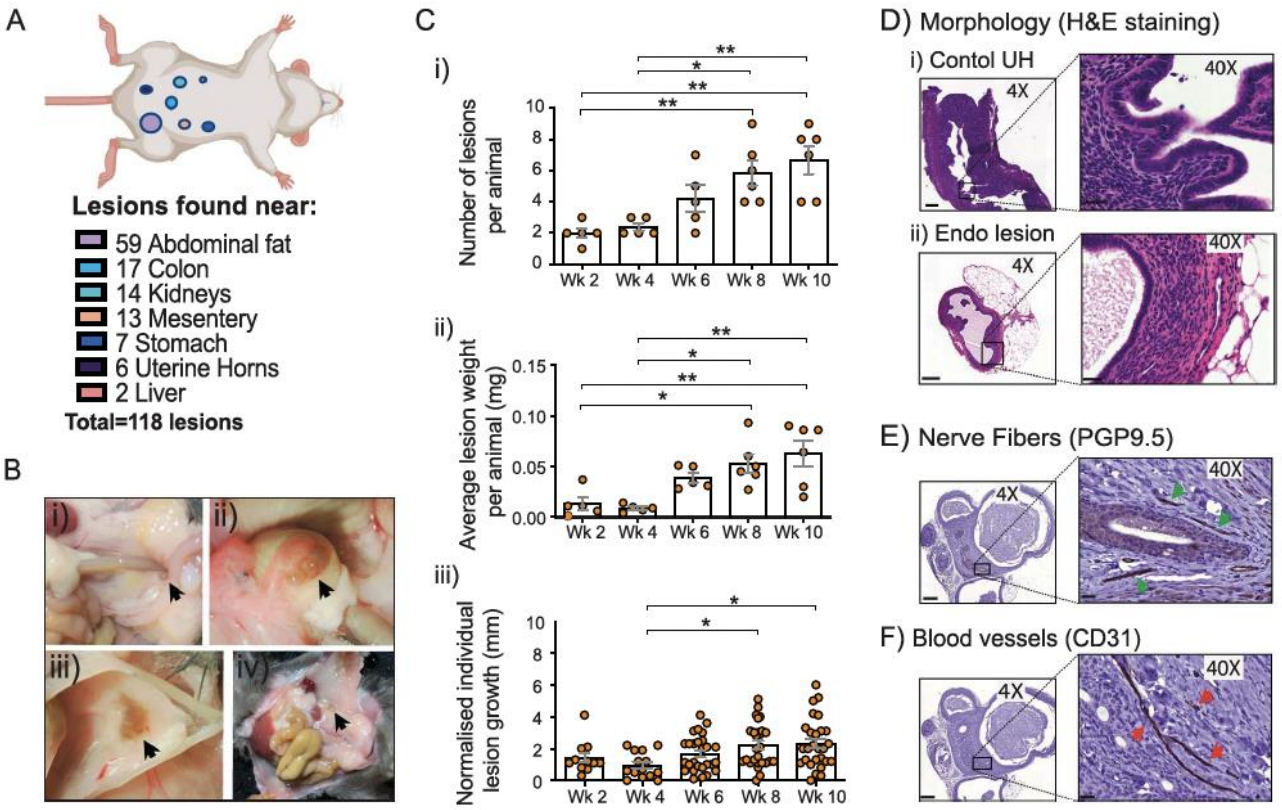

Figure 3.2: Inoculation of uterine horn fragments into the peritoneal cavity induces growth of endometriosis like lesions *in vivo*.

(A) Representative illustration showing the physical location of all endometriosis lesions found within all mice, collected between 2 and 10-weeks post Endo induction (N = 27 mice across all the time points). **(B)** Representative images comprising of endometrial lesions located **(i-ii)** near the colon and stomach as well as **(iii-iv)** within the abdominal fat in close proximity to the uterine horns. **(C)** Combined data showing lesion analysis over weeks 8-10 post-Endo induction, including **i)** the average number of lesions located per animal, **(ii)** the total lesion weight per animal (mg) and **(iii)** individual lesion growth per (mm), normalised to the size of inoculated tissue pieces. Data represent mean ± SEM and normalised to growth from day 0 (**P* < 0.05, ***P* < 0.01, ****P* < 0.001 ****P* < 0.001 and *****P* < 0.0001, one-way ANOVA with Turkey's multiple comparisons) from N = 5 to 6 mice per time point or n = 11 to 27 individual lesions per time point. **(D)** Representative H&E images of **(i)** control uterine horn tissue and **(ii)** fully developed endometriosis lesions, developing a similar structure to control endometrial tissue with endometrial glands and cell rich stroma. **(E)** Representative image taken from paraffin embedded sections stained with PGP9.5 to identify nerve fibres within endometriosis lesions. Green arrows illustrate nerve fibres running parallel to the plane of view. **(F)** Representative image taken from paraffin embedded sections stained with CD31 to identify endothelial cells within endometriosis lesions. Red arrows illustrate blood vessels running parallel to the plane of view. Images are shown at X4 magnification (scale bars represent 200 µm), accompanied by X40 magnified images (scale bars represent 20 µm). Created in part with BioRender.com.

3.5.2 Inflammatory mediators are altered in endometriosis mice.

Eleven individual inflammatory mediators present in the peritoneal fluid (PF) collected from mice with fully developed endometriosis (8-10 weeks after induction), were identified using a multiplex-array **(Figure 3.3)**. Compared to the PF from donor mice collected at day 0 the of model, peritoneal fluid collected in endometriosis mice at 8-10wks, showed a significant increase in VEGF **(Figure 3.3)** with a significant reduction in IL-13 **(Figure 3.3)**. There was no difference in the remaining 9 inflammatory mediators detected in the PF, including IL-1β, IL-6, IL-17, IL-33, MCP-1, RANTES, TNFα, βNGF and GM-CSF **(Figure 3.3)**.

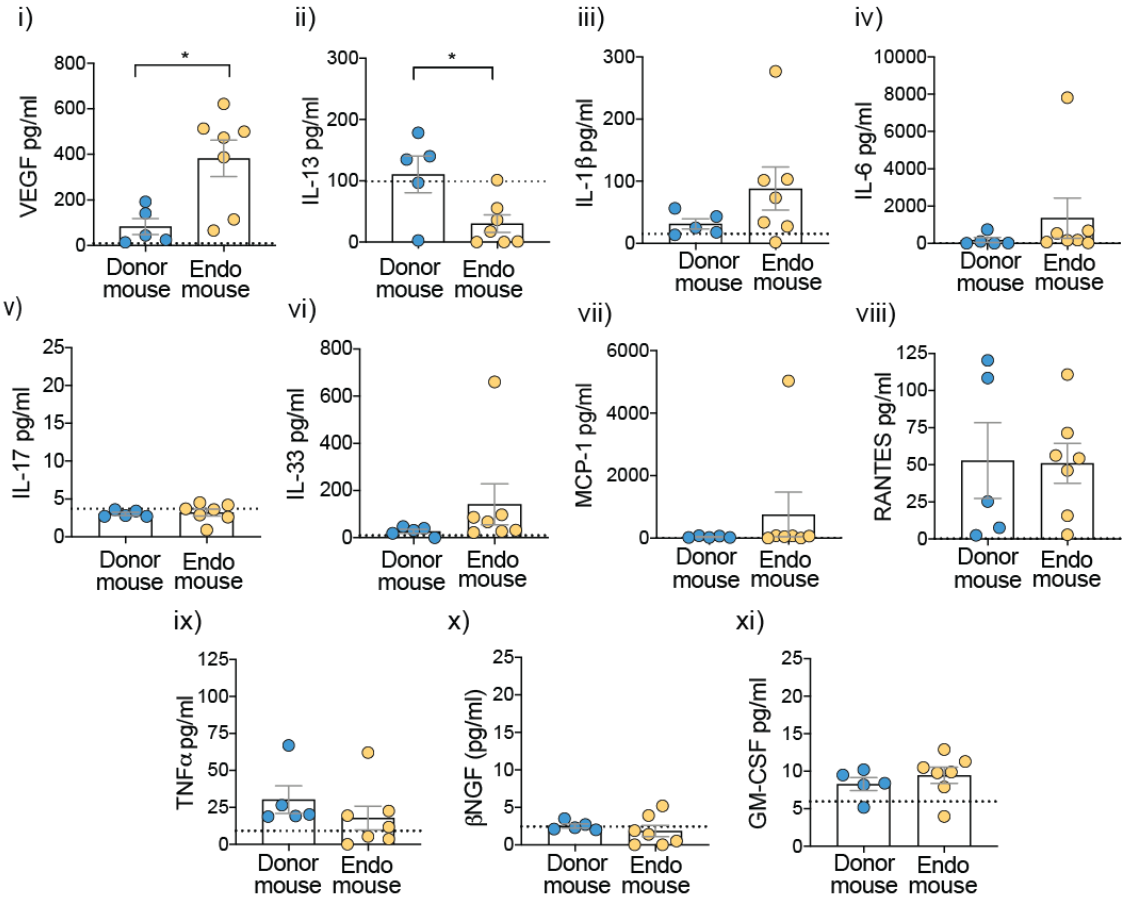

Figure 3.3: Cytokine analysis of peritoneal fluid (PF)

The PF of endometriosis mice contained significantly increased levels of **(i)** vascular endothelial growth factor (VEGF) and significantly reduced levels of **(ii)** interleukin-13 (IL-13), compared with the donor mice used to generate the endometriosis model. The abundance of all other analytes measured in the PF of mice with fully developed endometriosis was similar to those detected in the PF collected from donor mice. This includes **(iii)** interleukin 1β (IL-1β), **(iv)** interleukin 6 (IL-6), **(v)** interleukin 17 (IL-17), **(vi)** interleukin 33 (IL-33), **(vii)** monocyte chemoattractant protein 1 (MCP-1), **(viii)** regulated on activation, normal T-cell expressed and secreted (RANTES), **(ix)** tumour necrosis factor α (TNFα), **(x)** beta-nerve growth factor precursor (β-NGF), and **(xi)** granulocyte–macrophage colony-stimulating factor (GM-CSF). Data represent mean ± SEM with levels expressed as picograms per ml (pg/mL) of peritoneal fluid. **P* <0.05, unpaired two tailed Student *t* test for peritoneal fluid analytes β-NGF, GM-CSF, IL-13, IL-17, IL1β, RANTES, and VEGF and Mann–Whitney nonparametric test for PF analytes IL-33, IL-6, MCP-1, and TNFα. Data were obtained from n = 5 donor mice and n = 7 mice with fully developed endometriosis. Black dotted lines represent the lower limit of detection for each of the analytes. Each dot represents an individual animal.

Furthermore, when comparing inflammatory mediators found within the eutopic uterine horn tissue collected from donor mice to those found in endometriosis lesions at week 8-10, a significant increase was also seen in VEGF **(Figure** 3.4 **i)**. In contrast, there was a significant reduction in the levels of IL-1β, IL-13, IL-17, RANTES, TNFα, βNGF, and GM-CSF in endometriosis lesion collected from mice with fully developed endometriosis (8-10 weeks) compared to baseline conditions (Donor mouse) **(Figure** 3.4 **ii-viii)**; whilst IL-6, IL-33 and MCP-1 levels were not significant changed **(Figure** 3.4 **ix-xi)**.

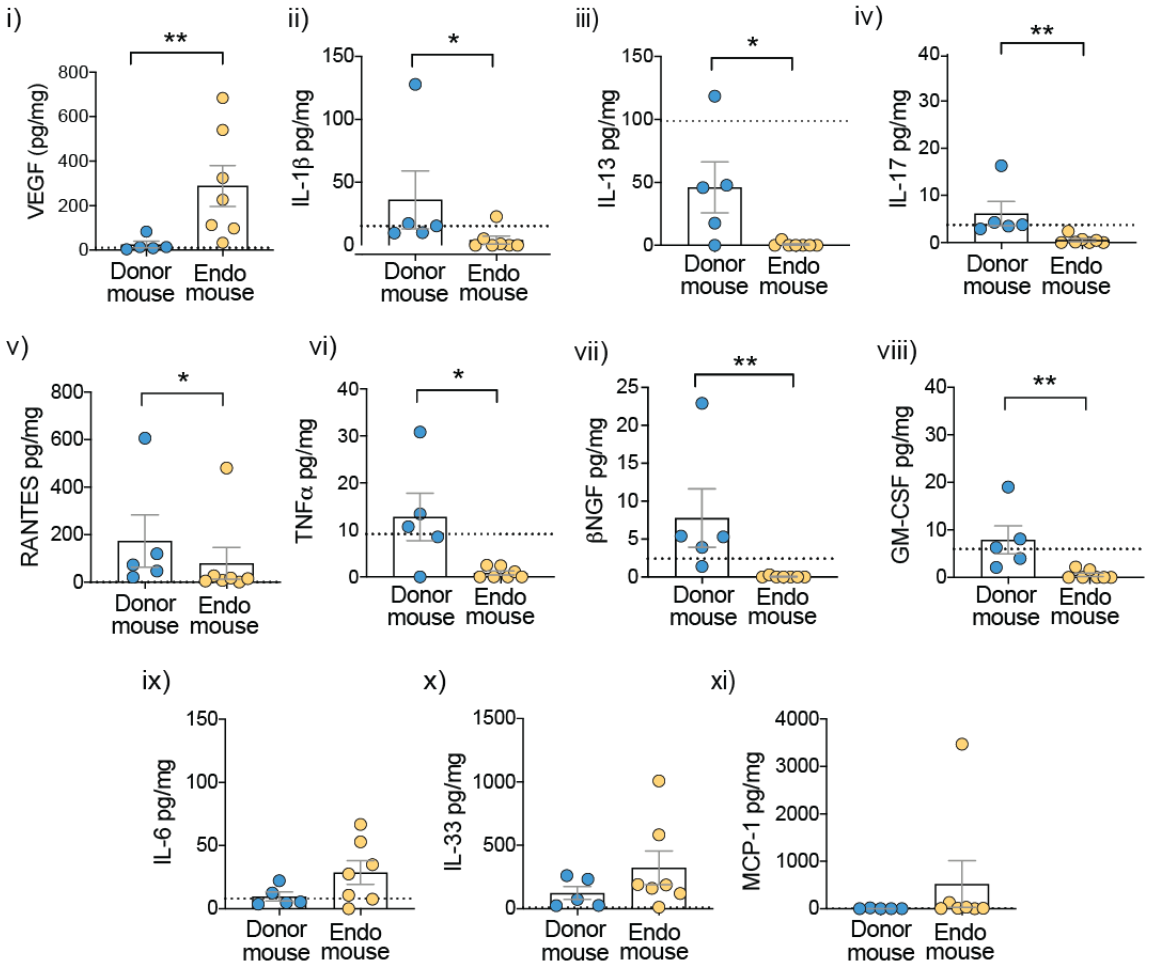

Figure 3.4: Cytokine analysis of whole endometriosis lesions

Homogenates of whole endometriosis lesions contained significantly increased levels of **(i)** Vascular Endothelial Growth Factor (VEGF), compared to uterine horn tissue collected at day 0 of the model from donor mice (Donor mouse). Endometriosis lesions also contained significantly decreased levels of analytes including **(ii)** IL-1β, **(iii)** IL-13, **(iv)** IL-17, **(v)** RANTES**, (vi)** TNFα, (vii) βNGF and **(viii)** GM-CSF), compared to uterine horn tissue collected at day 0 of the model from donor mice (Donor mouse). Levels of remaining analytes **(ix)** IL-6, **(x)** IL-33 and **(xi)** MCP-1 were unchanged within endometriosis lesions compared to uterine horn tissue from donor mice. Data represent mean ± SEM with levels expressed as picograms per mg (pg/mg) of protein. **P* <0.05, ***P* <0.01, unpaired two-tailed Student *t* test for analyte IL-6 and Mann-Whitney non-parametric test for analytes βNGF, GM-CSF, IL-13, IL-17, IL-1β, IL-33, RANTES, TNFα and VEGF. Data was obtained from N = 5 donor

mice and N = 7 mice with fully developed endometriosis. Black dotted lines represent the lower limit of detection for each of the analytes. Each dot represents data from an individual animal.

Having established a syngeneic mouse model of endometriosis, and gained an overview of the local inflammatory environment, we aimed to determine if these endometriosis mice developed chronic pelvic pain (CPP). For this, we completed a series of behavioural assays on fully conscious Endo and Sham mice, at 8-10 weeks following inoculation.

3.5.3 Enhanced sensitivity to vaginal and colorectal distension in mice with endometriosis.

Women with endometriosis often experience pain related to colonic and vaginal comorbidities [26, 38]. To investigate whether the development of endometriosis induced vaginal or colonic hypersensitivity in our mouse model of endometriosis, we measured the visceromotor response (VMR) to organ distension *in vivo* by recording electromyography (EMG) activity from electrodes surgically implanted into the abdominal muscles.

Vaginal distension (VD) alone evoked an increase in the VMR, with the degree of VMR related to the VD pressure. We found that there was a lack of VMR to VD in Sham mice at pressures ≤ 40mmHg. This range of pressures are therefore called non-noxious pressures. Sham mice showed increased VMR to VD at noxious pressures (60-80 mm Hg) **(Figure** 3.5**A and 3.5B)**. We found that Endo mice displayed pronounced hypersensitivity to VD *in vivo*, evident by significantly elevated VMRs to VD at 40 mm Hg-80 mm Hg distension pressures compared to Sham mice **(Figure** 3.5**A and 3.5B)**. The sum of all VMR responses (total AUC) to VD (20-80 mm Hg) was significantly increased in Endo mice compared to Sham **(Figure** 3.5**C i)**. Detailed analysis of the VMR responses at different distension pressures showed that Endo mice displayed allodynia (sum of AUC at non-noxious distension pressures (20-40 mm Hg; **Figure** 3.5**C ii**) and hyperalgesia (sum of AUC at noxious distension pressures (60-80 mm Hg; **Figure** 3.5**C iii**).

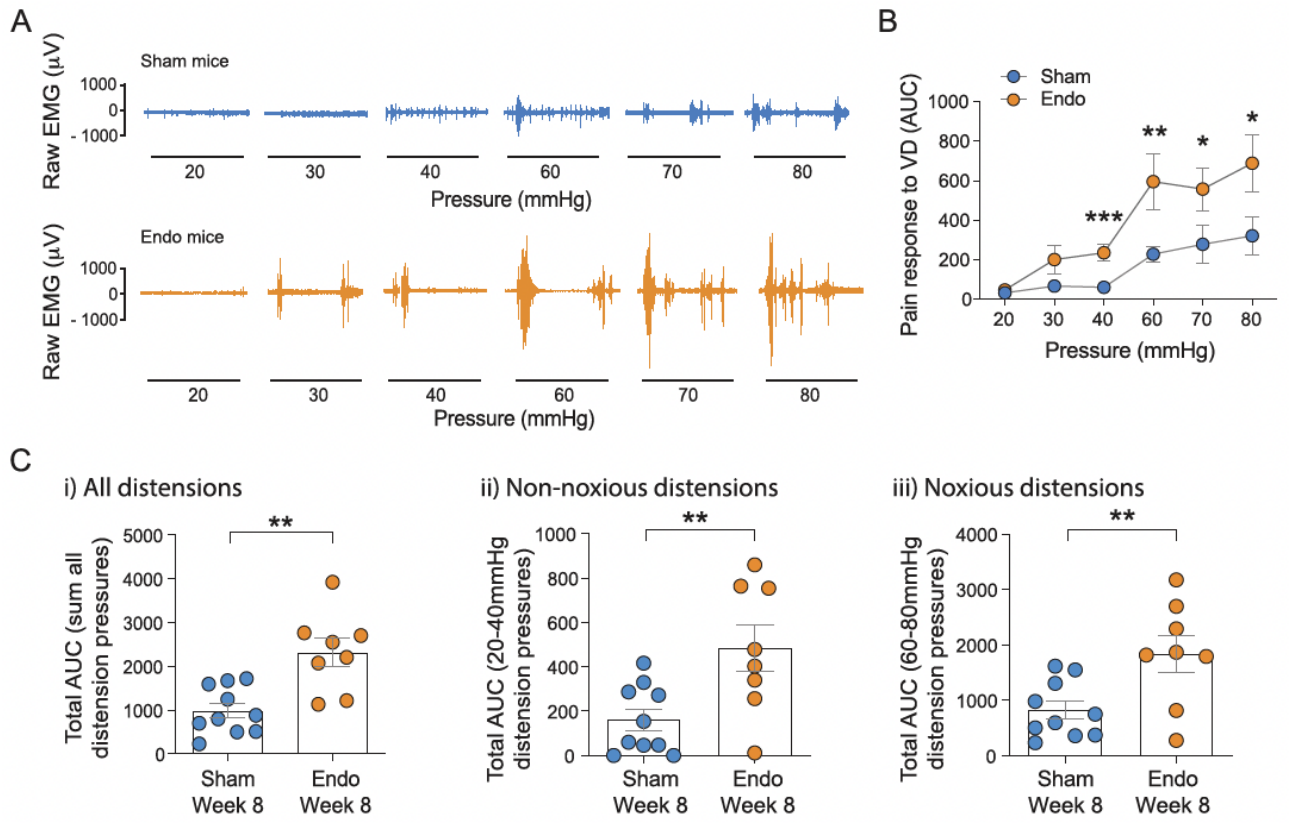

Figure 3.5: Endometriosis mice display enhanced pelvic pain evoked by vaginal distension *in vivo*.

(A) Representative electromyography (EMG) recordings at increasing vaginal distension (VD) pressures (mm Hg) in conscious mice after 8 weeks of either Sham or endo induction. **(B)** Grouped data showing increased visceromotor responses (VMR) to VD from Endo mice, compared with Sham mice from 40mmHg – 80mmHg (*P < 0.05, **P < 0.01, ***P < 0.001, generalised estimating equations followed by LSD post hoc test, from N = 10 Sham mice and N = 8 Endo mice). Data represent mean ± SEM. **(C)** Grouped data expressed as the total area under the curve (AUC) of the VMR to **(i)** all distension pressures (20-80 mm Hg), as well as separated into **(ii)** non-noxious (20-40 mm Hg) distension pressures and **(iii)** noxious (60-80 mm Hg) distension pressures of VD, shows significantly increased responses in Endo mice compared with Sham mice (**P <0.01, unpaired two-tailed Student *t* test, from N = 10 Sham mice and N = 8 Endo mice). Each dot represents the AUC from an individual animal. Data represent mean ± SEM.

We next aimed to determine whether endometriosis development also enhanced colonic pain sensitivity evoked by distension of the colorectum (CRD) in a similar way. An increase in colonic distension pressure evokes an increase in the VMR **(Figure 3.6A and 3.6B)**. We found that Endo mice developed pronounced hypersensitivity to CRD *in vivo*. This was evident by significantly elevated VMRs to CRD from distension pressures of 40 mm Hg and above compared to Sham mice as well as significantly increased VMR over the sum of all distension pressures (total AUC) **(Figure 3.6C i)**. Again, Endo mice developed allodynia (enhanced response at non-noxious distension

pressures (20-40 mm Hg)) **(Figure 3.6C ii)** and hyperalgesia (enhanced response at noxious distension pressures (50-80 mm Hg) **(Figure 3.6C iii)**.

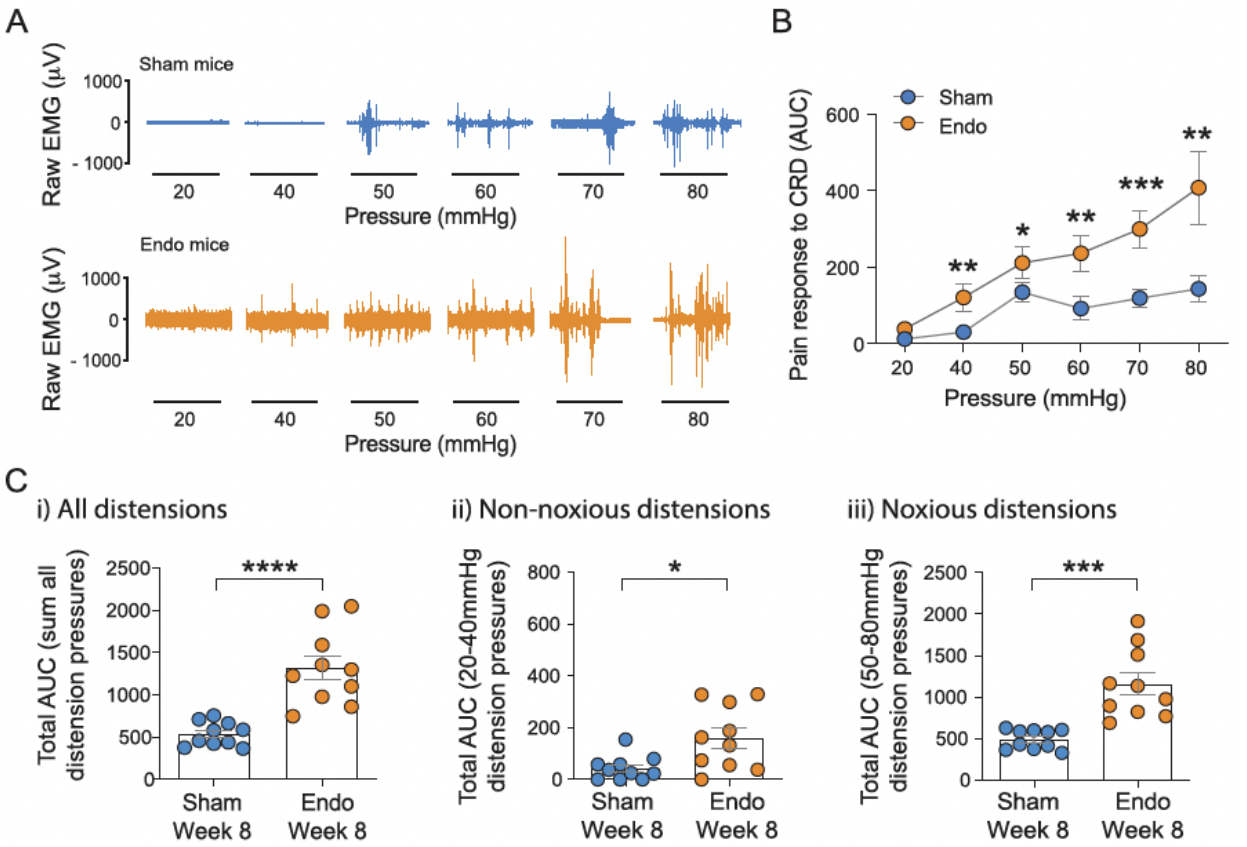

Figure 3.6: Endo mice display enhanced pelvic pain evoked by colorectal distension *in vivo*

(A) Representative electromyography (EMG) recordings at increasing colorectal distension (CRD) pressures (mm Hg) in conscious mice after 8 weeks of either **(i)** Sham or **(ii)** Endo mice. **(B)** Grouped data showing increased visceromotor responses (VMR) to CRD from Endo mice, compared with Sham mice from 40 mm Hg (**P* <0.05, ***P* <0.01 and ****P* <0.001, generalised estimating equations followed by LSD post hoc test, from N = 10 mice per group). Data represent mean ± SEM. **(C)** Grouped data expressed as the total area under the curve (AUC) of the VMR to **(i)** all distension pressures (20-80mmHg), as well as separated into **(ii)** non-noxious (20-40 mm Hg) distension pressures and **(iii)** noxious (50-80 mm Hg) distension pressures of CRD, showed significantly increased responses in Endo mice compared with Sham mice (**P* <0.05, ****P* <0.001, and *****P* <0.0001, unpaired two-tailed Student *t* test, from N = 10 mice per group). Each dot represents the AUC from an individual animal. Data represent mean ± SEM.

3.5.4 Mice with endometriosis develop enhanced cutaneous sensitivity to thermal stimuli.

In addition to CPP involving visceral organs, women with endometriosis also report somatic pain sensitivity [90]. To test whether the development of endometriosis in this model effected cutaneous sensitivity, mice underwent hot plate testing at a known noxious temperature of 54 ± 0.1 ^{o}C [284]. We found that Endo mice developed an enhanced sensitivity to noxious thermal stimulus, indicated by a reduced latency of reaction to the heat plate compared to their Sham counterparts **(Figure 3.7)**.

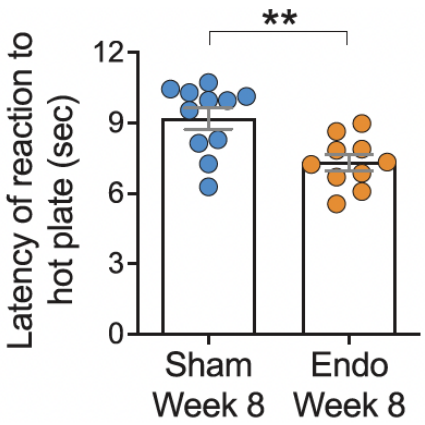

Figure 3.7: Endometriosis mice develop enhanced cutaneous thermal sensitivity.

Group data displaying the latency of reaction (seconds; sec) to the hot plate. Endo mice display a significantly reduced response time to noxious thermal stimuli compared to Sham mice. Data represent mean ± SEM (** $P < 0.01$, unpaired, two-tailed Student *t* test, from N = 11 Sham mice and N = 10 Endo mice). Dots represent values from individual mice.

Once we determined that Endo mice developed enhanced sensitivity to mechanical and thermal stimuli evoked across multiple organs, we aimed to determine whether the spontaneous behaviour of mice was also altered.

3.5.5 Mice with endometriosis display bladder dysfunction accompanied by hypersensitivity of sensory afferents innervating the bladder.

As women with endometriosis often suffer with comorbid bladder dysfunction [57, 58], it was important to investigate whether mice with fully developed endometriosis developed altered bladder function. To do this, we examined alterations in the spontaneous bladder-voiding patterns between day 0 and 8 weeks post Sham or Endo induction **(Figure 3.8A, 3.7B)**. Filter paper samples from Sham mice showed a similarly organised pattern of voiding at both day 0 and week 8 **(Figure 3.8A i)**. In comparison, mice developed a disrupted voiding pattern following the development of endometriosis, indicative of bladder dysfunction **(Figure 3.8B i)**. These changes were characterised by an increase in the total number of urine spots, in particular an increase in the number of small spots (100-1,000 dpi), in mice with fully developed endometriosis **(Figure 3.8B ii-iii)**, compared to Sham mice **(Figure 3.8A ii-iii)**.

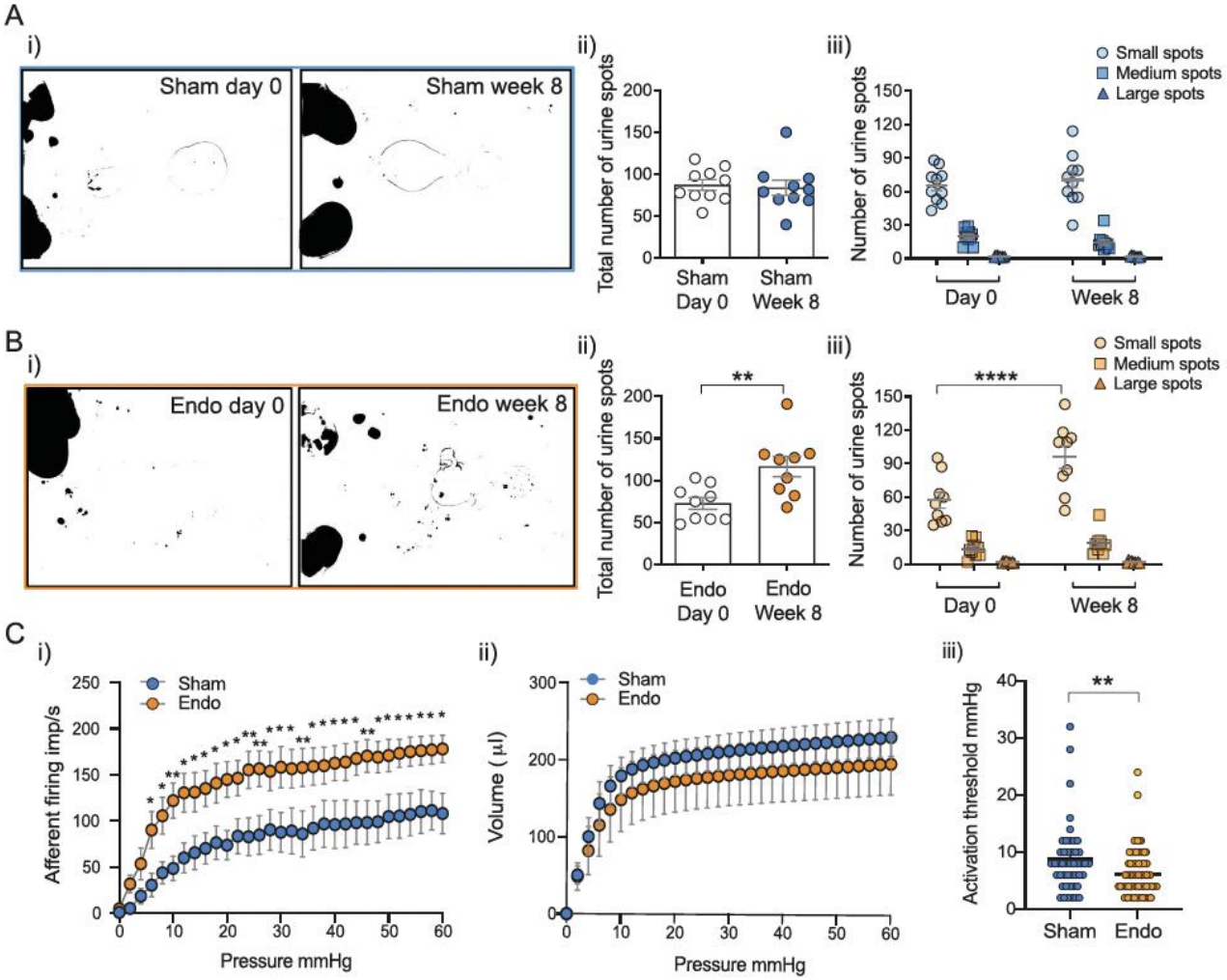

Figure 3.8: Endometriosis mice develop changes in spontaneous voiding patterns *in vivo* accompanied by altered afferent sensitivity *ex vivo*.

(A) (i) Representative images of voiding patterns between day 0 and 8 weeks following Sham induction. **(ii)** Grouped data of total urine spot count showing no difference between day 0 and 8 weeks ($P > 0.05$, unpaired two-tailed Student t test, from N = 10 mice). **(iii)** Grouped data showing no change in the total number of small (100-1,000dpi) medium (1,001-100,000dpi) or large (>100,001dpi) urine spots at both day 0 and 8 weeks in Sham mice ($P > 0.05$, two-way ANOVA with Bonferroni's multiple comparisons, from N = 10 mice). **(B) (i)** Representative images of voiding patterns between day 0 and 8 weeks following endo induction. **(ii)** Grouped data of total urine spot count shows a significant increase in the total spots following 8 weeks of endometriosis development (**$P < 0.01$, unpaired, two-tailed Student *t* test, from N = 9 mice). **(iii)** Grouped data shows a change in the total number of small urine spots (100-1,000 dpi) with no change in medium (1,001-100,000 dpi) or large (> 100,001 dpi) urine spots at between day 0 and 8 weeks post endo induction (****$P <$ 0.0001, two-way ANOVA with Bonferroni's multiple comparisons, from N = 9 mice). Data represent mean ± SEM. Dots represent values from individual mice. **(C) (i)** *Ex vivo* bladder afferent firing in response to a ramped increase in pressure is significantly increased in endometriosis mice, compared to their Sham counterparts (*P <0.05, **$P < 0.01$, two-way ANOVA followed by Fisher's LSD test, from N = 5 Sham mice and N = 5 Endo mice). **(ii)** There is no change in compliance of the bladder muscle with increasing volumes having a similar effect on pressure in both Sham and Endo mice ($P > 0.05$, two-way ANOVA followed by Sidak multiple comparisons test, from N = 5 Sham mice and N = 5 Endo mice). **(iii)** The activation threshold of individual afferents is significantly reduced in endometriosis mice compared to Sham (**$P < 0.01$, unpaired, two-tailed Student *t* test, from N = 5 Sham mice and N = 5 Endo mice. Data represent mean ± SEM).

To further elucidate whether the chronic changes seen in the bladder voiding patterns of endometriosis mice were due to alterations in bladder afferent mechanosensitivity (which will translate in an altered signal of the bladder's fullness state), we aimed to examine bladder afferent responses to bladder distension *ex vivo*. As pressure in the bladder increased from 0-60 mm Hg the rate of individual afferent firing in the pelvic nerve also increased. Sham mice displayed a steady increase in sensory nerve firing with increasing pressure from bladder filling **(Figure 3.8C i)**. Interestingly, we saw those afferent nerves innervating the bladder in Endo mice developed a significantly enhanced firing rate to bladder distension from as low as 6mmHg and continuing to 60 mm Hg, compared to Sham **(Figure 3.8C i)**. These changes in mechanosensitivity of bladder afferents were not due to a change in bladder muscle compliance as there was no significant difference in the pressure/volume relationship between Sham and Endo mice **(Figure 3.8C ii)**. When comparing the activation threshold of individual pelvic afferents nerves, we also found that the afferents of mice with endometriosis required significantly less pressure to trigger activation **(Figure 3.8C iii)** and therefore had lower activation thresholds.

3.5.6 The development of endometriosis alters the spontaneous behaviour of mice.

In addition to women with endometriosis being diagnosed with comorbidities affecting visceral organs, an association has been identified between endometriosis and psychological diseases including depression and anxiety [306]. To determine whether the development of endometriosis influences non-evoked behavioural patterns, we recorded the spontaneous behaviour of both Sham and Endo mice in an open field test using the behavioural spectrometer.

Mice from both Sham and Endo treated groups displayed no significant differences in total track length **(Figure 3.9A i-ii and B i)**. However, there was a significant reduction in exploratory behaviour, with Endo mice less likely to explore the centre field, indicated by a reduced centre field track length **(Figure 3.9B ii)**, reduced number of visits to the centre field **(Figure 3.9B iii)**, and remaining significantly closer to the outer wall **(Figure 3.9B iv)** compared to their Sham counterparts. Despite changes in exploratory behaviours, Endo mice showed no changes in their time engaged in any of the individual behaviours quantified, including grooming, orienting, rearing and locomotive behaviours **(Figure 3.9C-E)**.

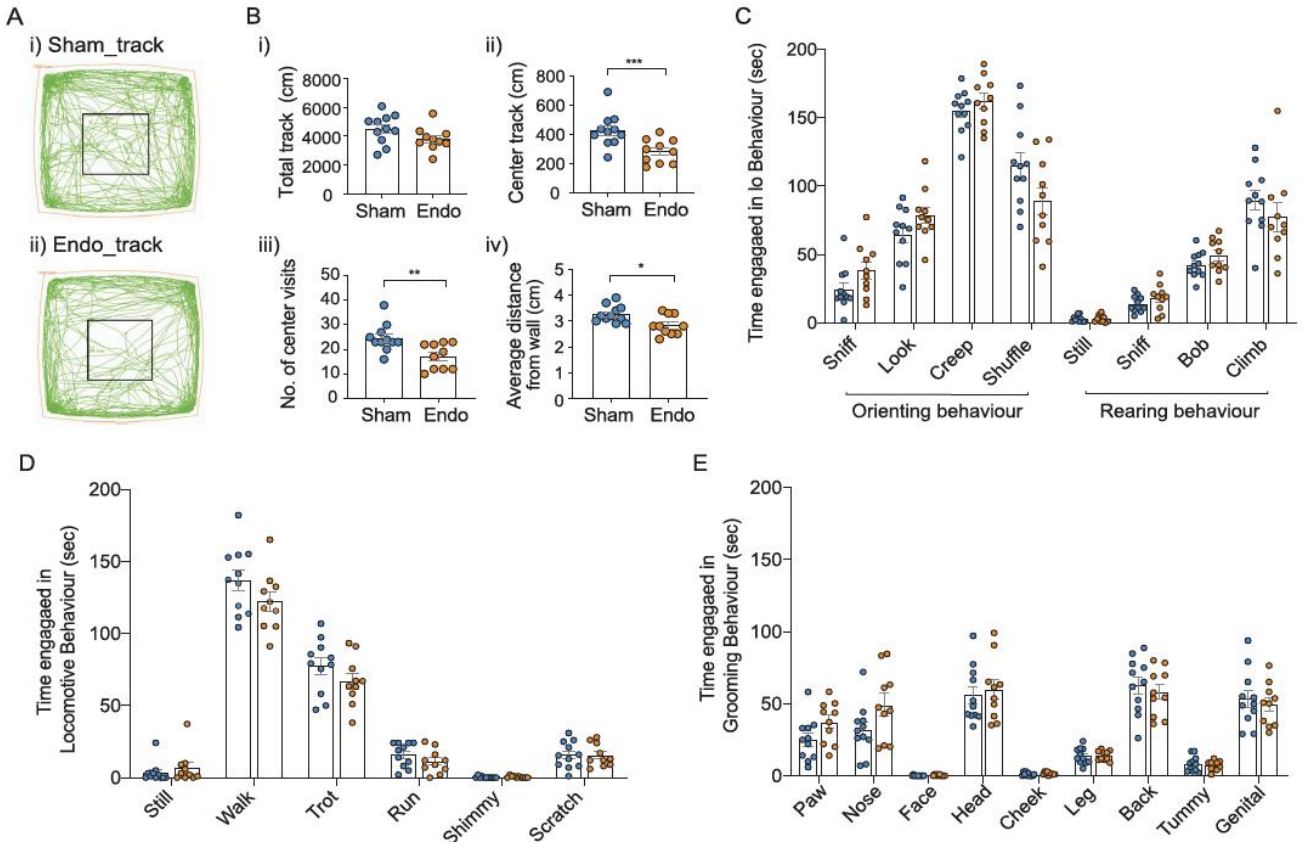

Figure 3.9: Endometriosis mice exhibit changes in spontaneous behavioural patterns.

(A) Representative track paths are shown for both **(i)** a Sham mouse and **(ii)** an Endo mouse, with the centre square represented in black. **(B)** Grouped data showed no difference in **(i)** the total track length between Sham and Endo mice, however the **(ii)** centre track length, **(iii)** the number of centre visits and **(iv)** the average distance from the outer walls was significantly reduced in Endo mice. **(C)** When looking at individual behaviours, there was no significant difference in time engaged in either individual orienting or rearing behaviours, **(D)** individual locomotive activities or **(E)** individual grooming locations. Data represent mean ± SEM. (*$P < 0.05$, **$P < 0.01$ and ***$P < 0.001$, unpaired, two-tailed Student *t* test, from N = 11 Sham and N = 10 endo mice). Dots represent values from individual mice.

3.6 Discussion

Endometriosis effects up to 10% of women worldwide, with the vast majority presenting with comorbidities associated with multiple visceral organs and chronic pelvic pain (CPP). Although endometriosis was first clinically defined as early as 1925, the underlying pathogenesis remains elusive. Furthermore, the mechanisms responsible for the development of CPP in endometriosis remains poorly understood [40, 231, 307]. With the multifaceted nature of endometriosis, it is important that an animal model recapitulates as many features of the human disease state as possible.

In this study, we used a syngeneic endometriosis mouse model, designed to mimic retrograde menstruation, to induce the development of endometrial lesions. Structurally, lesions contained distinct features of eutopic endometrial tissue, displaying both endometrial glands and stroma throughout. Both nerves and blood vessels were identified in these lesions, as well as elevated VEGF, an important factor for lesion development and maintenance [82], within the peritoneal fluid and endometriosis lesions themselves. The results presented in this study also demonstrate mice with endometriosis developed i) hypersensitivity across multiple visceral organs, ii) enhanced peripheral sensitivity to heat, and iii) anxiety-like behaviour. This draws similarities to what is observed in women with endometriosis, with patients at significantly higher risk of developing chronic pain conditions affecting visceral organs (notably including IBS, dyspareunia and IC/BPS) [38, 308] and psychological conditions including depression and anxiety [306, 309].

Interestingly, despite tissue being inoculated at week 0, we only saw a significant increase in lesions growth from week 6 post inoculation. One plausible explanation is that at early time points fragments of tissue may not have established into clearly visible lesions, or perhaps sprouting of new lesions (or even spontaneous resolution of some lesions) may occur at later time points, as recently shown nicely by Dorning *et al*. and Fattori *et al*. [197, 299]. Nevertheless, we were unable to determine whether this was the case, as we only have a “snapshot” of lesion’s development every 2 weeks, rather than a longitudinal visual identification of individual lesion development.

The enhanced inflammatory environment identified in some mouse models of endometriosis, including that presented in the autologous mouse model in Chapter 2 [197, 297], was not apparent in the syngeneic inoculation mouse model of endometriosis at 8-10 weeks post-induction. In contrast, we observed a significant reduction in IL-13 levels within the peritoneal fluid and reduced levels of IL-1β, IL-13, IL-17, RANTES, TNFα, βNGF, and GM-CSF within endometriosis lesions themselves.

Our data add to the growing inconsistencies around the importance of inflammation in endometriosis. To date, inflammatory cytokine concentrations have not proven effective in predicting endometriosis in women, with both early and severe stages of endometriosis offering inconclusive and varying cytokine patterns. For example, TNFα and IL-8 levels in the peritoneal fluid and serum

of women with endometriosis were found to decrease with disease severity [310]. Furthermore, Llarena *et al*., recently reported no difference in IL-8, MCP-1, TNFα or VEGF levels in the peritoneal fluid of women with endometriosis at any disease stage [311]. In contrast, cytokines including IL-1α, IL-1β and IL-6, were found elevated in women with advanced stage endometriosis, but were unchanged in women with mild endometriosis, compared to women without endometriosis [311]. A plausible explanation for such a variation may be due to macrophage activity and secretions during inflammation, which can vary between pro-inflammatory and pro-repair throughout the various stages of disease [312, 313]. In mice, a recent study found increased levels of neutrophils and inflammatory cytokines G-CSF, TNFα, IL-6 and VEGF, in the peritoneal fluid during in the early stages (days 1-3) of endometriosis development [298]. However, by day 7 and 28 both neutrophil infiltration and enhanced cytokines had returned to baseline levels [298]. Recently, a study using a mouse model of endometriosis induced by human endometrial tissue injection, reported a macrophage shift from inflammatory, in early development, to reparative in later stages [313]. To this end, the decreased levels of the several inflammatory cytokines measured in this study may reflect the more advanced stage endometriosis lesions collected in our study. Future studies elucidating changes in inflammatory mediators across multiple time points may enable us to further map their involvement in lesion's growth and endometriosis progression.

Other chronic pain conditions such as IBS, IC/BPS and fibromyalgia are defined by hyperalgesia in the absence of inflammation. However, inflammation is a known contributor to chronic pain pathogenesis, causing sensitization of neurons that can persist long-after the resolution of inflammation [88, 151]. Measuring multiple time points throughout early development and maintenance of endometriosis to determine how the inflammatory phenotype alters in this model would provide a clearer time course of inflammation but was beyond the scope of this study.

As changes in peripheral sensitivity were apparent in the absence of a local inflammatory environment, our data indicates that at the time point studied, pro-inflammatory cytokines are not essential for maintaining a chronic hypersensitive state once the disease is well established. This data therefore supports the notion that alternative mechanisms, such as chronic sensory afferent hypersensitivity, contribute to the maintenance of CPP in endometriosis.

Our data shows that Endo mice developed hypersensitive responses to vaginal, colonic, and cutaneous stimuli *in vivo*, as well as altered bladder sensory signalling *ex vivo*. Together this suggests that chronic changes in global sensitivity have occurred in these Endo mice. The concept of chronic changes in broader pain signalling have been shown in similar mouse model of endometriosis [197]. Evidence from other chronic pain disorders indicates that chronic sensitization of peripheral sensory neurons can induce long term structural and synaptic neuroplasticity in central sensory transduction pathways [151]. This process may be of particular relevance to endometriosis, as the disease often progresses for years prior to diagnosis and the subsequent initiation of

treatment or surgical removal of lesions. As such, there is ample time for chronic changes in peripheral and central sensory pathways to occur and may be why current therapeutic treatments, aimed at reducing inflammation and lesion removal, have mixed efficacy in alleviating CPP [35, 208, 231, 307].

Chronic changes in sensory function may also be responsible for the common comorbidities of endometriosis patients. We and others have found that chronic peripheral hypersensitivity can influence the excitability and function of peripheral neurons innervating distinct organs via a process called cross-organ sensitization [151]. Our data suggests that cross-organ sensitization developed in the Endo mice, as these mice, but not their Sham counterparts, developed hypersensitivity and altered function in multiple visceral organs. Visceral organs are particularly susceptible to cross-organ sensitization as they share overlapping sensory pathways, with pelvic nerves from the bladder, vagina, colon and uterus been shown to converge into the same dorsal root ganglion and levels of the spinal cord [231]. In some cases, axons innervating multiple organs have been shown to share a single cell body within the ganglion [92, 109, 110, 151].

Further support for these mechanisms occurring in our mouse model comes from our *ex vivo* bladder afferent recordings. Here we found that enhanced mechanosensitivity of pelvic afferents in response to bladder distension in Endo mice occurred despite no direct insult to the bladder. Physiologically, this enhanced mechanosensitivity indicates signalling of bladder fullness and/or discomfort at lower thresholds compared to Sham mice, supporting the induction of a hypersensitive, IC-like phenotype [110]. This identifies that not only does our endometriosis model develop CPP across multiple visceral organs, but that chronic changes to pain signalling in visceral organs have also established by 8-10 weeks of endometriosis development.

In addition to visceral hypersensitivity and indications of CPP, we were able to identify changes in the spontaneous behaviour of mice, with a reduction in exploratory behaviours in endometriosis mice compared to Sham. The reduction in this exploratory behaviour and tendency of Endo mice to remain closer to the wall and avoid central areas (considered to be an aversive place), also known as thigmotaxis, is a reported indication of anxiety in mice [314]. Although this is in contrast to what occurs in more the invasive surgical model of endometriosis characterised in Chapter 2, whereby the CPP experienced across visceral organs was not accompanied by changes in spontaneous behaviour [297], it does reflect what is seen in women with endometriosis and CPP [315]. Women with endometriosis are at a greater risk of developing depression and anxiety, with these psychological conditions reported by many women suffering from endometriosis [306, 315]. Interestingly, high levels of anxiety and depression have been suggested to actually amplify the severity of pain in women with endometriosis [306].

In conclusion, our study has successfully demonstrated the induction of an endometriosis phenotype in mice that concurrently induces CPP, manifested as enhanced sensitivity to pain across multiple visceral and non-visceral organs. Although further elucidating specific mechanisms was not in the scope of this study, we identified that changes in pain perception *in vivo* were also accompanied by hypersensitivity of pelvic afferents innervating the bladder, *ex vivo*. To this end, we propose that this mouse model of endometriosis provides an important tool for further research into peripheral and central mediation of CPP in endometriosis, which will ultimately allow us to identify treatments targeted towards the chronic changes in pain sensitivity in endometriosis, which are currently lacking.

CHAPTER 4: PHARMACOLOGICAL MODULATION OF VOLTAGE-GATED SODIUM (Na_V) CHANNELS ALTERS NOCICEPTION ARISING FROM THE FEMALE REPRODUCTIVE TRACT

4.1 Statement of Authorship

With permission from all authors, this chapter includes an earlier version of work found in the following publication:

Publication: Castro, J*., **J. Maddern***, A. Erickson, A. Caldwell, L. Grundy, A. M. Harrington and S. M. Brierley (2020). "Pharmacological modulation of voltage-gated sodium (Na_V) channels alters nociception arising from the female reproductive tract." Pain Jan;162(1):227-242. *Contributed equally to this work.

Parts of this chapter were presented by Dr. Joel Castro in an oral presentation at the 14th World Congress of Endometriosis and in abstract form in the Australian Pain Society Newsletter – Special Edition (volume 40, issue 4, May 2020).

Students' contribution to publication:

J. Maddern*: Involved in experimental design and performed VMR, pERK experiments, tissue collection and retrograde tracing as well as assisted with single cell RT-PCR. Contributed to data analysis and preparation of figures and tables. Contributed to manuscript writing and editing.

Estimated overall percentage contribution: 40%

Co-author contributions:

Dr J. Castro*: Involved in experimental design and developed/performed all *ex vivo* afferent recording experiments. Contributed to data analysis, figure preparation, wrote and edited the manuscript. Provided supervision and expert advice.

Dr A. Erickson: Performed all patch clamp experiments, collected single cells and assisted with single cell PCR. Contributed to data analysis, figure preparation and reviewed manuscript

A. Caldwell: Performed full tissue PCR experiments and analysis. Reviewed manuscript

Dr. L Grundy, Dr. A. M. Harrington: Reviewed manuscript and provided expert advice

Prof. S. Brierley: Provided expert advice, assisted with experimental design, supervision, and interpretation of data. Contributed with manuscript writing, editing and figure layout. Corresponding author.

4.2 Overview

Dyspareunia, also known as vaginal hyperalgesia, is a prevalent and debilitating symptom of gynaecological disorders such as endometriosis. Despite their potential importance in chronic pain development, the sensory pathways transmitting nociceptive information from female reproductive organs remain poorly characterised, even in their healthy state. Although we have been able to characterise 2 mouse models of endometriosis, the knowledge gap surrounding sensory signalling from the female reproductive tract is a limiting factor in further understanding changes occurring due to chronic disease progression in endometriosis.

The vagina is innervated by nerves that regulate muscle contractility, glandular secretions, immune cell interactions and convey non-noxious and noxious stimuli to the central nervous system (CNS) for processing. How these sensory neurons (afferents) detect/transmit pain from the vagina (a key organ often affected by endometriosis) is currently unknown, which ultimately limits the mechanistic understanding of vaginal pain and treatment development for endometriosis related-CPP. To address this knowledge gap, we examined, for the first time: (1) the mechanosensory properties of pelvic afferent nerves innervating the healthy naïve mouse vagina; (2) the expression profile of key ion channels expressed within these afferents, which govern their function; and (3) how pharmacological modulation of these channels alters vaginal nociceptive signalling *ex vivo, in vitro,* and *in vivo*.

4.3 Introduction

Endometriosis and vulvodynia affect approximately 10% of women worldwide [316-321], with up to 16% of women thought to experience vulvodynia at some stage in their lives [321]. Dyspareunia, also known as vaginal hyperalgesia or painful intercourse, is one of the most debilitating symptoms experienced by women with endometriosis and vulvodynia. Despite this, the aetiology and pathogenesis of chronic pain associated with endometriosis- and vulvodynia-induced dyspareunia remains to be identified [322-325].

The first step in the pain pathway are the primary sensory afferents that project from peripheral tissues to the CNS. The colon, bladder and female reproductive organs all receive input from pelvic sensory afferent pathways [191]. Whilst many studies have characterised the properties of sensory afferent nerves innervating the colon and bladder [151]; little is known about how mechanical stimuli is detected and transmitted from female reproductive organs to the CNS. Thirty years ago, Berkley's group showed that pelvic and hypogastric afferents innervating the rat female reproductive tract fired action potentials to a variety of mechanical and chemical stimuli [326-329]. Hormonal variations occurring across the estrous cycle, pregnancy and labour also modulate the mechanosensitivity of these afferents [330-332]. Remarkably, additional studies exploring the mechanosensory properties of sensory afferents innervating female reproductive organs are lacking.

Modulation of ion channels and receptors expressed by peripheral sensory afferent nerves has shown promise in the treatment of chronic pain arising from visceral organs [142, 161, 163, 206, 305, 333]. However, only a limited number of studies have investigated the expression of nociceptive ion channels within sensory neurons projecting to female reproductive organs. Amongst these, ion channel transient receptor potential vanilloid 1 TRPV1 [205], purinergic $P2X_3$ [334], the voltage-gated sodium (Na_V) channel $Na_V1.8$ [335] and the voltage-gated potassium channels (K_V) $K_V6.4$ and $K_V2.1$ [335] have been identified, but function was not explored [335].

Recent evidence shows that modulation of Na_V channels have potential in the management of acute and chronic visceral pain [161, 285, 333, 336, 337]. Na_V channels are important determinants of sensory neuron excitability, having an essential role in the generation and propagation of action potentials and the transduction of sensory stimuli [336, 338-340]. The Na_V channel family consists of 9 isoforms ($Na_V1.1$-$Na_V1.9$) that are distinguished by their relative sensitivity to the neurotoxin tetrodotoxin (TTX), characterised as either TTX-sensitive ($Na_V1.1$ – $Na_V1.4$, $Na_V1.6$, and $Na_V1.7$) or TTX-resistant ($Na_V1.5$, $Na_V1.8$, and $Na_V1.9$) [338, 339]. Numerous channelopathies in *SCN9A* ($Na_V1.7$), *SCN10A* ($Na_V1.8$), and *SCN11A* ($Na_V1.9$) have been demonstrated to alter pain sensitivity in humans [340, 341].

Given the lack of knowledge on the sensory afferent pathways innervating female reproductive organs, the aims of this study were: 1) to examine the mechanosensory properties of

sensory afferents innervating the mouse vagina; 2) to determine the expression profile of Na_V channels contained within these afferents, 3) their contribution to vaginal afferent excitability; and 4) to determine how pharmacological modulation of these channels alters nociceptive signalling and ultimately regulation of vaginal pain sensitivity *in vivo*.

4.4 Methods

4.4.1 Animals

The Animal Ethics Committees of the South Australian Health and Medical Research Institute (SAHMRI), and Flinders University approved all experiments involving animals (ethics number SAM342). All experiments conformed to the relevant regulatory standards and the ARRIVE guidelines. Virgin female C57BL/6J mice at 8-13 weeks of age were used and acquired from an in-house C57BL/6J breeding program (JAX strain #000664; originally purchased from The Jackson Laboratory (breeding barn MP14; Bar Harbor, ME; USA) within SAHMRI's specific and opportunistic pathogen-free animal care facility, as described in Chapter 2. Female mice were group housed in IVC cages and the littermate male mice were separated at weaning. All female mice use in this study were virgin (never been mated). Vaginal lavage or other cytology test to confirm cycle stage were not performed, but it has been reported that an extended absence of male pheromones leads to a state of anestrous (lee-boot effect) [274].

4.4.2 Pharmacological modulators

Veratridine, a non-selective agonist of Na_V channels, was purchased from Sigma-Aldrich (Australia). Tetrodotoxin (TTX), a selective blocker of TTX-sensitive Na_V channels, was purchased from Tocris Biosciences (Australia). At the concentration used in this study, veratridine (50 µM) has been shown to activate TTX-sensitive and TTX-resistant Na_V channels [305, 342], whereas TTX (0.5 µM) has been shown to selectively inhibit TTX-sensitive Na_V channels [305, 338].

4.4.3 *Ex vivo* afferent recording preparation from pelvic nerves innervating the female reproductive tract

On the day of experimentation, mice were humanely killed by CO_2 inhalation and the whole female reproductive tract was removed and afferent recordings from pelvic nerves innervating the vagina area were performed. Briefly, intact female reproductive organs (vagina and uterus) were removed along with the attached neurovascular bundle containing pelvic and pudendal nerves

(Figure 4.1**A)**. The whole tissue was transferred to ice-cold Krebs solution (in mM: 117.9 NaCl, 4.7 KCl, 25 $NaHCO_3$, 1.3 NaH_2PO_4, 1.2 $MgSO_4 \cdot (H_2O)7$, 2.5 $CaCl_2$, 11.1 D-glucose); and following further dissection, the distal and central portions of the female reproductive organs were opened longitudinally **(Figure** 4.1**B)**. The tissue was pinned flat, mucosal side up, in a specialised organ bath consisting of two adjacent compartments generated from clear acrylic (Danz Instrument Service, Adelaide, South Australia, Australia), the floors of which were lined with Sylgard (Dow Corning Corp., Midland, MI) **(Figure** 4.1**B)**. The neurovascular bundle containing the pelvic nerve was extended from the tissue compartment into the recording compartment where they were laid onto a mirror. A movable wall with a small "mouse hole" (to allow passage of the nerves) was lowered into position and the recording chamber filled with paraffin oil [343]. The organ compartment was superfused with Krebs solution, bubbled with carbogen (95% O_2, 5% CO_2) at a temperature of 34°C. The pelvic nerve was dissected away from the neurovascular bundle and from the nerve sheath surrounding the nerve under a dissecting microscope. Using fine forceps, the nerve trunk was teased apart into 6–10 bundles, which were individually placed onto a platinum recording electrode **(Figure** 4.1**B)**. A separate platinum reference electrode rested on the mirror in a small pool of Krebs solution adjacent to the recording electrode. Action potentials, generated by mechanical stimuli applied to the afferent's receptive field, were recorded by a differential amplifier, filtered, and sampled (20 kHz) using a 1401 interface (Cambridge Electronic Design, Cambridge, UK).

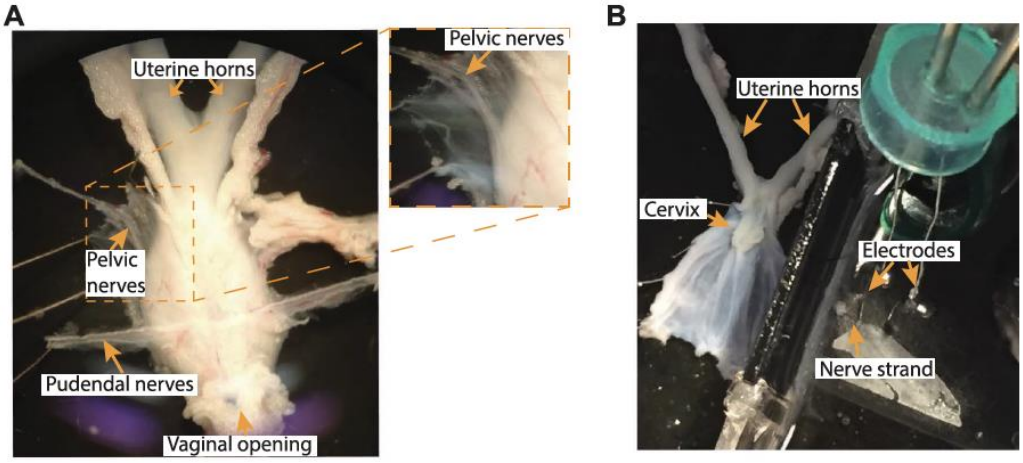

Figure 4.1: *Ex vivo* afferent recording preparation from the pelvic nerves innervating the female reproductive tract.

(A) Picture of a female reproductive tract (uterus and vagina) following removal from the mouse, and partially cleaned to expose pelvic and pudendal nerves. **(B)** Picture of our novel ex vivo single-unit extracellular afferent recording preparation from the pelvic nerves innervating the female reproductive tract. The picture demonstrates the female reproductive tract opened longitudinally and pinned flat, mucosal side up, in the left side of chamber constantly perfused with Krebs solution. Additionally, on the right-hand side of the chamber, the finely dissected pelvic nerve, still attached to the organs, lays on a glass plate within a separate chamber filled with paraffin oil to allow for nerve recordings.

4.4.3.1 Mechanosensory profile of pelvic afferents innervating the vagina

Receptive fields tested in this study were limited to the vagina (above vaginal opening and below cervix) and were identified by systematically stroking the mucosal surface of the vagina with a stiff brush to activate all subtypes of vaginal mechanoreceptors. In order to study baseline mechanosensory properties of the pelvic afferents innervating a particular receptive field within the vagina, three distinct mechanical stimuli were tested: i) static probing with calibrated von Frey hairs (vfh; 2 g force; applied 3 times for a period of 3 sec); ii) mucosal stroking of the vaginal surface with calibrated vfh (10-1000 mg force; applied 10 times each); or iii) circular stretch (5 g; applied for a period of 1 minute). Stretch was applied using a claw made from bent dissection pins attached to the tissue adjacent to the afferent receptive field and connected to a cantilever system with thread [343]. Weights were applied to the opposite side of the cantilever system to initiate stretch. Only circular, and not longitudinal, stretch was tested in this study. Once baseline mechanosensitivity was tested, a small chamber was then placed onto the mucosal surface of the vagina, surrounding the afferent receptive field. Residual Krebs solution within the chamber was aspirated and the Na_V channel pharmacological modulators, veratridine (50 µM) and TTX (0.5 µM), were applied in separate experimental preparations for 5 minutes each. Mechanical sensitivity of the afferent receptive field was then re-tested in response to the three distinct mechanical stimuli previously tested.

4.4.3.2 Statistical analysis of afferent recording data

Action potentials were analysed off-line using the Spike 2 (version 5.21) software (Cambridge Electronic Design, Cambridge, UK) and discriminated as single units based on distinguishable waveforms, amplitudes, and durations. Data are expressed as mean ± SEM. n = the number of afferents recorded, N = the number of animals used for those specific experiments. Data were statistically compared using Prism 7 software (GraphPad Software, San Diego, CA, USA) and, where appropriate, were analysed using paired or un-paired two-tailed Student *t* test and one- or two-way analysis of variance (ANOVA) with Bonferroni post hoc tests. Differences were considered statistically significant at $*P < 0.05$, $**P < 0.01$, $***P < 0.001$, $****P < 0.0001$.

4.4.4 Identification and culture of dorsal root ganglia (DRG) neurons innervating the vagina

Retrograde labelling was performed to identify DRG neurons innervating the vagina. Cholera toxin subunit B (0.5%) conjugated to AlexaFluor® 488 (diluted in 0.1 M phosphate buffer, pH = 7.35; Invitrogen, Carlsbad, CA) was injected (2 µL / injection site) at five different sites into the vaginal wall. Injections were made using a Hamilton syringe attached to a 23-gauge needle. A tunnelling method was used, whereby the tip of the needle is inserted into the vaginal wall, approximately 0.2 cm from the vaginal opening and tunnelled an additional 0.2 cm in a cranial direction within the vaginal wall. The tracer is then expelled as the needle is gradually extracted from the needle tract.

This ensures that a greater area of the vaginal wall is exposed to the dye compared to localised injections at the needle insertion points. Mice were then allowed to recover, housed individually and closely monitored. All mice recovered quickly and showed no adverse signs. Four days after vaginal tracing, mice were humanely euthanised via CO_2 inhalation and lumbosacral (LS; L5-S1) dorsal root ganglia (DRG) were removed. DRG were digested in Hanks' balanced salt solution (HBSS; pH 7.4; Life Technologies, #14170161) containing 2.5 mg/mL collagenase II (GIBCO, ThermoFisher Scientific, #17101015) and 4.5 mg/mL dispase (GIBCO, ThermoFisher Scientific, #17105041) at 37°C for 30 min. The collagenase-dispase solution was aspirated and replaced with HBSS containing collagenase (4.5 mg/mL) only for 10 minutes at 37°C. Following subsequent washes in HBSS, DRG were mechanically disrupted and cells dissociated in 600 µL complete DMEM (Dulbecco's Modified Eagle Media [DMEM; GIBCO, ThermoFisher Scientific, #11995065]; 10% Fetal Calf Serum [Invitrogen, ThermoFisher Scientific, MA, USA]; 2 mM L-glutamine [GIBCO, ThermoFisher Scientific, #25030081], 100 µM MEM non-essential amino acids [GIBCO, ThermoFisher Scientific, #11140076], 100 mg/mL penicillin/streptomycin [GIBCO, ThermoFisher Scientific, #15070063], and 96 µg/L nerve growth factor-7S [Sigma, N0513-0.1MG]) via trituration through fire-polished Pasteur pipettes of descending diameter, and centrifuged for 1 min at 50×*g* [158, 159, 285, 337, 344-346]. Neurons were resuspended in 300 µL complete DMEM and spot-plated (20 µL) onto 13 mm coverslips coated with laminin (20 µg/mL; Sigma-Aldrich, #L2020) and poly-D-lysine (800 µg/mL; ThermoFisher Scientific). Coverslips were incubated at 37°C in 5% CO_2 for 2-3 hours to allow neurons to adhere before flooding with 1.7 mL complete DMEM. Neurons collected for single-cell RT-PCR 12 to 24 hours post dissociation or were recorded from using patch-clamp electrophysiology 20 to 48 hours post dissociation.

4.4.5 Reverse transcription-polymerase chain reaction (RT-PCR) of individual vagina-innervating DRG neurons

4.4.5.1 Neuron collection and lysis

Dissociated DRG neurons from vagina-traced mice were perfused with bath solution and picked into the end of an air-filled wide aperture borosilicate glass pipette fabricated in the P-97 (Sutter Instruments, Novato, CA) pipette puller 12 to 24 hours post dissociation. A separate pipette was used to sample bath solution to assess RNA contamination. The end of the glass pipette containing the collected neuron was broken into a sterile Eppendorf tube containing 10 µL of lysis buffer with DNase (ThermoFisher, TaqMan Gene Expression Cells-to-CT Kit, cat # AM1728). Incubation with lysis buffer occurred for 5 to 10 minutes at room temperature, followed by addition of 1 µL DNase stop solution and incubation for a further 5 to 10 minutes at room temperature. Lysates were frozen on dry ice and stored at -80°C until cDNA synthesis was performed.

4.4.5.2 cDNA synthesis

Synthesis of cDNA was performed using the SuperScript VILO IV EzDNase (ThermoFisher, cat #11766050) kit according to manufacturer's instructions. Each cDNA synthesis batch included one reverse transcriptase (RT) negative control to assess genomic DNA contamination. Synthesised cDNA was stored at -20°C until PCR was performed.

4.4.5.3 RT-PCR

For each RT-PCR reaction, 10 µL of PCR Master mix, 0.5 µL of each TaqMan primer (see **Table** 4.1 below for details), 8 µL of water, and 1.6 µL cDNA from each sample was tested in singlicate for each target. *Tubb3* was used as a neuronal marker. RT controls, bath controls, negative controls (water instead of cDNA) were routinely included in PCR reactions, and a positive control test was performed for each primer using cDNA synthesised from whole DRG RNA. Assays were run for 50 cycles on a 7500 Fast Real-Time PCR System (Applied Biosystems, Victoria, Australia) machine, using 7500 Fast software, v2.0.6. Genes were considered expressed if a complete amplification curve was obtained within 50 cycles.

Table 4.1: TaqMan primers used for qRT-PCR and single cell RT-PCR, obtained from Life Technologies

GENE ALIAS	GENE TARGET	ASSAY ID
Hypoxanthine-guanine phosphoribosyltransferase 1 (reference gene)	*Hprt*	Mm00446968_m1
Glyceraldehyde 3-phosphate dehydrogenase (reference gene)	*Gapdh*	Mm99999915_g1
$Na_V1.1$	*Scn1a*	Mm00450580_m1
$Na_V1.2$	*Scn2a1*	Mm01270359_m1
$Na_V1.3$	*Scn3a*	Mm00658167_m1
$Na_V1.4$	*Scn4a*	Mm00500103_m1
$Na_V1.5$	*Scn5a*	Mm01342518_m1
$Na_V1.6$	*Scn8a*	Mm00488110_m1
$Na_V1.7$	*Scn9a*	Mm00450762_s1
$Na_V1.8$	*Scn10a*	Mm00501467_m1
$Na_V1.9$	*Scn11a*	Mm00449367_m1
Tubulin, beta 3 class III	*Tubb3*	Mm00727586_s1

4.4.6 Quantitative RT-PCR (qRT-PCR) of whole lumbosacral DRG and vaginal tissue

4.4.6.1 Tissue collection

DRG (L5-S1) and vaginal tissues were collected immediately after euthanasia by CO_2 inhalation. For DRG, whole lumbosacral DRG were surgically removed, snap frozen, and stored at -80°C before RNA extraction. Vaginal tissues were collected by removing the whole female reproductive tract and dissecting away the cervix, uterus and uterine horns. The remaining/sole vaginal tissue was then snap frozen and stored at -80°C before RNA extraction.

4.4.6.2 RNA extraction

RNA was extracted using the PureLink RNA Micro kit (Invitrogen, Victoria, Australia, cat #12183-016; DRG) or the PureLink RNA Mini kit (Invitrogen, cat #12183018A; vaginal tissue) followed by a DNAse treatment (Life Technologies, cat #12185-010) according to the manufacturer's instructions.

4.4.6.3 Quantitative Reverse transcription-polymerase chain reaction

QRT-PCR was performed using Express qPCR Supermix (Applied Biosystems, Victoria, Australia, cat # 11785200) with commercially available hydrolysis probes (TaqMan; Life Technologies, see **Table** 4.1 above for details) and RNAse-free water (AMBION, Victoria, Australia, cat #AM9916). For each reaction, 10 μL of qPCR SuperMix, 1 μL of TaqMan primer, 2 μL RT enzyme mix, 2 μL of water, and 5 μL of RNA (diluted in RNAse-free H_2O to approximately 100ng/well) from each sample was tested in duplicate for each Na_V channel subtype. *Hprt* and *Gapdh* were used as endogenous controls for all tissues. Assays were run for 50 cycles on a 7500 Fast Real-Time PCR System (Applied Biosystems) machine, using 7500 Fast software, v2.0.6. Quantity of mRNA is expressed as ΔCt relative to the geometric mean of reference genes Hprt and Gapdh.

4.4.7 Whole-cell current-clamp and voltage-clamp electrophysiology of vagina-innervating DRG neurons

Dissociated DRG neurons isolated from vagina-traced mice were recorded in current-clamp mode on day 1 post culturing (20 to 30 hours) and in voltage-clamp mode on day 1 and day 2 post culturing (20 to 48 hours). Neurons patched in this study were small to medium in size, with an average diameter of 27 ± 1 μm.

4.4.7.1 Solutions and pipettes

Intracellular current-clamp solution contained (in mM): 135 KCl; 2 $MgCl_2$; 2 MgATP; 5 EGTA-Na; 10 HEPES-Na; adjusted to pH 7.3. Extracellular (bath) current-clamp solution contained (in mM): 140 NaCl; 4 KCl; 2 $MgCl_2$; 2 $CaCl_2$; 10 HEPES; 5 glucose; adjusted to pH 7.4. Intracellular voltage-clamp solution contained (in mM): 60 CsF; 45 CsCl; 2 $MgCl_2$; 5 EGTA-Na; 10 HEPES-Cs; 30 TEA-

Cl; 2 MgATP; adjusted to pH 7.2 with CsOH, 280 mOsm. Extracellular (bath) voltage-clamp solution contained (in mM): 70 NaCl; 50 NMDG; 40 TEA-Cl; 4 CsCl; 2 $MgCl_2$; 2 $CaCl_2$; 10 HEPES; 5 Glucose; adjusted to pH 7.4, approximately 300 mOsm. Standard wall borosilicate glass pipettes (OD x ID x length: 1.5 mm x 0.86 mm x 7.5 cm, Harvard, cat # 64-0792) were pulled and fire-polished to 3-10 MΩ for current-clamp recordings, and 1-3 MΩ for voltage-clamp recordings using a P-97 (Sutter Instruments) pipette puller.

4.4.7.2 Protocols

Responses to TTX (0.1 μM continually perfused by a gravity) were recorded at 1 minute after start of perfusion. For current-clamp recordings, two baseline responses were measured (1 minute apart) to assess stability of recording. Only cells with a difference of ≤ 1 current step in rheobase at baseline were included in the analysis. For voltage-clamp recordings, maximum peak current was monitored until reaching a stable amplitude before proceeding with compound application. In current-clamp mode, neurons were held at -70 mV for 15 ms, hyperpolarised by a -20 pA current injection for 475 ms, then held at -70 mV for 100 ms. Stepwise depolarising pulses in increments of 10 pA were applied from holding potential of -70 mV with 2 sec repetition intervals to determine the rheobase (minimum amount of current required to fire an action potential). Current-voltage (I_{Na}-V) relationships were determined by application of a pre-pulse to -100 mV (100 ms), followed by a series of step pulses from -65 mV to +60 mV (5 mV increments (100 ms)), before returning to hold at -70 mV (repetition interval of 3 sec, P/8 leak subtraction). Voltage dependence of steady-state fast inactivation was determined by application of a series of pre-pulses from -110 to +2.5 mV (7.5 mV increments (100 ms)), then a pulse at -30 mV or -10 mV depending on current amplitude, followed by hold at -70 mV (50 ms) (3 second repetition interval).

Diameter measurement: To determine average neuron diameter, the smallest and largest width of the neuronal soma was measured using the microscope eyepiece reticle calibrated with a stage micrometre and averaged.

Exclusion criteria: For current-clamp recordings, neurons were not recorded if the resting membrane potential was more depolarized than -40 mV as this is an indicator of poor cell health. For voltage-clamp recordings, only recordings with voltage error of less than 5 mV were used for analysis.

4.4.7.3 Data acquisition and analysis

Recordings were amplified with Axopatch 200A, digitised with Digidata 1322A, sampled at 20 kHz, filtered at 5 kHz, recorded with pCLAMP 9 software (Molecular Devices), and analysed in Clampfit 10.3.2 (Molecular Devices), Prism v8.0.0 (GraphPad), and IBM SPSS Statistics v25.

4.4.8 In vivo vaginal distension activation of spinal cord dorsal horn neurons identification by phosphorylated MAP kinase ERK 1/2 (pERK)

4.4.8.1 In vivo vaginal distension

Vehicle (saline), veratridine (50 µM), or TTX (0.5 µM) were administered intravaginally via a small canula inserted into the mice vaginal canal under isoflurane anaesthesia. Immediately after, and still under anaesthesia, a 3 mm length (~4 mm diameter when fully inflated) balloon catheter was inserted into the vaginal canal. Mice were removed from the isoflurane chamber, and, on regaining consciousness, the balloon was distended for 30 seconds to 40 mm Hg applied via a syringe attached to a sphygmomanometer pressure gauge. After 30 seconds, the pressure was released, and the balloon deflated (0 mm Hg) for 10 seconds. This process was repeated 5 times. After the fifth distension, mice were given an anaesthetic overdose (0.125 mL/250 g Lethabarb) and by 5 minutes, had undergone transcardial perfuse fixation.

4.4.8.2 Transcardial perfuse fixation and tissue processing

After anaesthetic overdose, the chest cavity was opened and 0.5 mL of heparin saline was injected into the left ventricle followed by insertion of a 22-gauge needle, attached to tubing and a peristaltic perfusion pump. The right atrium was snipped, allowing for perfusate drainage. Warm saline (0.85% physiological sterile saline) was perfused before ice-cold 4% paraformaldehyde in 0.1 M phosphate buffer (Sigma-Aldrich, St. Louis, MO). After complete perfusion, L6-S2 spinal cord segments (determined by level of DRG root insertion points) were removed and postfixed in 4% paraformaldehyde in 0.1M phosphate buffer at 4°C for 18 to 20 hours. The lowest rib was used as an anatomical marker of T13. After post-fixation, spinal cords were cryoprotected in 30% sucrose/phosphate buffer (Sigma-Aldrich) overnight at 4°C and then an additional 24-hour incubation at 4°C in 50% OCT/30% sucrose/phosphate buffer solution before freezing in 100% OCT. Spinal cords were cryosectioned (10 µm thick) and placed onto gelatine-coated slides for immunofluorescence labelling. Spinal cord segments were serially sectioned and distributed over 6 slides, which were used for auto staining of neuronal activation marker phosphorylated MAP kinase ERK 1/2 (pERK) [112].

4.4.8.3 Spinal cord–phosphorylated MAP kinase ERK 1/2 (pERK) immunofluorescence

The spinal cord dorsal horn neurons activated by vaginal distension were identified by labelling for neuronal activation marker pERK using primary antibody (pERK; 1:800) in Antibody Diluent (S0809, Agilent DAKO) with 3,3′-Diaminobenzidine (DAB) / horseradish peroxidase (HRP) secondary antibody staining. After air drying for 1 hour, sections were post-fixed in formalin with a brief rinse in distilled water prior to target antigen retrieval with EnVision FLEX TRS Low pH target retrieval solution (citrate buffer, pH 6.1; K8005, Agilent DAKO). Nonspecific binding of secondary antibodies was blocked with Serum-Free Protein Block (X0909, Agilent DAKO). Tissue sections were incubated with primary antisera for 1 hour, washed and incubated for 3 minutes in Envision FLEX Peroxidase-blocking Reagent (GV823, Agilent DAKO), followed by 20-minute incubation with

Envision FLEX HRP Polymer (GV823, Agilent DAKO) for HRP binding. Negative controls were prepared as above with the primary antibody omitted. Sections were then washed in wash buffer (GC807, DAKO Omnis, Agilent) before a 10-minute incubation in EnVision FLEX Substrate Working Solution (DAB) for staining. Following further wash cycles, slides underwent a 3-minute incubation with Haematoxylin ready to use solution (K8018, Agilent DAKO) before being rinsed and removed from the DAKO Omnis, dehydrated in alcohol and cleared in xylene. Slides were mounted with Dibutylphthalate Polystyrene Xylene (DPX, Sigma-Aldrich) and cover slipped.

4.4.8.4 Microscopy

DAB/HRP-stained slides were imaged using a 3DHistech Panoramic 250 Flash II slide scanner at 40x using the autofocus setting (SAHMRI Histology Slide Scanning Service). Images of individual sections from L6–S2 regions were taken using digital pathology viewing software (QuPath 0.1.2) and analysed using ImageJ software. The images were not manipulated in any way.

4.4.8.5 Spinal cord pERK neuronal counts

Neuronal counts were analysed from previously saved digital photomicrographs, with only neurons with intact nuclei counted. The number of pERK-immunoreactive (IR) dorsal horn neurons/animal was obtained from a minimum of 6 sections/animal/spinal segment (L6-S2). The total number of pERK-IR neurons from the dorsal horn overall and selectively from dorsal horn regions was then averaged across mice following 40 mm Hg pressures of vaginal distension after vehicle, TTX (0.5 µM) or veratridine (50 µM) vaginal infusion prior to balloon insertion. The selective dorsal horn regions analysed were defined as the superficial dorsal horn (Lamina LI-II), lamina LIII-V, dorsal grey commissure (DGC), lateral spinal nucleus (LSN) and the sacral parasympathetic nucleus (SPN, only in S1-S2 spinal segments) (**Figure 4.2**). Selection of the dorsal horn regions were on based on previous published work [347] and the Allen Spinal Cord Atlas available from https://mousespinal.brain-map.org.

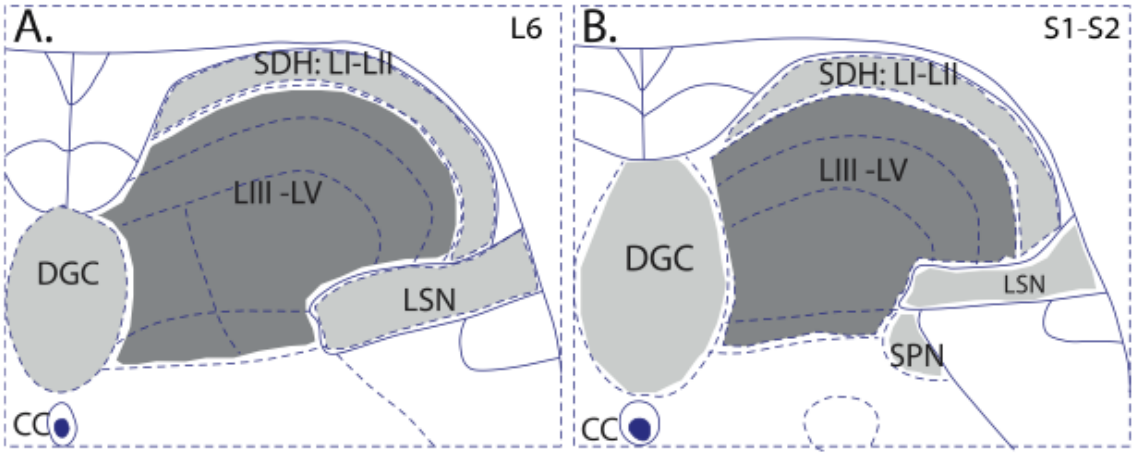

Figure 4.2: Schematic overview of the mouse lumbosacral spinal cord (L6-S2).

(A-B) Illustration of a cross section of the lumbosacral spinal cord (L6-S2) showing dorsal horn laminae and regions in which the number of pERK-IR neurons was compared between experimental groups. Map adapted from 2008 Allen Institute for Brain Science©. Allen Spinal Cord Atlas. Available from: https://mousespinal.brain-map.org.

4.4.8.6 Statistical analysis of pERK-IR

Ordinary one-way ANOVA followed by Bonferroni's multiple comparison post-hoc test was used to compare the number of pERK-IR neurons between different treatments in different regions of the dorsal horn. Differences were considered statistically significant at **P* <0.05, ***P* <0.01, ****P* <0.001. Averaged data values are expressed as mean ± SEM. Figures were prepared in GraphPad 7.02. Software (San Diego, CA, USA). N represents number of animals per group, whilst n represents the number of neurons or independent observations.

4.4.9 Visceromotor response (VMR) to vaginal distension (VD): assessment of vaginal pain sensitivity in vivo

The visceromotor response (VMR) is a nociceptive brainstem reflex consisting of the contraction of the abdominal muscles in response to noxious distension of hollow organs such as the vagina [92, 195] and the colorectum [110, 157, 159, 161, 279-281]. We recorded the VMR to vaginal distension (VD) as an objective measurement of vaginal sensitivity to pain in fully conscious animals [92, 115, 175, 176, 186, 195, 273, 282].

4.4.9.1 Surgical implantation of electromyography (EMG) electrodes

The VMR was objectively assessed by electromyography (EMG) to quantify abdominal muscle contractions in response to VD, as described in Chapter 2, with EMG electrodes implanted in the abdominal musculature at least 3 days prior to VMR assessment.

4.4.9.2 Assessing visceromotor responses (VMR) to vaginal distension (VD)

On the day of VMR assessment, animals were briefly sedated with isoflurane and vehicle (saline), veratridine (50 µM), or TTX (0.5 µM) were administered intravaginally via a small canula inserted into the vaginal canal, immediately followed by insertion of a 3-mm balloon catheter. VMR to VD was measured as described in Chapter 2. Distensions were applied from the non-noxious to the noxious range (20-30-40-60-70-80 mm Hg, 30 seconds duration at 3-minute intervals between consecutive distensions). Each VMR VD protocol was completed within 30 minutes of either saline, veratridine or TTX administration.

4.4.9.3 Statistical analysis of VMR to VD data

To quantify the magnitude of the VMR at each distension pressure, the area under the curve (AUC) during the distension (30 seconds) was corrected for the baseline activity (AUC pre-distension, 30 seconds). Total AUC was quantified by adding the individual AUC at each distension pressure. VMR data are presented as mean ± SEM, and N represents the number of animals. VMR data were statistically analysed by generalised estimating equations (GEE) followed by LSD post hoc test when appropriate using SPSS 23.0. Analysis and figures were prepared in GraphPad Prism 7 Software, San Diego, CA, USA. Differences were considered statistically significant at $*P < 0.05$, $**P < 0.01$, $***P < 0.001$.

4.5 Results

4.5.1 Mechanosensory profile of pelvic sensory afferents innervating the female reproductive tract

The peripheral terminals of sensory neurons innervating visceral organs are equipped to detect a variety of mechanical stimuli [142, 151]. There is a great body of knowledge illustrating how mechanical stimuli is detected by visceral organs such as the colon [112, 343, 348] and the bladder [162, 303, 305], however little is known about how mechanical stimuli is sensed by the female reproductive organs. To reduce this knowledge gap, we developed a novel *ex vivo* preparation to characterise the mechanosensory profile of pelvic afferents innervating the female reproductive tract of the mouse **(Figure** 4.1**)**.

We found that pelvic afferent nerve terminals had small (~0.5 mm) punctate receptive fields from which action potentials were evoked in response to the application of mechanical stimuli. Receptive fields for these individual afferents were distributed throughout the length of the vagina **(Figure** 4.3**A)**. Overall, the majority of afferents recorded were silent at rest, with only 21.4% (3 of 14) of the afferents showing low rates of spontaneous activity.

To examine the mechanosensory properties of the nerve fibres from a particular receptive field, three distinct mechanical stimuli were tested. We examined the effect of: i) static focal compression of the receptive field with a calibrated 2 g von Frey hairs (vfh) **(Figure** 4.3**B)**; ii) fine stroking of the vaginal mucosa surface with calibrated (10-1000 mg) vfh **(Figure** 4.3**C)**; and iii) 5 g circular stretch of the vagina, applied via a cantilever system **(Figure** 4.3**D)**. Interestingly, we found that the entire population of vaginal afferents tested (total of 14 afferents from 8 mice) responded to all three mechanical stimuli tested **(Figure** 4.3**E)**. We also found that fine stroking of the vaginal mucosal surface and static probing of the receptive fields readily evoked discharge of action potentials throughout the duration of the stimulus **(Figure** 4.3**B-C)**.

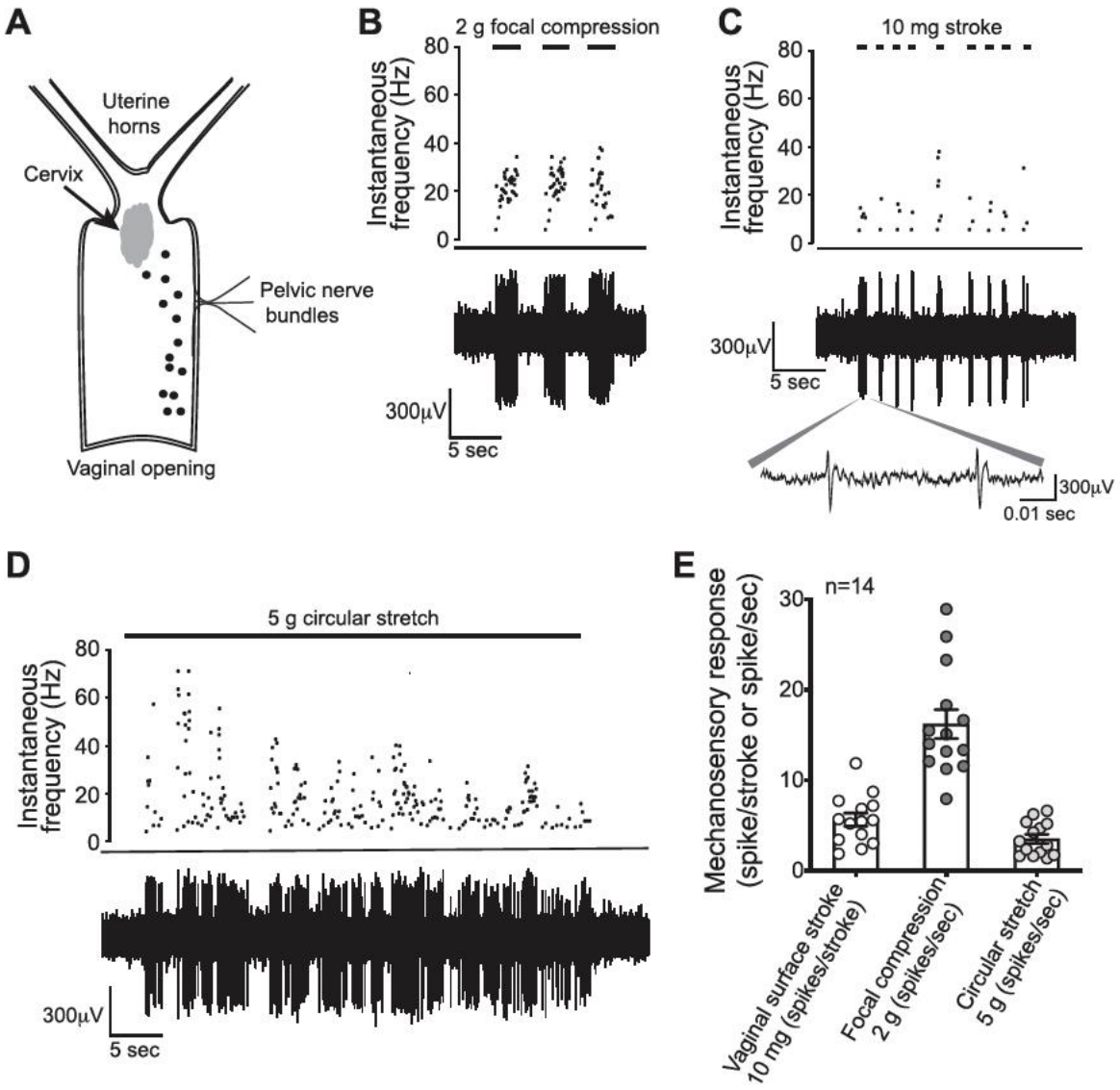

Figure 4.3: Mechanosensory profile of pelvic afferents innervating the mouse vagina

(A) Schematic diagram of the *ex vivo* female reproductive tract preparation. Pelvic afferent receptive fields (indicated by black circles) were distributed down the entire length of the vagina. **(B)** Representative traces obtained with our novel *ex vivo* single-unit extracellular nerve recording preparation, showing action potential discharge in response to focal compression of the afferent receptive field with a 2 g von Frey hair (vfh) filament. The same pelvic vaginal afferent also responded to **(C)** fine stroking of the vaginal mucosa surface with a 10 mg vfh, and **(D)** circular stretch of the whole tissue. The inset below panel C shows an enhanced area of the nerve recording, demonstrating individual action potentials. **(E)** Grouped data from *ex vivo* single-unit extracellular nerve recording preparation showing the response of 14 different pelvic vaginal afferents to the three mechanical stimuli tested. Grouped data are from n = 14 afferents from N = 8 mice. Data represent mean ± SEM.

4.5.2 Mechanically evoked responses of pelvic vaginal afferents can be modulated by targeting voltage-gated sodium (Na_V) channels

We have recently determined that Na_V channels expressed within the cell bodies of sensory afferents that travel from the colon and bladder to the central nervous system are potential

therapeutic targets for treatment of acute and chronic visceral pain [161, 285, 305, 333, 336, 337]. With this in mind, we used our novel *ex vivo* afferent recording preparation to determine whether pharmacological modulation of Na_V channels could alter mechanosensory properties of pelvic afferents innervating the vagina.

Application of the pan-Na_V channel agonist, veratridine, resulted in significant increases in pelvic vaginal afferent responses to focal compression **(Figure** 4.4**A)**, mucosal stroking **(Figure** 4.4**B)** and circular stretch **(Figure** 4.4**C)** compared with their normal baseline responses. Veratridine did not evoke action potential firing in the absence of mechanical stimuli.

Exposure of vaginal afferent endings to the neurotoxin TTX (blocker of the TTX-sensitive $Na_V1.1$-$Na_V1.4$, $Na_V1.6$, and $Na_V1.7$ channels) significantly reduced, but did not completely block, vaginal afferent responses to focal compression **(Figure** 4.4**D)**, mucosal stroking **(Figure** 4.4**E)**, and circular stretch **(Figure** 4.4**F)**. Overall, these findings indicating both TTX-sensitive and TTX-resistant Na_V channels are involved in vaginal afferent responses to mechanical stimulation.

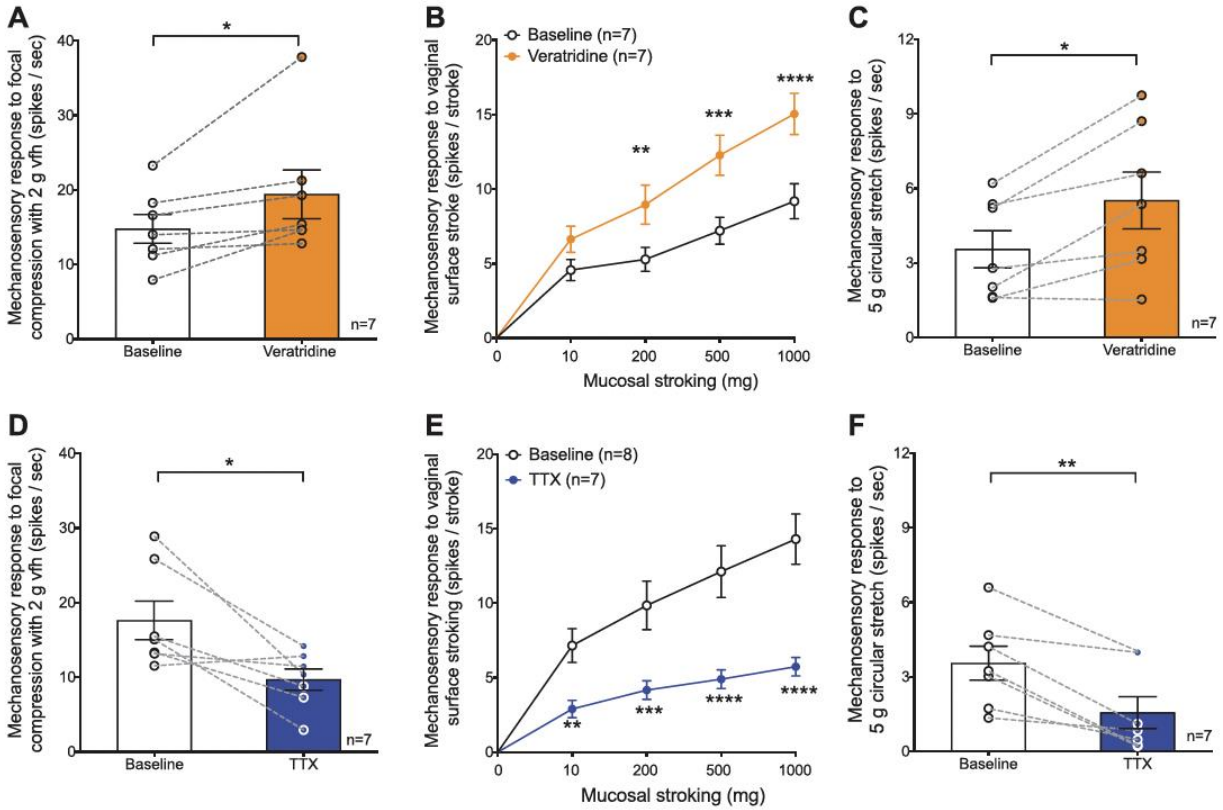

Figure 4.4: Responses of pelvic vaginal afferents to mechanical stimuli can be altered *ex vivo* by Na_V channel modulators

(A-C) Grouped data obtained with the *ex vivo* single-unit extracellular nerve recording preparation, showing that veratridine application (50 µM for 5 minutes) to the luminal side of the organ preparation increases pelvic vaginal afferent sensitivity to three different mechanical stimuli. **(A)** Baseline mechanosensory response (number of spikes per second) to focal compression of the vaginal afferent receptive field was significantly increased after incubation with veratridine (**P* <0.05, paired two-tailed Student *t* test, n = 7 afferents from N = 6 mice). Additionally, veratridine enhanced baseline mechanosensitivity of vaginal afferents to **(B)** mucosal stroking with calibrated von Frey hairs (***P*

<0.01 for 200 mg stroking, ***P <0.001 for 500 mg stroking and ****P <0.0001 for 1000 mg stroking, two-way ANOVA with Bonferroni post-hoc comparison tests, n = 7 afferents from N = 6 mice) and **(C)** circular stretch of the whole tissue (*P <0.05, paired two-tailed Student *t* test, n = 7 afferents from N = 6 mice). **(D-F)** Grouped data obtained with the *ex vivo* single-unit extracellular nerve recording preparation showing that tetrodotoxin application (TTX; 0.5 µM for 2 minutes) to the luminal side of the organ preparation decreases pelvic vaginal afferent sensitivity to three different mechanical stimuli. **(D)** The mechanosensory response (number of spikes per second) to focal compression of the vaginal afferent receptive field was significantly reduced after incubation with TTX (*P <0.05, paired two-tailed Student *t* test, n = 7 afferents from N = 5 mice). Additionally, TTX reduced the mechanosensitivity of vaginal afferents to **(E)** mucosal stroking with calibrated vfh (**P <0.01 for 10 mg stroking, ***P <0.001 for 200 mg stroking, ****P <0.0001 for 500 and 1000 mg stroking, two-way ANOVA with Bonferroni post-hoc comparison tests, n = 7 afferents from N = 5 mice) and (F) circular stretch of the whole tissue (**P <0.01, paired two-tailed Student *t* test, n = 7 afferents from N = 5 mice). Data represent mean ± SEM.

4.5.3 Pharmacological modulation of Na_V channels alters the excitability of dorsal root ganglia (DRG) sensory neurons innervating the vagina

Given the significant effect of Na_V channel modulation on altering pelvic vaginal afferent responses to mechanical stimuli, we investigated the relative expression of these channels within sensory neurons innervating the vagina, and whether pharmacological modulation of these channels could alter the electrophysiological properties of vaginal-innervating DRG neurons.

First, we investigated whether Na_V channels were indeed expressed by individual DRG sensory neurons innervating the vagina. Using single-cell RT-PCR, we determined mRNA expression of all members of the Na_V channel family ($Na_V1.1$-$Na_V1.9$) in 39 individual vagina-innervating DRG neurons, identified by retrograde labelling. Overall, we found that all Na_V channel family members were expressed throughout the population of retrogradely labelled vaginal-innervating DRG neurons examined **(Figure 4.5)**. We found three general patterns of expression, with Na_V channel transcripts expressed by either a large number ($Na_V1.7$: 100%, $Na_V1.8$: 97%), a moderate number ($Na_V1.9$: 62%; $Na_V1.6$: 59%; $Na_V1.2$: 54%; $Na_V1.1$: 33%) or a small number ($Na_V1.5$: 26%; $Na_V1.3$: 21%; $Na_V1.4$: 13%) of vaginal-innervating DRG neurons **(Figure 4.5A)**. The expression and co-expression patterns of Na_V channel transcripts was heterogeneous amongst neurons, with only a small proportion of cells expressing the same pattern of Na_V channel transcripts with no cells expressing the full repertoire of $Na_V1.1$-1.9 **(Figure 4.5B-C)**.

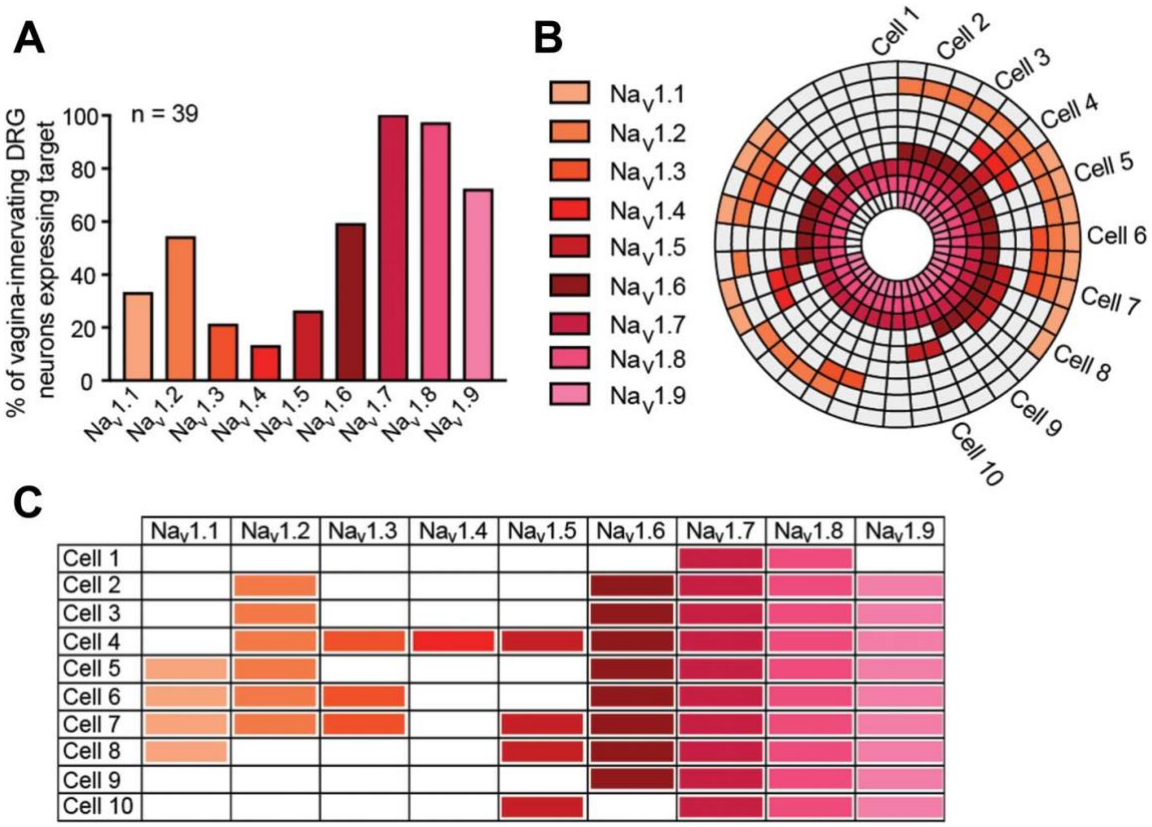

Figure 4.5: Voltage-gated sodium (Na_V) channels are expressed in DRG neurons innervating the mouse vagina

(A) Single-cell RT-PCR of retrogradely traced vagina-innervating LS DRG neurons shows the percentage of neurons expressing genes encoding Na_V channels (*Scn1a-Scn11a*) (n = 39 single cells from N = 5 mice). Our RT-PCR results revealed that 54% to 100% of all vagina-traced DRG neurons expressed $Na_V1.2$ (*Scn2a*: 54%), $Na_V1.6$ (*Scn8a*: 59%), $Na_V1.9$ (*Scn11a*: 72%), $Na_V1.8$ (*Scn10a*: 97%) and $Na_V1.7$ (*Scn9a*: 100%). Transcripts from the other members of the Na_V channel family were found in considerably fewer vaginal-innervating DRG neurons $Na_V1.4$ (*Scn4a*: 13%), $Na_V1.3$ (*Scn3a*, 21%), $Na_V1.5$ (*Scn5a*, 26%) and ($Na_V1.1$ (*Scn1a*, 33%). **(B)** Donut plot showing expression and co-expression of genes encoding Na_V channels ($Na_V1.1$-1.9) in 39 individual retrogradely traced vagina-innervating DRG neurons. Each colour represents an individual gene with expression marked by bold (see legend). *Scn1a* ($Na_V1.1$) is represented in the outer ring, and *Scn11a* ($Na_V1.9$) in the inner ring. Individual neurons are arranged radially, such that co-expression of genes in a single neuron can be easily identified running from outside to inside. **(B-C)** Individual neurons showed significant heterogeneity of expression and substantial co-expression of Na_V channels in individual retrogradely traced DRG neurons. Some cells express all the channel isoforms except $Na_V1.1$ (cell 4) or $Na_V1.4$ (cell 7), whilst other cells only express $Na_V1.7$, and $Na_V1.8$ (cell 1). The majority of the cells express mRNA for $Na_V1.6$ (59%), $Na_V1.7$ (100%), $Na_V1.8$ (97%) and $Na_V1.9$ (72%). DRG, dorsal root ganglia; RT-PCR, reverse transcription-polymerase chain reaction.

We also determined the mRNA expression profile of Na_V channel transcripts within the vaginal tissue, with QRT-PCR revealing an overall very low level of abundance **(Figure 4.6)**. $Na_V1.7$ was the most abundantly expressed Na_V channel in vaginal tissue, whilst $Na_V1.2$-1.6 had even lower

abundance **(Figure 4.6)**. $Na_V1.1$, $Na_V1.8$, $Na_V1.9$ expression in vaginal tissue was below detection limits **(Figure 4.6)**. Our QRT-PCR data showed that Na_V expression was approximately 200-1000-fold lower in vaginal tissue that in whole lumbosacral DRG **(Figure 4.6)**.

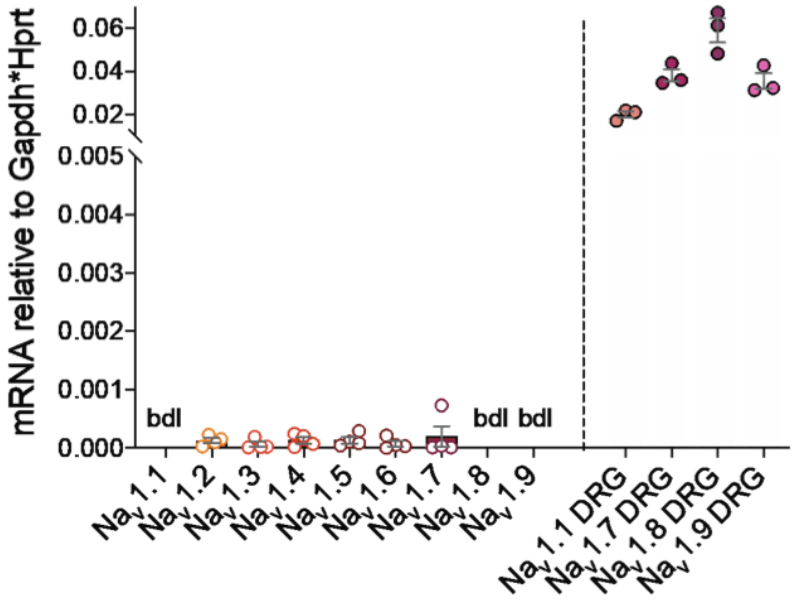

Figure 4.6: mRNA expression profile of Na_V transcripts within the mouse vagina and whole LS DRG.

Na_V channel ($Na_V1.1$- $Na_V1.9$) mRNA expression in vaginal tissue relative to the housekeeper genes Gapdh*Hprt (left of dashed line). $Na_V1.7$ is the most expressed Na_V transcript in the vagina. $Na_V1.2$-1.6 are barely detected, whilst $Na_V1.1$ and $Na_V1.8$-1.9 are below the level of accurate detection. Vaginal tissues were obtained from N = 4 mice. $Na_V1.1$ and $Na_V1.7$-1.9 expression in LS DRG (right of dashed line) are provided as a reference. LS DRG were bilaterally obtained from N = 3 mice. DRG, dorsal root Ganglia.

We next examined whether inhibition of TTX-sensitive Na_V channels could alter electrophysiological properties of isolated vagina-innervating DRG neurons using whole-cell patch-clamp electrophysiology **(Figure** 4.7**).** At baseline conditions in voltage-clamp mode, vagina-innervating DRG neurons exhibited large voltage-dependent sodium currents, which were significantly reduced in amplitude (by 40.9 ± 9.2%) following a 1-minute incubation with TTX **(Figure** 4.7**A i-iv)**. Furthermore, in current clamp mode the threshold for action potential generation (rheobase) was significantly increased (2.1 ± 0.2-fold) in the presence of TTX in 78% (35 of the 45) neurons examined **(Figure** 4.7**B i-iv)**. These findings reflect a decrease in neuronal excitability of vagina-innervating DRG neurons when TTX-sensitive Na_V isoforms are blocked. Overall, these results indicate that modulating Na_V channels expressed in sensory afferent neurons that innervate the female reproductive tract alters neuronal excitability, hence their ability to fire action potentials.

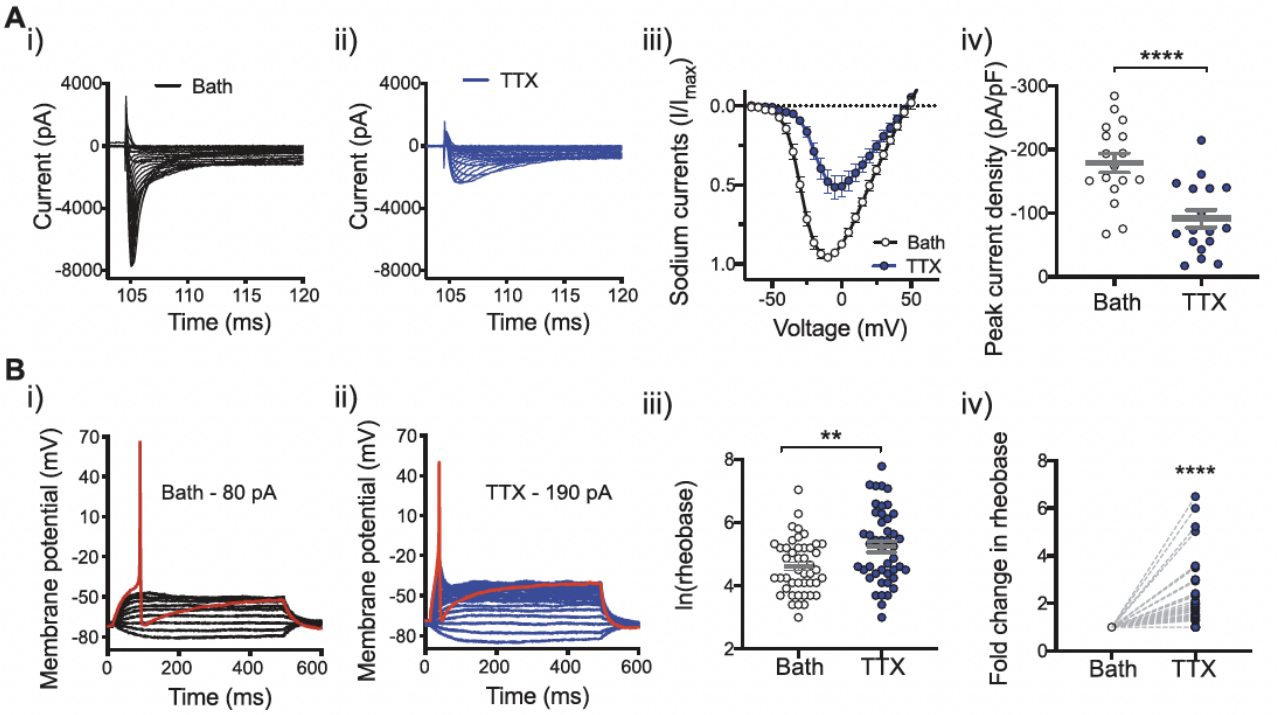

Figure 4.7: Inhibition of TTX-sensitive Na_V channels reduces sodium current density and excitability of DRG neurons innervating the vagina.

(A) Original whole-cell voltage-clamp recordings of a retrogradely traced vagina-innervating LS DRG neuron showing voltage-dependent sodium currents **(i)** before and **(ii)** after 1 min tetrodotoxin (TTX, 0.1 μM) addition. Sodium currents were evoked by a series of voltage step pulses from -65 mV to +60 mV (5 mV increments of 100 ms), before returning to hold at -70 mV (repetition interval of 3 sec, P/8 leak subtraction). **(iii)** In the presence of TTX (blue), sodium current influx in response to voltage steps occurs at more depolarised voltages, and the peak current is shifted in the depolarising direction compared to bath conditions (black). The measured current (I) at each voltage was normalised to the peak current (I_{max}), and each data point shown here is the averaged I/I_{max} ± SEM. **(iv)** Analysis of the average peak current density confirms a significant reduction in the presence of TTX compared to bath conditions (****P <0.0001, paired Students t test, n = 17 neurons from N = 4 mice), suggesting a significant contribution of TTX-sensitive channels to the voltage-gated sodium current in vagina-innervating LS DRG neurons. **(B)** Original whole-cell current-clamp recordings of a single retrogradely traced vagina-innervating DRG neuron during current ramp protocols. Each line represents a 10 pA increase in current. **(i)** In this example, 80 pA was the measured threshold current required to elicit an action potential (red trace) under control conditions, which following 1-minute incubation with TTX **(ii)** increased to 190 pA, indicating decreased neuronal excitability. **(iii)** Incubation with TTX increases the average current threshold (ln(rheobase)) in vagina-innervating DRG neurons compared with bath conditions (** P<0.01, paired two-tailed Student t test, n = 45 neurons from N = 6 mice). **(iv)** Fold change of rheobase from baseline highlights the individual changes to rheobase observed in the presence of TTX. 35 out of 45 cells exhibited sensitivity to TTX with an increase in rheobase higher than 15% from bath conditions. (****P <0.0001, paired two-tailed Student t test, n = 45 neurons from N = 6 mice). DRG, dorsal root ganglia.

4.5.4 Vaginal distension-evoked activation of dorsal horn neurons within the spinal cord can be manipulated by intravaginal administration of Na_V channel modulators

Following our findings of Na_V channel modulation *ex vivo and in vitro*, we investigated whether changes in vaginal afferent sensitivity, induced by pharmacological modulation of Na_V channels in the periphery, translates to changes in the nociceptive signal sent to the central nervous system (CNS) *in vivo*. Therefore, we aimed to determine whether increasing or decreasing the peripheral sensitivity of vaginal afferents, induced by either veratridine or TTX respectively, correspondingly altered neuronal activation within the spinal cord. In separate mice we performed *in vivo* vaginal distension after infusion of either saline (vehicle control), veratridine, or TTX and compared the number of phosphorylated-MAP-kinase-ERK-immunoreactive (pERK-IR) dorsal horn neurons in the lumbosacral (LS; L6-S2) spinal cord **(Figure** 4.8**).** After saline infusion, vaginal distension resulted in pERK-IR neurons being present within the superficial dorsal horn (SDH; laminae LI-II), throughout the deep dorsal horn (DDH; LIII-V) and in the dorsal grey commissure (DGC). A number of pERK-IR neurons were also present within the region of the lateral spinal nucleus (LSN) and the sacral parasympathetic nucleus (SPN) in sacral spinal segments **(Figure** 4.8**)**.

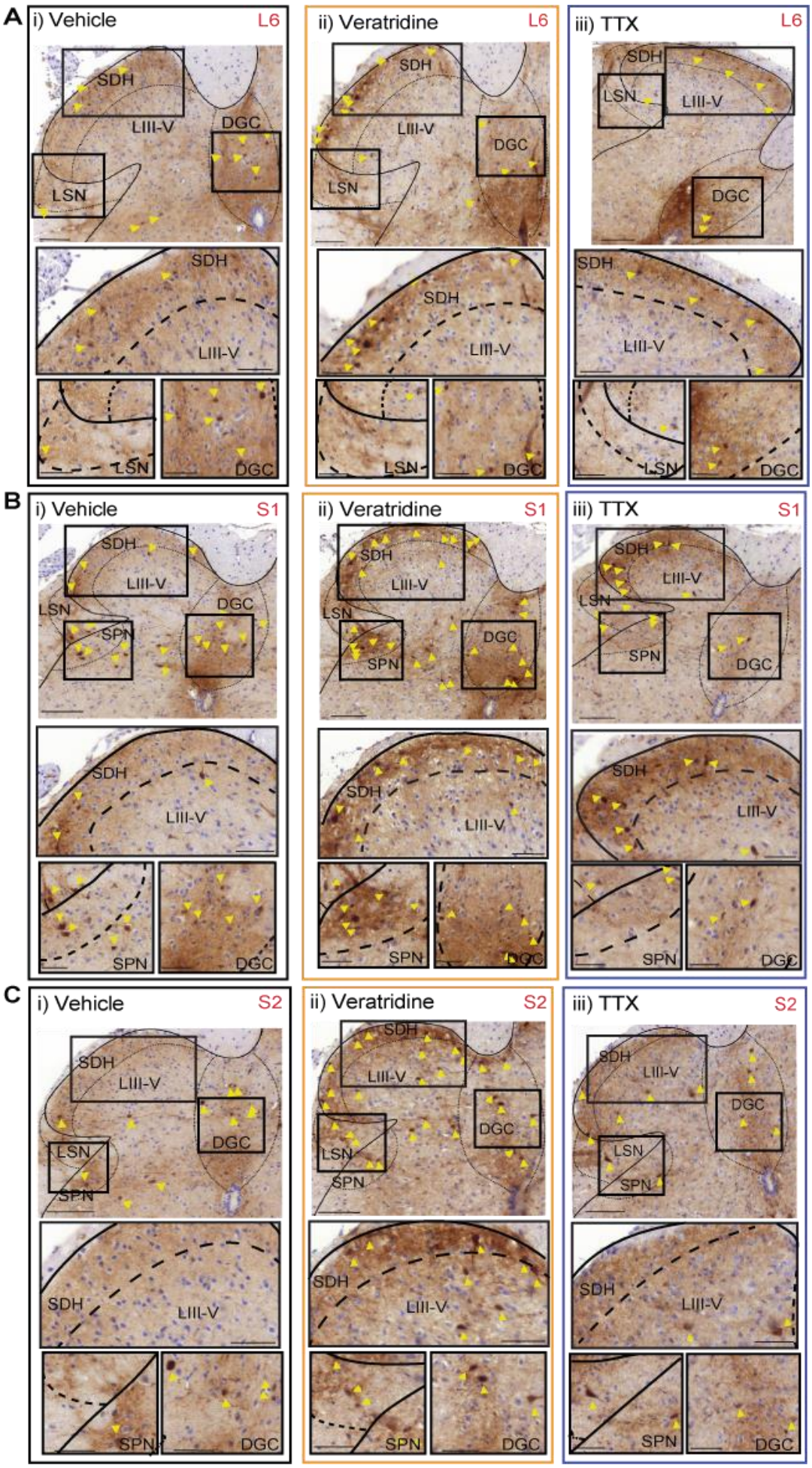
A
i) Vehicle
L6
SDH
LIII-V
DGC
LSN
ii) Veratridine
L6
iii) TTX
L6
B
i) Vehicle
S1
SPN
ii) Veratridine
S1
iii) TTX
S1
C
i) Vehicle
S2
ii) Veratridine
S2
iii) TTX
S2

Figure 4.8: pERK signalling in lumbosacral regions (LS: L6, S1 and S2) of the spinal cord in response to vaginal distension *in vivo*.

(A-C) Representative images of cross-sections from the **(A)** lumbar (L6) and **(B)** sacral (S1) and **(C)** sacral (S2) spinal cord labelled for pERK-IR from mice treated with **(i)** saline, **(ii)** 50 µM veratridine or **(iii)** 0.5 µM TTX prior to vaginal distension. Yellow arrowheads indicate pERK-IR neurons. Scale bars in upper panels represent 100 µm. The bottom panels for both A and B are higher magnification images of the different spinal area areas highlighted in the top panels. Yellow arrowheads indicate pERK- IR neurons. Scale bars in lower panel represent 50 µm. DGC, dorsal grey commissure; LSN, lateral spinal nucleus; SPN, sacral parasympathetic nucleus; SDH, superficial dorsal horn.

We then showed that the number of pERK-IR neurons evoked by vaginal distension is significantly increased by intravaginal administration of veratridine **(Figure** 4.9**A)** and decreased by TTX **(Figure** 4.9**A)**. Further analysis of the different regions of the dorsal horn showed that vaginal infusion of veratridine prior to distension resulted in significantly more pERK-IR dorsal horn neurons relative to saline infusion within the SDH **(Figure** 4.9**B)** and the LSN **(Figure** 4.9**E)**. In contrast, compared with vehicle veratridine treatment did not significantly alter the numbers of pERK-IR neurons within the DDH **(Figure** 4.9**C)**, DGC **(Figure** 4.9**D)**, or the SPN **(Figure** 4.9**F)**. In comparison, vaginal distension following intravaginal application of TTX resulted in a significant decrease in the total number of pERK-IR dorsal horn neurons relative to saline infusion, with significant reductions specifically within the DGC **(Figure** 4.9**D)**.

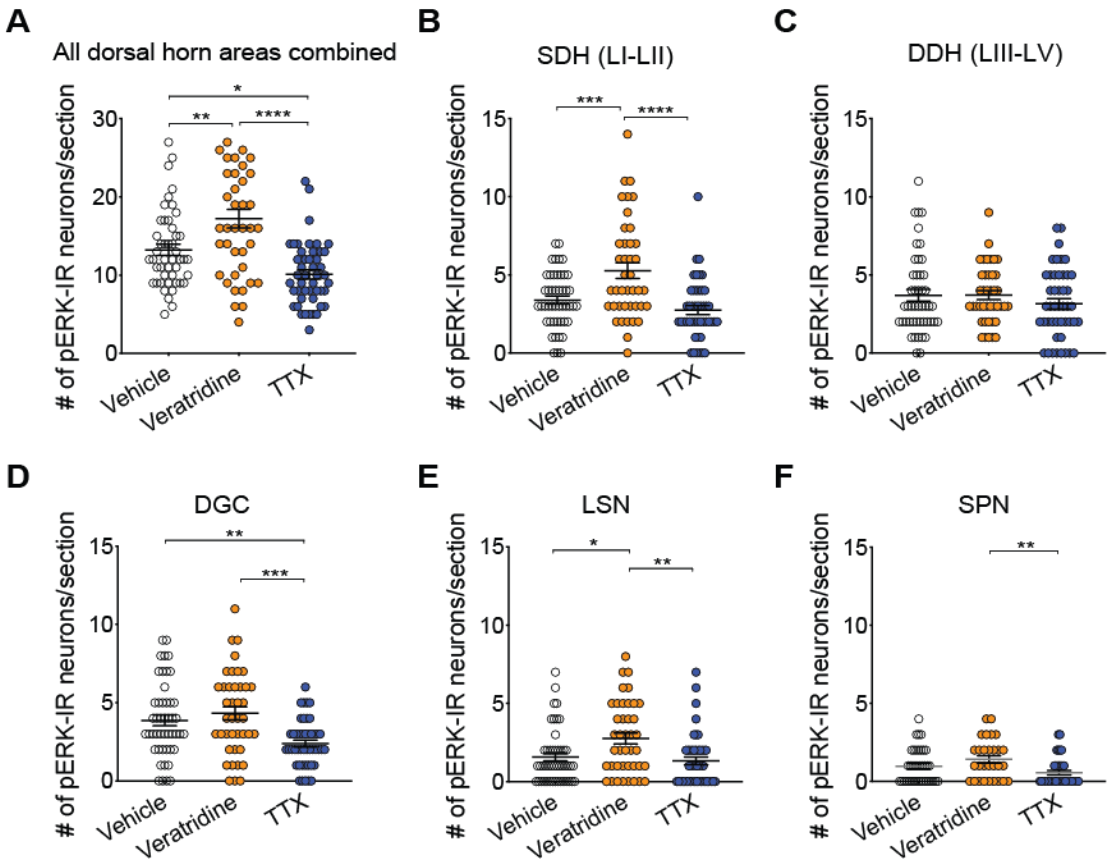

Figure 4.9: Intravaginal administration of Na_v channel modulators alters signalling in the dorsal horn of the spinal cord in response to vaginal distension *in vivo*

(A) Number of pERK-IR neurons/section of all dorsal horn areas combined. Compared with vehicle, veratridine significantly increased the number of pERK-IR neurons in response to vaginal distension (***P* <0.01), whilst TTX administration significantly reduced the number of pERK-IR neurons in response to vaginal distension (**P* <0.05). **(B-F)** individual areas of the dorsal horn showing pERK-IR induced by vaginal distension. pERK-IR was significantly increased following vaginal distension after veratridine administration compared to vehicle, with significantly greater numbers of pERK-IR neurons occurring in the **(B)** superficial dorsal horn (SDH; ****P* <0.0001) and **(C)** lateral spinal nucleus (LSN; **P* <0.05). pERK-IR was significantly decreased following vaginal distension after TTX administration compared to saline, with significantly fewer pERK-IR neurons occurring in the **(D)** dorsal grey commissure (DGC; ***P* <0.01). No significant difference was observed between veratridine and saline or TTX and saline in the **(C)** deep dorsal horn (DDH), nor the **(F)** sacral parasympathetic nucleus (SPN). Data are represented as the number of pERK-IR neurons per section of LS (L6-S2 unless stated otherwise) spinal cord, from minimum of 6 sections per mouse, from N = 4 mice. Data represent mean ± SEM. One-way ANOVA followed by Bonferroni's multiple comparison post-hoc test.

These *in vivo* results indicate that veratridine-induced increases in the peripheral sensitivity of vaginal afferent endings leads to enhanced signalling within the spinal cord. Conversely, vaginal administration of TTX can reduce spinal cord neuronal activation evoked by vaginal distension.

Interestingly, the changes in the number of pERK-IR neurons in response to veratridine mainly occurred within specific regions of the dorsal horn distinct from those affected by TTX.

4.5.5 Pain sensitivity to vaginal distension can be modulated *in vivo* by targeting Na_V channels intravaginally

We next investigated whether the observed alteration in the signalling in the CNS translates to changes in pain sensitivity evoked by vaginal distension in conscious animals. In order to measure vaginal pain sensitivity *in vivo* we measured the visceromotor response (VMR) to increasing vaginal distension (VD) pressures by recording electromyography (EMG) activity from electrodes surgically implanted into the abdominal muscles.

Vaginal distension evokes an increase in the VMR and the degree of VMR is related to the amount of pressure applied to the vagina **(Figure** 4.10**)**. We found that mice administered intravaginally with veratridine displayed pronounced hypersensitivity to vaginal distension *in vivo*. This is indicated by significantly elevated VMRs to VD to all distension pressures compared to mice intravaginally treated with vehicle **(Figure** 4.10**A-C)**. Conversely, intravaginal administration of TTX significantly reduced VMRs to VD compared to mice intravaginally treated with vehicle, suggestive of an analgesic effect **(Figure** 4.10**A-C)**.

Taken together, these findings indicate that pharmacological modulation of Na_V channels at the periphery alters sensory signalling at the afferent and spinal cord levels, ultimately translating to modulation of pain sensitivity evoked by vaginal distension *in vivo*.

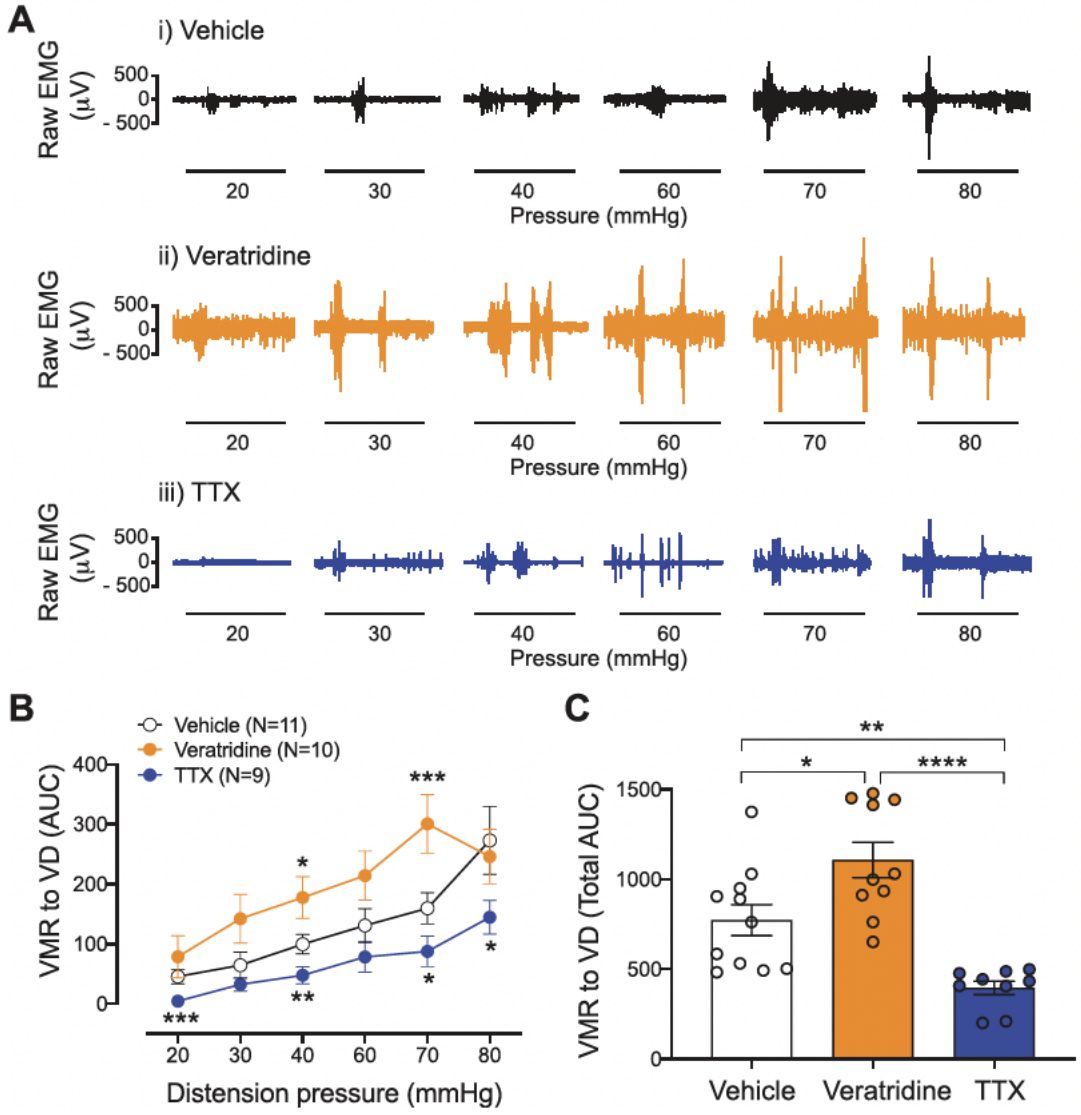

Figure 4.10: Pain evoked by vaginal distension can be modulated by intravaginal targeting of Na_V channels *in vivo*.

(A) Representative electromyography (EMG) recordings at increasing vaginal distension (VD) pressures (mm Hg) in mice intravaginally administered with either **(i)** vehicle, **(ii)** veratridine (50 µM) or **(iii)** TTX (0.5 µM) 10 mins before EMG recordings. Horizontal bars shows the length of time for each distension (30 seconds). **(B)** Grouped data showing visceromotor responses (VMR) to vaginal distension (VD) from mice intravaginally treated with vehicle (black), veratridine (orange) and TTX (blue). Veratridine treatment significantly increased the VMRs to VD compared with vehicle-treated mice (**P* <0.05 at 40 mm Hg; and ****P* <0.001 at 70 mm Hg, generalised estimating equations followed by LSD post hoc test. N = 10 vehicle and N = 11 veratridine treated mice). Conversely, TTX treatment significantly reduced the VMRs to VD compared with vehicle-treated mice (****P* <0.001 at 20 mm Hg; ***P* <0.01 at 40 mm Hg; and **P* <0.05 at 70 and 80 mm Hg, generalised estimating equations followed by LSD post hoc test. N = 10 vehicle and N = 9 TTX treated mice). **(C)** Grouped data expressed as the total area under the curve (total AUC). Each dot represents the total AUC (sum of the AUCs obtained at each distension pressure) from an individual animal. Intravaginal administration of veratridine (orange) significantly increased the VMR responses to VDs, compared to vehicle treatment (**P* <0.05). Conversely, intravaginal administration of TTX (blue) significantly decreased the VMR responses to VDs, compared to vehicle treatment (**P* <0.01). Veratridine- and TTX-treated groups showed an enhanced difference in their total AUC (**P* <0.0001). One-way

ANOVA with Bonferroni post-hoc comparison test, from N = 10 vehicle, N = 11 veratridine and N = 9 TTX treated mice). Data represent mean ± SEM.

4.6 Discussion

In this study we determine how pelvic afferents innervating the mouse vagina are broadly tuned to detect a variety of mechanical stimuli. We also show how activation of these afferents leads to activation of neurons within the dorsal horn of the spinal cord and pain-related behaviours *in vivo*. We also identify, for the first time, the complete expression profile of Na_V channels within individual retrogradely traced vaginal-innervating DRG neurons. Finally, we demonstrate that Na_V channel modulators are able to alter i) the responsiveness of pelvic vaginal afferents to mechanical stimuli; ii) the excitability of isolated vaginal-innervating DRG neurons; iii) nociceptive signalling into the spinal cord and ultimately iv) pain sensation evoked by vaginal distension in conscious animals.

The female reproductive tract is innervated by sensory afferents from the hypogastric, pelvic, and pudendal nerves [189, 203, 331, 332, 349-353]. These afferents have been shown to fire action potentials in response to mechanical and chemical stimuli applied within the uterus, cervix, and vagina of anaesthetised rats [326-329]. Remarkably, further studies examining the mechanosensory properties of these afferents and how their modulation alters the transmission of sensory information to the CNS are lacking.

In the current study, using a single unit *ex vivo* recording preparation, we show that pelvic afferents innervating the mouse vagina are tuned to detect a variety of mechanical stimuli. Utilising a flat sheet preparation, where the vagina was opened longitudinally and pinned flat, we show that the receptive fields of pelvic afferent endings were found scattered throughout the whole length of the vagina. Receptive fields were distributed ipsilaterally to the pelvic nerve branch where the recordings were made. Characterisation of afferent mechanosensitivity showed that 100% of the afferents examined responded to all three mechanical stimuli tested, suggesting polymodality. We found that focal compression of the receptive field or gentle stroking of the mucosa surface with calibrated vfh evoked slowly adapting responses, with responses that start and end with the stimuli. Circular stretch of the vagina evoked either a sustained or moderately adapting response. Additionally, we showed that baseline responses to stroking stimulation of the mucosa were graded, where action potential frequency increased with increased stroke intensity. Overall, the mechanosensory properties of pelvic afferents innervating the mouse vagina are similar to those found in rats by Prof. Berkley's studies ~30 years ago [326-329].

We also demonstrate, for the first time, a direct role for Na_V channels in mediating afferent signalling from the vagina. Specifically, we showed that vaginal afferent mechanosensitivity, neuronal activation within the spinal cord and pain responses to vaginal distension could all be significantly augmented by pan-Na_V activation with veratridine. This suggests activation of Na_V

channels can drive vaginal pain transmission, which is consistent with observations in other visceral organs. For example, intravesical instillation of veratridine significantly enhances bladder afferent sensitivity to graded distension [305]. Similarly, in the colon pan-Na_V activation with Pacific ciguatoxin (P-CTX-1) activates colonic afferents and correspondingly neurons within the spinal cord [285]. Furthermore, accidental consumption of P-CTX-1 or veratridine in humans, manifests as acute and severe abdominal pain [285, 354, 355].

In the current study we also show that TTX significantly reduces vaginal afferent function and neuroexcitability, whilst reducing Na_V currents in vaginal-innervating DRG neurons. Correspondingly, this results in a reduced number of pERK-IR neurons within the dorsal horn of the spinal cord and reduces pain responses to noxious vaginal distension. Notably, TTX significantly reduced, but did not abolish these responses, implicating both TTX-S ($Na_V1.1$-$Na_V1.4$, $Na_V1.6$, and $Na_V1.7$) and TTX-R ($Na_V1.5$, $Na_V1.8$ and $Na_V1.9$) channels in this response.

Our single cell RT-PCR data showed distinct and overlapping expression profiles of the various members of the Na_V family within individual vagina-innervating neurons. Notably, the majority of the neurons expressed at least one TTX-sensitive ($Na_V1.7$) and one TTX-resistant ($Na_V1.8$) isoform. This single cell RT-PCR data indicate that the TTX-sensitive component is most likely attributable to combinations of $Na_V1.1$, $Na_V1.2$, $Na_V1.6$, and $Na_V1.7$, which were found to be expressed in a high proportion of vagina-innervating DRG neurons. Although studies have yet to directly investigate a role for $Na_V1.1$ or $Na_V1.6$ in pelvic vaginal afferents, studies in the colon show these two isoforms play key roles in signalling nociceptive information in response to mechanical stimuli [161, 333, 337]. In contrast, $Na_V1.7$ does not appear to contribute to either colonic or bladder nociception, at least in healthy conditions [356], whilst there is currently no functional data to support a role of $Na_V1.2$ in visceral sensory signalling [336]. For the TTX-resistant component, $Na_V1.8$, and $Na_V1.9$ are likely the main contributors as they are highly expressed in vagina-innervating DRG neurons and contribute to other forms of visceral pain [285, 357]. In contrast, the other TTX-R subunit $Na_V1.5$ is poorly expressed in vagina-innervating DRG neurons. Furthermore, our QRT-PCR data identified extremely limited expression of Na_V channel subtypes within the vaginal tissue, suggesting the effects of veratridine and TTX on modulating afferent mechanosensitivity occurs through an afferent mechanism, and not due to secondary changes within the vaginal tissue.

Our findings here regarding the TTX sensitivity and Na_V isoform expression profile of vaginal-innervating DRG neurons contrast sharply with those in other visceral organs. For example, both the sodium current density of bladder-innervating neurons and bladder afferent responses to distension and are almost completely abolished by TTX. Correspondingly, intra-bladder TTX administration dramatically reduces the number of dorsal horn neurons being activated by bladder distension [305]. These findings suggest a large TTX-sensitive component and a small TTX-resistant component in bladder-innervating DRG neurons. In contrast, vaginal-innervating DRG neurons have a more

balanced TTX-sensitive and TTX-resistant contribution, which is likely borne by fewer vaginal neurons expressing $Na_V1.1$, $Na_V1.3$ and $Na_V1.6$ compared with bladder-innervating DRG neurons [305]. Colon-innervating DRG neurons also demonstrate TTX-sensitive and TTX-resistant components [358], although more of these neurons express $Na_V1.1$, $Na_V1.2$, $Na_V1.3$ and $Na_V1.9$ [356] than vagina-innervating LS DRG neurons. These findings are important, as the complete Na_V channel expression profile in afferent neurons innervating female reproductive organs has not previously been reported; with only one study showing $Na_V1.8$ expression in afferents innervating the mouse uterus [335]. These findings provide novel alternatives to regulate sensation arising from these visceral organs, as discussed below.

In the present study, we show that intravaginal administration of the pan-Na_V activator veratridine, increases vaginal sensory signalling into the spinal cord (measured by an increase of pERK-IR neurons) in response to vagina distension. Notably, veratridine-induced increases in pERK-IR neurons were localised to the superficial dorsal horn (SDH) and the lateral spinal nucleus (LSN). Both of these regions have significant roles in relaying nociceptive signalling into various pain processing centres of brain [359, 360]. Conversely, TTX reduced the number of pERK-IR neurons. However, this reduction occurred primarily within the dorsal grey commissure (DGC), which in sacral spinal regions, is known to be important to signalling visceral sensation within dorsal columns [361]. These findings correspond well with our observation that *in vivo* intravaginal administration of veratridine significantly increase the visceromotor response to vaginal distension, whilst TTX significantly reduced these responses compared to vehicle-treated mice. Interestingly, as alterations in the visceromotor response to vaginal distension in animals treated with either veratridine or TTX occurred across all distension pressures, this suggests that Na_V channels mediate the transmission of both non-noxious and noxious stimuli.

It is well documented that women with endometriosis and vulvodynia experience dyspareunia twice as often as healthy women [362, 363]. It is also well known that pelvic afferents innervating other visceral organs, such as the colon and bladder, become hypersensitive to mechanical stimuli in animal models of irritable bowel syndrome (IBS) [157-161] and interstitial cystitis/bladder pain syndrome (IC/BPS) [162, 163], which ultimately leads to CPP in humans. Whether the dyspareunia, experienced by women with endometriosis and vulvodynia, could be explained by vaginal afferents developing hypersensitivity to mechanical stimuli remains to be identified. However, this study provides novel findings advancing the understanding of vaginal sensation that can be used to recognise and explore changes in states of chronic pelvic pain associated with endometriosis and vulvodynia. As recent reports show the potential of targeting Na_V channels for the treatment of acute and chronic visceral pain [11-15], a similar strategy to treat pain arising from the female reproductive organs may be possible. This concept is supported by our findings, providing the first direct demonstration for a role of Na_V channels in regulating vaginal sensation *in vivo*.

In conclusion, our findings demonstrate that modulation of the electrophysiological properties of afferents innervating the female reproductive tract, by targeting Na_V channels expressed within these afferents, lead to changes in nociceptive signalling sent to the CNS and ultimately regulated vaginal pain sensitivity evoked by vaginal distension *in vivo*. These findings contribute towards the understanding of how mechanical stimuli is detected and transmitted from healthy female reproductive organs and uncovers potential molecular targets to investigate as novel therapeutics to manage dyspareunia associated with endometriosis and vulvodynia. With this in mind, Chapter 5 will focus on whether we can employ selective targeting of ion channels within vaginal-innervating sensory afferents as a treatment option for vaginal pain associated with endometriosis.

CHAPTER 5: PHARMACOLOGICAL INHIBITION OF VOLTAGE GATED SODIUM CHANNEL (Na_V) 1.7 REDUCES VAGINAL HYPERSENSITIVITY IN A SYNGENEIC MOUSE MODEL OF ENDOMETRIOSIS

5.1 Co-contribution statement

Electrophysiology experiments, associated analysis and graphs included in this chapter were produced by colleague and co-supervisor, Dr. Joel Castro.

Pharmacological modulators used in these experiments were developed and provided by our collaborators, with thanks to:

Prof. Irina Vetter's group from Institute for Molecular Bioscience, The University of Queensland (OD1) and Prof. Glenn King's group from Australian Research Council Centre of Excellence for Innovations in Peptide and Protein Science, The University of Queensland (Tsp1a).

5.2 Overview

Throughout Chapter 4, we present evidence that healthy pelvic vaginal afferents are broadly tuned to detect a variety of mechanical stimuli in mice. Moreover, we showed that pharmacological modulation of voltage-gated sodium (Na_V) channel activity in these afferents results in altered sensory signalling from the vagina, seen as changes in mechanosensitivity, nociceptive signalling within the spinal cord and ultimately altered pain responses, *in vivo* [220]. This provided the first direct confirmation that both TTX-sensitive ($Na_V1.1$-$Na_V1.4$, $Na_V1.6$, and $Na_V1.7$) and TTX-resistant ($Na_V1.5$, $Na_V1.8$ and $Na_V1.9$) Na_V channels play a substantial role in regulating physiological sensation in the vaginal; however, the role of specific Na_V channel isoforms was not directly explored. In this study, we investigate the role of voltage-gated sodium channel isoform 1.7 ($Na_V1.7$) in vaginal sensation. Importantly, using our syngeneic inoculation model of endometriosis presented in Chapter 3, we build on our knowledge to identify a specific role of $Na_V1.7$ in endometriosis associated vaginal pain. The aims of this study were to: 1) establish whether vaginal sensory signalling can be modulated by targeting $Na_V1.7$ channels expressed in the vagina; 2) directly measure whether the mechanosensitive properties of vaginal-innervating pelvic afferents is altered with the development of endometriosis; and 3) determine whether $Na_V1.7$ has a direct role in altered vaginal nociceptive signalling in endometriosis.

5.3 Introduction

The chronic pelvic pain (CPP) experienced by women with endometriosis is commonly associated with visceral organs including the bowel, bladder, and reproductive tract, with many women developing comorbidities such as irritable bowel syndrome (IBS), interstitial cystitis/bladder pain syndrome (IC/BPS) and vulvodynia [187, 364]. Dyspareunia, or vaginal hyperalgesia/painful intercourse, is a debilitating symptom experienced by many women with endometriosis and vulvodynia [362, 363, 365].

Peripheral sensory afferents are an essential first step in the visceral pain pathway, transmitting nociceptive signals from visceral organs to the central nervous system (CNS) for processing. Hypersensitivity of sensory afferents innervating key visceral organs has been demonstrated in animal models of chronic diseases such as IBS and IC/BPS [151, 157-163]. Membrane receptors and ion channels expressed within these afferents tightly regulate their activation and ultimately their sensitivity to detect a range of stimuli. Targeted modulation of specific ion channels expressed within the sensory neurons of both the bowel and the bladder has demonstrated potential in the treatment of visceral hypersensitivity associated with these chronic conditions [142, 161, 163, 206, 305, 333, 366]. Unfortunately, there remains inadequate knowledge surrounding specific functional ion channel roles in sensory neuronal signalling from the female reproductive tract, currently limiting their targeted approach in treatment of vaginal pain.

In Chapter 4, we identified that all Na_V channel isoforms ($Na_V1.1$-1.9) were differentially expressed within vaginal-innervating dorsal root ganglion (DRG) neurons [220]. Moreover, we showed that sensory signals arising from the mouse vagina could be pharmacologically modulated by broad targeting of Na_V channels *ex vivo, in vitro* and *in vivo.* In this chapter, we will investigate the specific contribution of $Na_V1.7$ to vaginal sensation. Our interest was based on our finding that the $Na_V1.7$ transcript was expressed in 100% of vaginal-innervating neurons [220]. Furthermore, it has been suggested that $Na_V1.7$ has a critical role in nociception, with SCN9A (the gene encoding the α subunit of $Na_V1.7$) mutations leading to altered pain sensitivity in humans [367, 368]. For example, loss-of-function mutations of SCN9A are associated with congenital insensitivity to pain, a rare disorder characterised by a near-total loss of pain sensitivity [369]. In contrast, gain-of-function mutations of SCN9A in humans induces enhanced pain perception, associated with pain syndromes such as primary inherited erythromelalgia (burning pain of the limbs) [370-372], paroxysmal extreme pain disorder [371] and some forms of small-fibre neuropathy [373]. $Na_V1.7$ is also proposed to play a role in peripheral sensitization following inflammation [374] and the pathophysiology of chronic visceral pain associated with IBS [336, 366], however, whether it plays a modulating role in endometriosis associated vaginal pain sensation is yet to be determined.

With this in mind, this chapter will utilise highly selective pharmacological modulators of $Na_V1.7$ channels, including the $Na_V1.7$ activator, OD1, and the $Na_V1.7$ inhibitor, Tsp1a, to establish whether targeting $Na_V1.7$ in the vagina can modulate the mechanosensitive properties of vaginal-innervating pelvic afferents, *ex* vivo. We will then determine whether this modulation translates into altered vaginal nociceptive signalling, *in* vivo. Finally, we will elucidate whether $Na_V1.7$ contributes to the vaginal hypersensitivity developed in our pre-clinical mouse model of endometriosis.

5.4 Methods

5.4.1 Animals

All animal experiments conformed to the relevant regulatory standards and ARRIVE guidelines, covered by the Animal Ethics Committee of the South Australian Health and Medical Research Institute (SAHMRI), approved under ethics SAM342. Naïve, female C57BL/6J mice were acquired from an in-house C57BL/6J breeding programme (Jax strain #000664; originally purchased from The Jackson Laboratory (breeding barn MP14; Bar Harbor, ME; USA) within SAHMRI's specific and opportunistic pathogen-free animal care facility, as described in Chapter 2. All female mice use in this study were virgin (never been mated) and housed in the absence of males from weening. Vaginal lavage or other cytology test to confirm cycle stage were not performed, but it has been reported that an extended absence of male pheromones leads to a state of anestrous (lee-boot effect) [274].

5.4.2 Pharmacological modulators

Pharmacological modulation of $Na_V1.7$ channels was achieved using modulators provided by collaborators including: The α-Scorpion Toxin OD1, a selective agonist of $Na_V1.7$ channels, chemically synthesized by Prof Irina Vetter's research group at the University of Queensland, Brisbane, Australia [375] and the tarantula derived peptide Tsp1a, a selective $Na_V1.7$ channel inhibitor, chemically synthesized from Prof Glenn King's research group at the University of Queensland, Brisbane, Australia [366].

5.4.3 Syngeneic inoculation mouse model of endometriosis induction

The syngeneic inoculation method of endometriosis induction described in Chapter 3 was used to generate endometriosis (Endo) or sham control animals (Sham) for the experimental results found within this chapter. All mice received a low dose (0.05 mg/kg) of analgesic buprenorphine prior to the commencement of each surgical procedure. Detailed methods of endometriosis induction have been presented in Chapter 3 [376] and are briefly outlined below.

5.4.3.1 Ovariectomy surgery

Prior to surgical induction of endometriosis, female mice were ovariectomised in order to deplete endogenous steroid production, as described in Chapter 2 [297]. Ovariectomised mice were given an intraperitoneal injection (i.p.) of 100 µg/kg estradiol benzoate (or Progynon-B) to maintain

steady levels of circulating estrogen [276, 277] and allowed to recover for a minimum of 5 days before random allocation to either Endo or Sham induction groups.

5.4.3.2 Endometriosis (Endo) and Sham induction

Following ovariectomy recovery, Endo or Sham induction was performed using the syngeneic inoculation method of endometrial fragments **(Figure 5.1A)**, as described in Chapter 3 [376]. All animals recovered well from surgical procedures within 5 days and no signs of distress or unusual pain behaviours were observed. To maintain steady levels of circulating estrogen over endometriosis development, both Endo and Sham mice were given a weekly i.p. injection of 100 µg/kg estradiol benzoate until *in vivo* or *ex vivo* experiments **(Figure 5.1B).**

5.4.4 *Ex vivo* and *In vivo* assessment of visceral hypersensitivity

As demonstrated in Chapter 3, endometriosis mice develop endometriosis lesions throughout the peritoneal cavity and display signs of CPP by 8-10 weeks of endometriosis development in this model [376]. Therefore, to examine the role of $Na_V1.7$ in vaginal pain sensitivity in endometriosis, all experiments presented in this chapter were performed following a minimum of 8 weeks of endometriosis development **(Figure 5.1B)**. A dedicated group of mice were used for *ex vivo* electrophysiology experiments (N = 8 Sham and N = 8 Endo) with a separate group for *in vivo* experiments measuring pain evoked by distension of the vagina (N = 10 Sham and N = 10 Endo mice). All mice included in experiments were examined during dissection to confirm the growth of endometriosis lesions in Endo mice, and the absence of any lesions in Sham mice.

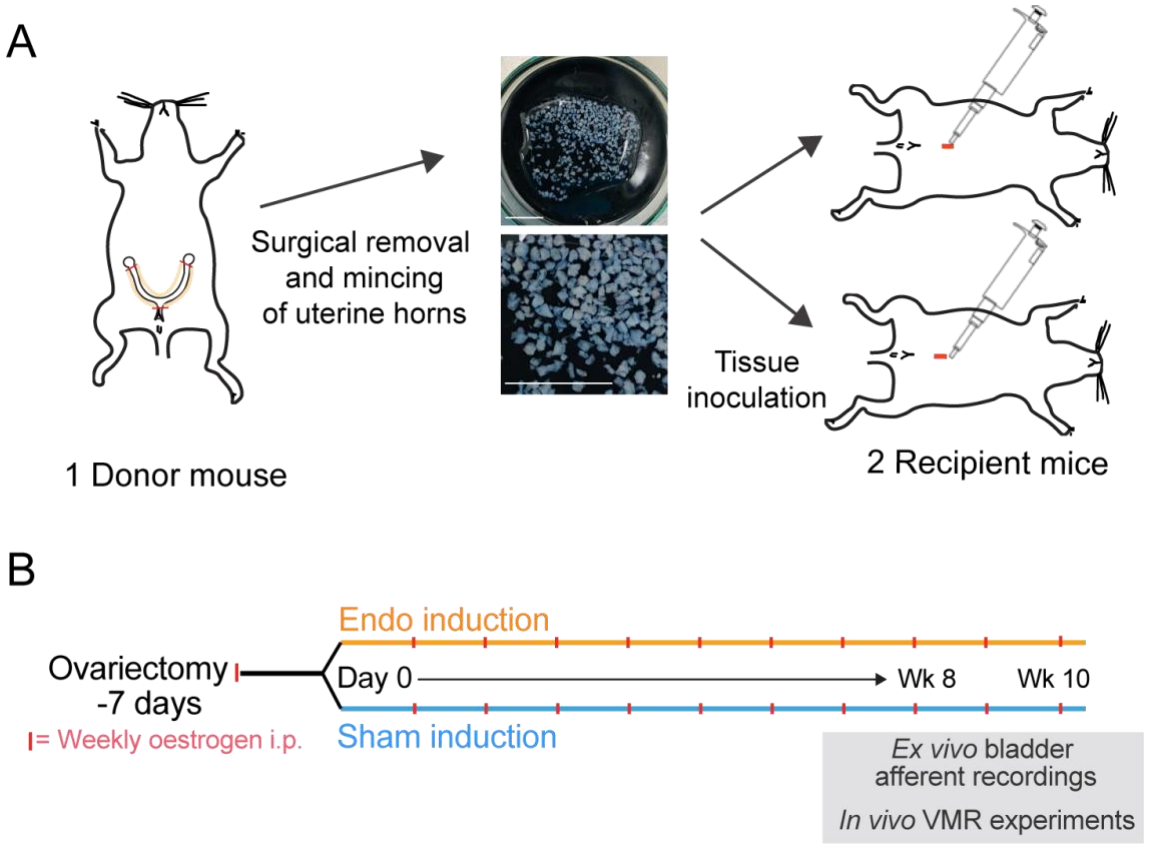

Figure 5.1: Schematic diagram of interventions performed and timeline of experimental studies.

(A) Schematic diagram demonstrating endometriosis induction via uterine horn tissue inoculation. Uterine horns are surgically removed from 1 donor C57BL/6J mouse, cleared of excess fat and connective tissue and transferred to a clean dissecting dish containing 0.5mL of PBS (penicillin (100 U/mL) and streptomycin (100 mg/mL). Uterine horns are then minced into small segments (measurement bars represent 1cm). The resulting minced uterine horn tissue is then equally injected into 2 recipient mice through a small midline abdominal incision. Sham mice receive PBS (penicillin (100 U/mL) and streptomycin (100 mg/mL) only. **(B)** Schematic diagram representing the timeline for experimental studies performed. Seven days prior to Endo or Sham induction, all mice receive an ovariectomy and commence weekly i.p. estradiol injections (red lines). Following 7 days of recovery, mice undergo either Endo or Sham induction. Endometriosis is then allowed to develop whilst all mice continue to receive weekly estradiol injections to maintain circulating levels of estrogen. All *in vivo* and *ex vivo* experiments were completed between 8 and 10 weeks in both Sham and Endo mice.

5.4.5 *Ex vivo* afferent recording preparation from the pelvic nerve innervating the vagina

Using the novel *ex vivo* pelvic afferent recording preparation presented in Chapter 4, we characterised the responses of afferents innervating the mouse vagina, demonstrating their ability to detect various mechanical stimuli which can be pharmacologically modulated with Na_v channel targeting [220]. In this chapter, this technique was used to specifically elucidate a role of $Na_V1.7$ in

vaginal afferent signalling and identify whether this may be involved in the enhanced pain following endometriosis development.

5.4.5.1 Mechanosensory properties of pelvic afferents innervating the vagina

Receptive fields tested in this study were limited to the length of the vagina (above vaginal opening and below the cervix) **(Figure 5.2A)**. Baseline mechanosensory properties of the pelvic afferents innervating a particular receptive field within the vagina, were recorded to 3 distinct mechanical stimuli, as described in Chapter 4 [220]. The 3 mechanical stimuli tested included: (1) static probing with calibrated von Frey hairs (vfh; 2 g force; applied 3 times for a period of 3 seconds); (2) mucosal stroking of the vaginal surface with calibrated vfh (10-1000 mg force; applied 10 times each); and (3) circular stretch (5 g; applied for a period of 1 minute).

Once baseline afferent mechanosensitivity was recorded, a small chamber was placed onto the mucosal surface of the vagina, surrounding the afferent receptive field. Residual Krebs solution within the chamber was removed and the $Na_V1.7$ channel pharmacological modulators, OD1 ($Na_V1.7$ agonist, 100 nM for 5 minutes) or Tsp1a ($Na_V1.7$ inhibitor, 200 nM for 5 minutes), were applied, in separate experimental preparations. The concentrations of both OD1 and Tsp1a were chosen due to their potent and selective modulation of $Na_V1.7$ channels at these concentrations [366, 377]. Mechanical sensitivity of the afferent receptive field was then retested in response to the 3 distinct mechanical stimuli previously recorded.

5.4.6 *In vivo* assessment of evoked vaginal pain by quantification of visceromotor responses (VMR).

The visceromotor response (VMR) to vaginal distension (VD) has been a successful technique to objectively measure vaginal sensitivity to pain *in vivo* [115, 186, 195, 220, 273, 282, 297, 376]. Using VMR to VD, we were able to demonstrate, in Chapter 4, that vaginal sensitivity can be pharmacologically modulated from the vagina. VMR was assessed by recording the electromyography (EMG) activity from electrodes transplanted in the abdominal muscles to increasing VD pressures, as detailed in Chapter 2 and described previously [220, 297, 376]. In this chapter, we will utilise this technique to specifically examine the role of $Na_V1.7$ in vaginal sensory signalling and determine whether it plays a role in vaginal pain in endometriosis. Detailed methods can be found in Chapter 2 and are briefly described below.

5.4.6.1 Surgical implantation of electromyography (EMG) electrodes

Surgical implantation of 2 EMG electrodes into the abdominal musculature was completed as described in Chapter 2. At the end of surgery, mice received an antibiotic (Baytril®; 5 mg/kg s.c. injection) and analgesic (buprenorphine; 0.05 mg/kg s.c. injection) as well as their final dose of 100 µg/kg estradiol benzoate (i.p.). Mice were monitored for recovery in their home cages for a minimum of 3 days before the experimental VMR protocol.

5.4.6.2 Assessing visceromotor responses (VMR) to vaginal distension (VD)

Assessment of VMR to graded vaginal distensions (VD) (20-30-40-60-70 mm Hg for 30 seconds duration each pressure, separated by 3-minute interval) was performed in a similar fashion to that described in Chapter 2. In this study, we assessed VMR responses to VD in the same animal at baseline (vehicle treatment) and after treatment with $Na_V1.7$ inhibitor, Tsp1a. We have previously shown that a single bolus dose of 200nM Tsp1a delivered intracolonically can normalise colonic hypersensitivity in a mouse model of colonic visceral hypersensitivity (CVH) [366]. Vehicle (saline) or $Na_v1.7$ inhibitor (Tsp1a 200 nM) were administered intravaginally (50 µL). Following the final VD distension after saline treatment, mice were returned to their cage for a minimum of 3 hours before repeating the VD protocol in the presence of Tsp1a. Each VMR to VD protocol was completed within 30 minutes of either saline or Tsp1a administration. Any mice with damaged electrodes that prevented both interventions were excluded from paired analysis.

To quantify the magnitude of the VMR at each VD pressure, the area under the curve (AUC) during the distension was corrected for baseline activity (30 seconds AUC pre-distension). The AUC for the total AUC (all distension pressures), non-noxious AUC (pressures 20 and 30 mm Hg) and noxious AUC (pressures between 40 and 70 mm Hg) was quantified by adding the individual AUC at each VD pressure.

5.4.7 Statistical analysis

Data was graphed using Prism 9 software (GraphPad Software, San Diego, CA, USA) and presented as mean ± standard error of the mean (SEM), with n representing the number of afferents recorded and N representing the number of animals per group. Normality of data was assessed using the Shapiro-Wilk test prior to all statistical analysis. Data were analysed where appropriate using a paired or unpaired two-tailed Student *t* tests for groups of equal variances; or using the Wilcoxon or Mann-Whitney nonparametric test for groups with unequal variances. Data comparing more than two groups were analysed using an ordinary one- or two-way analysis of variance (ANOVA) with Bonferroni or Kruskal-Wallis multiple comparisons post hoc tests. VMR distension data were analysed using generalised estimating equations (GEE) followed by least significant difference (LSD) post hoc test when appropriate, using SPSS 27.0. Differences were considered statistically significant at $*P < 0.05$, $**P < 0.01$, $***P < 0.001$ and $****P < 0.0001$.

5.5 Results

5.5.1 Activation of $Na_V1.7$ sensitizes vaginal-innervating pelvic afferents to mechanical stimuli in Sham control mice

We show in Chapter 4 that broad activation of Na_V channels with the pan-Na_V agonist, veratridine, resulted in a significant increase in pelvic vaginal afferent responses to vaginal surface stroking, focal compression and circular stretch [220]. With this in mind, we aimed to use our recently developed *ex vivo* afferent recording preparation to further elucidate the role of $Na_V1.7$ in the mechanosensitivity of pelvic afferents innervating the vagina.

Application of the selective $Na_V1.7$ agonist, OD1 (100 nM), to the receptive field on the luminal surface of vaginal tissue of Sham mice resulted in significant hypersensitivity to all 3 mechanical stimuli tested **(Figure 5.2A-D)**. Specifically, action potential firing of vaginal afferents to vaginal surface stroking with calibrated von Frey hairs (vfh) were significantly elevated at 200, 500 and 1000 mg of force following OD1 incubation **(Figure 5.2B)**. Focal compression (2 g vfh) of afferent receptive fields in the presence of OD1 also achieved a significant increase in action potential firing compared to baseline responses **(Figure 5.2C)**. Pelvic afferents also became hypersensitive to circular stretch (5 g) in the presence of OD1, with significantly elevated action potential firing rate **(Figure 5.2D i)** as well as reduced latency to the first evoked action potential **(Figure 5.2D ii)**. Interestingly, OD1 evoked spontaneous action potential firing following mechanical stimulation in 50% of afferents, a phenomenon not seen following baseline mechanical stimulation **(Figure 5.2E i-ii)**.

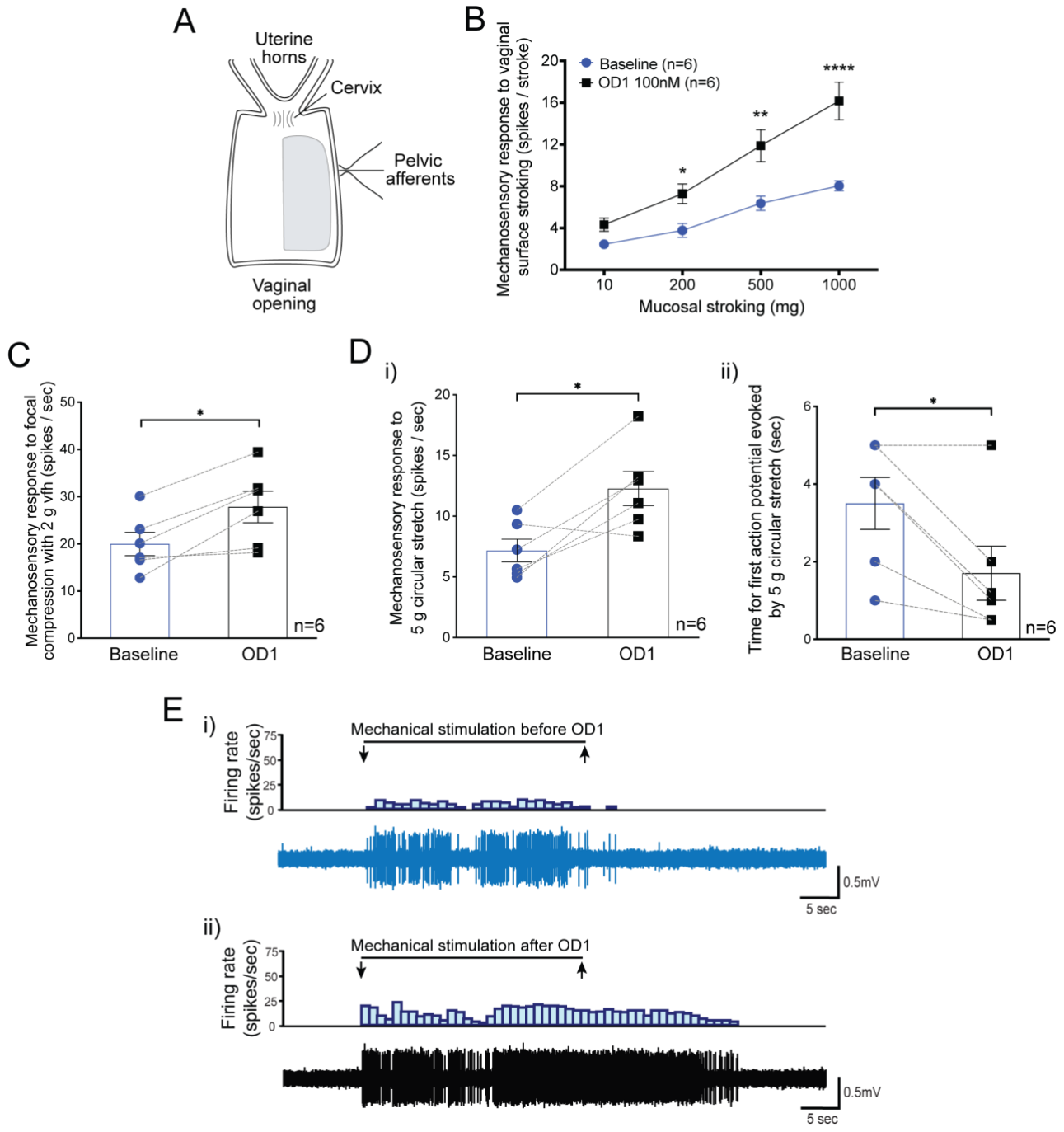

Figure 5.2: Activation of $Na_V1.7$ with OD1 (100 nM) sensitizes vaginal-innervating pelvic afferents to a variety of mechanical stimuli in Sham control mice.

(A) Schematic diagram of the *ex vivo* electrophysiology preparation for measuring vaginal-innervating pelvic afferents in female mice. Receptive field of pelvic afferents recorded were located along the length of vaginal tissue (indicated by shaded grey area). Grouped data **(B-D)** obtained with this preparation in Sham control mice show that luminal activation of $Na_V1.7$ with OD1 (100 nM for 5 mins, black) significantly increased baseline (blue) mechanosensation to 3 different mechanical stimuli. **(B)** OD1 significantly increased the mechanosensory responses (spikes/sec) to vaginal surface stroking with calibrated von Frey hairs (vfh) from 200 mg to 1000 mg (**P* <0.05, ***P* <0.01, *****P* <0.0001, two-way ANOVA with Bonferroni post hoc comparison tests). **(C)** Focal compression of the afferent receptive fields on vaginal surface with a 2 g vfh filament were also increased following incubation (**P* <0.05, paired Students *t*-test). **(D) i)** Mechanosensitivity of pelvic afferents to circular stretch (5g) of the whole vaginal tissue was also significantly enhanced following OD1 incubation. **ii)**

a reduction in the time to elicit the first action potential was also significantly reduced following OD1 incubation (*P <0.05, paired Student t test). **(E) ii)** spontaneous firing of action potentials following mechanical stimulation was also demonstrated following OD1 incubation, **i)** this phenomenon did not occur before OD1 application. Data represent mean ± SEM with n = 6 afferents from N = 3 Sham control mice. Vfh: von Frey hair; ANOVA: analysis of variance**.**

5.5.2 Inhibition of $Na_V1.7$ has no effect on vaginal-innervating pelvic afferents mechanosensitivity in Sham mice, *ex vivo*

Considering $Na_V1.7$ activation with OD1 was able to sensitize vaginal afferent receptive fields in Sham mice, we wanted to see whether inhibition of $Na_V1.7$ with Tsp1a would reduce baseline afferent responses. Understanding this would allow us to elucidate an *ex vivo* role for $Na_V1.7$ in vaginal afferent signalling in healthy conditions.

Interestingly, we found that incubation with the specific $Na_V1.7$ inhibitor, Tsp1a (200 nM) had no effect on baseline action potential firing rates of pelvic vaginal afferents to all 3 mechanical stimuli tested **(Figure 5.3A-C)**. This included no change to baseline mechanosensory responses to vaginal surface stroking **(Figure 5.3A i-ii)**, focal compression (2 g vfh) **(Figure 5.3B i-ii)** or 5 g circular stretch **(Figure 5.3C i-ii)**. Inhibition of $Na_V1.7$ with Tsp1a also had no effect on the afferent firing rate or the time to first evoked action potential **(Figure 5.3C iii)**. Overall, these findings suggest that $Na_V1.7$ does not play a significant role in healthy baseline vaginal sensory signalling, *ex vivo*.

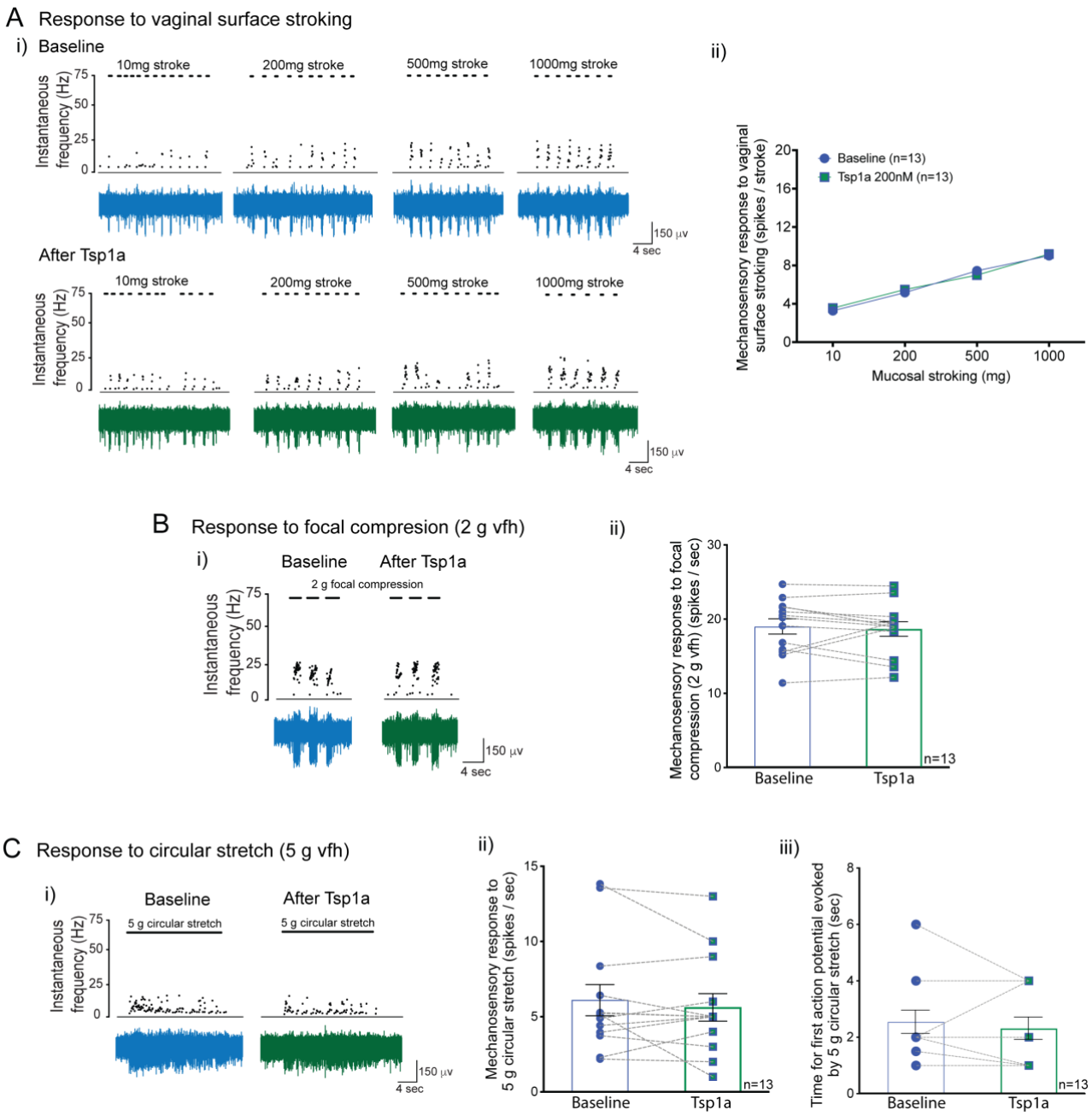

Figure 5.3: Inhibition of $Na_V1.7$ with Tsp1a (200 nM) does not alter the mechanosensitivity of vaginal-innervating pelvic afferents in Sham control mice.

(A-C) Representative traces of electrophysiological recordings together with grouped data show that luminal inhibition of $Na_V1.7$ with Tsp1a (green) has no effect on the baseline (blue) mechanosensation of pelvic afferents to 3 different mechanical stimuli. **(A)** Tsp1a had no effect on baseline mechanosensory responses (spikes/sec) to vaginal surface stroking with calibrated vfh across all ranges tested between 10 mg and 1000 mg (P >0.05, two-way ANOVA with Bonferroni post hoc comparison tests). **(B)** The firing rate (spikes/sec) in response to focal compression of the afferent receptive fields on the luminal vaginal surface with a 2 g vfh filament was also unchanged following incubation with Tsp1a (P >0.05, paired Student t test). **(C)** **i)** Mechanosensitivity of pelvic afferents to circular stretch (5 g) of the whole vaginal tissue also showed no change following Tsp1a incubation. **iii)** the time to elicit the first action potential remained similar following incubation with Tsp1a (P >0.05, paired Student t test). Data represent mean ± SEM with n = 13 afferents from N = 4 Sham control mice. Vfh: von Frey hair; ANOVA: analysis of variance.

5.5.3 $Na_V1.7$ inhibition has no effect on vaginal sensation in Sham mice, *in vivo*

After identifying that $Na_V1.7$ inhibition had no effect on vaginal afferent mechanosensitivity of Sham mice, *ex vivo*, we wanted to see whether inhibiting $Na_V1.7$ channels directly within the vagina could modulate the vaginal sensation of Sham mice, *in vivo.* For this, we recorded the visceromotor responses (VMR) to graded vaginal distension (VD) as previously described in Chapter 2, 3 and 4 [220, 297, 376]. We evaluated the VMR to non-noxious (20-30 mm Hg) and noxious (40-70 mm Hg) distensions pressures, to determine whether mice experience signs of allodynia (pain to non-noxious stimuli) or hyperalgesia (enhanced pain to noxious stimuli).

Vaginal distension (VD) in Sham mice evokes a staged increase in VMR, proportional to the amount of pressure applied **(Figure 5.4A-B)**. Similar to the results seen in the *ex vivo* preparation, direct inhibition of $Na_V1.7$ with intravaginal Tsp1a did not alter the VMR response to VD across any distension pressure in Sham mice **(Figure 5.4A-B)**. Furthermore, the total response (area under the curve; AUC) remains unchanged in the presence of Tsp1a **(Figure 5.4C i).** Additional sub-analysis revealed that Tsp1a application did not alter the VMR responses at non-noxious **(Figure 5.4C ii)** nor noxious **(Figure 5.4C iii)** distension pressures. Taken together, these findings suggest that $Na_V1.7$ does not contribute to the baseline vaginal afferent firing and sensory responses evoked by vaginal distension in control conditions.

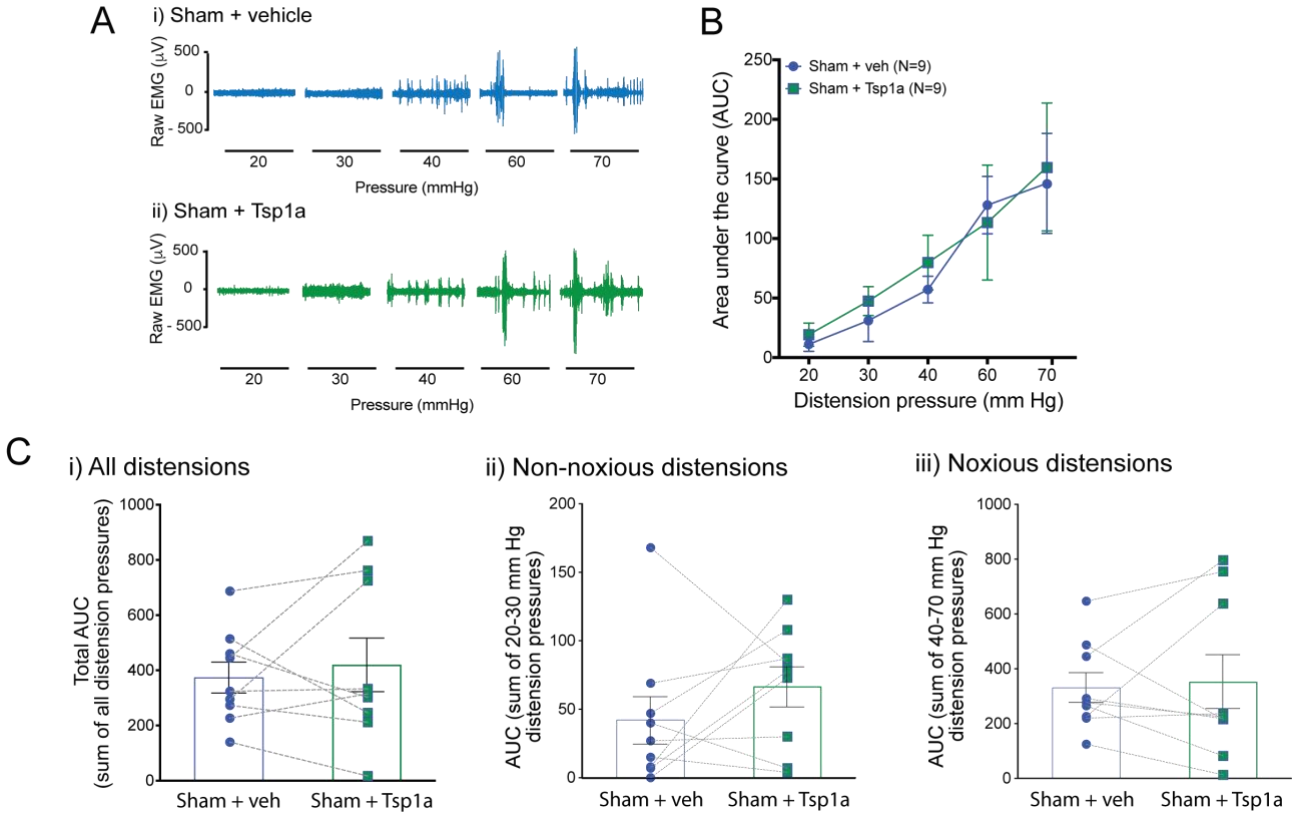

Figure 5.4: Inhibition of $Na_V1.7$ with Tsp1a (200 nM) does not alter pain evoked by vaginal distension in Sham control mice

(A) Representative electromyography (EMG) recordings at increasing vaginal distension (VD) pressures (horizontal bars represent 30 sec VD at pressures between 20-70 mm Hg) in conscious Sham control mice following intravaginal administration of **i)** vehicle (saline, blue) followed by **ii)** Tsp1a (200 nM) (green). **(B)** Group data shows no difference in the visceromotor responses (VMR) to VD across all distension pressures from Sham control mice, treated with vehicle (blue) or Tsp1a (green). (*P* >0.05 generalised estimating equations followed by LSD post hoc test). **(C)** grouped data for the **i)** total AUC across all distension pressures, **ii)** non-noxious (20-30 mm Hg) distension pressures and **iii)** noxious (40-70 mm Hg) distension pressures shows that the VMR responses following vehicle administration were unchanged with Tsp1a treatment (green). Each dot represents the total AUC (sum of the AUCs obtained at each distension pressure) from an individual animal. *P* >0.05, paired Student *t* test. Data represent mean ± SEM from N = 9 Sham control mice. EMG: electromyography; VD: vaginal distension; AUC: area under the curve; VMR: visceromotor response; LSD: least significant difference.

With these results in mind, we next wanted to investigate whether $Na_V1.7$ channels play a role in abnormal vaginal sensation developed in our pre-clinical mouse model of endometriosis. In Chapter 3 we demonstrate that sensory afferents innervating the bladder develop mechanical hypersensitivity in a syngeneic inoculation mouse model of endometriosis [376]. Although sensitization of the peripheral sensory system that innervates the female reproductive tract is also suggested to occur in endometriosis [141, 172, 231], it has not yet been demonstrated. With this in mind, we first explored whether sensory afferents innervating the vagina of mice with endometriosis developed afferent hypersensitivity.

5.5.4 Vagina-innervating pelvic afferents from endometriosis mice develop hypersensitivity

Using our *ex vivo* pelvic afferent preparation, we compared the response of vaginal-innervating afferents to 3 different mechanical stimuli, in both Sham mice and mice with fully developed endometriosis (Endo) **(Figure 5.5)**. Vaginal afferents from Sham mice displayed an expected steady increase in action potential firing in response to increasing stroking pressures **(Figure 5.5A i-ii)**. In comparison, vaginal afferents from Endo mice showed enhanced action potential firing to the same vaginal surface stroking, particularly at the higher stroking pressures, 500-1000 mg **(Figure 5.5A i-ii)**. Although there was no significant difference in the response of vaginal afferents from Endo mice to focal compression (2 g vfh) **(Figure 5.5B i-ii)**, significant hypersensitivity of vaginal afferents was present in response to circular stretch of the whole vaginal tissue in Endo mice. These vaginal afferents displayed an increased afferent firing rate **(Figure 5.5C i-ii)** as well as a significant reduction in the latency to first evoked action potential **(Figure 5.5C iii)**.

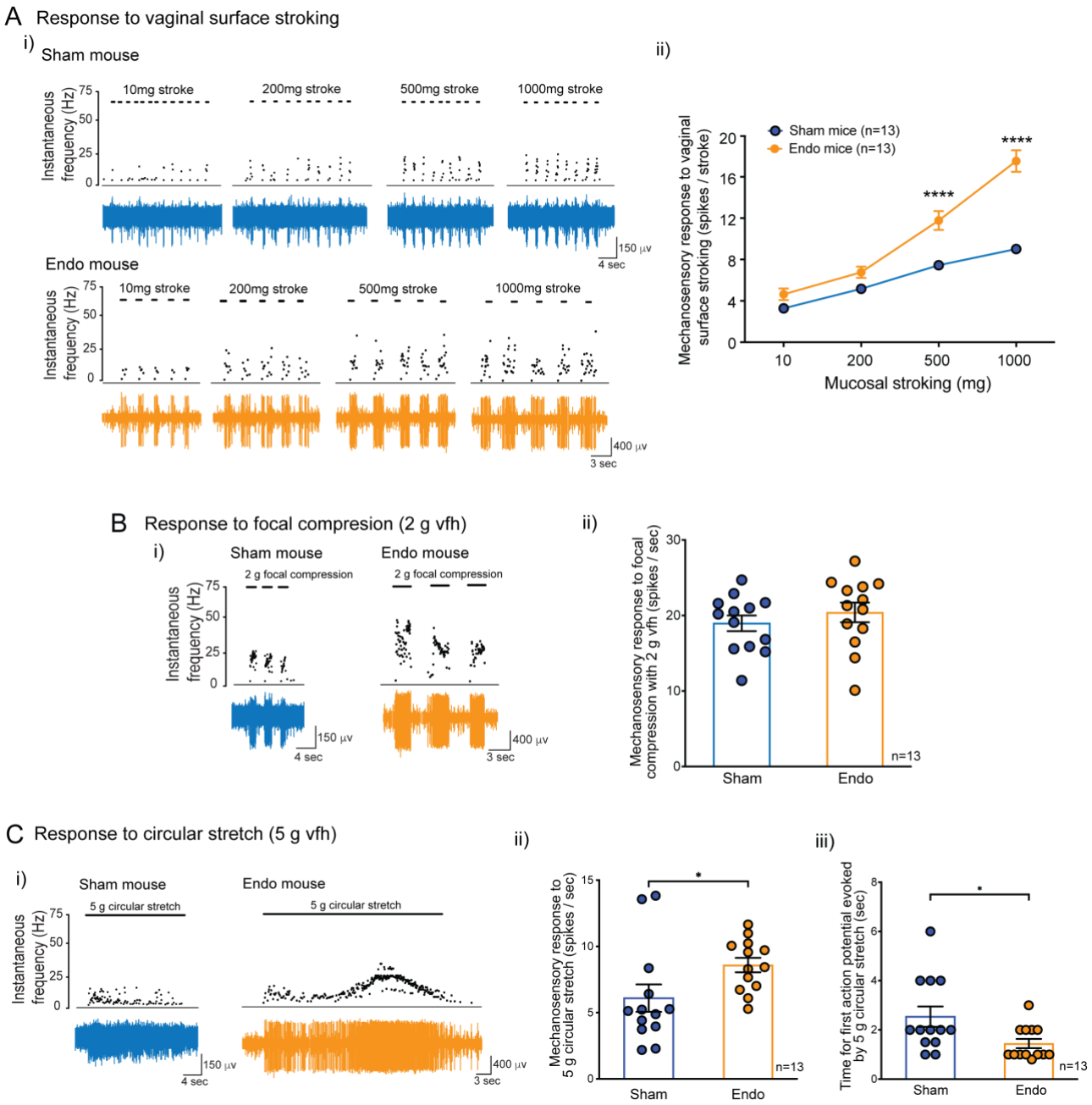

Figure 5.5: Vagina-innervating pelvic afferents from mice with endometriosis developed hypersensitivity to mechanical stimuli

(A-C) Representative traces of electrophysiological recordings together with grouped data obtained from Sham (blue) and Endo (orange) mice using the *ex vivo* vaginal afferent preparation shows that the development of endometriosis in mice leads to significantly enhanced mechanosensitivity in response to surface stroking and circular stretch but not to focal compression. **(A)** Endometriosis mice exhibit a significantly increased mechanosensory responses (spikes/sec) to vaginal surface stroking with calibrated vfh at both 500 mg and 1000 mg (****P <0.0001, two-way ANOVA with Bonferroni post hoc comparison tests). **(B)** Focal compression of the afferent receptive fields on the vaginal surface with a 2 g vfh filament was similar in mice with endometriosis compared to their Sham counterparts (P >0.05, un-paired Student t test). **(C) i-ii)** The mechanosensitivity of pelvic afferents to circular stretch (5g) of the whole vaginal tissue was significantly enhanced in mice with endometriosis compared to Sham mice. **iii)** This was also apparent with a significant reduction in the time taken (seconds) to elicit the first action potential following 5 g circular stretch, in endometriosis mice compared to Sham controls (*P <0.05, un-paired Student t test). Data represent mean ± SEM with n = 13 afferents from N = 4 Sham mice and n = 13 afferents from N = 4 Endo mice. Vfh: von Frey hair; ANOVA: analysis of variance.

5.5.5 Inhibition of $Na_V1.7$ reduces mechanical hypersensitivity of vaginal afferents in endometriosis mice, *ex vivo*

Considering our previous findings, which indicate that $Na_V1.7$ channels (SCN9A) were expressed in 100% of sensory afferents innervating the vagina [220], and a demonstrated role of $Na_V1.7$ channels in heightened nociception [378], we sought to determine whether $Na_V1.7$ channels were contributing to the vaginal hypersensitivity developed by mice with endometriosis.

Using the selective $Na_V1.7$ inhibitor, Tsp1a (100 nM), applied directly to the mucosal surface of the vagina, we show that the heightened vaginal afferent mechanosensory responses present in endometriosis mice were significantly attenuated **(Figure 5.6)**. Specifically, the mechanosensory response of vaginal afferents to all 3 mechanical stimuli tested, including surface stroke **(Figure 5.6A)**, focal compression **(Figure 5.6B)** and circular stretch **(Figure 5.6C i-ii)** were significantly reduced in the presence of Tsp1a. Furthermore, incubation with Tsp1a delayed afferent response to mechanical stimuli, inducing a significantly increased time to the first evoked action potential **(Figure 5.6C iii)**.

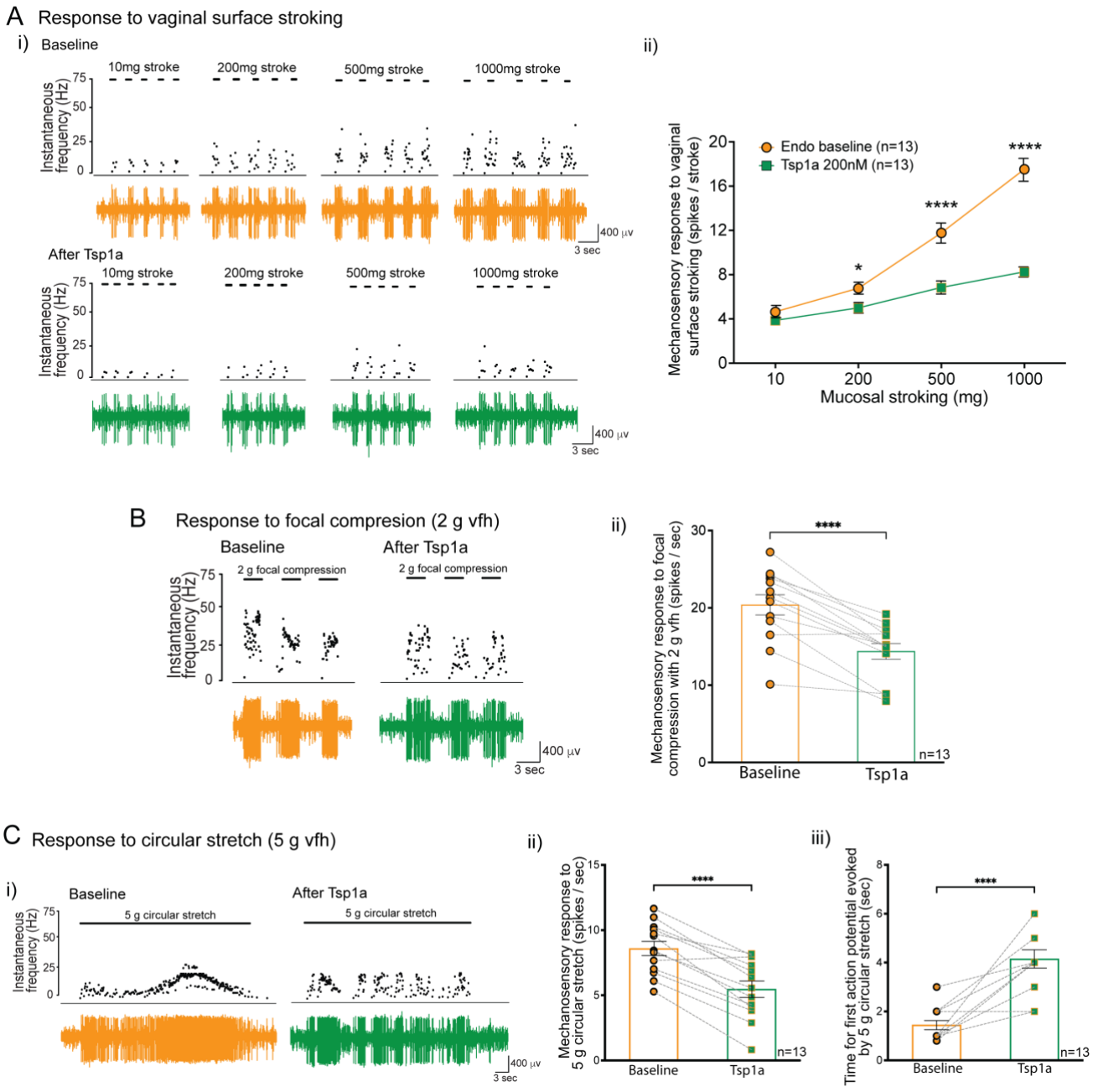

Figure 5.6: Inhibition of $Na_V1.7$ with Tsp1a (200 nM) reduces the mechanosensitivity of vaginal-innervating afferents in mice with endometriosis.

(A-C) Representative traces of electrophysiological recordings together with grouped data show that luminal inhibition of $Na_V1.7$ with Tsp1a (green) significantly reduces the developed hyper-mechanosensation of pelvic afferents to 3 different mechanical stimuli seen in endometriosis mice (orange). **(A)** Tsp1a reduced baseline mechanosensory responses (spikes/sec) to vaginal surface stroking with calibrated vfh across ranges 200 mg and 1000 mg (*P >0.05, ****P <0.0001, two-way ANOVA with Bonferroni post hoc comparison tests). **(B)** The firing rate (spikes/sec) in response to focal compression of the afferent receptive fields on the luminal vaginal surface with a 2 g vfh filament was significantly reduced following incubation with Tsp1a (****P <0.0001, paired Student t test). **(C) i-ii)** The enhanced mechanosensitivity of pelvic afferents to circular stretch (5 g) of the whole vaginal tissue was also reduced following Tsp1a incubation. **iii)** This was also seen with an increased time to elicit the first action potential following incubation with Tsp1a (****P >0.0001, paired Student t test). Data represent mean ± SEM with n = 13 afferents from N = 4 Endo mice. Vfh: von Frey hair; ANOVA: analysis of variance.

5.5.6 Inhibition of $Na_V1.7$ channels reverses vaginal allodynia and hyperalgesia developed by mice with endometriosis

To determine whether the demonstrated role of $Na_V1.7$ in vaginal hypersensitivity in endometriosis, *ex vivo,* translates to an alteration in vaginal sensory responses, *in vivo*, we first aimed to confirm our previous finding, that mice with endometriosis displayed enhanced vaginal pain sensitivity evoked by VD using VMR [297]. In line with the hypersensitivity demonstrated in vaginal innervating afferents *ex vivo*, we found that our Endo mice indeed developed enhanced vaginal sensitivity across all distension pressures, *in vivo* **(Figure 5.7A-B)**. This hypersensitivity was evident as an increase in the total AUC **(Figure 5.7B)** as well as a significant increase at both non-noxious **(Figure 5.7C)** and noxious **(Figure 5.7D)** VD pressures, displaying the development of both allodynia and hyperalgesia in Endo mice.

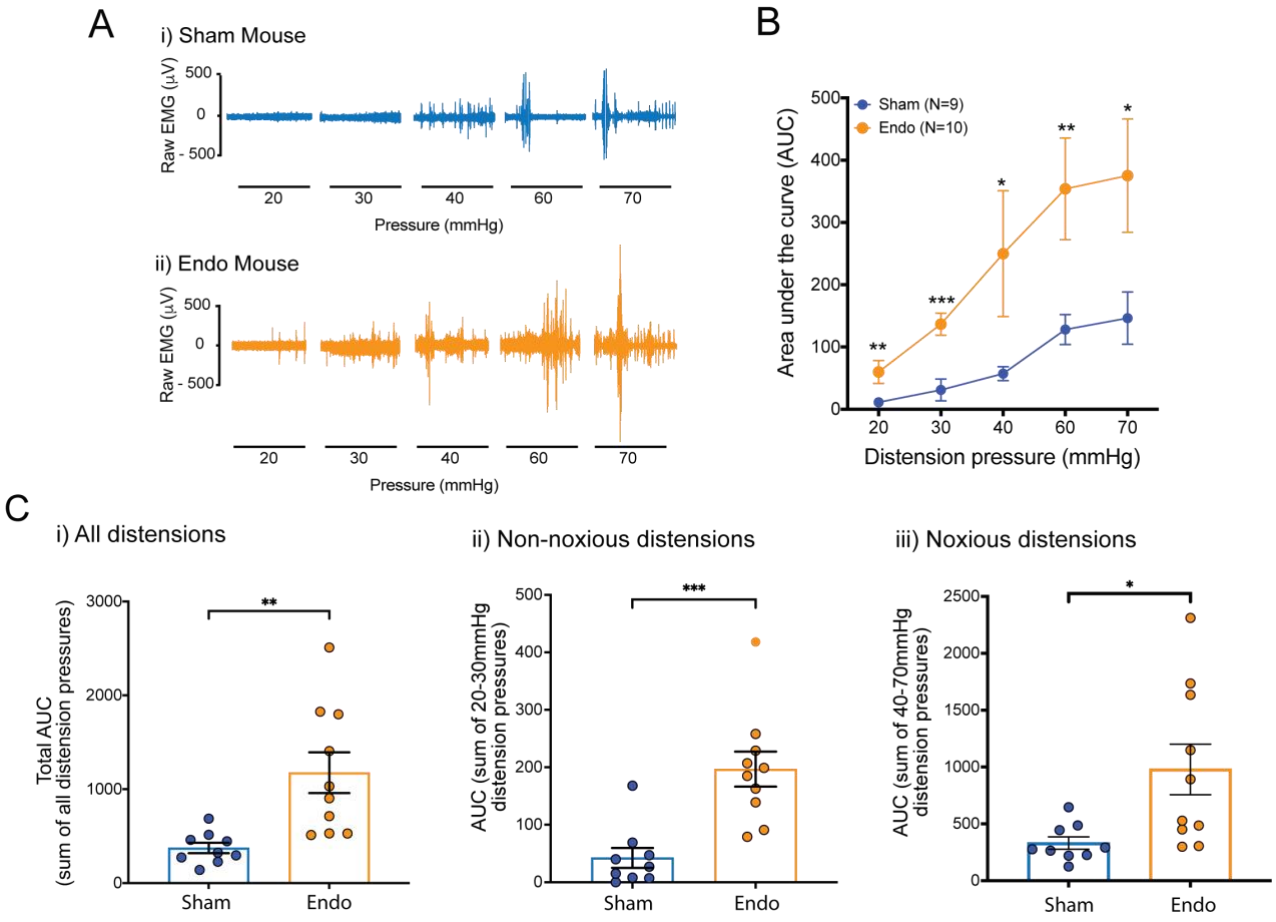

Figure 5.7: Mice with endometriosis display allodynia and hyperalgesia evoked by vaginal distension *in vivo*.

(A) Representative EMG recordings at increasing vaginal distension (VD) pressures (horizontal bars represent 30 sec VD at pressures between 20-70 mm Hg) in Sham control mice (blue) and Endo mice (orange). **(B)** Group data of the of the area under the curve (AUC) of visceromotor responses (VMR) to VD across all distension pressures from Sham control mice and endo mice. Endo mice displayed enhanced VMR responses across all distension pressures compared to their Sham counterparts (**P* <0.05, ***P* <0.01, ****P* <0.001, generalised estimating equations followed by LSD post hoc test). **(C)** grouped data for the **i)** total AUC across all distension pressures, **ii)** non-noxious (20-30 mm Hg) distension pressures and **iii)** noxious (40-70 mm Hg) distension pressures shows that the VMR responses of endo mice were significantly elevated across all distension pressures, as well as displaying allodynia at non-noxious distension pressures and hyperalgesia at noxious distension pressures. Each dot represents the total AUC (sum of the AUCs obtained at each distension pressure) from an individual animal. **P* <0.05, ***P* <0.01, ****P* <0.001, un-paired Student *t* test. Data represent mean ± SEM from N = 9 mice Sham and N = 10 Endo mice. EMG: electromyography; LSD: least significant difference.

After confirming that Endo mice developed vaginal allodynia and hyperalgesia, we investigated whether inhibition of $Na_V1.7$ channels could revert the vaginal hypersensitivity present in mice with endometriosis. We found that $Na_V1.7$ inhibition with a single intravaginal dose of Tsp1a significantly reduced VMR to non-noxious VD pressures, 20-30 mm Hg, as well as the noxious pressure, 60 mm Hg **(Figure 5.8A-B)** in Endo mice. $Na_V1.7$ inhibition with Tsp1a was able to reduce the total VMR response (total AUC) to VD **(Figure 5.8C i)**, reducing both the allodynia at non-noxious pressures **(Figure 5.8C ii)** as well as hyperalgesia at noxious pressures **(Figure 5.8C iii)**. Interestingly, the reduction in response to VD generally normalised the hypersensitivity developed in Endo mice to levels similar to those of Sham mice. This included a reduction to the total response **(Figure 5.8B and 5.8D i)**, non-noxious distension response **(Figure 5.8B and 5.8D ii),** and noxious distension response **(Figure 5.8B and 5.8D iii)** to be comparable to that of Sham mice.

Taken together these results suggest that $Na_V1.7$ plays a role in the aberrant vaginal sensory signalling developed in mice with endometriosis. Importantly, the reversal of vaginal pain in endometriosis mice returned to responses experienced by Sham mice, maintaining a baseline level of vaginal sensation equivalent to those without endometriosis.

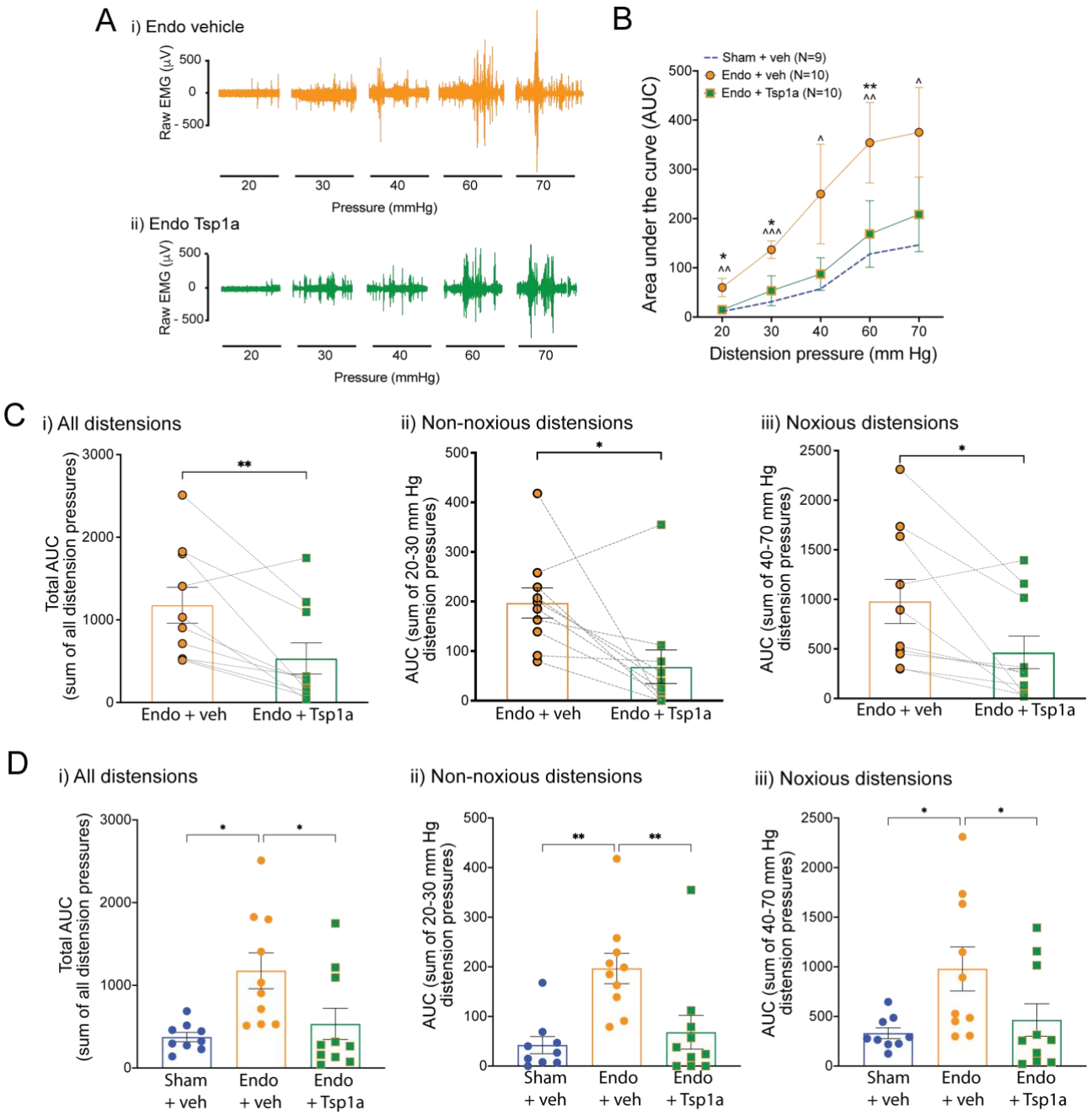

Figure 5.8: Inhibition of $Na_V1.7$ with Tsp1a (200nM), reduced allodynia and hyperalgesia evoked by vaginal distension in mice with endometriosis, reducing VMR responses to levels seen in Sham mice.

(A) Representative electromyography (EMG) recordings at increasing vaginal distension (VD) pressures (horizontal bars represent 30 sec VD at pressures between 20-70 mm Hg) in mice with endometriosis (Endo) following intravaginal administration of **i)** vehicle (saline, orange) followed by **ii)** Tsp1a (200 nM) (green). **(B)** Grouped data shows a significant reduction in the visceromotor responses (VMR) to VD at 20-30 mm Hg and 60 mm Hg between Endo mice treated with vehicle (orange) and Tsp1a (green). Endo mice treated with Tsp1a returned to similar VMR as Sham control mice (blue dotted line) (**P* <0.05, ***P* <0.01 in Endo + veh vs Endo + Tsp1a; ^*P* <0.05, ^^*P* <0.01 and ^^^P<0.001 Endo + veh vs Sham + veh; GEE followed by LSD post hoc test). **(C)** grouped data for the **i)** total AUC across all distension pressures, **ii)** non-noxious (20-30 mm Hg) distension pressures and **iii)** noxious (40-70 mm Hg) distension pressures shows that VMR responses following vehicle administration (orange) were reduced with Tsp1a treatment (green) across all pressure ranges. Each dot represents the total AUC (sum of the AUCs obtained at each distension pressure) from an individual animal. (**P* <0.05, ***P* <0.01, paired Student *t* test). **(D)** Grouped data of the **i)**

total AUC across all distension pressures, **ii)** non-noxious (20-30 mm Hg) distension pressures and **iii)** noxious (40-70 mm Hg) distension pressures illustrates that the reduction in allodynia and hyperalgesia developed in mice with endometriosis returns to levels like those seen in Sham + veh treated mice. (**P* <0.05, ***P* <0.01, One-way ANOVA with Kruskal-Wallis post hoc comparison). Data represent mean ± SEM from N = 9 Sham and N = 10 Endo mice.

5.6 Discussion

Vaginal pain is experienced by many women that suffer from endometriosis, however, the mechanisms contributing to this chronic pain are poorly understood. In Chapter 4, we demonstrated that healthy pelvic vaginal afferents were tuned to detect a variety of mechanical stimuli in mice. We identified that modulating voltage gated sodium (Na_V) channel activity was able to alter sensory signalling from the vagina, leading to modified mechanosensory responses, nociceptive signalling within the spinal cord and ultimately altered pain responses *in vivo* [220]. Whilst this provided the first direct confirmation that both TTX-sensitive ($Na_V1.1$-$Na_V1.4$, $Na_V1.6$, and $Na_V1.7$) and TTX-resistant ($Na_V1.5$, $Na_V1.8$ and $Na_V1.9$) Na_V channels play a tangible role in regulating vaginal sensation, identifying the contribution of individual Na_V channel isoforms had not yet been explored. Of particular interest, the TTX-sensitive isoform $Na_V1.7$ was expressed in 100% of vaginal innervating sensory neurons and, although $Na_V1.7$ does not appear to contribute to visceral nociception in healthy conditions [356], it may have a role in the development and maintenance of chronic pain [379]. Building on our previous results, this chapter focused specifically on the role of $Na_V1.7$ in vaginal pain signalling and importantly, examined its contribution to the aberrant pain signalling developed in endometriosis.

In this study, utilising a single unit *ex vivo* afferent recording preparation, we were able to determine that by targeting the most favourably expressed Na_V channel in vaginal innervating neurons, $Na_V1.7$, we were able to modulate the mechanosensitivity of sensory afferents in control mice. Using the α scorpion toxin OD1 to selectively activate $Na_V1.7$, we significantly enhanced the mechanosensory responses of afferents innervating the vagina, demonstrating that vaginal mechanosensory drive could be elevated by pharmacological activation of $Na_V1.7$. Physiologically, $Na_V1.7$ plays a key role in setting the activation threshold of sensory afferent terminals, with its activation triggering depolarization of afferent nerves and action potential firing [378, 380, 381]. In genetic gain-of-function mutations, the enhanced activity of $Na_V1.7$ in sensory neurons maintains them in a hyperexcitable state, increasing action potential firing and ultimately driving sensory signalling, even in the absence of stimuli [380]. Kinetically, following its activation $Na_V1.7$ is slow to close and subsequently inactivate [378, 382]. In line with this, we saw spontaneous firing in half of vaginal afferent fibres once mechanical stimuli had ceased. In this instance, targeted $Na_V1.7$ activation with OD1, followed by its slow closed-state inactivation, disrupts resting threshold equilibrium in such a way that it maintains sensory neurons in a hyperexcitable state, even in the absence of further stimuli, and action potentials continue to fire [377].

We then examined whether selective inhibition of $Na_V1.7$ would alter the sensitivity of vaginal afferents to mechanical stimulation in control mice. In contrast to the modulating effect seen with OD1, select inhibition of $Na_V1.7$ with the tarantula derived peptide Tsp1a did not alter the capacity of vaginal-innervating afferents to respond to the same mechanical stimuli. The lack of modification

to mechanosensitivity was further supported by VMR to VD studies, where Tsp1a also had no effect on baseline vaginal pain sensation recorded in conscious control mice. These results are consistent with the notion that $Na_V1.7$ channels do not appear to contribute to visceral nociception in healthy conditions [356, 366].

Although $Na_V1.7$ channels do not appear to have a role in healthy vaginal sensory afferent signalling, altered pain responses in human $Na_V1.7$ functional mutations, as well research using some chronic disease models, has identified that altered $Na_V1.7$ channel activity may drive heightened pain and nociception in chronic pain [366, 381, 382]. As peripheral afferent sensitization is proposed to develop following chronic development of disease where chronic visceral pain manifests, such as IBS and IC/BPS [157-163] the involvement of $Na_V1.7$ in endometriosis associated CPP is of interest. Insight into the differential roles of $Na_V1.7$ in various stages of inflammatory disease has been built using animal models of visceral hypersensitivity. For example, in a mouse model of inflammatory colitis, where colitis mice experience colonic hypersensitivity [110, 158], the expression of $Na_V1.7$ remained unchanged in colonic DRG neurons in an acute model (7 days) [383] however it became upregulated in a model of chronic visceral hypersensitivity (CVH) (4 weeks) compared to controls [379]. Similarly, increased levels of $Na_V1.7$ in DRG neurons are found in a rat model of painful diabetic neuropathy, where both mechanical allodynia and thermal hyperalgesia have been demonstrated at 4 weeks following diabetes induction [384, 385]. As endometriosis is a chronic inflammatory disease, with an average of 8-12 years to diagnosis, chronic inflammation has had time to impart significant influence on CPP mechanisms [67-69]. With the frequent involvement of several visceral organs, hypersensitivity of visceral afferents, as seen in other chronic conditions, may play a key role in the diverse CPP developed in endometriosis.

In Chapter 3, we identified that sensory afferents innervating the bladder of endometriosis mice, which exhibit signs of visceral pain, became hypersensitive to mechanical stimuli compared to the bladder afferents of their Sham counterparts [376]. Expanding on these findings, the results presented in this chapter demonstrate, for the first time, that endometriosis development also induces hypersensitivity of vaginal-innervating sensory afferents. Together, these results continue to demonstrate that endometriosis development can alter afferent sensitivity across multiple visceral organs, although the mechanisms involved remain largely unknown. As $Na_V1.7$ has been of key interested in the transduction of visceral nociceptive pain in chronic inflammatory diseases, we aimed to determine whether it had a role in the pathophysiology of endometriosis associated CPP.

In this study, we have been able to identify a specific role for $Na_V1.7$ in endometriosis associated vaginal afferent hyperexcitability, allodynia and hyperalgesia. By measuring the sensitivity of the vaginal afferents of endometriosis mice, in the presence of $Na_V1.7$ inhibitor Tsp1a, we were able to illustrate that selective inhibition of $Na_V1.7$ can normalise endometriosis induced vaginal afferent sensitivity, *ex vivo*. Translating this to nociceptive behavioural changes *in vivo*, we

further demonstrated that $Na_V1.7$ inhibition with a single intravaginal dose of Tsp1a was able to normalise the vaginal hypersensitivity induced by endometriosis development in conscious mice. Of significance, Tsp1a was able to reverse endometriosis associated vaginal allodynia and hyperalgesia but did not abolish the important baseline sensory functions of vaginal sensation, maintaining sensitivity similar to that seen in Sham control mice. These results also reflect those seen with Tsp1a and Sham mice, with no additional reduction below baseline sensory levels. This finding is important, as maintaining baseline functional levels of vaginal sensation are important for physiological and sexual function in women with endometriosis. Of promise, these analgesic results on vaginal hypersensitivity are akin what was recently shown using a mouse model of CVH [366]. These studies nicely demonstrated that intracolonic $Na_V1.7$ inhibition with Tsp1a (200 nM) was able to normalise elevated VMR to colorectal distension (CRD) to baseline levels in CVH mice but did not affect VMR responses to CRD in healthy mice [366].

As endometriosis is an estrogen-dependent inflammatory disease effecting women of reproductive age, the link between estrogen receptors and $Na_V1.7$ is an important relationship to consider. The estrogen receptor β agonist, 2,3-bis(4-hydroxy-phenyl)-propionitrile has been demonstrated to drive expression of SCN9A, the gene encoding $Na_V1.7$, in human embryonic stem cells with a nociceptive phenotype [168]. It has also been demonstrated that macrophages, activated with peritoneal fluid from women with endometriosis, can enhance the expression of SCN9A in cultured human sensory neurons [257]. Within human tissue samples, elevated levels of SCN9A have also been found in endometriosis lesions collected from women with pain compared to the peritoneum of women without endometriosis/without pain [168]. While changes in the expression profile of $Na_V1.7$ relating to key endometriosis factors including estrogen, peritoneal fluid, and endometriosis lesions themselves have been discovered, the functional role of $Na_V1.7$ in sensory signalling in endometriosis, had not yet been explored. The results presented in this chapter provide the first direct link between $Na_V1.7$ and vaginal pain signalling and demonstrate an enhanced, and importantly reversible, role in endometriosis associated vaginal hyperalgesia.

Although $Na_V1.7$ is a widely accepted pain target, largely due to genetic mutations impacting pain sensitivity in humans, the translation to clinical significance as a treatment for chronic pain is unfortunately lacking. Other Na_V channel isoforms are known to play a vital role in key physiological processes, including maintaining cardiac rhythm ($Na_V1.5$) and motor neuron function ($Na_V1.6$). This signifies the need for highly effective selectivity if $Na_V1.7$ targeted pharmacological therapeutics are to be successfully implemented in the treatment of chronic pain [386, 387]. Demonstrating encouraging results, indirect targeting of $Na_V1.7$ activity in sensory neurons by specifically inhibiting $Na_V1.7$ trafficking and surface expression, with compound 194, saw thermal and mechanical hypersensitivity reversed in a rodent model of neuropathic pain [388, 389]. More directly, promising analgesic responses have been demonstrated in basic rodent models of chemical-, thermal- and

acid-induced pain using centipede venom peptide μ-SLPTX-Ssm6a, which selectively inhibits human $Na_V1.7$ [390]. Similarly, $Na_V1.7$ inhibition using the novel blocker QLS-81 was able to normalise mechanical hypersensitivity of the hind paw in a mouse model of spinal nerve injury and spontaneous pain-like behaviours in acute inflammatory pain model induced by formalin injection, with no adverse effects on cardiac or locomotor activity [391]. Together with recently published results using the tarantula derived peptide Tsp1a to reverse colonic hypersensitivity in a mouse model of CVH [366], as well as the findings presented in this chapter, direct pharmacological targeting of $Na_V1.7$ is providing novel insight into its potential therapeutic role in sensory nociception in chronic visceral pain.

In conclusion, the results presented herein identifies the concurrent development of hyperexcitable vaginal afferents in a pre-clinical mouse model of endometriosis that has been shown to develop bladder afferent hypersensitivity as well as indications of widespread CPP [376]. The successful attenuation of vaginal afferent hypersensitivity and vaginal pain in mice with endometriosis treated intravaginally with Tsp1a occurred whilst maintaining baseline sensory functions. This suggests that pharmacological inhibition of $Na_V1.7$ may be a viable therapeutic treatment for chronic vaginal pain associated with endometriosis. Whether $Na_V1.7$ may play a role in additional visceral organ sensitivity seen in endometriosis, like that demonstrated in common comorbidities including IBS and BPS, was out of the scope of the current study but would provide an exciting link in understanding the mechanisms involved in endometriosis associated widespread CPP.

Ultimately, further understanding the mechanisms by which endometriosis induces chronic pain across multiple visceral organs will help identify targeted treatment options to alleviate CPP experienced by women with endometriosis. This brings us to the final results chapter of this thesis, which will elucidate whether the fluid surrounding visceral organs can directly activate visceral-innervating sensory neurons and explore whether heightened neuronal activation with the development of endometriosis may play a role in endometriosis associated CPP.

CHAPTER 6: PERITONEAL FLUID FROM MICE AND WOMEN WITH ENDOMETRIOSIS AND CHRONIC PELVIC PAIN INDUCES HEIGHTENED ACTIVATION OF VISCERAL INNERVATING SENSORY DORSAL ROOT GANGLION NEURONS

6.1 Co-contribution Statement

The work presented in this chapter was partly funded by a 'HDR Student Small Research Grant' awarded by the Flinders Health and Medical Research Institute.

Special thanks to Prof. Stuart Brierley and Dr. Joel Castro for training in experimental design, protocols, analysis, and interpretation of the data presented within this chapter. Special thanks also to Dr. Mariana Brizuela and Dr. Aenea Hendry for assistance and training in cell culture.

Human peritoneal fluid samples used in these experiments were collected as part of the Melbourne Endometriosis Research Cohort (MERC) at the Royal Women's Hospital (Melbourne, Australia) and provided by our collaborators A/Prof Martin Healey, Dr. Sarah Holdsworth-Carson and Prof. Peter Rogers.

The $Na_V1.8$-Cre mice used to generate $Na_V1.8$xGCaMP6s mice used in this chapter were kindly donated by A/Prof Wendy Imlach from Monash University (Melbourne, Australia)

6.2 Overview

It is widely accepted that the aberrant inflammatory profile of the peritoneal fluid (PF) is an innate pathology that contributes to endometriosis development in humans [230]. In Chapter 2, we were able to show that the inflammatory environment within the PF of our pre-clinical endometriosis model resembled that seen in women with endometriosis, developing elevated inflammatory cytokines including interleukins (IL) IL-1β, IL-6, IL-17, IL-33 and VEGF [297]. While this aberrant environment has been described to support the growth and chronic development of endometriosis [39, 230, 392], it has also been suggested that the chronic inflammatory milieu within PF may have a direct role in the generation of endometriosis associated CPP [106, 231], although this is yet to be demonstrated.

Our access to PF from both mice and women with endometriosis that experience CPP, as well as specialised $Na_V1.8$xGCaMP6s mice that allow us to visualise sensory neuron activity, provides us with the unique opportunity to directly determine whether PF has a direct functional role in sensory neuron activation. Utilising these tools, the aims of this final chapter were to: (1) determine whether PF collected from mice and women with endometriosis is able to directly activate or sensitize visceral sensory neurons innervating visceral organs of healthy mice and (2) examine whether different subtypes of PF, collected from both mice and women with endometriosis and CPP, induces distinctive neuronal activation profiles that may contribute to CPP development in endometriosis.

6.3 Introduction

To date, the majority of research into mechanisms of CPP development has focused on endometriotic lesions, most commonly found throughout the pelvic cavity, as the primary source of endometriosis associated pain [231]. Although lesion-specific pain is apparent, with lesions on visceral organs being able to induce locally-associated visceral pain [36, 393], the severity of CPP is not frequently correlated with the stage of disease or location of lesions [36, 37, 72]. This disconnect suggests that additional and lesion independent mechanisms may also contribute to the generation of CPP in endometriosis.

Endometriosis associated CPP can present as diffuse 'pelvic' pain or can be associated with visceral comorbidities affecting organs such as the colon, bladder, and vagina. Surrounding these pelvic organs is a small volume of peritoneal fluid (PF) that maintains a moist environment, acting as a dynamic medium to facilitate the exchange of immune cells and ultimately maintain homeostasis within the peritoneal cavity [394]. In women, part of this physiological role is to provide an innate immune environment that tightly controls the elimination of ectopic endometrial cells following retrograde menstruation, which naturally occurs in up to 90% of women [42, 43]. However, in endometriosis, a chronic imbalance in this immune response is thought to disrupt ectopic cell clearance, which ultimately contributes to the growth and maintenance of endometriotic lesions [39, 392]. Ectopic lesion development further compounds this aberrant inflammatory environment within the PF of women with endometriosis, as they, themselves, continue to release proinflammatory and neurogenic factors into the surrounding fluid [54].

It has been suggested that the chronic inflammatory milieu within PF of women with endometriosis may have a direct role in the generation of endometriosis-associated CPP [106, 231]. Recently, a study examining peritoneal immune cells in the PF of women with endometriosis found a strong correlation between peritoneal macrophage abundance and the severity of CPP [395]. This link between the inflammatory environment within the PF and CPP has also been demonstrated in a pre-clinical mouse model, where peritoneal macrophage depletion reduced endometriosis associated mechanical hyperalgesia [257]. In addition to the role of immune cells, increased levels of several soluble inflammatory factors including tumor necrosis factor-α (TNFα), nerve growth factor (NGF), Regulated on Activation Normal T cell Expressed and Secreted (RANTES, also known as C-C chemokine ligand 5: CCL5), and interleukins (IL) IL-8 and IL-1β, have also been found within the PF of endometriosis patients who report pain [81, 96-98]. This altered inflammatory milieu within the PF presents an opportunity for interaction with sensory neurons in and around nearby visceral organs [99, 100]. This direct interaction may play a functional role in visceral nociception [396], however direct experimental evidence is currently lacking.

Peripheral sensory neurons innervate the serous membrane lining the peritoneal cavity, including both the parietal and visceral peritoneum [397, 398], as well as visceral organs within the peritoneal space [396, 399, 400]. Spatially, the neurons innervating the viscera would be the same neurons intrinsically exposed to PF within the peritoneal cavity. Activation of these sensory neurons by a variety of mechanical, chemical, or inflammatory stimuli, acts as the first step in the visceral pain pathway, initiating nociceptive signalling to the central nervous system (CNS) for processing and subsequent pain perception. In addition to direct activation of sensory neurons, a chronic inflammatory environment could lead to sensitization of peripheral nociceptive fibres, which translates to allodynia (pain in response to stimulus that was not painful prior to inflammatory insult) or hyperalgesia (increased sensitivity to noxious stimuli) [88, 151]. Peripheral sensitization induced by chronic exposure to proinflammatory mediators has been suggested to play a role in allodynia and hyperalgesia seen in endometriosis patients [78]. Whilst we have shown, in Chapters 3 and 5, that peripheral sensory nerve fibres innervating visceral organs such as the vagina and bladder develop mechanical hypersensitivity in a mouse model of endometriosis [220, 376], a direct functional link between the aberrant inflammatory milieu within the peritoneal cavity and altered peripheral neuron activation has not yet been explored.

With this in mind, the aims of these experiments were to: (1) determine whether PF from mice and women with endometriosis is able to directly activate or sensitize visceral sensory neurons of healthy female mice and (2) examine whether different subtypes of PF collected from patients with endometriosis and/or CPP induces distinctive neuronal activation profiles.

6.4 Methods

6.4.1 Animal and human ethics

The Animal Ethics Committee of the South Australian Health and Medical Research Institute (SAHMRI) approved all experiments involving animals (ethics number SAM342 and SAM195). All animal experiments conformed to the relevant regulatory standards and ARRIVE guidelines. For endometriosis and Sham induction for collection of peritoneal fluid (PF), female C57BL/6J mice at 6 weeks of age were acquired from an in-house specific and opportunistic pathogen-free animal care facility C57BL/6J breeding programme (Jax strain #000664; originally purchased from The Jackson Laboratory; Bar Harbor, ME, USA). For *in vitro* experiments, female genetically encoded Ca^{2+} imaging mice, heterozygous for $Na_V1.8$-Cre (kindly donated by A/Prof Imlach, Monash University) and crossed with GCaMP6s (Jax strain #024106; originally purchased from The Jackson Laboratory; Bar Harbor, ME, USA) were acquired from the SAHMRI in-house breeding programme at 10-12 weeks of age. Mice were grouped house, as described in Chapter 2. All female mice use in this study were virgin (never been mated) and housed in the absence of males from weening. Vaginal lavage or other cytology test to confirm cycle stage were not performed, but it has been reported that an extended absence of male pheromones leads to a state of anestrous (lee-boot effect) [274].

Human PF sample collection was approved by the human research ethics committee for ongoing research programs at the Royal Women's Hospital (Melbourne, Australia). Ethics approval included project 10/43 (Royal Women's Hospital Tissue Bank) and Project 16/43 (Identification and function of genes that increase risk for endometriosis) as part of the Melbourne Endometriosis Research Cohort (MERC). All patients provided informed consent for PF sample collection and approved use in animal studies.

6.4.2 Collection of peritoneal fluid (PF)

Peritoneal fluid (PF) samples were collected from both mice and humans as described below. Samples were allocated to distinct treatment groups based on mouse phenotype **(Table 6.3)** or patient criteria pre-determined by MERC. A detailed description of human PF grouping criteria is provided in section 'Patient PF sample groups' below **(Table 6.3)**. A control treatment which comprised a 50:50 dilution of PBS:HEPES buffer in the absence of any PF was included for all groups.

6.4.2.1 Mouse PF samples

Mouse PF samples were collected ten weeks after endometriosis induction surgery, using the auto-transplantation method of endometriosis induction. Detailed methodology of endometriosis induction can be found in Chapter 2. Briefly, five uterine horn fragments were surgically transplanted within the peritoneal cavity of mice to induce endometriosis development: 3 fragments within the intestinal mesentery and two around the uterus. Peritoneal fluid was collected using a 200 µL PBS flush immediately prior to euthanasia, as described in Chapter 2. Approximately 100 µL of the PF flush was collected, snap frozen and stored at -80 °C until use. Peritoneal fluid was also collected from mice that had undergone Sham surgery (sutures placed at the sites mentioned above, in the absence of any endometrial tissue). Any PF samples that had been contaminated with blood or tissue were discarded.

Samples were grouped into Sham Mouse PF (N = 3) and Endo Mouse PF (N = 3) based on either sham (Sham) or endometriosis (Endo) induction surgery at the initiation of model development **(Table 6.3)**. At 8-10 weeks following endometriosis development and concurrent development of CPP, we have shown that the PF from Endo mice contains elevated inflammatory cytokines similar to those found in women, including interleukins (IL) -1β, IL-6, IL-17, IL-33 and VEGF (Chapter 2) [297]

Table 6.1: Mouse peritoneal fluid (PF) sample groups for *in vitro* experiments

Mouse PF group	Chronic pelvic pain (CPP)	Number of Mice
Sham	No CPP	N=3
Endo	CPP	N=3

PF, peritoneal fluid; CPP, Chronic pelvic pain; N = the number of unique mouse samples

6.4.2.2 Human PF samples

Human PF samples were collected from pre-menopausal women, not currently on hormone treatment, as part of an ongoing research program at the Royal Women's Hospital (Melbourne, Australia) with the Melbourne Endometriosis Research Cohort (MERC), with special thanks to our collaborators A/Prof. Martin Healey, Dr. Sarah Holdsworth-Carson and Prof. Peter Rogers. Samples of PF were collected from women at the commencement of laparoscopic surgery, with one to 15 mL collected neat from the peritoneal cavity of each patient. Once collected, samples were centrifuged at 4 °C for 5 minutes at 900 gs. Aliquots of 250-1000 µL were taken, with care to avoid cellular debris, and stored at -80 °C until use. Any contaminated samples were discarded, and samples with visible blood content were excluded from Ca^{2+} imaging experiments. A total of 18 individual patient samples

were used in this study, collected from patients with a mean age of 33.7 years, a mean weight of 66.64 kgs and mean BMI of 25.3 **(Table 6.2).**

Table 6.2: Patient characteristics of PF sample cohort

Patient Characteristics (N=18)	
Age in years	33.7 ± 6.69
Weight in Kgs	66.64 ± 11.2
BMI in kg/m^2	25.3 ± 3.81

Values are presented as mean ± standard deviation.

6.4.2.2.1 Patient PF sample groups

For patient groups, PF samples were allocated to the following 4 cohorts by MERC at the time of PF collection, based on histologically confirmed endometriosis and patient report of experiencing non-cyclical pelvic pain **(Figure 6.1)**. Final groups included Group 1: No Endo No CPP (N = 2), Group 2: No Endo + CPP (N = 6), Group 3: Endo No CPP (N = 4) and Group 4: Endo + CPP (N = 6) **(Table 6.3)**.

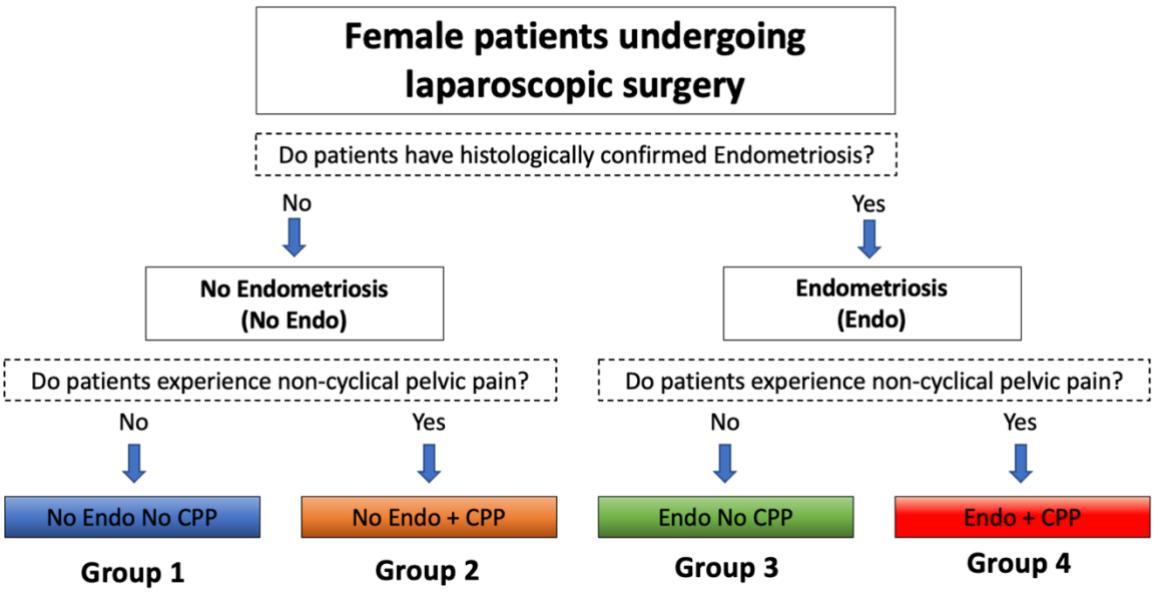

Figure 6.1: Schematic diagram of patient criteria for PF sample treatment subtypes.

Peritoneal fluid of patients undergoing laparoscopic surgery were collected and subsequently grouped in response to pre-determined criteria. Patients were grouped as 'No Endo' and 'Endo' based on whether they had been diagnosed with histologically confirmed endometriosis. These patients were then grouped into subtypes depending on whether they experienced non-cyclical pelvic pain (regular pelvic pain unrelated to menstruation). Final PF subtypes included: Group 1: No Endo No CPP (blue); Group 2: No Endo + CPP (orange); Group 3: Endo No CPP (green) and Group 4: Endo + CPP (red). CPP: chronic pelvic pain.

Table 6.3: Peritoneal fluid (PF) patient sample groups for *in vitro* experiments

Patient PF group	Chronic pelvic pain (CPP)	Number of Patients
No Endo	No CPP	N=2
	CPP	N=6
Endo	No CPP	N=4
	CPP	N=6

PF, peritoneal fluid; CPP, Chronic pelvic pain; N = the number of unique patient samples

6.4.3 GCaMP imaging

As mechanisms involved in visceral pain signalling differ from somatic sources such as the skin or muscle, identifying sensory neurons that specifically innervate the viscera is important when trying to determine relevant mechanisms involved in CPP [397, 401]. Using intraperitoneal (i.p.) tracing, Peeters *et al*. identified that 5% of all neurons within thoracolumbar (TL9-L1) dorsal root ganglia (DRG) were visceral innervating neurons, and that these neurons shared overlapping sensory pathways with visceral organs [396].

In this study, we performed live cell Ca^{2+} imaging on isolated i.p. traced sensory DRG neurons *in vitro*, as an indicator of neuronal activity [402]. We performed primary cell culture of DRG collected from healthy naïve female $Na_V1.8$xGCaMP6s mice. $Na_V1.8$xGCaMP6s mice express a slow and stable genetically encoded fluorescent Ca^{2+} indicator in cells containing the voltage gated sodium channel 1.8 ($Na_V1.8$). Changes in GCaMP6s fluorescence indicates changes in intracellular Ca^{2+}, which is an indicator of neuronal activation [402]. These mice are particularly useful for our Ca^{2+} imaging experiments as more than 95% of visceral afferents are unmyelinated C-fibres known to express $Na_V1.8$, which are suggested to play an important role in nociceptive action potential firing [336, 403]. $Na_V1.8$ is also found highly expressed in sensory nerves innervating key visceral organs known to be affected by endometriosis associated CPP [220, 285, 305]. Together, these tools provides us with an ultrasensitive technique for measuring changes in intracellular Ca^{2+} within visceral-innervating sensory neurons, as an indicator of neuronal activation [404].

6.4.3.1 Identification and culture of dorsal root ganglion (DRG) neurons innervating the peritoneal cavity

Retrograde labelling was performed to fluorescently identify DRG neurons innervating the peritoneal cavity of healthy female $Na_V1.8$xGCaMP6s mice. For this, Cholera toxin subunit B (CT-B) conjugated to AlexaFluor (AF) 594 (500 µg, Invitrogen, CA, USA) was dissolved in 500 µL of 0.1 M

phosphate buffer (pH 7.35). Under light isoflurane, half (250 µL) of the diluted CT-B AF594 (1 µg/µL) was injected (i.p.) into the peritoneal cavity of each mouse; spread evenly across four injection sites over the abdomen to facilitate dispersion across the peritoneal cavity. Following the final i.p. injection, the abdomen was gently massaged for 30 seconds to encourage thorough spreading of nerve tracer to 'capture' as many nerve endings within the peritoneal cavity as possible. Mice were monitored on recovery and housed individually for 3-4 days following i.p. tracer injection. All mice recovered quickly and showed no adverse clinical signs.

Three to four days following i.p. tracing, mice were humanely euthanised via CO_2 inhalation and the bi-lateral thoracolumbar (T9-L2) and lumbosacral (L5-S2) DRG were removed. These DRG levels were chosen as a previous study by Peeters *et al*., employing this technique, identified the largest i.p. traced population within T9-L1 DRG neurons [396] and L5-S2 are known to contain neurons that innervate visceral organs [109, 151, 231]. DRG were dissociated using the protocol described in Chapter 4 [220]. Following dissociation, neurons from T9-L1 and L5-S2 were combined and resuspended in 250 µL of complete DMEM and immediately spot plated (20 µL) onto 12 x 13 mm coverslips pre-coated with laminin (20 µg/mL; Sigma-Aldrich, #L2020) and poly-D-lysine (800 µg/mL; ThermoFisher Scientific). Coverslips were incubated at 37 °C in 5% CO_2 for 2 hours to allow neurons to adhere to the coverslip before flooding with 1 mL complete DMEM. Neurons were maintained at 37 °C in 5% CO_2 until used for Ca^{2+} imaging studies, 18-28 hours post dissociation.

6.4.3.2 In vitro *live cell calcium imaging*

Live cell Ca^{2+} imaging was performed to establish whether PF can directly activate sensory neurons and to evaluate whether PF sensitizes sensory neurons to subsequent stimulation with the TRPV1 agonist, capsaicin. TRPV1 is a nociceptive ion channel that acts as a molecular sensor and potentiates responses to painful stimuli. TRPV1 can integrate responses to stimuli such as acidosis, oxidative stress, and inflammatory mediators and is known to be involved in visceral nociceptive signalling [135, 165, 166, 405, 406].

For each experiment, a single coverslip of cultured DRG neurons was placed in a specialized chamber at room temperature, connected to a steady state perfusion system and washed with HEPES buffer (10 mM HEPES sodium salt [4-(2-hydroxyethyl)piperazine-1-ethanesulfonic acid sodium salt; Sigma, #H7006], 140 mM NaCl [Chem Supply, #SA046], 4 mM KCl [Chem Supply, #PA054], 5 mM D-glucose anhydrous [Chem Supply, #GA018], 2 mM $CaCl_2$ [Scharlau, #CA01951000], and 2 mM MgCl2 [Sigma, #M8266], pH 7.40). Fluorescent images were acquired with a Nikon TE300 Eclipse microscope combined with a Sutter DG-4/OF wavelength switcher, and a Photonic Science ISIS-3 intensified CCD camera, operated by MetaFluor Fluorescence Ratio Imaging Software (Molecular Devices, CA). An initial light microscope image was taken to identify all neurons present within the field, as well as provide a visual assessment of overall cell health.

Following this, a subsequent image of the same field was taken using the Rhod-2 Filter set (ET545/25x (excitation) and ET607/70m (emission)) to identify red fluorescence emitted by traced visceral innervating neurons which had incorporated the nerve tracer CTB-594 **(Figure 6.2A)**. This image was used to quantify the percentage of individual i.p. traced neurons per experiment and identify neurons for analysis presented within this chapter**.** For live cell Ca^{2+} imaging experiments, a sequence of images of raw GCaMP6s fluorescence (used to record changes in intracellular Ca^{2+}) were taken with a Fluo-4 Filter set (ET480/40x (excitation) and ET535/50m (emission)). Images were taken every 5 seconds across the duration of each experiment at 10x magnification. Data were recorded and analysed offline using MetaFluor Fluorescence Ratio Imaging Software (Molecular Devices, CA).

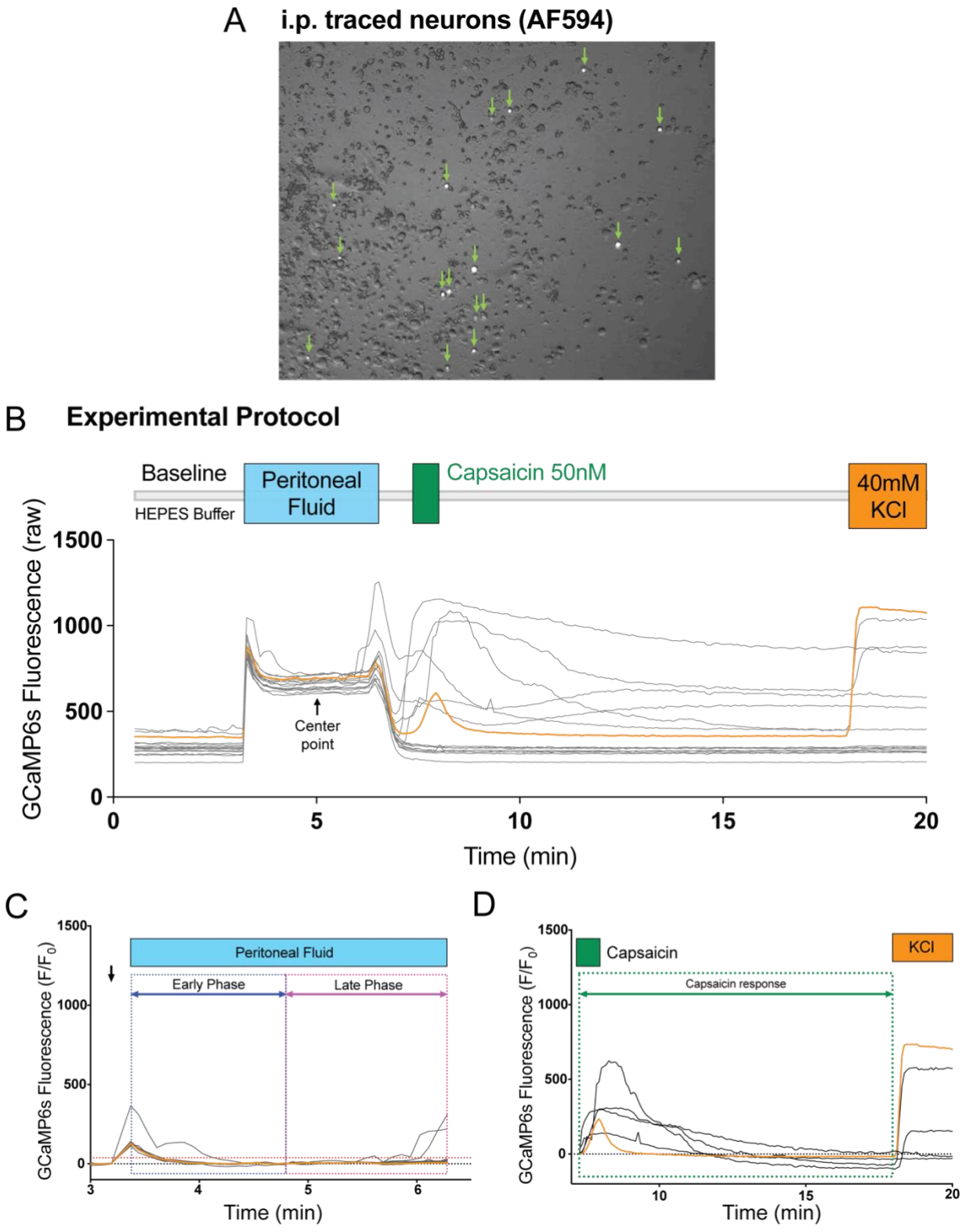

Figure 6.2: Intraperitoneal (i.p.) traced neurons, experimental protocol, and analysis.

(A) Representative light microscope image displaying the field of view of a single coverslip used in an experimental protocol. Green arrows indicate intraperitoneal (i.p.) AF594 traced neurons cultured from T9-L2 and L5-S2 DRG. **(B)** A schematic diagram accompanied by a raw trace that depicts the full experimental timeline for all calcium imaging experiments performed, including all control, mouse peritoneal fluid (PF) and human PF experimental samples. Timeline includes a

baseline (3 min), peritoneal fluid incubation (3 min), washout (30 sec), 30 second Capsaicin (50 nM) treatment, a washout period (10 min) and finally high KCl (40 mM) at the end of each experiment. Data are recorded as a change in the CGaMP6s fluorescence (raw) over time with each line representing an individual traced neuron. Orange trace represents a single example neuron throughout the protocol. Black arrow represents center point of PF incubation for normalisation protocol. **(C-D)** Following normalisation of raw experiments, the PF response and the capsaicin response is graphed as a change in CGaMP6s fluorescence (F) over a baseline fluorescence of 0 (F_0). The orange trace represents the same neuron in (B) following normalisation. **(C)** Neuronal response to PF incubation is analysed as the whole response (blue bar), as well as early and late phase of response, indicated by the blue and pink box respectively. **(D)** The capsaicin response window includes capsaicin treatment period (30 sec) and the subsequent washout period, as indicated by the green box. F_0 is represented by the black dotted line and the red dotted line represents 'PF response' threshold.

6.4.3.3 Experimental protocol

The experimental protocol remained consistent between both mouse and human PF groups, as well as control, and comprised an initial baseline recording (3 mins), PF incubation (or PBS:HEPES for control) (3 mins), a 30 second HEPES wash, Capsaicin (50 nM in HEPES) stimulation (30 sec), a 10-minute HEPES wash and finally a KCl (40 mM in HEPES) stimulation (Figure 6.2C). All PF samples were tested individually, with each PF sample tested on 2 separate days and 2 separate mice to account for differences across individual cell cultures. Only one PF sample was tested per coverslip, with the cells discarded at the conclusion of each full PF treatment protocol. Baseline recordings and wash periods using HEPES buffer, as well as the capsaicin and KCl treatments were completed using the inbuilt steady state slow perfusion system to maintain controlled flow of solutions. For PF treatments, HEPES buffer was removed manually and slowly replaced with the PF treatment using a pipette to minimise mechanical disruption to the cells. This manual process was necessary due to the small volume of PF that could not be transferred through the perfusion system. As there were small volumes of some PF samples, the experimental sample of all PF samples tested was diluted 50:50 in HEPES buffer to maintain consistency.

6.4.3.4 Normalisation, response analysis, and exclusion criteria

As there is variability in raw cell fluorescence **(Figure 6.2B)**, all responses were normalised to a baseline fluorescence of 0 (F_0). For this, the 3 data points immediately prior to both PF addition and capsaicin stimulation were averaged and set as baseline (F_0) **(Figure 6.2C-D)**. In addition to normalising all cells to F_0, further standardization was required to account for an artificial inflection seen with the addition of PF samples, which was inconsistent between sample groups and across the field of view. For this, the center point **(Figure 6.2C)** in the 'PF response window' was set as baseline (F_0). The center point was chosen as it allowed us to capture both early and late responses to PF. The set response window for PF analysis was consistent between all groups, with the artificial

inflection points excluded from analysis **(Figure 6.2C)**. All normalised data are presented as the change in fluorescence from baseline fluorescence (F/F_0).

For analysis, PF responders were identified as cells with an increase in GCaMP6s fluorescence of over 3x the baseline variability (12.69 ± 0.57, mean ± SEM from n = 623 neurons) of all traced neurons, recognizing an increase over 38.07 fluorescent units as a response to PF (red dotted line; **Figure 6.2C)**. For capsaicin and KCl, a response was identified as an increase of more than 10% from baseline fluorescence. In all graphs, the total response is presented as the total area under the curve (AUC) and the peak of response is the maximum point of GCaMP6s fluorescence (peak 'Y axis' response). For PF responses, the AUC was also calculated during the initial (early phase) and delayed (late phase) of response (blue and pink box respectively, **Figure 6.2C**). Sub-analysis of the PF response in the early and late phases allowed us to analyse the initial response profile (which is rapid and transient) and the late response (which is slower and sustained). For capsaicin, the response window included 30 second capsaicin treatment and subsequent washout period of 10 minutes (green box, **Figure 6.2D**).

Cells were classified as having low viability and excluded from final analysis if they did not respond to any stimulus, including PF, capsaicin or KCl. Cells that were negative in fluorescence following normalisation were excluded from further analysis.

6.4.4 Statistical analysis

Grouped data are presented as mean ± SEM with normality of data assessed using the Shapiro-Wilk test prior to all statistical analysis. Where appropriate, data were analysed using a two-way analysis of variance (ANOVA) with Bonferroni post-hoc multiple comparisons or Kruskal-Wallis nonparametric ANOVA with Dunn's multiple comparisons. Each dot represents an individual experiment or neuron, where n = the number of individual traced neurons and N = the number of unique PF samples per group. Percentage responders are presented as % neurons responding per group. Differences between number of responders per group were analysed using Fishers Exact tests. Differences for all analysis were considered statistically significant at $*P < 0.05$, $**P < 0.01$, $***P < 0.001$ and $****P < 0.0001$ unless otherwise indicated. Data were analysed using GraphPad Prism 9 (version 9.3.1) Software (San Diego, CA, USA).

6.5 Results

6.5.1 Peritoneal fluid from Endo mice activates a large subset of visceral innervating sensory neurons identified by i.p. tracing

Peritoneal fluid (PF) is known to contain a variety of mediators essential for maintaining physiological homeostasis in the local peritoneal environment [394]. Whilst it is suggested that women with endometriosis have an aberrant inflammatory environment within the PF, it is not known whether this PF can directly act on visceral-innervating sensory neurons, and as such, whether the PF itself may be involved in the generation of endometriosis associated CPP.

We first developed a technique to identify visceral-innervating sensory neurons, by injecting the fluorescent nerve tracer, CTB-AF594, into the peritoneal cavity of healthy mice, as described above. In line with previously reported i.p. tracing protocols [396], we found that the average % of traced neurons per mouse ranged between 2.86% ± 0.26 (Mouse 4) and 4.46% ± 0.34 (Mouse 5) (mean ± SEM), with an average of 3.82% ± 0.29 traced neurons **(Figure 6.3)**.

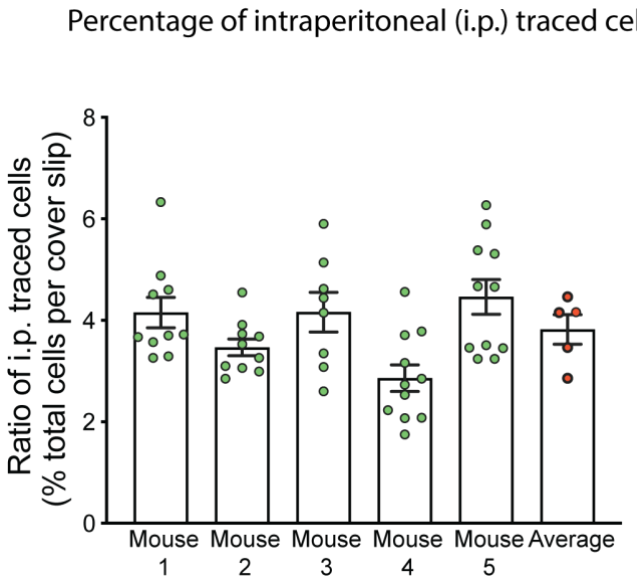

Figure 6.3: Intraperitoneal (i.p.) tracing identifies visceral innervating neurons.

Grouped data showing the ratio (% of total cells) of traced neurons per coverslip from each mouse (green dots) and the average % of traced neurons from all mice (red dots). Each red dot represents the average from mouse 1-5 respectively. Data are represented as mean ± SEM from n = 8-11 coverslips per mouse and N = 5 mice.

We then proceeded to evaluate the effect of PF collected from Sham mice and mice with endometriosis on the activity of visceral-innervating sensory neurons cultured from i.p traced $Na_V1.8$-GCaMP6S healthy mice. For this, we measured the fluorescence of the Ca^{2+} sensor, CGaMP6s, as an indicator of neuronal activation, as described above. Using this approach, we showed that

incubation with PBS:HEPES buffer (Control), did not significantly alter the activity of i.p. traced DRG neurons *in vitro*. This was evident as no single traced neuron recorded an increase in CGaMP6s fluorescence above 'response threshold' **(Figure 6.4A)**. In contrast, we found that incubation with PF collected from Sham mice (Sham mouse PF) caused a direct activation in a subset of i.p. traced sensory neurons (35.7% or 25 out of 72) **(Figure 6.4B and 6.4D)**. Interestingly, we found that the PF from mice with endometriosis and CPP (Endo Mouse PF) activated a significantly larger number of sensory neurons (72.4% or 55 out of 76) compared to Sham Mouse PF **(Figure 6.4C-6.4D)**. These results confirm that PF can directly activate sensory neurons and show that PF from endometriosis mice have a heightened capacity to activate more DRG neurons, *in vitro*.

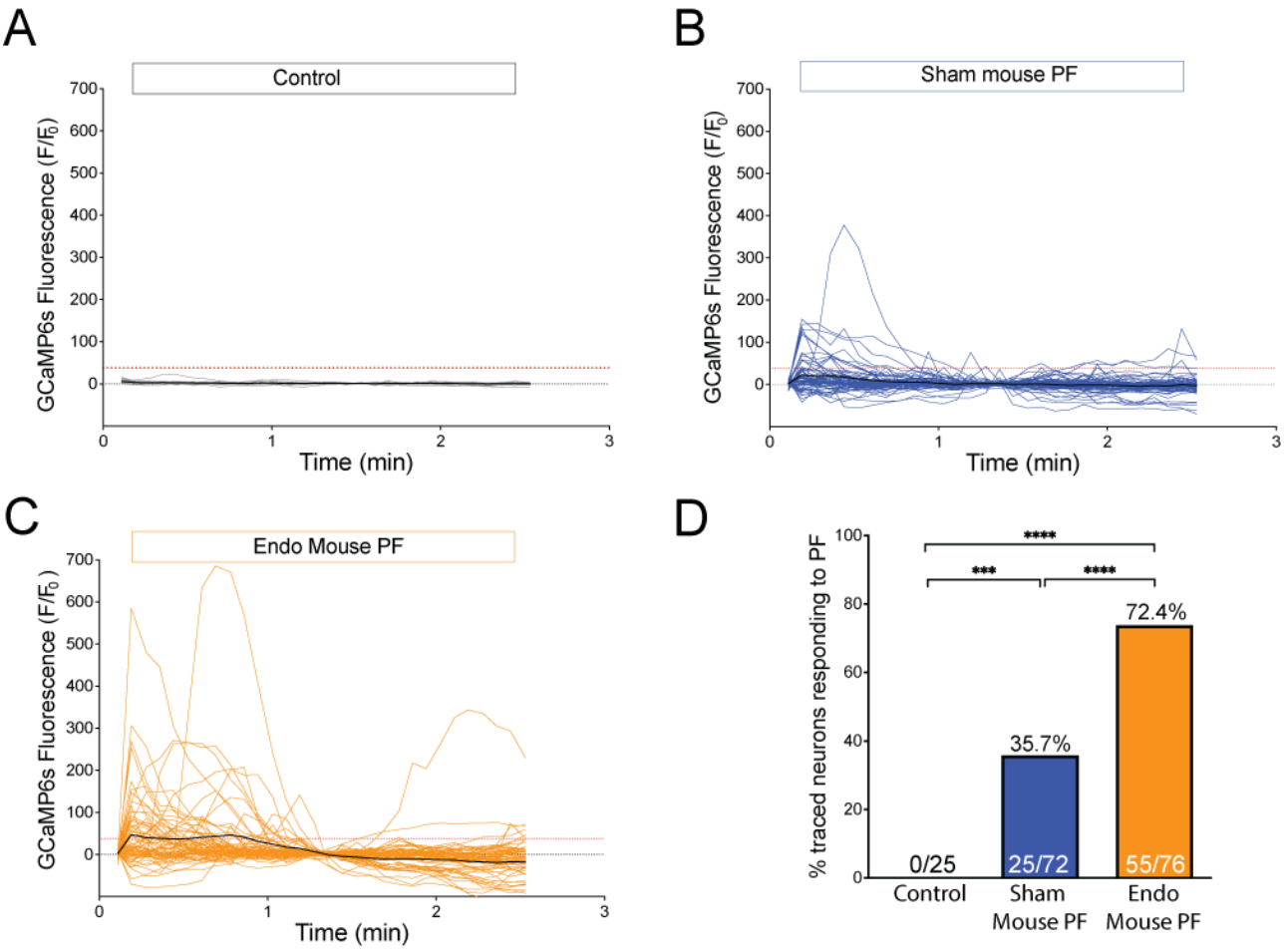

Figure 6.4: The peritoneal fluid (PF) from mice activates a subset of intraperitoneal (i.p.) innervating neurons from healthy female mice.

(A-C) Grouped traces showing the direct effect of **A)** Control (grey), **B)** Sham mouse PF (blue) and **C)** Endo Mouse PF (orange) incubation on individual i.p. traced neurons. Each coloured line represents a single neurons response over time, including Control (n = 25), Sham Mouse PF (n = 72) and Endo Mouse PF (n = 76) individual neurons. Black trace represents the average response of all traced neurons per treatment group (mean), black dotted line represents baseline (0), and red dotted line represents 'response threshold' (3x baseline variability, 38.07 fluorescent units). **(D)** The percentage (%) of traced neurons responding (above threshold) to PF incubation was greatest in Endo Mouse PF treated neurons, with grouped data showing a significantly larger % of traced neurons responding to the PF of Endo mice compared to both Sham Mouse PF and Control; Fishers exact tests, ***P <0.001, ****P <0.0001. PF: peritoneal fluid.

A detailed analysis of the average response profile to each PF showed that compared to Sham Mouse PF, the PF from Endo mice induced the largest activation of visceral-innervating sensory neurons **(Figure 6.5A)**. This effect was apparent when analysing the activation profile of individual neurons to PF, calculated as the peak (maximum GCaMP6s fluorescence) **(Figure 6.5B)** and total response (total area under the curve (AUC) of GCaMP6s fluorescence) **(Figure 6.5C)**. Moreover, we found that Endo Mouse PF generated the largest activation in the initial phase of the response, with the maximum peak occurring directly after PF addition **(Figure 6.5D i)**. Interestingly, neuronal activation induced by PF was transient in nature, with GCamp6s fluorescence returning to baseline levels (pre-PF addition) 1.3 minutes after PF addition **(Figure 6.5D ii)**. These results suggest that while both mouse PF subtypes can directly and transiently activate sensory neurons, the PF from mice with endometriosis and CPP induces a significantly heightened neuronal activation.

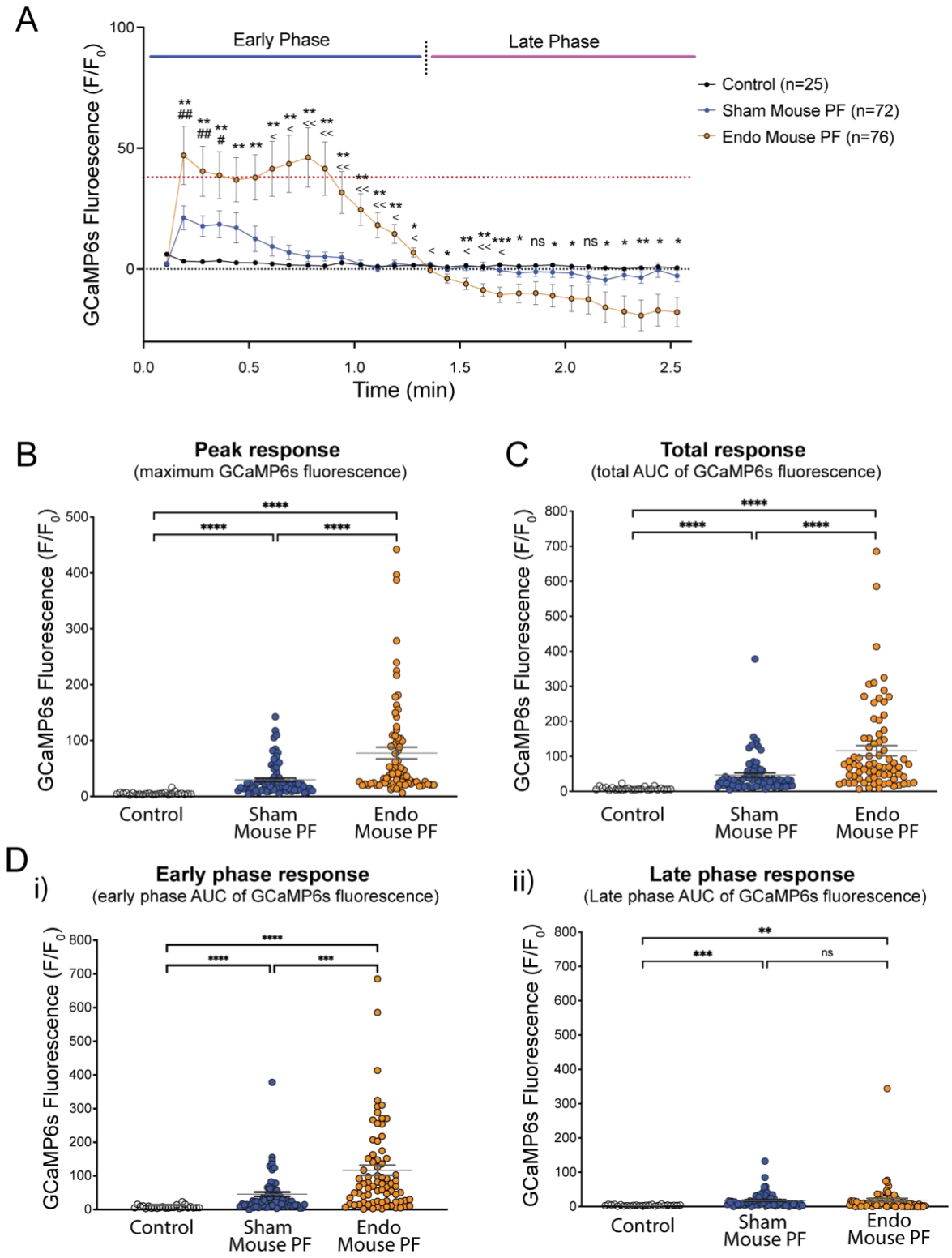

Figure 6.5: The peritoneal fluid (PF) from mice with endometriosis enhances neuronal activation of intraperitoneal (i.p.) traced neurons.

(A) Grouped data shows the total response profile (including early (blue bar) and late (pink bar) phases of response) from all traced neurons responding in each treatment group, including control (n = 25, N = 2), Sham Mouse PF (n = 72, N = 3) and Endo Mouse PF (n = 76, N = 3) incubation. Data are graphed as mean ± SEM, where n= the number of individual traced neurons and N represented number of unique samples tested. Data are analysed using a two-way ANOVA with Bonferroni post-hoc comparisons where $^{\#}$ = Sham Mouse PF vs control, * = Endo Mouse PF vs Control and $^{<}$ = Sham Mouse PF vs Endo Mouse PF. (Ns *P* >0.05, **P* <0.05, ***P* <0.01 and ****P*

<0.001). **(B)** The peak response (maximum GCaMP6s fluorescence) was the largest during incubation with Endo Mouse PF compared to both Control and Sham Mouse PF treatment groups. **(C)** The total response (total AUC of GCaMP6s fluorescence) was also significantly elevated in Endo Mouse PF treatment compared to control and Sham Mouse PF. **(D)** Detailed analysis of the total AUC of GCaMP6s fluorescence in the i) early phase and ii) late phase of response shows the enhanced response to Endo mouse PF treatment compared to Sham Mouse PF occurred during the first half of PF incubation. In comparison, analysis of the late response shows an increased response from both Sham and Endo Mouse PF compared to control, although the elevated response to Endo PF was not seen in this sustained phase of response. Data are presented as mean ± SEM from individual neurons, including control (n = 25, N = 2), Sham Mouse PF (n = 72, N = 3) and Endo Mouse PF (n = 76, N = 3). Each individual dot represents an individual neuron. Data are analysed using Kruskal-Wallis non-parametric analysis of variance with Dunn's multiple comparisons between groups where ns P >0.05, ***P* <0.01, ****P* <0.001, *****P* <0.0001. PF: peritoneal fluid.

6.5.2 Peritoneal fluid from mice with endometriosis does not sensitise visceral-innervating neurons to subsequent algesic stimuli

Peripheral sensitization of sensory neurons has been shown to occur in other chronic pain conditions such as rheumatoid arthritis, osteo arthritis and IBS [135, 142, 165] and has been suggested to play a role in CPP in endometriosis [78]. Following our results demonstrating that the PF from endometriosis mice caused enhanced neuronal activation compared to Sham Mouse PF, we wanted to determine whether incubation with Endo Mouse PF was able to sensitize sensory neurons to a subsequent algesic stimuli. For this, we measured the response of neurons to capsaicin (an agonist of the nociceptive ion channel TRPV1) after incubation with PF from Sham and Endo mice.

Treating sensory neurons with capsaicin induced rapid activation of a large subset of neurons regardless of whether they were pre-treated with PBS:HEPES Control **(Figure 6.6A)**, Sham Mouse PF **(Figure 6.6B)** or Endo Mouse PF **(Figure 6.6C)**. Moreover, the percentage of traced neurons responding to capsaicin was similar regardless of pre-treatment, with 18 out of 25 from Control (72%), 52 out of 72 from Sham Mouse PF (72.2%) and 49 out of 76 from Endo Mouse PF (64.4%) **(Figure 6.6D)**.

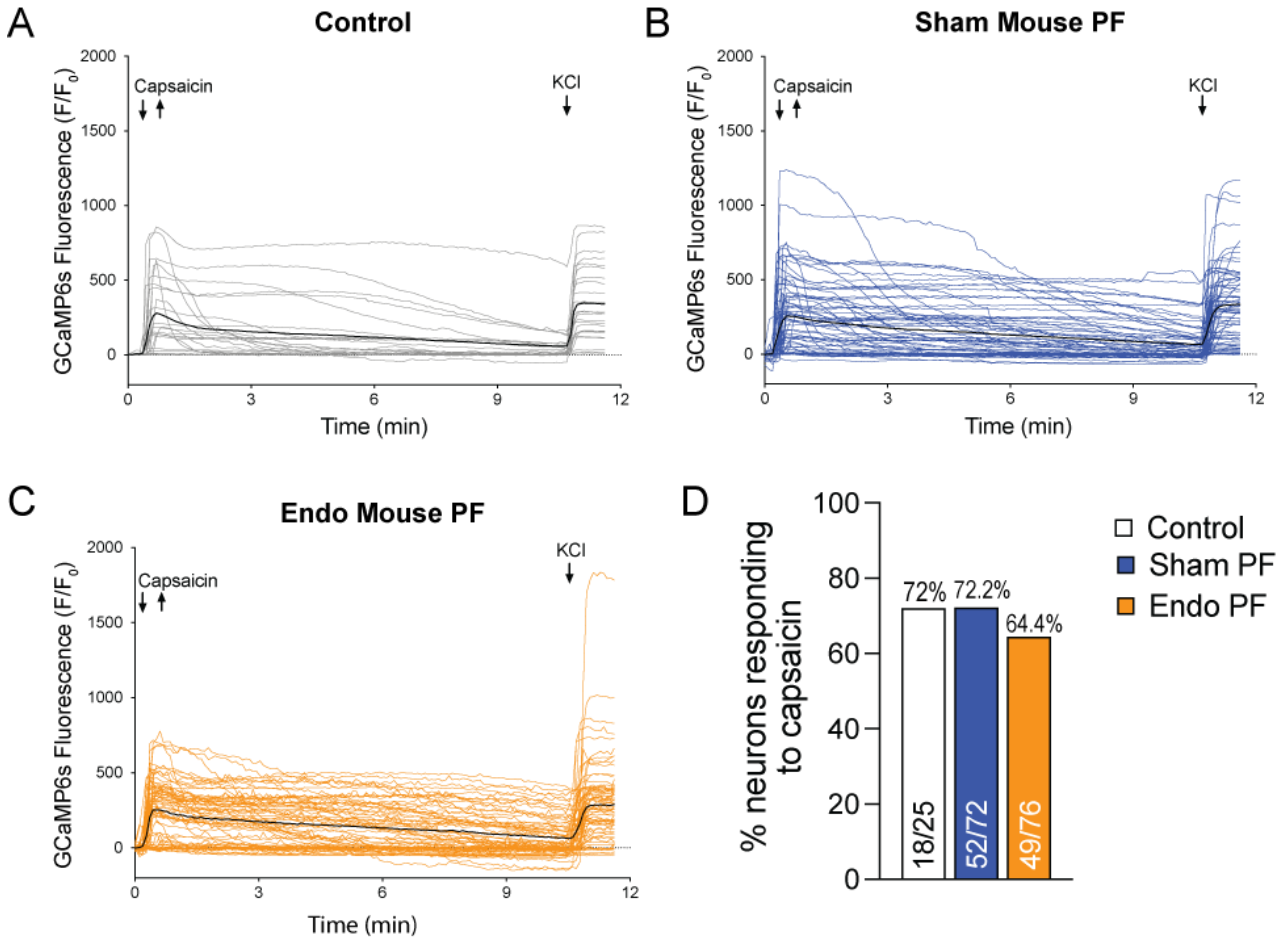

Figure 6.6: Capsaicin response of i.p. traced neurons following PF incubation.

Grouped traces showing the effect of TRPV1 agonist, capsaicin (50 nM) on neurons pre-treated with **(A)** Control (PBS:HEPES) (grey, n = 25), **(B)** Sham Mouse PF (blue, n = 72) and **(C)** Endo Mouse PF (orange, n = 76). Each coloured line represents a single i.p. neurons response over time to both 50 nM capsaicin and subsequent 40 mM KCl, black representative trace depicts average response of all traced neurons per group (mean), black dotted line represents baseline (0). **(D)** The percentage of single i.p. traced neurons that responded to capsaicin was similar across all groups. *P* >0.05 Fishers exact tests. PF: peritoneal fluid.

Analysis of the capsaicin response revealed that the total response profile was similar across treatment groups **(Figure 6.7A)**. Detailed analysis of capsaicin responses showed that pre-treatment with either PF group had no effect on the peak **(Figure 6.7B)** nor total response to capsaicin **(Figure 6.7C)**. We did find a small difference in the time taken to reach peak fluorescence following pre-treatment with Endo Mouse PF (1.14 ± 0.27 mins) compared to Control (peak at 1.39 ± 0.47 mins), however, there was no difference between Endo Mouse PF and Sham Mouse PF (peak at 1.29 ± 0.32 mins) (mean ± SEM) **(Figure 6.7D)**. Interestingly, both Sham Mouse PF and Endo mouse PF induced a slight shift to the left during the initiation of capsaicin response compared to Control, increasing GCaMP6s fluorescence faster in this early phase **(Figure 6.7E i-ii)**. Taken together, these results show that 3-minute incubation with PF from endometriosis mice does not appear to acutely alter the response of sensory neurons to TRPV1 activation compared to Sham Mouse PF.

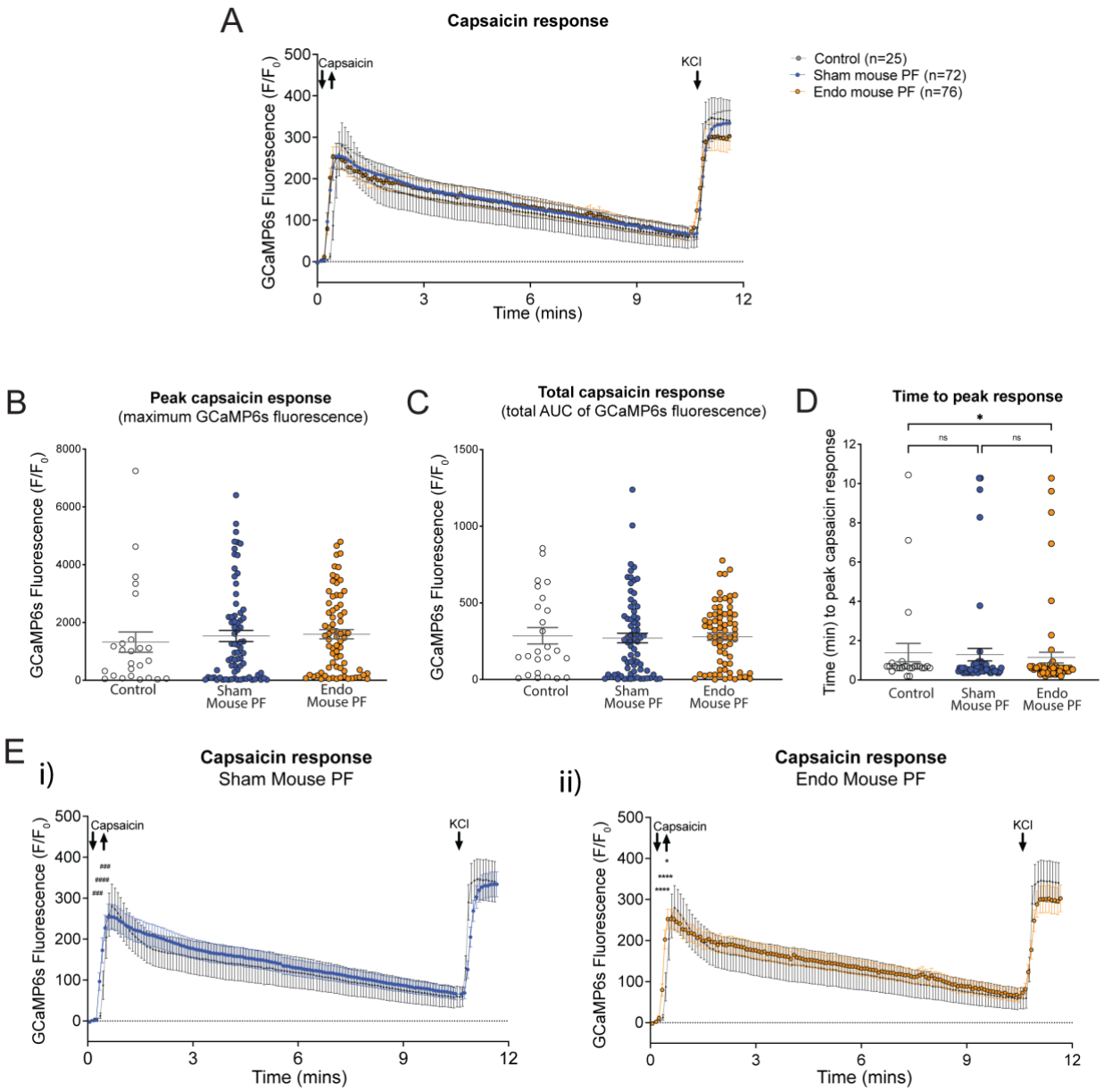

Figure 6.7: Peritoneal fluid from mice does not alter capsaicin responses in healthy intraperitoneal (i.p.) neurons.

(A) Grouped data from all traced neurons responding to control (n = 25, N = 2), Sham mouse PF (n = 72, N = 3) and Endo mouse PF (n = 76, N = 3) incubation, where n = number of neurons and N = number of individual samples. **(B)** Grouped data shows no difference in the peak capsaicin response (maximum GCaMP6s fluorescence) in i.p. traced neurons between Control, Sham mouse PF and Endo mouse PF pre-treated neurons. **(C)** Grouped data also shows no difference in the total capsaicin response (total AUC). **(D)** Grouped data shows a significantly reduced time (mins) to peak capsaicin response following Endo mouse PF incubation compared to control but no difference following Sham mouse PF incubation. **(E)** Separated out into the capsaicin response following **i)** Sham mouse PF and **ii)** Endo mouse PF incubation, statistical analysis shows significant increase in CGaMP6s fluorescence within the first 25 seconds compared to control in both PF incubations. Data are analysed using a two-way ANOVA with Bonferroni post-hoc comparisons where $^{\#}$= Sham mouse PF vs control, *= Endo mouse PF vs control (*P <0.05, ***P <0.001 and ****P <0.0001). All data are represented as mean ± SEM of the response from all i.p. traced neurons, where each dot represents a single neuron from each group. Data were analysing using Kruskal-Wallis non-parametric analysis of variance with Dunn's multiple comparisons between groups, ns P >0.05 and *P <0.05. PF: peritoneal fluid.

6.5.3 Endo Mouse PF recruits significantly more capsaicin responding and non-responding neurons than PF from Sham mice

As TRPV1 expressing neurons are often implicated in nociceptive signalling, we sought to determine whether the increased activation of sensory neurons seen in Endo Mouse PF treatment was due to additional recruitment of TRPV1-positive neurons or alternatively TRPV1-negative neurons. To address this, we separated the PF response analysis into TRPV1-positive neurons (capsaicin responders) and TRPV1-negative neurons (capsaicin non-responders) **(Figure 6.8A-C)**. We found that both Sham Mouse PF and Endo Mouse PF recruited a significant number of TRPV1-positive neurons, with Endo Mouse PF recruiting a larger number of these capsaicin responding neurons (81.6% or 40 out of 49) **(Figure 6.8A)**. Interestingly, we saw a marked recruitment of TRPV1-negative neurons (capsaicin non-responders) using Endo Mouse PF (55.6% or 15 out of 27), with this subset of sensory neurons not significantly activated by Sham Mouse PF (20% or 4 out of 20) **(Figure 6.8A)**.

To further elucidate the role of TRPV1-positive and -negative neurons in the heightened sensory neuronal activation seen with Endo Mouse PF, we also separated the peak and total PF responses into capsaicin responders **(Figure 6.8B)** and non-responders **(Figure 6.8C)**. In TRPV1-positive neurons, both the peak **(Figure 6.8B i)** and total **(Figure 6.8B ii)** responses was significantly elevated in the presence of both Endo and Sham Mouse PF compared to Control, with Endo Mouse PF inducing the largest neuronal activation in both analysis profiles. In comparison, in TRPV1-negative neurons, the peak **(Figure 6.8C i)** and total **(Figure 6.8C ii)** response was only significantly elevated above Control in Endo Mouse PF treated neurons and there was no longer a difference between Sham Mouse PF and Control.

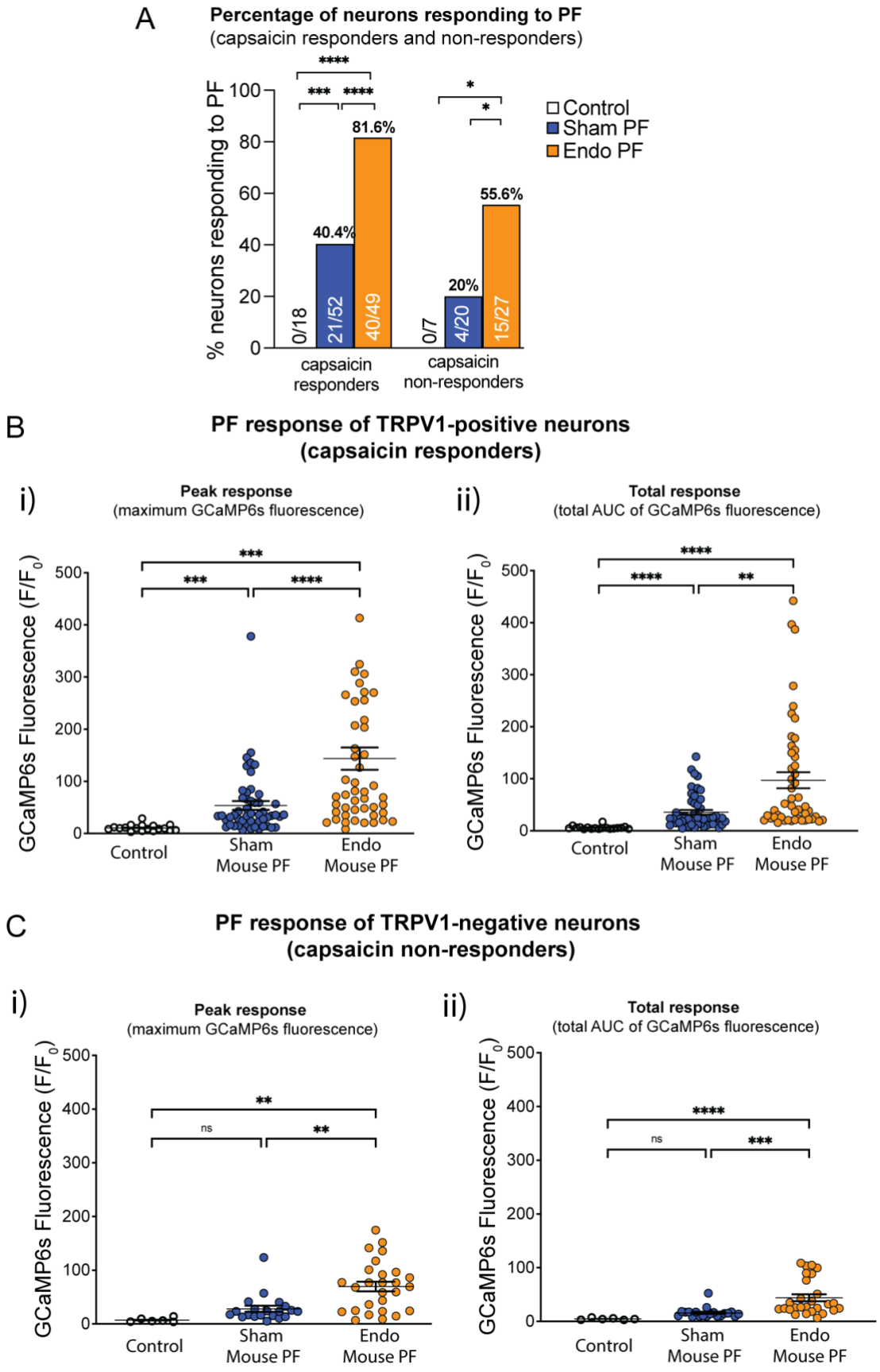

Figure 6.8: The peritoneal fluid (PF) from endometriosis mice activates significantly more capsaicin responding and non-responding neurons.

(A) The percentage of neurons responding to PF were made up of both capsaicin responders and non-responders, with the largest percentage of both neuron types responding to Endo Mouse PF. As Control treatment did not increase GCaMP6s fluorescent above 'response threshold' in any

traced neurons, there were 0% of capsaicin responders (0 out of 18) and non-responders (0 out of 7) activated. Fishers Exact tests; *P <0.05, ***P <0.001, ****P <0.0001. **(B)** Grouped data of the capsaicin responders only shows that both **i)** the peak (maximum GCaMP6s fluorescence) and **ii)** total PF response (total AUC of GCaMP6s fluorescence) was significantly increased during incubation with Endo Mouse PF (n = 49) compared to Sham Mouse PF (n = 52) and Control (n = 18) treated neurons. **(C)** Grouped data of capsaicin non-responders also shows that both **i)** the peak and **ii)** total PF response was significantly increased during incubation with Endo Mouse PF (n = 27) compared to Sham Mouse PF (n = 20) and Control (n = 7) treated neurons. Data are represented as mean ± SEM. Each individual dot represents an individual neuron. Data are analysed using Kruskal-Wallis non-parametric analysis of variance with Dunn's multiple comparisons between groups; ns P >0.05, **P <0.01, ***P <0.001, ****P <0.0001. PF: peritoneal fluid.

In summary, we were able to determine that PF from mice is able to directly activate a subset of visceral innervating sensory neurons, with heightened neuronal activation with the PF from mice with endometriosis and CPP. While we found no indication the PF induced neuronal sensitization to subsequent TRPV1 activation, separating PF response profiles into capsaicin responding and non-responding neurons gave us an indication of different neuron subtypes activated by each PF. Overall, we observed significant activation of TRPV1-positive neurons by both Sham and Endo Mouse PF, however, Endo Mouse PF incubation recruited an additional subset of TRPV1-negative neurons that were not activated by Sham Mouse PF. These results strongly implicate both TRPV1-positive and -negative neurons in the differential response seen with Endo Mouse PF.

Extending these results, we wanted to investigate whether the PF from women with endometriosis and CPP were also able to activate and/or sensitize sensory neurons innervating the viscera of healthy naïve mice. With access to 4 distinct subtypes of human PF, including women with or without endometriosis that presented with/without CPP, we have the unique ability to further translate our pre-clinical findings. This will allow us to determine whether the enhanced activation seen with Endo Mouse PF is associated with endometriosis development alone, or whether these results correlate with concurrent CPP development.

6.5.4 PF from humans with CPP directly activates a large proportion of visceral innervating sensory neurons from healthy mice.

As detailed in the methods section, we have access to 4 different types of human PF including: i) PF from healthy women (Group 1: No Endo - No CPP), ii) PF from women that have CPP unrelated to endometriosis (Group 2: No - Endo + CPP), iii) PF from women that have clinically diagnosed endometriosis but do not experience CPP (Group 3: Endo - No CPP), and finally iv) PF from women that have endometriosis and experience CPP (Group 4: Endo + CPP). We found that, similar to the PF from mice, all subtypes of PF from women were able to directly activate a subset of i.p traced sensory neurons from healthy mice **(Figure 6.9A-E)**. The percentage of neurons

responding to PF was lowest in the groups without CPP, including Group 1: No endo No CPP (5.8% or 5 out of 86 neurons) and Group 3: Endo No CPP (24.7% or 23 out of 93 neurons) **(Figure 6.9F).** Interestingly, both PF subtypes collected from women that suffered CPP activated the largest number of sensory neurons, with Group 3: No endo + CPP activating 51% (77 out of 151) and Group 4: Endo + CPP activating the highest number of sensory neurons, with 64.2% (97 out of 151) of neurons directly activated with this PF **(Figure 6.9F)**.

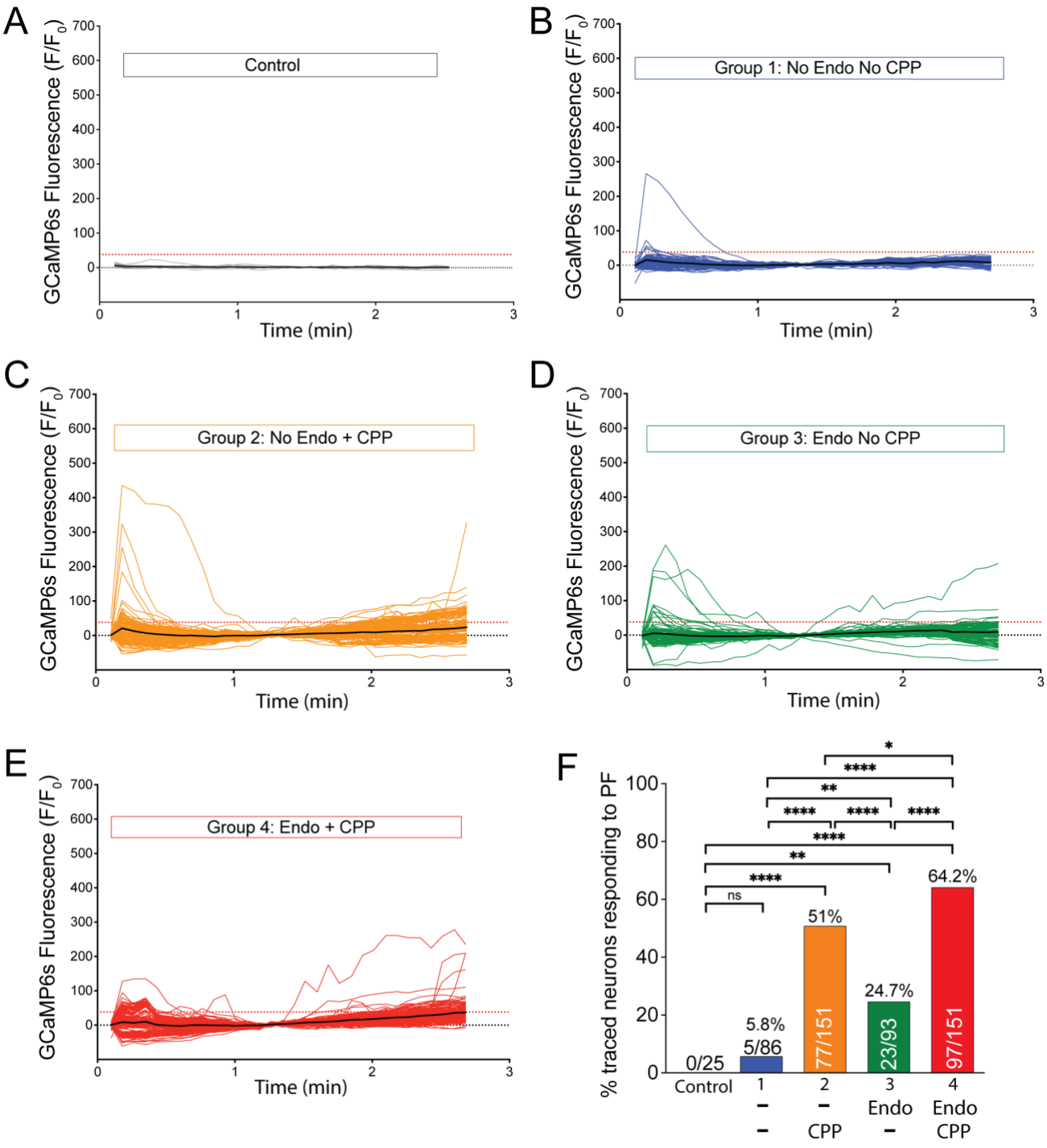

Figure 6.9: The peritoneal fluid (PF) from humans activates subsets of intraperitoneal (i.p.) innervating neurons from healthy female mice.

(A-E) Grouped traces showing the direct effect of treatment with **(A)** Control (PBS:HEPES) (grey, n = 25), **(B)** Group 1: No Endo No CPP PF (blue, n = 86), **(C)** Group 2: No Endo + CPP PF (orange, n = 151), **(D)** Group 3: Endo No CPP PF (green, n = 93) and **(E)** Group 4: Endo + CPP PF (red, n = 151) incubation on individual traced neurons. Each coloured line represents a single neurons response over time. Black trace represents the average response of all traced neurons (mean), black dotted line represents baseline (0) and red dotted line represents 'response threshold' (3x baseline variability). **(F)** The percentage (%) of traced neurons responding (above threshold) to PF incubation was significantly different between all groups, except Group 1: No endo No CPP group compared to Control. Grouped data show that Group 4: Endo + CPP PF activated the largest number of i.p. traced neurons. Fishers Exact tests; ns $P > 0.05$, *$P < 0.05$, **$P < 0.01$, ****$P < 0.0001$. CPP: chronic pelvic pain.

When looking at the activation response profile of all average traced neurons throughout PF incubation, we found distinct neuronal activation profiles induced from each PF subtype **(Figure 6.10A-B)**. Interestingly, and in contrast to mouse PF, we found that in addition to a transient activation observed in the first half of PF incubation, all types of PF induced a secondary/late sustained activation of sensory neurons innervating the viscera of healthy mice. Moreover, we found that the largest responses occurred during this second/late sustained response, with the PF collected from women that suffer from CPP inducing a larger neuronal activation (Group 2: No Endo + CPP, **Figure 6.10B ii**, and Group 4: Endo + CPP, **Figure 6.10B iv**)), compared to PF from women that do not experience CPP (Group 1: No Endo No CPP **(Figure 6.10B i)** and Group 3: Endo no CPP **(Figure 6.10B iii))**

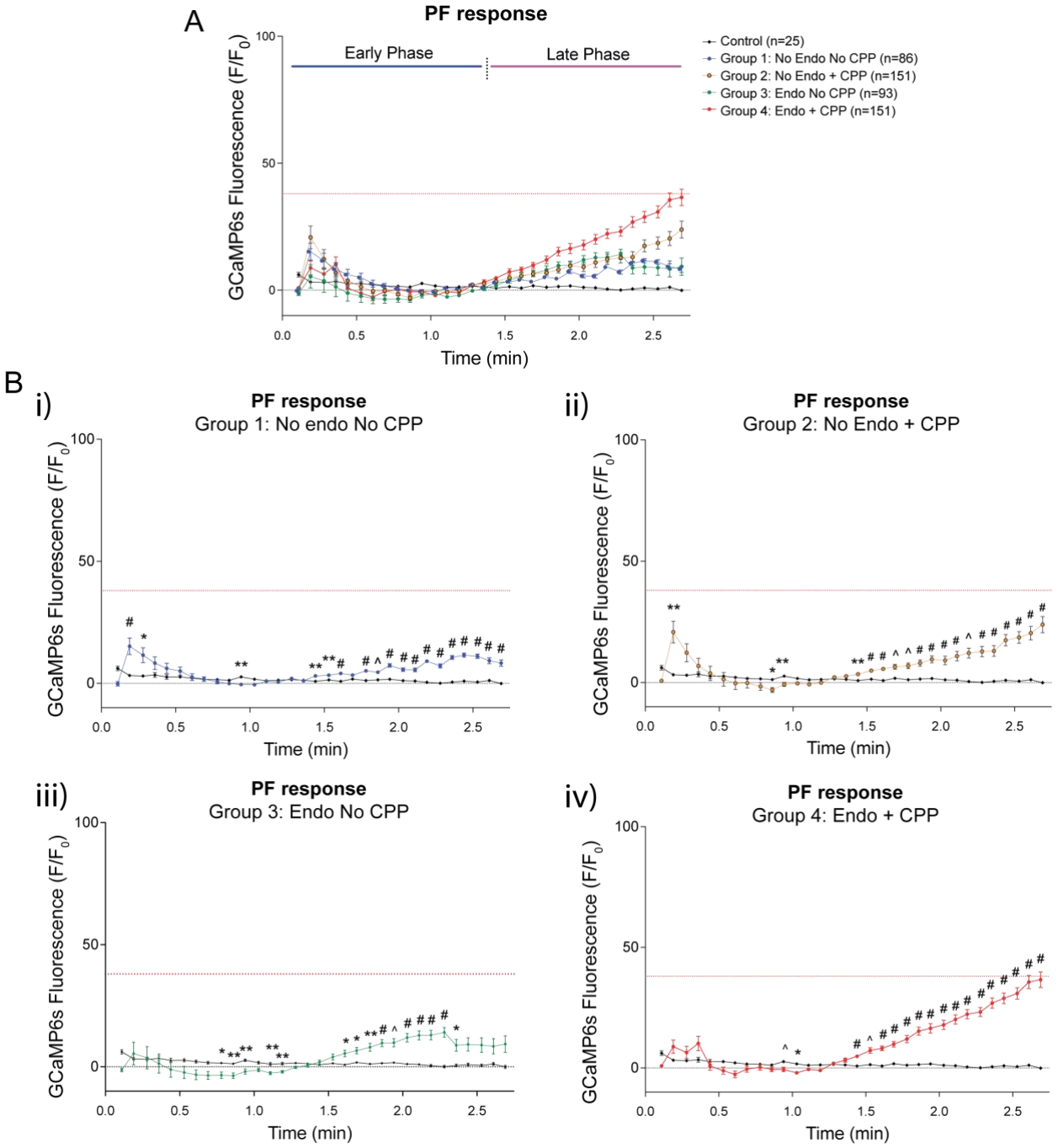

Figure 6.10: Peritoneal fluid from women enhances neuronal activation of visceral sensory neurons from healthy mice.

(A) Grouped data from all traced neurons (including early (blue bar) and late (pink bar) phases of response) in response to control (n = 25, N = 2), Group 1: No Endo No CPP PF (n = 86, N = 2), Group 2: No Endo + CPP PF (n = 151, N = 6), Group 3: Endo No CPP PF (n = 93, N = 4) and Group 4: Endo + CPP PF (n = 151, N = 6) incubation. Data are graphed as mean ± SEM, where n = the number of individual traced neurons and N represented number of unique samples tested. **(B)** Data presented for individual treatment groups compared to control shows that all PF subtypes, including **i)** Group 1: No Endo No pain, **ii)** Group 2: No Endo + CPP, **iii)** Group 3: Endo No CPP and **iv)** Group 4: Endo + CPP significantly increased CGaMP6s fluorescence over PF incubation. Data are graphed as mean ± SEM and analysed using a two-way ANOVA with Bonferroni post-hoc comparisons where **P* <0.05, ***P* <0.01 and ^*P* <0.001 and #*P* <0.0001). CPP: chronic pelvic pain.

These results were more evident when analysing the profile of the response of individual neurons **(Figure 6.11)**, which showed that all PF subtypes from women with endometriosis and/or CPP (Group 2: No Endo + CPP, Group 3: Endo No CPP, and Group 4: Endo + CPP) induced a significantly larger peak **(Figure 6.11A)** and total **(Figure 6.11B)** response than that seen in PF from Group 1: No Endo No CPP. Interestingly, the largest total responses were seen in PF from patient groups that experienced CPP, with no difference between Group 2: No Endo + CPP and Group 4: Endo + CPP (**Figure 6.11B**).

Interestingly, and in contrast to the mouse PF response profile, there were minimal differences in the early (rapid and transient) phase of response, with no difference between any PF subtype when compared to Group 1: No Endo No CPP **(Figure 6.11C i)**. However, the PF from both group of patients experiencing CPP were significantly higher than PF from the Endo only group (i.e. Group 2: No Endo + CPP and Group 4: Endo + CPP compared to Group 3: Endo No CPP, **Figure 6.11C i)**, suggesting specific soluble factors within the PF from patients with CPP drives this early activation phase. In comparison, the late sustained phase of response revealed elevated neuronal activation to all PF subtypes compared to Group 1: No Endo No CPP **(Figure 6.11C ii)**. Interestingly, in this phase, Group 4: Endo + CPP was significantly higher than all other PF treated groups **(Figure 6.11C ii)**.

These results indicate that whilst all PF types can activate a subset of sensory neurons, the capacity of PF from humans to directly activate neurons is enhanced in the presence of CPP, regardless of endometriosis development. However, there appears to be an additive effect with the combination of endometriosis and CPP on sustained neuronal activation.

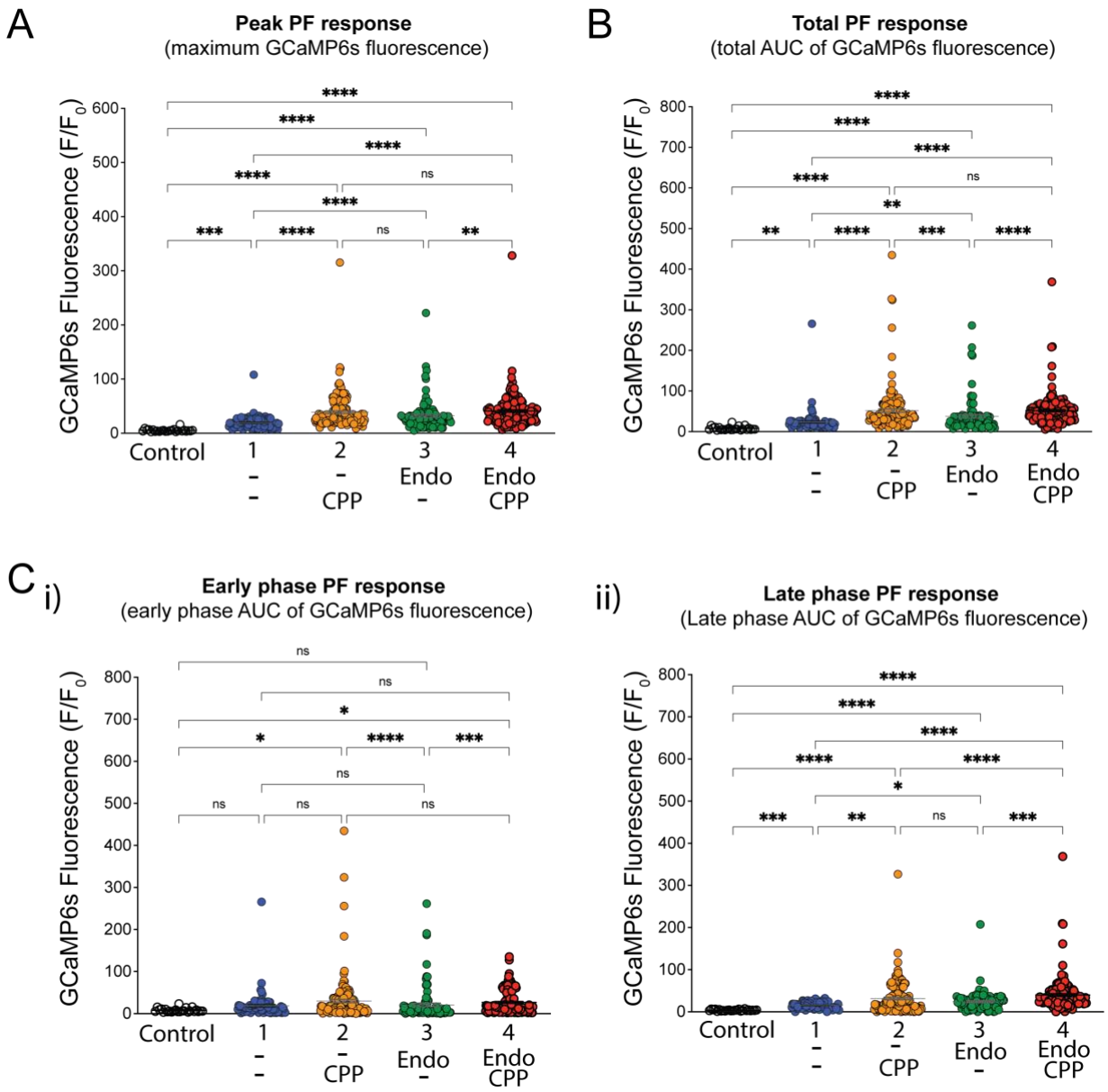

Figure 6.11: The peritoneal fluid (PF) from women enhances neuronal activation of intraperitoneal (i.p.) traced neurons

Grouped data showing **(A)** the peak response (maximum GCaMP6s fluorescence) was increased in all PF treatment groups compared to control, with Group 2: No Endo + CPP and both Endo groups (Group 3 and 4) being further increased over Group 1: No Endo No CPP. **(B)** Grouped data of the total response (total AUC of GCaMP6s fluorescence) also shows a significant increase in all PF treatment groups compared to control with the largest response seen in PF groups that experience CPP (Group 2 and 4). **(C)** Detailed analysis of the total AUC of GCaMP6s fluorescence in the **i)** early and **ii)** late phase of response shows the largest increase in AUC was during the late phase, with increases in all PF groups compared to both Control and Group 1: No Endo No CPP, in the second half of PF incubation. Data are presented as mean ± SEM from individual neurons, including control (n = 25, N = 2), Group 1: No Endo No CPP PF (n = 86, N = 2), Group 2: No Endo + CPP PF (n = 151, N = 6), Group 3: Endo No CPP PF (n = 93, N = 4) and Group 4: Endo + CPP PF (n = 151, N = 6). Each individual dot represents an individual neuron. Data are analysed using Kruskal-Wallis non-parametric analysis of variance with Dunn's multiple comparisons between groups where ns $P > 0.05$, ** $P < 0.01$, *** $P < 0.001$, **** $P < 0.0001$.

6.5.5 Peritoneal fluid from four patient cohorts has differential effects on capsaicin responses in DRG neurons

After confirmation that the PF from women can directly activate sensory neurons, with an increased response to groups with endometriosis and CPP, we again investigated whether incubation with PF could sensitize the neurons to subsequent algesic stimuli. Again, we measured the response of the TRPV1 agonist capsaicin following PF incubation from each patient group **(Figure 6.12A-E)**. Similar to what we saw in mice, we found that capsaicin activated a similar number of neurons regardless of the type of PF they were previously exposed to **(Figure 6.12F)**.

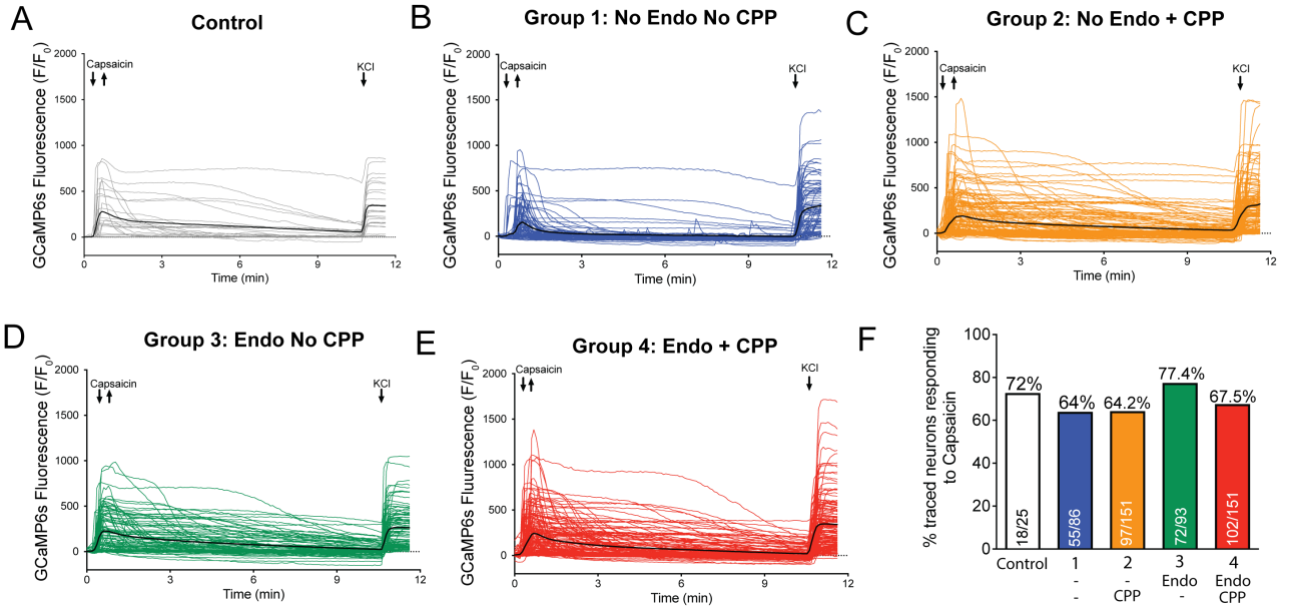

Figure 6.12: Capsaicin response of i.p. traced neurons following PF incubation.

Grouped traces showing the effect of TRPV1 agonist, capsaicin (50nM) on neurons pre-treated with **(A)** Control (PBS:HEPES) (grey, n= 25), **(B)** Group 1: No Endo No CPP (blue, n = 86), **(C)** Group 2: No Endo + CPP (orange, n = 151), **(D)** Group 3: Endo No CPP (green, n = 93) and **(E)** Group 4: Endo + CPP (red, n = 151). Each coloured line represents a single neurons response over time to 50 nM capsaicin and subsequent 40 mM KCl, black representative trace depicts average response of all traced neurons per group (mean), black dotted line represents baseline (0). **(F)** The percentage of i.p. traced neurons that responded to capsaicin was similar across all groups. *P* >0.05 Fishers exact tests. CPP: chronic pelvic pain

To better visualise the effect of capsaicin, we compared the capsaicin response following pre-treatment with each PF subtype against Control **(Figure 6.13A-B)**. Interestingly, results revealed a significant reduction in the capsaicin response in sensory neurons pre-treated with PF from Group 1: No Endo No CPP **(Figure 6.13B i)**. In contrast, the response with the PF from Group 2: No Endo

+ CPP **(Figure 6.13B ii)**, Group 3: Endo No CPP **(Figure 6.13B iii)** and Group 4: Endo + CPP **(Figure 6.13B iv)** did not mirror this reduction.

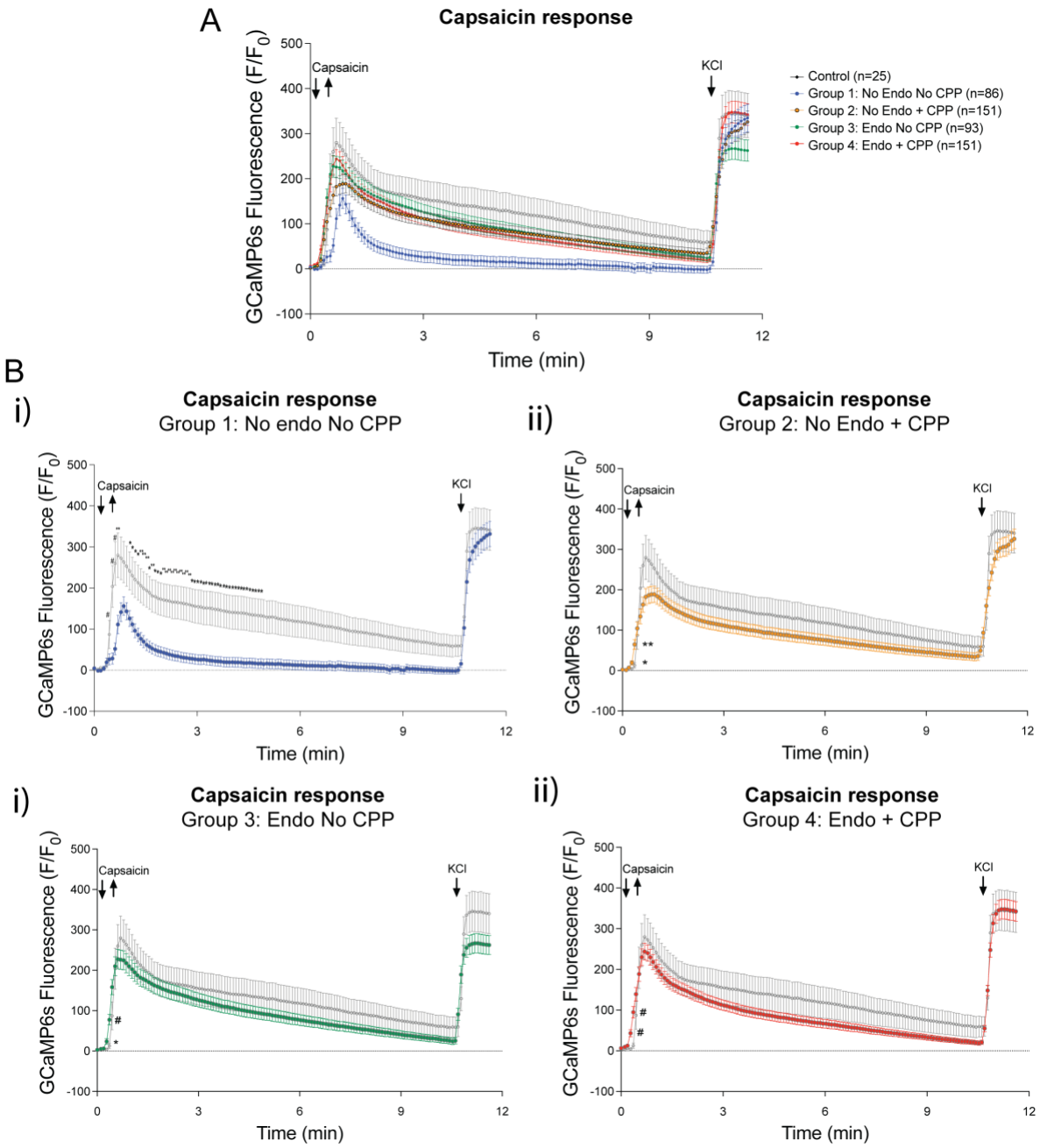

Figure 6.13: Peritoneal fluid (PF) from women does not sensitize healthy intraperitoneal (i.p.) neurons to TRPV1 activation.

(A) Grouped data from all traced neurons in response to control (n = 25, N = 2), Group 1: No Endo No CPP PF (n = 86, N = 2), Group 2: No Endo + CPP PF (n = 151, N = 6), Group 3: Endo No CPP PF (n = 93, N = 4) and Group 4: Endo + CPP PF (n = 151, N = 6) where n = number of neurons and N = number of individual samples. **(B)** Data presented for individual treatment groups compared to control, including **i)** Group 1: No Endo No pain, **ii)** Group 2: No Endo + CPP, **iii)** Group 3: Endo No CPP and **iv)** Group 4: Endo + CPP, shows that Group 1: No Endo No CPP significantly reduced the capsaicin response following PF incubation. In comparison, there was minimal change following incubation with all other PF subtypes compared to control. Data are graphed as mean ± SEM and analysed using a two-way ANOVA with Bonferroni post-hoc comparisons where *P <0.05, **P <0.01 and ^P <0.001 and $^{\#}P$ <0.0001). CPP: chronic pelvic pain.

Supporting the individual response profiles, the PF from Group 1: No Endo No CPP significantly reduced the peak capsaicin response **(Figure 6.14A)** as well as increased the time to peak response **(Figure 6.14B)** compared to all other PF subtypes. However, the total capsaicin response (total AUC of GCaMP6s fluorescence) was not different between any group **(Figure 6.14C)**. These results suggest that the PF from Group 1: No Endo No CPP patients may contain soluble factors that induce a basal inhibition of sensory neurons to subsequent TRPV1 activation.

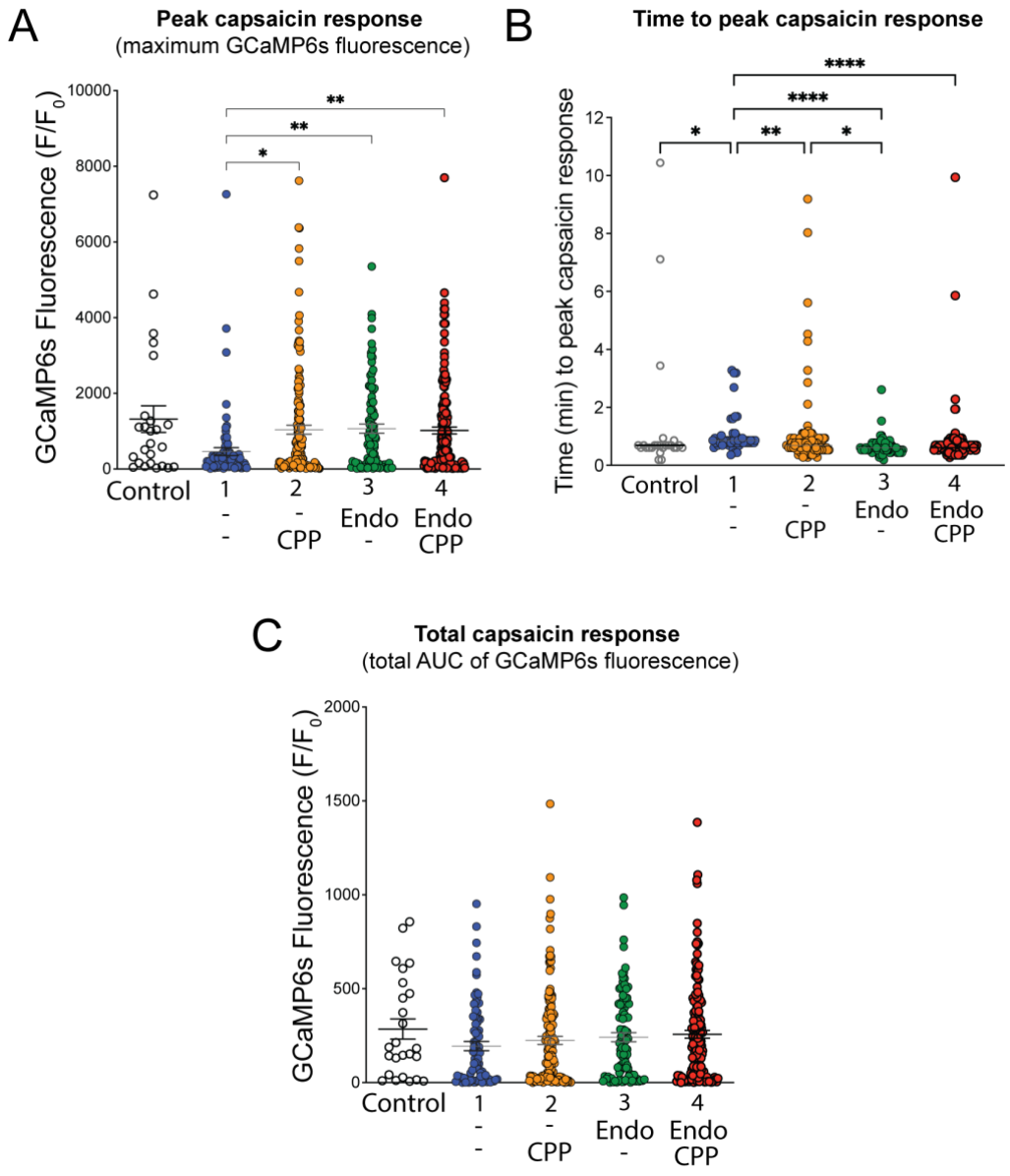

Figure 6.14: Peritoneal Fluid (PF) from women with No Endo No CPP reduced the peak capsaicin response.

(A) Grouped data shows a significant reduction in the peak capsaicin response (maximum GCaMP6s fluorescence) in i.p. traced neurons between following incubation with Group 1: No Endo No CPP PF compared to all other PF treatment groups. **(B)** Grouped data shows a significant increase in time (mins) to reach peak capsaicin response following incubation with Group 1: No Endo No CPP PF compared all other treatments. **(C)** Grouped data shows no difference in the total capsaicin response (total AUC of GCaMP6s fluorescence) between any treatment group. All data are

represented as mean ± SEM, where each dot represents a single neuron from each group. Data were analysing using Kruskal-Wallis non-parametric analysis of variance with Dunn's multiple comparisons between groups, ns $P > 0.05$, *$P < 0.05$, **$P < 0.01$, ***$P < 0.001$, ****$P < 0.0001$.

6.5.6 PF from women who experience CPP activates more capsaicin responding and non-responding neurons

So far, we have shown that PF from women with endometriosis and CPP induced enhanced activation of sensory neurons compared to the PF from women without Endo and CPP **(Figure 6.9, Figure 6.10, Figure 6.11).** Moreover, we demonstrated that PF did not sensitize the neurons to a subsequent application of an algesic stimuli (capsaicin) **(Figure 6.12, Figure 6.13, Figure 6.14)**. Finally, in line with what we had seen in mouse PF studies, we wanted to determine whether the enhanced activation of sensory neurons induced by the PF of women with endometriosis and CPP was due to differential recruitment of TRPV1 expressing neurons. For this, we separated the PF response analysis into TRPV1-positive neurons (capsaicin responders) and TRPV1-negative neurons (capsaicin non-responders) **(Figure 6.15A-C)**. We found that significantly more TRPV1-positive neurons responded to PF from women that experienced CPP (Group 2: No Endo + CPP and Group 4: Endo + CPP), with Group 4: Endo + CPP activating the largest number of both TRPV1-positive neurons (67.7% or 69 out of 102 neurons) and TRPV1-negative neurons (57.1% or 28 out of 49 neurons) **(Figure 6.15A)**. In addition, we found that Group 2 (No Endo + CPP) also activated a significant number of TRPV1-negative neurons (44.4% or 24 out of 54 neurons), and that Group 3 (Endo no CPP) almost exclusively activated a proportion of TRPV1-positive neurons and did not recruit additional TRPV1-negative neurons **(Figure 6.15A).**

To further explore the contribution of TRPV1-positive and -negative neurons in the differential sensory neuron activation seen between all subtypes of PF, we performed additional analysis by separating the PF responses into neurons that subsequently responded to capsaicin or not **(Figure 6.15B-C)**. We found that PF from women with endometriosis and/or CPP (Group 2: No Endo + CPP, Group 3: Endo No CPP and Group 4: Endo + CPP) elicited the highest responses in TRPV1-positive neurons compared to PF from women without Endo or CPP (Group 1) **(Figure 6.15B)**. In contrast, in TRPV1-negative neurons, PF from women with CPP (Group 2: No Endo + CPP and Group 4: Endo + CPP) were the only ones to cause significant activation compared to women without CPP **(Figure 6.15C)**.

Overall, we observed increased activation of TRPV1-positive and TRPV1-negative neurons in the groups that experience CPP, regardless of endometriosis diagnosis. In contrast, we observed minimal activation of TRPV1-negative neurons in groups that do not experience CPP. This strongly suggests that the recruitment of TRPV1-negative neurons is a differentiating factor between CPP and non CPP groups, which may reveal a driving factor in the generation of CPP.

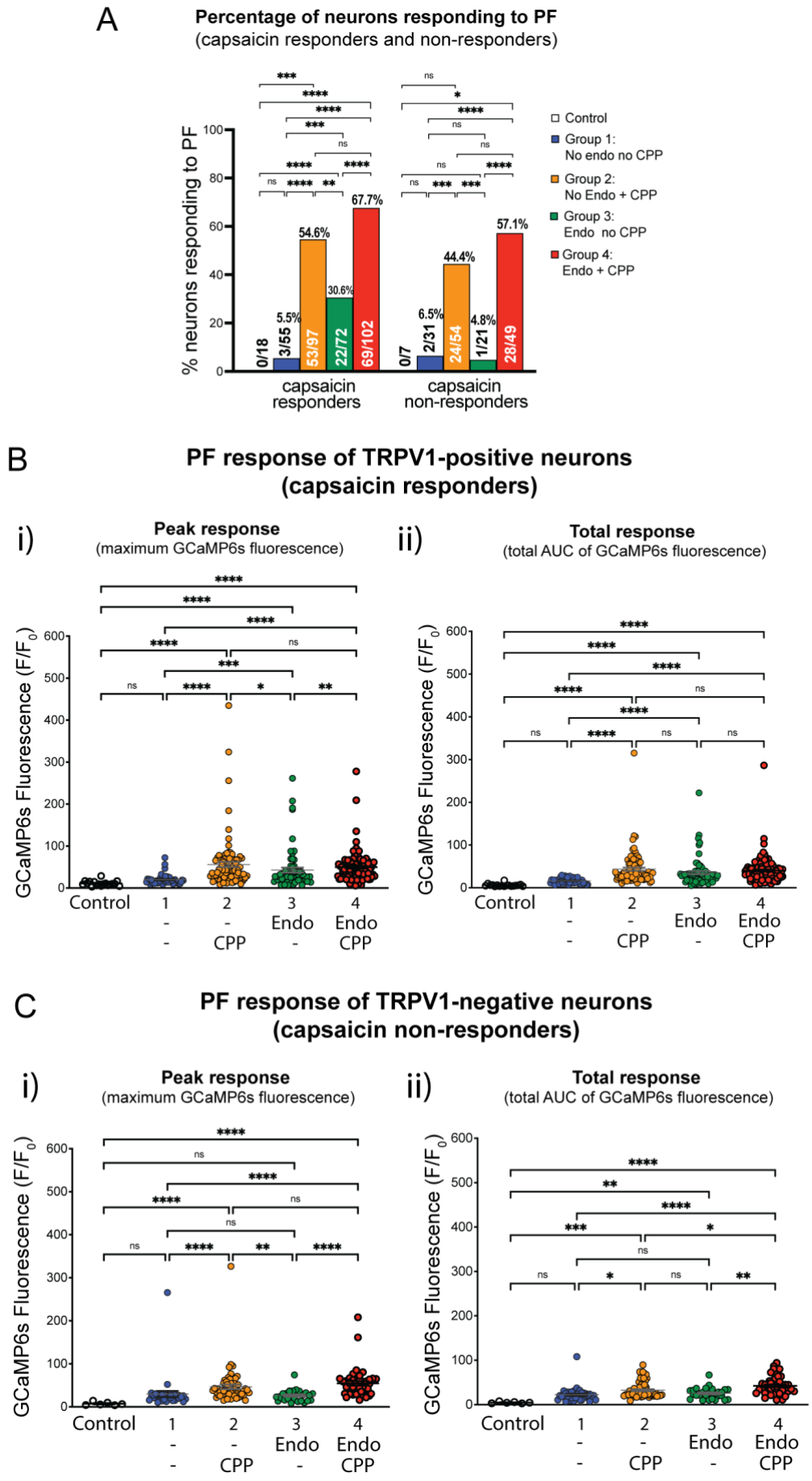

Figure 6.15: Peritoneal fluid (PF) from women who experience CPP activates significantly more TRPV1-positive and TRPV1-negative neurons.

(A) Grouped data shows neurons responding to PF were made up of both capsaicin responders and non-responders, with the largest percentage of both neuron subtypes responding to the PF from women who experienced CPP, with Group 4: Endo + CPP activating the largest number of both capsaicin responders and non-responders. Fishers Exact tests; ns P >0.05, *P <0.05, **P <0.01, ***P <0.001, ****P <0.0001. **(B)** Grouped data of the TRPV1-positive neurons (capsaicin responders) shows that **i)** the peak PF response (maximum GCaMP6s fluorescence) was the largest incubation with the PF of women that experience CPP, either without (Group 2: No Endo + CPP, n = 97) or with (Group 4: Endo + CPP, n = 102) compared to those that don't (Group 1: No Endo No CPP, n = 55 and Group 3: Endo No CPP, n = 72) and control (n = 19) treated neurons. **ii)** The total PF response (total AUC of GCaMP6s fluorescence) was similarly elevated in both CPP subtypes. **(C)** Grouped data of TRPV1-negative neurons (capsaicin non-responders) also shows that both **i)** the peak PF response and **ii)** the total PF response was significantly increased during incubation with PF from women who experience CPP (Group 2: No Endo + CPP, n = 54) or with (Group 4: Endo + CPP, n = 49) compared to those that don't (Group 1: No Endo No CPP, n = 31 and Group 3: Endo No CPP, n = 21) and control (n = 7) treated neurons. Data are represented as mean ± SEM from individual neurons. Each individual dot represents an individual neuron. Data are analysed using Kruskal-Wallis non-parametric analysis of variance with Dunn's multiple comparisons between groups; ns P >0.05, **P <0.01, ***P <0.001, ****P <0.0001. CPP: chronic pelvic pain.

6.6 Discussion

Recognised as an inflammatory condition, endometriosis has been linked with an increase in several inflammatory cytokines/chemokines, growth factors, neutrophils, and prostaglandins within the peritoneal fluid (PF) [81-84]. This aberrant environment within the peritoneal cavity presents an opportunity for direct interaction of soluble factors within the PF with nearby sensory nerves, initiating pain. The current study aimed to determine whether PF from either mice and women with endometriosis and CPP can directly activate visceral innervating sensory neurons and/or alter their response to subsequent algesic stimuli. To explore this, we used a combined approach, utilising i) i.p. nerve tracing to identify visceral innervating neurons, ii) a transgenic line of mice expressing the fluorescent Ca^{2+} sensor (GCaMP6s) in $Na_V1.8$ positive sensory neurons (>95 % of visceral innervating neurons [285, 305]{Castro, 2020 #221}), and iii) PF samples collected from both mice and women with and without endometriosis and/or CPP.

Our results showed that PF from both mice and humans can directly activate a subset of healthy i.p. innervating neurons from $Na_V1.8$xGCaMP6s mice. As $Na_V1.8$ is primarily expressed on small, peripheral sensory neurons involved in nociception [403, 407]{Castro, 2020 #221}, we can infer that PF is able to directly activate visceral sensory neurons, which are likely to be involved in pain sensation. We found that the PF from mice with an Endo + CPP phenotype activated a significantly larger population of visceral neurons compared to Sham controls. Importantly, these results were replicated using human PF, where PF from Endo + CPP patients also activated the largest population of visceral neurons compared to human PF subtypes without endometriosis and/or CPP. These results gave us a direct indication that the development of endometriosis and CPP alters the PF in such a way that it can heighten sensory neuron activation. This finding supports the hypothesis that the aberrant peritoneal environment developed in endometriosis may directly contribute to CPP in endometriosis.

In addition to these findings with endometriosis and CPP, our access to four distinct subtypes of PF patient samples allowed us to uncover an association with enhanced neuronal activation and patient experience of CPP alone. Multiple visceral organs can be associated with widespread CPP, and, for the first time, our data directly links PF with activation of visceral sensory neurons. Specifically, we identified that the PF from patients who experienced CPP, regardless of an endometriosis diagnosis, activated the largest number of sensory neurons, displaying increased maximum and total neuronal responses, compared to PF subtypes without CPP. We did see an additive effect with the development of endometriosis and CPP, which suggests the combination of pathologies further drives neuronal activation.

We have previously shown, in the pre-clinical mouse model of endometriosis described in Chapter 2, that the PF of Endo mice contains elevated inflammatory cytokines, including interleukin

(IL) IL-1β, IL-6, IL-17, and IL-33 as well as vascular endothelial growth factor (VEGF). Moreover, we found that tumour necrosis factor-α (TNFα) and Monocyte chemoattractant protein 1 (MCP-1) were slightly elevated, although not significantly. TNFα, and IL-1β are found elevated within the PF of endometriosis patients who reported CPP [81, 96-98, 155]. Notably, these mediators are suggested to directly activate sensory nerve endings [99, 100, 156], which could explain the increased neuronal activation seen in our experiments with the PF from both mice and women with endometriosis and CPP. While out of scope of the current study, future experiments looking at the molecular profile of soluble factors within PF samples from mice and women would provide insight to key mechanisms that may be driving the elevated neuronal activation seen in both endometriosis and CPP development.

Aside from direct activation of sensory neurons, peripheral sensitization of sensory neurons can occur in response to inflammatory mediators at the site of tissue injury [408]. In the current study, we aimed to determine whether the inflammatory environment within the PF can alter the response of sensory neurons to subsequent TRPV1 activation (i.e., induce neuronal sensitization). TRPV1 is a non-selective cation channel that acts as a molecular sensor and is strongly linked to altered pain perception, particularly in inflammation [165, 406]. TRPV1-positive neurons are found in a high percentage of visceral innervating neurons in mice [409]. This was supported by our results across all treatment groups, which showed between 64.2% and 77.4% of all visceral traced neurons responded to capsaicin. Despite the high number of TRPV1-positive neurons, we found that acute treatment with the PF from mice or women with endometriosis and/or CPP did not sensitize visceral innervating neurons to TRPV1 activation induced by capsaicin. While there did not appear to be an acute neuronal sensitization in response to any PF, the ability of endometriosis to ultimately alter neuronal sensitivity to this algesic stimuli throughout chronic disease progression may ultimately drive a sensitized response. This concept is important, as TRPV1 can undergo acute and reversible sensitization, which our results suggest did not occur, or can be upregulated and sensitized due to an overall increase in functional TRPV1 channels over time, which would not occur in the short time frame of these experiments [410]. The neuroplasticity of sensory nerves occurs over chronic disease progression, the combination of which ultimately acts to drive changes in peripheral sensitivity [88, 135, 151, 170, 171]. Interestingly, elevated expression of TRPV1 has been found on both the peritoneum and adhesions of women with endometriosis, which correlated with enhanced pain intensity [136, 168, 169]. To this end, our results reflect the acute effects of PF and don't necessarily exclude the ability of PF to ultimately sensitize sensory neurons throughout various stages of disease progression.

Interestingly, we did see a significant reduction in response to TRPV1 activation in Group 1: No endo No CPP human PF treated neurons. The PF from this subtype appears to induce an inhibitory environment for algesic stimulation of sensory neurons, suggesting there may be a

physiologically protective role of the PF to regulate pain sensation in healthy conditions. Importantly, this appears to be lost with the development of endometriosis and/or CPP. Losing this sensory inhibition would ultimately contribute to elevated pain signalling compared to healthy women, even without enhanced sensitization. However, it should be considered that, although the results seen with the PF from women were significant, the number of Group 1: No endo No CPP samples were limited (N = 2 samples) due the reduced number of 'healthy' women undergoing peritoneal surgery appropriate for PF collection. Moreover, the number of Control neurons was approximately one third of those used in other PF treatment groups, and more numbers of each group would be needed to confirm results.

Nevertheless, the notion that an inhibitory component exists which reduces afferent sensitivity in healthy conditions, and is then lost in inflammatory conditions such as IBS, has previously been described [411]. It has previously been shown that soluble mediators released by healthy human peripheral blood mononuclear cells (PMBCs) significantly reduced muscular-mucosal afferent firing of mouse colonic pelvic afferents, *ex vivo* [411]. In direct contrast, inflammatory mediators released from PMBCs of IBS patients increased the same mechanosensory responses [411]. Although these studies applied supernatants to intact colonic tissue for *ex vivo* afferent recordings rather than cultured DRG neurons like in our studies, similar inhibitory mechanisms may explain the response to healthy PF. To this end, it would be beneficial to determine whether direct application of this 'healthy' PF to sensory afferents in intact tissue would result in a similar reduced afferent firing rate, *ex vivo.* Interestingly, we did not see the same reduction in capsaicin response that was seen using human Group 1: No Endo No CPP PF following incubation with Sham Mouse PF. However, Sham mice undergo an ovariectomy and surgical suturing procedures to mimic those used in surgical induction of endometriosis. It is plausible that these procedures alter the PF environment in such a way that it is not reflective of a 'healthy' PF environment. Therefore, it would also be of interest to collect PF from naïve female mice for use in future studies to further explore the presence of an inhibitory role of healthy PF and the loss of this contributing to CPP.

In order to differentiate neuronal subtypes activated by the PF of each group, we classified traced neurons as either TRPV1-positive or TRPV1-negative based on their response to the TRPV1 agonist, capsaicin. We found that PF from both mice and women with endometriosis and CPP recruited the largest percentage of TRPV1-positive neurons out of all groups, activating 81.6%. (Endo mouse PF) and 67.7% (Group 4: Endo + CPP) respectively. Interestingly, the PF from women without endometriosis but that did experience CPP also activated a large number (54.8%) of TRPV1-positive neurons. These results are not surprising, given the acceptance that TRPV1-positive neurons are frequently associated with nociception. TRPV1 has been associated in chronic pain development in inflammatory conditions such as arthritis and IBS [135, 142, 165, 412] and has recently been implicated in endometriosis associated pain [136, 167, 169]. In the viscera, TRPV1 is

broadly expressed in a subset of polymodal neurons known as peptidergic neurons [151, 413], often co-expressed with transducer channels including transient receptor potential cation channel member ankyrin 1 (TRPA1) and the acid sensing ion channel ASIC3 [413]. TRPV1 is not only activated by capsaicin but can either directly or indirectly integrate responses to stimuli such as acidosis, oxidative stress, and inflammatory mediators [135, 166, 405, 414], all of which occur in endometriosis [81, 85, 96-98, 102]. The mechanisms by which PF is activating TRPV1-positive neurons, i.e., via direct TRPV1 activation or second messenger, such as another channel co-expressed within these neurons, was out of scope of these studies. However, our results support a role for TRPV1-positive neurons in CPP-associated sensory neuron activation.

Although TRPV1-positive peptidergic neurons are the most prominent in the viscera [415], we also found significant activation of a subset of TRPV1-negative neurons in response to both mouse and human PF with an endometriosis and CPP phenotype. Interestingly, in human studies, there was a stark difference in TRPV1-negative neurons activated between groups that experience CPP (Group 2: No Endo + CPP (44.4%) and Group 4: Endo + CPP (57.1%) and those that do not (Group 1: No Endo No CPP (6.5%) and Group 3: Endo No CPP (4.8%)). Of particular interest, the results gained using PF from women that were diagnosed with endometriosis but did not experience CPP showed that this PF subtype almost exclusively activated TRPV1-positive neurons (with 30.6% of TRPV1-positive neurons activated compared to only 4.8% of TRPV1-negative neurons). Taken together, our results suggests that while endometriosis development itself may enhance TRPV1-positive neuron activity, the mechanisms required to induce CPP may have a large component driven by recruitment of TRPV1-negative neurons.

Recent RNAseq data has identified a non-peptidergic neuron cluster (TRPV1-negative neurons) in colonic innervating DRG neurons [413]. These TRPV1-negative neurons contained high expression levels of other receptors including purinergic receptor P2X3, MAS-related G-protein coupled receptor D (MRGPRd) and Na_V channels $Na_V1.7$, $Na_V1.8$ and $Na_V1.9$. P2X3 receptors are known to mediate acute and chronic inflammatory neuropathic pain [416] and, along with TRPV1, are essential for nociception [417]. Moreover, P2X3 receptor expression in endometrial lesions correlates with pain severity [418]. However, although P2X3 was found in the TRPV1-negative neuron clusters, it was also found co-expressed with TRPV1 [419]. While the results gained in these experiments provide important information on neuron subtypes that respond to PF, to identify direct mechanisms future studies will need to utilise pharmacological inhibitors or genetically modified mice that lack channels of interest. It would also be beneficial to identify receptors and ion channels present specifically on these visceral innervating neurons. These studies would provide central information to identify key signalling pathways in visceral neurons that may contribute to CPP signalling from the peritoneal cavity.

In the experiments presented within this chapter, Ca^{2+} imaging was used as a surrogate measure of neuronal activation, with increases in GCaMP6s fluorescence signifying neuronal activity. Single cell Ca^{2+} imaging provides the combined advantage of a high throughput preparation, facilitating the testing of multiple samples with the selective identification of a key subset of fluorescently traced neurons. This distinction allowed us to determine the effect of various subtypes of PF on a physiologically relevant neuronal population, which is difficult achieve in an intact system. However, it is important to note that intracellular Ca^{2+} is not a direct proxy for action potential firing, and we cannot explicitly conclude from these experiments alone that PF does in fact enhance nociceptive signalling. Measuring direct firing of action potentials in response to PF subtypes with *ex vivo* electrophysiology would facilitate a more direct measurement of afferent firing. Ultimately, translating these *in vitro* findings to *in vivo* changes in pain like behaviours would nicely translate these studies to a whole-body system. For example, utilising behavioural techniques such as those described in the mouse model development Chapters 2 and 3, such as VMR and abdominal vfh, following acute i.p. administration of PF from and endometriosis and CPP phenotype, would be a translational set of experiments to nicely elucidate a direct role of PF in acute pain signalling.

In conclusion, this study has demonstrated that PF collected from mice or women experiencing CPP (in the presence or absence of endometriosis) can directly activate a distinct subset of visceral innervating sensory neurons. The combination of endometriosis and CPP in both mice and women significantly increased neuronal activation. This highlights a fundamental role of the aberrant inflammatory PF in altered sensory signalling. While there is a clear role for TRPV1-positive neurons in endometriosis and CPP, our studies revealed a TRPV1-negative component associated with CPP development in women. Whether or not enhanced neuronal activation translates to heightened pain signalling is an important next step to confirm its role in endometriosis associated CPP generation. The findings presented in this chapter further support the paradigm shift from endometrial lesions as the primary source of CPP in endometriosis and continues to expand into altered sensory signalling mechanisms. As a complex disease, considering the synergistic effects of various mechanisms contributing to endometriosis associated CPP expands the potential to identify much needed therapeutic targets to ultimately decrease morbidity associated with this debilitating condition.

CHAPTER 7: OVERALL DISCUSSION

As discussed in Chapter 1, the development of endometriosis associated CPP is multifactorial in nature, with a series of complex mechanisms likely to contribute to its development [231]. A major contributing factor in the shortage of effective therapeutic strategies is the lack of knowledge surrounding the mechanisms of endometriosis associated CPP. Despite a clear increase in endometriosis research published over the last 10 years, pre-clinical studies have failed to translate to effective clinical outcomes [228]. Unfortunately, the reproducibility of pre-clinical animal models that recapitulate the full spectrum of disease may be a translational block when considering progress in endometriosis related research [228]. To address this, the first aim of this thesis was to develop two mouse models of endometriosis for the study of CPP mechanisms. Both methods of endometriosis induction characterised within this thesis have previously been utilised in both rats and mice. Although their use has contributed to various areas of endometriosis research (see Chapter 1), detailed analysis of the development of CPP across multiple visceral organs had not yet been explored, limiting their use in CPP research.

7.1 Pre-clinical mouse models of endometriosis

Ectopic endometrial cell growth outside of the uterus defines endometriosis, with peritoneal endometriosis found in and around the peritoneum and visceral organs the most commonly located [250, 420]. However, women with endometriosis rarely develop a single lesion subtype, with a combination of both superficial peritoneal lesions as well as deep infiltrating lesions often develop [66]. By developing two mouse models of endometriosis, we revealed that differences in the method of induction ultimately translated to slight differences in endometriosis phenotype at 10 weeks. This is not unexpected, as small variations in endometriosis disease modelling, like those we have presented, have been suggested to mimic variations in endometriosis subtypes/heterogeneity like that which is seen naturally in women [299]. A recent study by Dorning *et al.* illustrated that even slight variations in donor uterine tissue type inoculated into the peritoneal cavity of mice resulted in clear differences in both disease progression and pain phenotype [299].

7.1.1 Endometrial lesion development and progression

In our studies, we found that surgical transplantation of uterine horn tissue (Chapter 2) as well as inoculation of minced uterine horn tissue into the peritoneal cavity of mice (Chapter 3)

successfully initiated the growth and development of endometriotic lesions in similar locations to those found in women and similar animal models [252, 276, 421, 422]. These ectopic endometrial lesions maintained histological characteristics resembling that which would confirm endometriosis in women, including the presence of endometrial glands and stroma [277, 286].

Using the transplant method of endometriosis induction, large full thickness uterine horn tissue biopsies were transplanted in direct contact with large blood vessels and associated nerves alongside visceral organs, in a controlled manner. This surgical model of endometriosis has been suggested to reflect more mature endometriosis development, bypassing the initial attachment phase of disease [423]. The resulting growth and development of lesions in this model displayed similarity to deep infiltrating endometriosis, which most often affects structures including the uterus and digestive tract [424, 425]. When considering the growth rate of endometriotic lesions, we saw significant growth of lesions occurring earlier in the transplant model compared to the inoculation model. The size of uterine tissue as well as the invasiveness of translocation method is a significant difference between both mouse models developed within this thesis. It is possible that the surgical trauma of induction, as well as the larger size of eutopic tissue surgically attached alongside visceral organs compared to inoculation, may support the development of a more progressed and deep infiltrating disease.

In comparison, the inoculation of minced uterine horn induced random growth of lesions in superficial peritoneal locations, such as on the abdominal wall, within abdominal fat, and within the connective tissue of visceral organs [376]. It is suggested that this induction method, which more closely replicates retrograde menstruation, resembles initial stages of disease development, including attachment, inflammation, and neuroangiogenesis [423]. In this method, small tissue fragments need to attach at locations suitable for continued lesion growth, a process bypassed in the transplant method. The resulting endometrial lesions bear more resemblance to superficial peritoneal endometriosis development, a common form of endometriosis seen in approximately 80% of cases [420]. As there is no way to determine whether lesions collected in our animals were from original tissue inoculation and at what point they established, the growth measurements presented in our studies may not be reflective of original lesion growth. For example, in a small number of mice, sprouting of new lesions from established lesions has recently been reported to occur at 6 weeks of endometriosis development using the inoculation method [299]. This new lesion sprouting has not yet been reported to occur in the transplant model. As such, longitudinal, non-invasive imaging of lesion development would provide an elegant alternative to understanding variations between early lesion growth and establishment within both models.

Importantly, both deep infiltrating and superficial peritoneal lesions are suggested to contribute to pelvic pain via different mechanisms [140, 426]. Specifically, deep infiltrating endometriosis has a stronger association with local pain, which could partially be explained by local

inflammation (discussed in section 7.1.3 below) and nerve encapsulation and compression [140], whereas superficial peritoneal endometriosis may be driven by an altered macrophage profile and lesion inflammation [426]. While different mechanisms may occur depending on lesion subtype developed within each model, the combination of factors leading to CPP will provide useful insight which compliments the complexity of disease.

7.1.2 Adhesions

Adhesions are bands of connective tissue that can cause fusion of structures that are normally separated, including visceral organs, muscle and surrounding connective tissues [427]. Pain mapping of patients with suspected adhesion associated CPP found the highest pain scores were in patients where adhesions had fused visceral organs such as the ovaries, bladder or small intestine with the parietal peritoneum [428, 429]. Although the underlying pathophysiology of adhesions in endometriosis is not well understood [292], women with endometriosis have an enhanced risk of developing peritoneal adhesions, through either spontaneous development [430] or following surgery [431]. Studies have identified up to 80% of women with endometriosis also have pelvic adhesions, with a higher incidence in women with advanced stage endometriosis [287, 432]. Interestingly, in our studies, the development of adhesions was only apparent in the transplant method of endometriosis induction. Inflammation in the peritoneal environment has been implicated in both endometriosis development as well as endometriosis-related surgical adhesions [292, 433]. It is likely that the invasive surgical nature of endometriosis induction in the transplant model is conducive in the development of adhesions. Performing endometriosis induction at various stages of post-ovariectomy healing has demonstrated that acute inflammation associated with surgical trauma can significantly promote the development of adhesions as well as endometriosis growth in mice [291]. Supporting the advanced stage of disease suggested to develop in the transplant model, adhesions are a pathology reflective of a more severe disease phenotype in women and is often found accompanying deep endometriosis [66, 433]. Despite the increased risk of adhesion formation in endometriosis, the role, if any, that adhesions play in CPP experienced by women with endometriosis remains unclear and recent studies have reported no correlation between patient-reported pain and the presence of adhesions [434].

7.1.3 Local inflammatory environment in endometriosis

Differences in the local inflammatory environment within the peritoneal fluid (PF) were also observed between our mouse models of endometriosis. Cytokines within the PF following endometriosis induction by surgical transplantation more closely resembled the inflammatory environment within the PF of many women with endometriosis, developing elevated interleukins -1β,

-6, -17, -33 and VEGF [297]. In comparison, VEGF was the only elevated pro-inflammatory cytokine measured within the PF of endometriosis mice developed using the inoculation method [376]. As noted within Chapter 3, this data adds to the growing inconsistencies around the importance of inflammation in endometriosis development [376]. Interestingly, inflammatory mediators in the PF and serum of women with endometriosis can vary depending on disease stage and severity [310, 311]. For example, one study found elevated mediators including IL-1α, IL-1β and IL-6 in advanced stage endometriosis only [311]. Conversely, a study in mice found that levels of some neutrophils and inflammatory cytokines, including TNFα, IL-6, and VEGF, were increased in the early days of development but had returned to baseline levels by 4 weeks of endometriosis development [298]. It remains unknown whether the aberrant inflammatory environment in women with endometriosis is an underlying defect in the immune system that supports endometriosis formation or rather a consequence of endometriosis development itself [230]. The inconsistencies within the PF in various studies illustrates that the inflammatory profile within the PF echoes the heterogeneity of endometriosis development.

When comparing the inflammatory mediators present within our mouse models, the difference may be reflective of a deep-infiltrating lesion subtype found in the transplant model of endometriosis, often associated with advanced disease, compared to the superficial lesion development in the inoculation model. Moreover, as mentioned above, the surgical nature of the transplantation model and additional formation of adhesions may also drive the inflammatory cascade, ultimately altering the inflammatory environment. The less invasive nature of the inoculation model avoids the disruptive inflammatory response that would occur in the transplant model, which would be more reflective of the early stages of disease initiation following retrograde menstruation. Unfortunately, it is difficult to draw parallels between inflammatory mediators reported in similar models of endometriosis, as the majority of rodent models reported in the literature follow endometriosis development over a shorter duration (days/weeks) [250], and variations similar to that which we see may also exist if later time points were included. Measuring inflammatory cytokines across the full development of endometriosis would give us a better understanding the inflammatory environment between both models of endometriosis development, however, was not in the scope of these studies. Despite these differences in local inflammation within the peritoneum at 8-10 weeks, both models of endometriosis developed a CPP phenotype reflective of that experienced by women with endometriosis.

7.1.4 Development of enhanced spontaneous and evoked ‘pain-like’ behaviours in both mouse models of endometriosis

Women with endometriosis are 13 times more likely to experience abdominal pain than healthy women [32], enhanced by a high comorbidity rate with other visceral pain syndromes

including irritable bowel syndrome (IBS), inflammatory bowel disease (IBD), interstitial cystitis/bladder pain syndrome (IC/BPS), and dyspareunia [26, 27, 38, 56-58]. To this end, characterizing the development of enhanced pain across multiple visceral organs in these pre-clinical models of endometriosis, using both spontaneous and evoked behavioural measurements, was essential to their establishment as models of CPP in endometriosis. The results presented in this thesis were the first to identify the concurrent development of vaginal, colonic, cutaneous, and bladder sensory comorbidities within both pre-clinical models of endometriosis [297, 376].

Despite similarities in a CPP phenotype, altered spontaneous behaviours associated with the development of anxiety was only developed in the inoculation model of endometriosis [376]. This behavioural difference, combined with differential lesion development and local inflammatory environment within the PF, supports the concept that mechanisms driving development of CPP may vary between models. With this in mind, it has recently been suggested that a single standardized model is not likely to provide translational benefit, but rather, preclinical research using multiple models may support more robust pre-clinical data and lead to stronger clinical outcomes [299]. This is important, as the development of endometriosis in women is complex, and the ability to use models that reflect different subgroups of endometriosis observed in women may offer key translatable findings relevant to heterogenous disease mechanisms.

7.1.5 Recognizing limitations

Within this thesis, we have successfully been able to characterise two independent mouse models of endometriosis for the study of CPP mechanisms. Though both mouse models provide practical contributions to CPP research in endometriosis, some limitations in their translation need to be considered. Notably, the most obvious limitation is the difference in cyclical menstruation and natural formation of endometriosis in rodents when compared to human disease development [254]. In women, this physiological process of menstruation would continually drive the innate immune response and facilitate cyclical introduction of new ectopic endometrial cells. While we can mimic the process of retrograde menstruation, the recurrent cyclical retrograde menstruation as well as cyclical bleeding from ectopic lesions does not occur in mice. Furthermore, ovariectomized mice were used in our study to enable control over fluctuating hormones, as cyclical variation in hormone levels has been shown to influence pain perception [435]. Although this enables us to reduce hormonal fluctuations impacting pain-like behavioural measurements, it does limit its effectiveness to support research into mechanisms associated with fertility and the role of natural hormone cycling in endometriosis development and cyclical CPP. Finally, endometriosis is a chronic disease that is often diagnosed after years of development facilitating complex disease progression [30, 67-69]. While we have characterised more chronic development compared to many studies looking at earlier time points, the disease progression may not encompass long term alterations in CPP processing

occurring over years of disease development. This long-term progression is difficult to replicate in rodent models in shorter time frames, however, the characterization of both models of endometriosis, which reflect different disease stages, is important for future mechanistic studies.

7.2 Pre-clinical models to investigate endometriosis mediated CPP

7.2.1 Differential mechanisms contributing to CPP in our mouse models of endometriosis?

As discussed in Chapter 1, various mechanisms are suggested to be involved in CPP development in endometriosis, with a combination likely contributing to endometriosis associated CPP. The similarities of the transplant model to deep infiltrating endometriosis on visceral structures may predispose the development of mechanisms more closely related to local inflammation or peripheral inflammation/sensitization due to local infiltrating lesions. In the transplant model endometrial lesions are surgically attached alongside the uterus which may result in the compression or encapsulation of nearby pelvic nerves. This may be relevant as high pain scores in women with endometriosis correlates with a higher density of nerves and nerve encapsulations [126, 127, 140]. In contrast, the inoculation model reflects more superficial peritoneal lesion development and there did not appear to be any deep infiltrating lesions. It is therefore unlikely that compression and encapsulation of local nerves has occurred, although we cannot rule this out.

Another clear difference between models was revealed with PF cytokine analysis at 8-10 weeks of endometriosis development. In our inoculation model of endometriosis, hyperalgesia of visceral organs remained despite the lack of an elevated inflammatory environment within the PF when compared to the transplant model. Taken at face value, these results suggest that elevated pro-inflammatory cytokines in the PF are not the only factor for sustained chronic hypersensitivity in the inoculation model. However, in future experiments it would be beneficial to look at the inflammatory environment throughout endometriosis development, and expand the panel of mediators measured, as the snapshot provided in these experiments does not give us a complete profile to draw conclusions. Interestingly, CPP in the absence of sustained inflammation occurs in other chronic pain conditions such as IBS, IC/BPS and fibromyalgia. In these conditions, inflammation is known to contribute to hyperalgesia by inducing sensitization of afferents which remains long-after the resolution of inflammation [88, 151]. With this in mind, measuring local inflammation within visceral organs themselves would be of benefit when considering CPP mechanisms associated with these organs.

7.2.2 Peripheral sensitization of visceral innervating afferents in endometriosis

As discussed in Chapter 1, neuroplasticity of peripheral sensory nerves, where structural or synaptic changes occur to shift neuronal function to a sensitized state may play a role in visceral hypersensitivity seen in endometriosis. In order to further elucidate these mechanisms, we first explored the peripheral sensory pathways involved in healthy vaginal nociception in mice. The work presented in Chapter 4 was the first to illustrate how pelvic vaginal afferents are broadly tuned to detect a variety of mechanical stimuli. Using the vaginal afferent recording technique developed in these studies, we were able to demonstrate that pelvic afferents innervating the vagina of endometriosis mice developed peripheral hypersensitivity, like that we had seen developed in bladder innervating afferents in Chapter 3. Although previous studies using a rat model of surgically induced endometriosis have shown vaginal hyperalgesia is correlated to increased vaginal innervation [268], studies directly measuring the sensitivity of visceral innervating afferents has not yet been performed in the surgical model of endometriosis. Therefore, future studies using the transplant model of endometriosis presented in this thesis to measure afferent hypersensitivity of visceral afferents would be an important addition. It would also be interesting to see if the hypersensitivity of bladder and vaginal innervating afferents is also seen in colonic afferents. Further understanding of afferent hypersensitivity in endometriosis, and the breadth at which this occurs, will be important for future targeting of CPP associated with specific visceral organs.

7.2.3 Central and cross-organ sensitization

Studies have shown that inflammatory changes in central spinal processing pathways occur using a similar inoculation model of endometriosis in mice [436]. In these studies, Dodds *et al*. described activation of astrocytes and microglia within the spinal cord of mice with endometriosis, a phenomenon which may drive central sensitization and cross-organ sensitization in endometriosis [436]. Both central and cross-organ sensitization would contribute to CPP across multiple visceral organs due to the overlap of shared neuronal pathways for nociceptive processing. This is especially relevant as visceral organs including the bladder and vagina are innervated by shared pelvic nerves. Although central mechanisms of CPP development in endometriosis were out of scope of the studies presented in this thesis, it would be interesting to determine whether this neuroinflammation also occurs in the transplant model of endometriosis.

7.3 The role of the peritoneal fluid (PF) in endometriosis mediated CPP

As discussed in Chapter 1, it is considered that immune dysfunction enables endometrial lesion formation throughout the peritoneal cavity in women with endometriosis [39], however, there may also be a role for the PF in CPP development [106, 231]. The final aim of this thesis was to determine whether soluble factors within the PF may be able to drive CPP in endometriosis. Various studies continue to report inconsistencies in the inflammatory environment within the PF of women with endometriosis at various stages of disease and lesion subtype [101, 310, 311]. Similarly, we also reported differences in PF cytokines between the inoculation and surgical induction methods in mice [297, 376]. This heterogeneity makes it difficult to elucidate mechanisms in which the PF may drive CPP in endometriosis. The use of capsaicin in our studies did enable us to determine a differential role for both TRPV1-positive and -negative neuronal pathways, however, without further analysis of soluble factors within the PF samples used in these studies, the mechanisms by which neuronal activation occurs are difficult to determine.

7.3.1 A role for TRPV1-negative neurons in CPP

TRPV1 has long been implicated in inflammatory pain, and as such, has been the target for drug development in human pain conditions including osteoarthritis, headaches, neuropathic pain and cancer pain [437]. We saw that the PF from both mice and women with Endometriosis and CPP activated the largest number of both TRPV1-positive and TRPV1-negative cultured sensory DRG neurons innervating the mouse viscera. Interestingly, the PF from women with endometriosis but that do not experience CPP almost exclusively activated TRPV1-positive neurons, with TRPV1-negative neurons not contributing in this CPP-free subgroup. These results suggest that while TRPV1-positive pathways may be activated by underlying mechanisms associated with endometriosis development, there may be an independent role for TRPV1-negative neurons in CPP generation. Supporting this concept, we saw elevated activation of TRPV1-negative sensory neurons using the PF collected from women suffering CPP, but that did not have endometriosis. The ability of PF from women who suffer from CPP (regardless of endometriosis diagnosis) to recruit a subset of sensory neurons (TRPV1-negative) that are not recruited by PF of women that do not experience CPP may help explain how PF drives CPP. Without examining the soluble factors within the PF, we cannot draw comparisons on specific mechanisms by which enhanced sensory neuron activation occurs with CPP subtypes. By drawing on underlying pathologies, independent of endometriosis, that induce peritoneal inflammation and CPP, we can draw similarities with the aberrant release of inflammatory mediators in endometriosis which may help explain the elevated sensory drive.

Other conditions which may alter the inflammatory environment within the PF and are known to cause pelvic pain include pelvic inflammatory disease, ovarian cysts, peritoneal cysts, and adhesions [438]. Pelvic inflammatory disease affects sexually active women of reproductive age and is characterised by infection of the female genital tract, with intra-abdominal infections releasing local inflammatory mediators [438, 439]. Ovarian cysts can cause chronic pain in women, with the rupture of cysts releasing inflammatory fluid into the peritoneal cavity, contributing to intense pain [438, 440]. In a similar way, peritoneal cysts can occur following pelvic surgery, infection, or cancer [441] and are associated with chronic pain and inflammation in the peritoneum. Interestingly, adhesions alone have also been implicated as a cause for CPP in women without endometriosis [442]. These examples are ways in which inflammation in and around visceral organs may contribute to a dynamic inflammatory environment. Future studies should compare soluble factors within the PF of the CPP subtypes, both with and without endometriosis, as well as the PF subtypes that do not experience CPP. This would help determine what mediators may be activating both TRPV1-positive and -negative neuronal pathways and allow us to determine key differences which may be driving CPP.

7.3.2 The role of PF combined with chronic changes in sensory pathways following endometriosis development

Finally, when considering the potential mechanisms for endometriosis associated CPP generation induced from the PF, it should also be considered that additional activation of cultured sensory neurons seen in Chapter 6 were obtained using healthy neurons. While this enabled us to elucidate an acute and direct effect of PF on sensory neuron activation, it does not account for the interaction with chronic changes due to endometriosis development, such as peripheral and central sensitization. With an average delay in diagnosis of endometriosis of up to 12 years [30, 67-69], the pain experienced by most women is succeeding chronic disease development and multiple mechanisms are likely to be involved. As mentioned in Chapter 1, long-term development of endometriosis can sensitize peripheral sensory neurons, as was described in vaginal and bladder innervating afferents in our endometriosis mice (Chapter 3 and 5). Adding to peripheral sensitization, sensitized sensory nerve fibres contribute to sustained inflammation, initiating a pro-inflammatory feedback loop known as neurogenic inflammation [231]. This neurogenic inflammation occurs in chronic pain conditions which are often co-diagnosed with endometriosis, such as IC/BPS and IBS, where chronic neurogenic inflammation contributes to chronic pain [88, 147, 149, 150]. In addition to sensitization of existing visceral neurons, an increase in the number of sensory afferents has been found in the endometrium of women with endometriosis [123].

This highlights the complexity of mechanisms contributing to CPP, and to build on our findings, we need to take the knowledge gained in healthy neuron experiments and combine it with our mouse models of endometriosis. Further understanding the long-term changes in neuronal

sensitivity induced by endometriosis and combining it with the acute affects generated by PF, will give us a more complete understanding of how these mechanisms interact in chronic disease to drive CPP.

7.4 Therapeutic strategies for the treatment of endometriosis associated CPP

7.4.1 Modulation of peripheral sensitization by targeting membrane channels and receptors

Various membrane receptors and ion channels contribute to sensory afferent hypersensitivity including voltage gated sodium channels (Na_V), voltage gated calcium channels (Ca_V), purinergic ion channels and cannabinoid receptors [164]. Modulation of ion channels expressed within sensory neurons innervating visceral organs, such as the colon and the bladder, has shown to be a promising approach in the treatment of CPP associated with both IBS and OAB [142, 161, 163, 206, 305, 333, 366]. In Chapter 4, we explored this concept by targeting peripheral ion channels to alter the responsiveness of healthy pelvic vaginal afferents. Within this chapter, we demonstrated how pharmacological modulation of Na_V channels within the vagina could alter vaginal nociceptive signalling. This chapter was important as it uncovered the ability to modulate sensory signals from the vagina, by targeting the first step in the pain pathway, the peripheral sensory afferents [220]. Translating this to endometriosis associated vaginal pain, the results presented in Chapter 5, using selective inhibitors of $Na_V1.7$ channels, suggest that similar approach may be beneficial in endometriosis. It will be important to determine whether there is a similar role for $Na_V1.7$ in endometriosis associated pain originating from other visceral organs such as the colon or the bladder, which also express high levels of $Na_V1.7$ in associated DRG neurons [285, 305]. In addition, further understanding other ion channels and receptors that may be involved in endometriosis associated pain in these visceral organs would help uncover additional therapeutic targets.

7.4.2 Targeting the inflammatory environment in the PF to treat CPP

Direct targeting of individual cytokines in the PF of endometriosis patients has been attempted to control pain, however, has not had much success. For example, clinical trials targeting the elevated levels of TNFα, which is suggested to be associated with pain, failed to reduce dysmenorrhoea, dyspareunia or pelvic tenderness in women with endometriosis [443]. In comparison, indirect targeting of inflammatory mediators within the PF with antioxidants has shown more promise [103]. It is thought that by targeting oxidative stress within the PF of women with endometriosis (see Chapter 1) using antioxidants will ultimately reduce inflammatory mediators

within the PF that are thought to directly activate sensory neurons. Interestingly, vitamin E and C significantly reduced PF levels of RANTES, IL-6 and MCP-1 in women with endometriosis and/or infertility and also led to a reduction in pelvic pain scores and dyspareunia [103]. More recently, a similar study recruiting endometriosis only patients saw a reduction in pelvic pain, dysmenorrhea, and dyspareunia in response to vitamin E and C, although specific inflammatory mediators were not measured [444]. Although there has not been success in direct targeting of individual factors within the PF, the results seen with antioxidants and related reduction in inflammatory mediators are promising. While our studies focus on CPP in endometriosis, the results described in our studies may also help understand CPP developed in other inflammatory conditions like those mentioned above and similar treatments may also be translatable to these conditions.

7.5 Concluding remarks

In conclusion, the work presented in this thesis contributes two different pre-clinical mouse models of endometriosis and position them for vital research into CPP mechanisms in endometriosis. Both induction methods led to the successful development of endometrial lesions and, importantly, induced indications of spontaneous and evoked pain across multiple visceral organs including the bladder, colon, and vagina. The differences in endometriosis induction methods between the two models may stimulate alternative disease progression and ultimately represent distinctive mechanisms underlying the heterogenous disease that develops in women. Using these models, we were able to illustrate the development of peripheral sensory hypersensitivity of vaginal and bladder afferents. Moreover, we showed that inhibiting key ion channels, governing the function of these peripheral sensory afferents, was an effective strategy to revert hypersensitivity and CPP in endometriosis. We were also able to demonstrate a role for the altered PF in endometriosis in visceral-innervating sensory neuron function, identifying key neuronal pathways which may drive CPP. Ultimately, the research presented in this thesis contributes to future research in endometriosis associated CPP and has uncovered potential therapeutic avenues for the treatment of CPP in endometriosis.

CHAPTER 8: REFERENCES

1. Martucci, K.T. and S.C. Mackey, *Neuroimaging of Pain: Human Evidence and Clinical Relevance of Central Nervous System Processes and Modulation.* Anesthesiology, 2018. **128**(6): p. 1241-1254.
2. Merskey, H.E., *Classification of chronic pain: Descriptions of chronic pain syndromes and definitions of pain terms.* Pain, 1986.
3. Bonica, J.J. and J.F. Hoffman, *The Management of Pain with Special Emphasis on the Use of Analgesic Blocks in Diagnosis, Prognosis, and Therapy.* Anesthesia & Analgesia, 1954. **34**(5): p. 57-58.
4. Treede, R.-D., et al., *A classification of chronic pain for ICD-11.* PAIN, 2015. **156**(6).
5. Treede, R.-D., et al., *Chronic pain as a symptom or a disease: the IASP Classification of Chronic Pain for the International Classification of Diseases (ICD-11).* PAIN, 2019. **160**(1).
6. IASP, *Classification of Chronic Pain: Description of Chronic Pain Syndromes and Definition of Pain Terms. Second Edition.*, H. Merskey. and N. Bogduk., Editors. 2011, IASP Press: https://www.iasp-pain.org/publications/free-ebooks/classification-of-chronic-pain-second-edition-revised/.
7. Goldberg, D.S. and S.J. McGee, *Pain as a global public health priority.* BMC public health, 2011. **11**: p. 770-770.
8. Jackson, T., et al., *A Systematic Review and Meta-Analysis of the Global Burden of Chronic Pain Without Clear Etiology in Low- and Middle-Income Countries: Trends in Heterogeneous Data and a Proposal for New Assessment Methods.* Anesthesia & Analgesia, 2016. **123**(3).
9. Breivik, H., et al., *Survey of chronic pain in Europe: prevalence, impact on daily life, and treatment.* Eur J Pain, 2006. **10**(4): p. 287-333.
10. Pitcher, M.H., et al., *Prevalence and Profile of High-Impact Chronic Pain in the United States.* The journal of pain, 2019. **20**(2): p. 146-160.
11. Clauw, D.J., et al., *Reframing chronic pain as a disease, not a symptom: rationale and implications for pain management.* Postgraduate Medicine, 2019. **131**(3): p. 185-198.
12. Turk, D.C., H.D. Wilson, and A. Cahana, *Treatment of chronic non-cancer pain.* The Lancet, 2011. **377**(9784): p. 2226-2235.
13. Manchikanti, L. and A. Singh, *Therapeutic opioids: a ten-year perspective on the complexities and complications of the escalating use, abuse, and nonmedical use of opioids.* Pain physician, 2008. **11**(2 Suppl): p. S63-S88.
14. Raffaeli, W. and E. Arnaudo, *Pain as a disease: an overview.* Journal of pain research, 2017. **10**: p. 2003-2008.
15. Fillingim, R.B., et al., *Sex, gender, and pain: a review of recent clinical and experimental findings.* The journal of pain, 2009. **10**(5): p. 447-485.
16. Fayaz, A., et al., *Prevalence of chronic pain in the UK: a systematic review and meta-analysis of population studies.* BMJ open, 2016. **6**(6): p. e010364-e010364.
17. Mills, S.E.E., K.P. Nicolson, and B.H. Smith, *Chronic pain: a review of its epidemiology and associated factors in population-based studies.* British journal of anaesthesia, 2019. **123**(2): p. e273-e283.
18. Gerdle, B., et al., *Prevalence of widespread pain and associations with work status: a population study.* BMC musculoskeletal disorders, 2008. **9**: p. 102-102.
19. Mogil, J.S., *Sex differences in pain and pain inhibition: multiple explanations of a controversial phenomenon.* Nature Reviews Neuroscience, 2012. **13**(12): p. 859-866.
20. Pagé, M.G., et al., *As if one pain problem was not enough: prevalence and patterns of coexisting chronic pain conditions and their impact on treatment outcomes.* Journal of pain research, 2018. **11**: p. 237-254.
21. Ahangari, A., *Prevalence of chronic pelvic pain among women: an updated review.* Pain Physician, 2014. **17**(2): p. E141-7.
22. Vincent, K., *Chronic pelvic pain in women.* Postgrad Med J, 2009. **85**(999): p. 24-9.

23. Andrews, J., et al., *AHRQ Comparative Effectiveness Reviews*, in *Noncyclic Chronic Pelvic Pain Therapies for Women: Comparative Effectiveness*. 2012, Agency for Healthcare Research and Quality (US): Rockville (MD).
24. Gordon, H.G., et al., *When pain is not the whole story: Presenting symptoms of women with endometriosis.* Aust N Z J Obstet Gynaecol, 2022.
25. Aredo, J.V., et al., *Relating Chronic Pelvic Pain and Endometriosis to Signs of Sensitization and Myofascial Pain and Dysfunction.* Seminars in reproductive medicine, 2017. **35**(1): p. 88-97.
26. Schomacker, M.L., et al., *Is endometriosis associated with irritable bowel syndrome? A cross-sectional study.* Eur J Obstet Gynecol Reprod Biol, 2018. **231**: p. 65-69.
27. Jess, T., et al., *Increased risk of inflammatory bowel disease in women with endometriosis: a nationwide Danish cohort study.* Gut, 2012. **61**(9): p. 1279-83.
28. Simoens, S., L. Hummelshoj, and T. D'Hooghe, *Endometriosis: cost estimates and methodological perspective.* Hum Reprod Update, 2007. **13**(4): p. 395-404.
29. Rogers, P.A.W., et al., *Research Priorities for Endometriosis.* Reproductive sciences (Thousand Oaks, Calif.), 2017. **24**(2): p. 202-226.
30. Nnoaham, K.E., et al., *Impact of endometriosis on quality of life and work productivity: a multicenter study across ten countries.* Fertil Steril, 2011. **96**(2): p. 366-373 e8.
31. Adamson, G., S. Kennedy, and L. Hummelshoj, *Creating solutions in endometriosis: Global collaboration through the World Endometriosis Research Foundation*. Vol. 2. 2010. 3-6.
32. Ballard, K.D., et al., *Can symptomatology help in the diagnosis of endometriosis? Findings from a national case-control study--Part 1.* BJOG, 2008. **115**(11): p. 1382-91.
33. Porpora, M.G., et al., *Correlation between endometriosis and pelvic pain.* J Am Assoc Gynecol Laparosc, 1999. **6**(4): p. 429-34.
34. Shakiba, K., et al., *Surgical treatment of endometriosis: a 7-year follow-up on the requirement for further surgery.* Obstet Gynecol, 2008. **111**(6): p. 1285-92.
35. Abbott, J., et al., *Laparoscopic excision of endometriosis: a randomized, placebo-controlled trial.* Fertil Steril, 2004. **82**(4): p. 878-84.
36. Hsu, A.L., et al., *Relating pelvic pain location to surgical findings of endometriosis.* Obstet Gynecol, 2011. **118**(2 Pt 1): p. 223-30.
37. Schliep, K.C., et al., *Pain typology and incident endometriosis.* Hum Reprod, 2015. **30**(10): p. 2427-38.
38. Surrey, E.S., et al., *Risk of Developing Comorbidities Among Women with Endometriosis: A Retrospective Matched Cohort Study.* Journal of Women's Health (15409996), 2018. **27**(9): p. 1114-1123.
39. Giudice, L.C. and L.C. Kao, *Endometriosis.* Lancet, 2004. **364**(9447): p. 1789-99.
40. Sampson, J.A., *Peritoneal endometriosis due to the menstrual dissemination of endometrial tissue into the peritoneal cavity.* American Journal of Obstetrics and Gynecology, 1927. **14**(4): p. 422-469.
41. Halme, J., et al., *Retrograde menstruation in healthy women and in patients with endometriosis.* Obstet Gynecol, 1984. **64**(2): p. 151-4.
42. O, D.F., et al., *The Presence of Endometrial Cells in Peritoneal Fluid of Women With and Without Endometriosis.* Reprod Sci, 2017. **24**(2): p. 242-251.
43. Kruitwagen, R.F., et al., *Endometrial epithelial cells in peritoneal fluid during the early follicular phase.* Fertil Steril, 1991. **55**(2): p. 297-303.
44. Tal, A., et al., *Endometrial cells contribute to preexisting endometriosis lesions in a mouse model of retrograde menstruationdagger.* Biol Reprod, 2019. **100**(6): p. 1453-1460.
45. Liu, D.T. and A. Hitchcock, *Endometriosis: its association with retrograde menstruation, dysmenorrhoea and tubal pathology.* Br J Obstet Gynaecol, 1986. **93**(8): p. 859-62.
46. Critchley, H.O., et al., *The endocrinology of menstruation--a role for the immune system.* Clin Endocrinol (Oxf), 2001. **55**(6): p. 701-10.
47. Symons, L.K., et al., *The Immunopathophysiology of Endometriosis.* Trends Mol Med, 2018. **24**(9): p. 748-762.
48. Halme, J., S. Becker, and R. Wing, *Accentuated cyclic activation of peritoneal macrophages in patients with endometriosis.* Am J Obstet Gynecol, 1984. **148**(1): p. 85-90.

49. Banu, S.K., et al., *Cyclooxygenase-2 regulates survival, migration, and invasion of human endometriotic cells through multiple mechanisms.* Endocrinology, 2008. **149**(3): p. 1180-9.
50. Amaral, V.F., et al., *Positive correlation between serum and peritoneal fluid CA-125 levels in women with pelvic endometriosis.* Sao Paulo Med J, 2006. **124**(4): p. 223-7.
51. Chuang, P.C., et al., *Inhibition of CD36-dependent phagocytosis by prostaglandin E2 contributes to the development of endometriosis.* Am J Pathol, 2010. **176**(2): p. 850-60.
52. Oosterlynck, D.J., et al., *The natural killer activity of peritoneal fluid lymphocytes is decreased in women with endometriosis.* Fertil Steril, 1992. **58**(2): p. 290-5.
53. Dmowski, W.P., H. Gebel, and D.P. Braun, *Decreased apoptosis and sensitivity to macrophage mediated cytolysis of endometrial cells in endometriosis.* Hum Reprod Update, 1998. **4**(5): p. 696-701.
54. Laux-Biehlmann, A., T. d'Hooghe, and T.M. Zollner, *Menstruation pulls the trigger for inflammation and pain in endometriosis.* Trends Pharmacol Sci, 2015. **36**(5): p. 270-6.
55. Sourial, S., N. Tempest, and D.K. Hapangama, *Theories on the pathogenesis of endometriosis.* Int J Reprod Med, 2014. **2014**: p. 179515.
56. Signorile, P.G., et al., *Endometriosis: A Retrospective Analysis of Clinical Data from a Cohort of 4,083 Patients, With Focus on Symptoms.* In Vivo, 2022. **36**(2): p. 874-883.
57. Chung, M.K., R.P. Chung, and D. Gordon, *Interstitial cystitis and endometriosis in patients with chronic pelvic pain: The "Evil Twins" syndrome.* JSLS : Journal of the Society of Laparoendoscopic Surgeons, 2005. **9**(1): p. 25-29.
58. Tirlapur, S.A., et al., *The 'evil twin syndrome' in chronic pelvic pain: a systematic review of prevalence studies of bladder pain syndrome and endometriosis.* Int J Surg, 2013. **11**(3): p. 233-7.
59. Hickey, M., K. Ballard, and C. Farquhar, *Endometriosis.* BMJ, 2014. **348**: p. g1752.
60. Chapron, C., et al., *Rethinking mechanisms, diagnosis and management of endometriosis.* Nat Rev Endocrinol, 2019. **15**(11): p. 666-682.
61. Nisenblat, V., et al., *Combination of the non-invasive tests for the diagnosis of endometriosis.* Cochrane Database Syst Rev, 2016. **7**: p. Cd012281.
62. Riazi, H., et al., *Clinical diagnosis of pelvic endometriosis: a scoping review.* BMC Womens Health, 2015. **15**: p. 39.
63. Pugsley, Z. and K. Ballard, *Management of endometriosis in general practice: the pathway to diagnosis.* Br J Gen Pract, 2007. **57**(539): p. 470-6.
64. Guerriero, S., et al., *Transvaginal ultrasound vs magnetic resonance imaging for diagnosing deep infiltrating endometriosis: systematic review and meta-analysis.* Ultrasound Obstet Gynecol, 2018. **51**(5): p. 586-595.
65. Van den Bosch, T. and D. Van Schoubroeck, *Ultrasound diagnosis of endometriosis and adenomyosis: State of the art.* Best Pract Res Clin Obstet Gynaecol, 2018. **51**: p. 16-24.
66. Zondervan, K.T., C.M. Becker, and S.A. Missmer, *Endometriosis.* N Engl J Med, 2020. **382**(13): p. 1244-1256.
67. Hadfield, R., et al., *Delay in the diagnosis of endometriosis: a survey of women from the USA and the UK.* Hum Reprod, 1996. **11**(4): p. 878-80.
68. Husby, G.K., R.S. Haugen, and M.H. Moen, *Diagnostic delay in women with pain and endometriosis.* Acta Obstet Gynecol Scand, 2003. **82**(7): p. 649-53.
69. Arruda, M.S., et al., *Time elapsed from onset of symptoms to diagnosis of endometriosis in a cohort study of Brazilian women.* Hum Reprod, 2003. **18**(4): p. 756-9.
70. *Classification of endometriosis. The American Fertility Society.* Fertil Steril, 1979. **32**(6): p. 633-4.
71. *Revised American Society for Reproductive Medicine classification of endometriosis: 1996.* Fertil Steril, 1997. **67**(5): p. 817-21.
72. Vercellini, P., et al., *Association between endometriosis stage, lesion type, patient characteristics and severity of pelvic pain symptoms: a multivariate analysis of over 1000 patients.* Hum Reprod, 2007. **22**(1): p. 266-71.
73. Adamson, G.D., *Endometriosis classification: an update.* Curr Opin Obstet Gynecol, 2011. **23**(4): p. 213-20.
74. Johnson, N.P., et al., *World Endometriosis Society consensus on the classification of endometriosis.* Hum Reprod, 2017. **32**(2): p. 315-324.

75. Chapron, C., et al., *Anatomical distribution of deeply infiltrating endometriosis: surgical implications and proposition for a classification.* Human Reproduction, 2003. **18**(1): p. 157-161.
76. Stegmann, B.J., et al., *Using location, color, size, and depth to characterize and identify endometriosis lesions in a cohort of 133 women.* Fertil Steril, 2008. **89**(6): p. 1632-6.
77. Sutton, C.J., et al., *Prospective, randomized, double-blind, controlled trial of laser laparoscopy in the treatment of pelvic pain associated with minimal, mild, and moderate endometriosis.* Fertil Steril, 1994. **62**(4): p. 696-700.
78. Morotti, M., K. Vincent, and C.M. Becker, *Mechanisms of pain in endometriosis.* Eur J Obstet Gynecol Reprod Biol, 2017. **209**: p. 8-13.
79. Patel, B.G., et al., *Pathogenesis of endometriosis: Interaction between Endocrine and inflammatory pathways.* Best Pract Res Clin Obstet Gynaecol, 2018. **50**: p. 50-60.
80. Zheng, P., et al., *Research on central sensitization of endometriosis-associated pain: a systematic review of the literature.* J Pain Res, 2019. **12**: p. 1447-1456.
81. Barcz, E., P. Kaminski, and L. Marianowski, *Role of cytokines in pathogenesis of endometriosis.* Med Sci Monit, 2000. **6**(5): p. 1042-6.
82. Donnez, J., et al., *Vascular endothelial growth factor (VEGF) in endometriosis.* Hum Reprod, 1998. **13**(6): p. 1686-90.
83. Sacco, K., et al., *The role of prostaglandin E2 in endometriosis.* Gynecol Endocrinol, 2012. **28**(2): p. 134-8.
84. Králíčková, M. and V. Vetvicka, *Immunological aspects of endometriosis: a review.* Annals of translational medicine, 2015. **3**(11): p. 153-153.
85. Reeh, P.W. and K.H. Steen, *Tissue acidosis in nociception and pain.* Prog Brain Res, 1996. **113**: p. 143-51.
86. Holzer, P., *Acid sensing by visceral afferent neurones.* Acta Physiol (Oxf), 2011. **201**(1): p. 63-75.
87. Tokushige, N., et al., *Nerve fibres in peritoneal endometriosis.* Human Reproduction, 2006. **21**(11): p. 3001-3007.
88. Brierley, S.M. and D.R. Linden, *Neuroplasticity and dysfunction after gastrointestinal inflammation.* Nat Rev Gastroenterol Hepatol, 2014. **11**(10): p. 611-27.
89. Chiu, I.M., C.A. von Hehn, and C.J. Woolf, *Neurogenic inflammation and the peripheral nervous system in host defense and immunopathology.* Nature Neuroscience, 2012. **15**: p. 1063.
90. Bajaj, P., et al., *Endometriosis is associated with central sensitization: a psychophysical controlled study.* J Pain, 2003. **4**(7): p. 372-80.
91. Woolf, C.J., *Central sensitization: implications for the diagnosis and treatment of pain.* Pain, 2011. **152**(3 Suppl): p. S2-15.
92. Ge, P., et al., *Linaclotide treatment reduces endometriosis-associated vaginal hyperalgesia and mechanical allodynia through viscerovisceral cross-talk.* Pain, 2019.
93. Berbic, M. and I.S. Fraser, *Immunology of normal and abnormal menstruation.* Womens Health (Lond), 2013. **9**(4): p. 387-95.
94. Brosens, I.A., *Endometriosis—A disease because it is characterized by bleeding.* American Journal of Obstetrics and Gynecology, 1997. **176**(2): p. 263-267.
95. Burney, R.O. and R.B. Lathi, *Menstrual bleeding from an endometriotic lesion.* Fertil Steril, 2009. **91**(5): p. 1926-7.
96. Scholl, B., et al., *Correlation between symptoms of pain and peritoneal fluid inflammatory cytokine concentrations in endometriosis.* Gynecol Endocrinol, 2009. **25**(11): p. 701-6.
97. Bedaiwy, M.A., et al., *Prediction of endometriosis with serum and peritoneal fluid markers: a prospective controlled trial.* Hum Reprod, 2002. **17**(2): p. 426-31.
98. Ryan, I.P., et al., *Interleukin-8 concentrations are elevated in peritoneal fluid of women with endometriosis.* Fertil Steril, 1995. **63**(4): p. 929-32.
99. Liang, Y., et al., *Villainous role of estrogen in macrophage-nerve interaction in endometriosis.* Reprod Biol Endocrinol, 2018. **16**(1): p. 122.
100. Wu, J., et al., *Macrophage and nerve interaction in endometriosis.* J Neuroinflammation, 2017. **14**(1): p. 53.

101. Zhou, J., et al., *Peritoneal Fluid Cytokines Reveal New Insights of Endometriosis Subphenotypes.* Int J Mol Sci, 2020. **21**(10): p. 3515.
102. Santulli, P., et al., *Protein oxidative stress markers in peritoneal fluids of women with deep infiltrating endometriosis are increased.* Hum Reprod, 2015. **30**(1): p. 49-60.
103. Santanam, N., et al., *Antioxidant supplementation reduces endometriosis-related pelvic pain in humans.* Transl Res, 2013. **161**(3): p. 189-95.
104. Wright, K.R., B. Mitchell, and N. Santanam, *Redox regulation of microRNAs in endometriosis-associated pain.* Redox Biol, 2017. **12**: p. 956-966.
105. Ray, K., et al., *Oxidation-sensitive nociception involved in endometriosis-associated pain.* Pain, 2015. **156**(3): p. 528-39.
106. Asante, A. and R.N. Taylor, *Endometriosis: the role of neuroangiogenesis.* Annu Rev Physiol, 2011. **73**: p. 163-82.
107. Berkley, K.J., *A life of pelvic pain.* Physiol Behav, 2005. **86**(3): p. 272-80.
108. de Groat, W.C., D. Griffiths, and N. Yoshiimura, *Neural Control of the Lower Urinary Tract*, in *Comprehensive Physiology*. 2015. p. 327-396.
109. Grundy, L. and S.M. Brierley, *Cross-organ sensitization between the colon and bladder: to pee or not to pee?* Am J Physiol Gastrointest Liver Physiol, 2018. **314**(3): p. G301-g308.
110. Grundy, L., et al., *Chronic linaclotide treatment reduces colitis-induced neuroplasticity and reverses persistent bladder dysfunction.* JCI Insight, 2018. **3**(19): p. e121841.
111. Harrington, A.M., et al., *Sprouting of colonic afferent central terminals and increased spinal mitogen-activated protein kinase expression in a mouse model of chronic visceral hypersensitivity.* J Comp Neurol, 2012. **520**(10): p. 2241-55.
112. Harrington, A.M., et al., *Colonic afferent input and dorsal horn neuron activation differs between the thoracolumbar and lumbosacral spinal cord.* Am J Physiol Gastrointest Liver Physiol, 2019. **317**(3): p. G285-g303.
113. Weinstein, B.M., *Vessels and nerves: marching to the same tune.* Cell, 2005. **120**(3): p. 299-302.
114. Greaves, E., et al., *Estrogen receptor (ER) agonists differentially regulate neuroangiogenesis in peritoneal endometriosis via the repellent factor SLIT3.* Endocrinology, 2014. **155**(10): p. 4015-26.
115. McAllister, S.L., et al., *Endometriosis-induced vaginal hyperalgesia in the rat: role of the ectopic growths and their innervation.* Pain, 2009. **147**(1-3): p. 255-64.
116. Bulun, S.E., *Endometriosis.* N Engl J Med, 2009. **360**(3): p. 268-79.
117. Hammond, M.G., et al., *The effect of growth factors on the proliferation of human endometrial stromal cells in culture.* Am J Obstet Gynecol, 1993. **168**(4): p. 1131-6; discussion 1136-8.
118. Lin, Y.J., et al., *Neutrophils and macrophages promote angiogenesis in the early stage of endometriosis in a mouse model.* Endocrinology, 2006. **147**(3): p. 1278-86.
119. Shifren, J.L., et al., *Ovarian steroid regulation of vascular endothelial growth factor in the human endometrium: implications for angiogenesis during the menstrual cycle and in the pathogenesis of endometriosis.* J Clin Endocrinol Metab, 1996. **81**(8): p. 3112-8.
120. Nisolle, M., et al., *Morphometric study of the stromal vascularization in peritoneal endometriosis.* Fertil Steril, 1993. **59**(3): p. 681-4.
121. Skaper, S.D., *Neurotrophic Factors: An Overview.* Methods Mol Biol, 2018. **1727**: p. 1-17.
122. Yan, D., X. Liu, and S.W. Guo, *Nerve fibers and endometriotic lesions: partners in crime in inflicting pains in women with endometriosis.* Eur J Obstet Gynecol Reprod Biol, 2017. **209**: p. 14-24.
123. Tokushige, N., et al., *High density of small nerve fibres in the functional layer of the endometrium in women with endometriosis.* Hum Reprod, 2006. **21**(3): p. 782-7.
124. Wang, G., et al., *Rich innervation of deep infiltrating endometriosis.* Hum Reprod, 2009. **24**(4): p. 827-34.
125. McAllister, S.L., N. Dmitrieva, and K.J. Berkley, *Sprouted innervation into uterine transplants contributes to the development of hyperalgesia in a rat model of endometriosis.* PLoS One, 2012. **7**(2): p. e31758.
126. McKinnon, B., et al., *Endometriosis-associated nerve fibers, peritoneal fluid cytokine concentrations, and pain in endometriotic lesions from different locations.* Fertil Steril, 2012. **97**(2): p. 373-80.

127. Mechsner, S., et al., *A pilot study to evaluate the clinical relevance of endometriosis-associated nerve fibers in peritoneal endometriotic lesions.* Fertil Steril, 2009. **92**(6): p. 1856-61.
128. Kajitani, T., et al., *Possible involvement of nerve growth factor in dysmenorrhea and dyspareunia associated with endometriosis.* Endocr J, 2013. **60**(10): p. 1155-64.
129. Morotti, M., et al., *Peripheral changes in endometriosis-associated pain.* Hum Reprod Update, 2014. **20**(5): p. 717-36.
130. Miyashita, M., et al., *Expression of Nerve Injury-Induced Protein1 (Ninj1) in Endometriosis.* Reprod Sci, 2019. **26**(8): p. 1105-1110.
131. Tokushige, N., et al., *Effects of hormonal treatment on nerve fibers in endometrium and myometrium in women with endometriosis.* Fertil Steril, 2008. **90**(5): p. 1589-98.
132. Chao, M.V., *Neurotrophins and their receptors: a convergence point for many signalling pathways.* Nat Rev Neurosci, 2003. **4**(4): p. 299-309.
133. Anaf, V., et al., *Hyperalgesia, nerve infiltration and nerve growth factor expression in deep adenomyotic nodules, peritoneal and ovarian endometriosis.* Hum Reprod, 2002. **17**(7): p. 1895-900.
134. Bjorling, D.E., et al., *Modulation of nerve growth factor in peripheral organs by estrogen and progesterone.* Neuroscience, 2002. **110**(1): p. 155-67.
135. Wang, Y., *The functional regulation of TRPV1 and its role in pain sensitization.* Neurochem Res, 2008. **33**(10): p. 2008-12.
136. Bohonyi, N., et al., *Local upregulation of transient receptor potential ankyrin 1 and transient receptor potential vanilloid 1 ion channels in rectosigmoid deep infiltrating endometriosis.* Mol Pain, 2017. **13**: p. 1744806917705564.
137. Anaf, V., et al., *Increased nerve density in deep infiltrating endometriotic nodules.* Gynecol Obstet Invest, 2011. **71**(2): p. 112-7.
138. Wang, G., et al., *Hyperinnervation in intestinal deep infiltrating endometriosis.* J Minim Invasive Gynecol, 2009. **16**(6): p. 713-9.
139. Tulandi, T., A. Felemban, and M.F. Chen, *Nerve fibers and histopathology of endometriosis-harboring peritoneum.* J Am Assoc Gynecol Laparosc, 2001. **8**(1): p. 95-8.
140. Anaf, V., et al., *Relationship between endometriotic foci and nerves in rectovaginal endometriotic nodules.* Hum Reprod, 2000. **15**(8): p. 1744-50.
141. Arnold, J., et al., *Imbalance between sympathetic and sensory innervation in peritoneal endometriosis.* Brain Behav Immun, 2012. **26**(1): p. 132-41.
142. Sadeghi, M., et al., *Contribution of membrane receptor signalling to chronic visceral pain.* Int J Biochem Cell Biol, 2018. **98**: p. 10-23.
143. Aziz, Q., *Complementary alternative medicine and autonomic nervous system and functional bowel disorders.* Autonomic Neuroscience, 2013. **177**(1): p. 42-43.
144. Heitkemper, M., et al., *Evidence for autonomic nervous system imbalance in women with irritable bowel syndrome.* Dig Dis Sci, 1998. **43**(9): p. 2093-8.
145. Pluchino, N., et al., *Estrogen receptor-alpha immunoreactivity predicts symptom severity and pain recurrence in deep endometriosis.* Fertil Steril, 2020. **113**(6): p. 1224-1231 e1.
146. Ma, W. and R. Quirion, *Does COX2-dependent PGE2 play a role in neuropathic pain?* Neurosci Lett, 2008. **437**(3): p. 165-9.
147. van der Kleij, H.P.M., P. Forsythe, and J. Bienenstock, *Autonomic Neuroimmunology*, in *Encyclopedia of Neuroscience*, L.R. Squire, Editor. 2009, Academic Press: Oxford. p. 1003-1008.
148. Bacci, M., et al., *Macrophages are alternatively activated in patients with endometriosis and required for growth and vascularization of lesions in a mouse model of disease.* Am J Pathol, 2009. **175**(2): p. 547-56.
149. Straub, R.H. and C. Schradin, *Chronic inflammatory systemic diseases: An evolutionary trade-off between acutely beneficial but chronically harmful programs.* Evol Med Public Health, 2016. **2016**(1): p. 37-51.
150. Bordman, R. and B. Jackson, *Below the belt: approach to chronic pelvic pain.* Can Fam Physician, 2006. **52**(12): p. 1556-62.
151. Grundy, L., A. Erickson, and S.M. Brierley, *Visceral Pain.* Annu Rev Physiol, 2019. **81**: p. 261-284.

152. Iyengar, S., M.H. Ossipov, and K.W. Johnson, *The role of calcitonin gene-related peptide in peripheral and central pain mechanisms including migraine.* Pain, 2017. **158**(4): p. 543-559.
153. St-Jacques, B. and W. Ma, *Peripheral prostaglandin E2 prolongs the sensitization of nociceptive dorsal root ganglion neurons possibly by facilitating the synthesis and anterograde axonal trafficking of EP4 receptors.* Exp Neurol, 2014. **261**: p. 354-66.
154. Neziri, A.Y., et al., *Correlation between altered central pain processing and concentration of peritoneal fluid inflammatory cytokines in endometriosis patients with chronic pelvic pain.* Reg Anesth Pain Med, 2014. **39**(3): p. 181-4.
155. Overton, C., et al., *Peritoneal fluid cytokines and the relationship with endometriosis and pain.* Hum Reprod, 1996. **11**(2): p. 380-6.
156. Hughes, P.A., et al., *Sensory neuro-immune interactions differ between irritable bowel syndrome subtypes.* Gut, 2013. **62**(10): p. 1456-65.
157. Castro, J., et al., *Cyclic analogues of alpha-conotoxin Vc1.1 inhibit colonic nociceptors and provide analgesia in a mouse model of chronic abdominal pain.* Br J Pharmacol, 2018. **175**(12): p. 2384-2398.
158. Castro, J., et al., *Linaclotide inhibits colonic nociceptors and relieves abdominal pain via guanylate cyclase-C and extracellular cyclic guanosine 3',5'-monophosphate.* Gastroenterology, 2013. **145**(6): p. 1334-46 e1-11.
159. Castro, J., et al., *Activation of pruritogenic TGR5, MrgprA3, and MrgprC11 on colon-innervating afferents induces visceral hypersensitivity.* JCI Insight, 2019. **4**(20).
160. Sadeghi, M., et al., *Structure-Activity Studies Reveal the Molecular Basis for GABAB-Receptor Mediated Inhibition of High Voltage-Activated Calcium Channels by alpha-Conotoxin Vc1.1.* ACS Chem Biol, 2018. **13**(6): p. 1577-1587.
161. Salvatierra, J., et al., *NaV1.1 inhibition can reduce visceral hypersensitivity.* JCI Insight, 2018. **3**(11).
162. Grundy, L., A. Caldwell, and S.M. Brierley, *Mechanisms Underlying Overactive Bladder and Interstitial Cystitis/Painful Bladder Syndrome.* Front Neurosci, 2018. **12**: p. 931.
163. Michel, M.C. and Y. Igawa, *Therapeutic targets for overactive bladder other than smooth muscle.* Expert Opin Ther Targets, 2015. **19**(5): p. 687-705.
164. de Carvalho Rocha, H.A., et al., *Main ion channels and receptors associated with visceral hypersensitivity in irritable bowel syndrome.* Annals of gastroenterology, 2014. **27**(3): p. 200-206.
165. Basbaum, A.I., et al., *Cellular and molecular mechanisms of pain.* Cell, 2009. **139**(2): p. 267-84.
166. Tominaga, M. and D. Julius, *Capsaicin receptor in the pain pathway.* Jpn J Pharmacol, 2000. **83**(1): p. 20-4.
167. Lian, Y.L., et al., *Elevated expression of transient receptor potential vanilloid type 1 in dorsal root ganglia of rats with endometriosis.* Mol Med Rep, 2017. **16**(2): p. 1920-1926.
168. Greaves, E., et al., *Elevated peritoneal expression and estrogen regulation of nociceptive ion channels in endometriosis.* The Journal of clinical endocrinology and metabolism, 2014. **99**(9): p. E1738-E1743.
169. Rocha, M.G., et al., *TRPV1 expression on peritoneal endometriosis foci is associated with chronic pelvic pain.* Reprod Sci, 2011. **18**(6): p. 511-5.
170. Ma, F., L. Zhang, and K.N. Westlund, *Reactive oxygen species mediate TNFR1 increase after TRPV1 activation in mouse DRG neurons.* Mol Pain, 2009. **5**: p. 31.
171. Kajihara, H., et al., *New insights into the pathophysiology of endometriosis: from chronic inflammation to danger signal.* Gynecol Endocrinol, 2011. **27**(2): p. 73-9.
172. Berkley, K.J., A.J. Rapkin, and R.E. Papka, *The pains of endometriosis.* Science, 2005. **308**(5728): p. 1587-9.
173. Fuentes, I.M. and J.A. Christianson, *The Influence of Early Life Experience on Visceral Pain.* Front Syst Neurosci, 2018. **12**: p. 2.
174. Pierce, A.N. and J.A. Christianson, *Stress and chronic pelvic pain.* Prog Mol Biol Transl Sci, 2015. **131**: p. 509-35.
175. Pierce, A.N., et al., *Vaginal hypersensitivity and hypothalamic-pituitary-adrenal axis dysfunction as a result of neonatal maternal separation in female mice.* Neuroscience, 2014. **263**: p. 216-30.

176. Pierce, A.N., et al., *Neonatal vaginal irritation results in long-term visceral and somatic hypersensitivity and increased hypothalamic-pituitary-adrenal axis output in female mice.* Pain, 2015. **156**(10): p. 2021-31.
177. Anaf, V., et al., *Pain, mast cells, and nerves in peritoneal, ovarian, and deep infiltrating endometriosis.* Fertil Steril, 2006. **86**(5): p. 1336-43.
178. Schulke, L., et al., *Dendritic cell populations in the eutopic and ectopic endometrium of women with endometriosis.* Hum Reprod, 2009. **24**(7): p. 1695-703.
179. Ji, R.-R., et al., *Neuroinflammation and Central Sensitization in Chronic and Widespread Pain.* Anesthesiology, 2018. **129**(2): p. 343-366.
180. Koelbaek Johansen, M., et al., *Generalised muscular hyperalgesia in chronic whiplash syndrome.* Pain, 1999. **83**(2): p. 229-34.
181. Harris, R.E., et al., *Elevated insular glutamate in fibromyalgia is associated with experimental pain.* Arthritis Rheum, 2009. **60**(10): p. 3146-52.
182. Nijs, J., et al., *How to explain central sensitization to patients with 'unexplained' chronic musculoskeletal pain: practice guidelines.* Man Ther, 2011. **16**(5): p. 413-8.
183. Li, T., et al., *Endometriosis alters brain electrophysiology, gene expression and increases pain sensitization, anxiety, and depression in female mice.* Biol Reprod, 2018. **99**(2): p. 349-359.
184. Vincent, K., et al., *Dysmenorrhoea is associated with central changes in otherwise healthy women.* Pain, 2011. **152**(9): p. 1966-1975.
185. As-Sanie, S., et al., *Functional connectivity is associated with altered brain chemistry in women with endometriosis-associated chronic pelvic pain.* The Journal of Pain, 2016. **17**(1): p. 1-13.
186. Nagabukuro, H. and K.J. Berkley, *Influence of endometriosis on visceromotor and cardiovascular responses induced by vaginal distention in the rat.* Pain, 2007. **132 Suppl 1**: p. S96-103.
187. Chung, M.K., et al., *The evil twins of chronic pelvic pain syndrome: endometriosis and interstitial cystitis.* JSLS, 2002. **6**(4): p. 311-4.
188. Pezzone, M.A., R. Liang, and M.O. Fraser, *A model of neural cross-talk and irritation in the pelvis: implications for the overlap of chronic pelvic pain disorders.* Gastroenterology, 2005. **128**(7): p. 1953-64.
189. Wesselmann, U., *Neurogenic inflammation and chronic pelvic pain.* World J Urol, 2001. **19**(3): p. 180-5.
190. Winnard, K., et al., *Cross-system viscerovisceral interactions: influence of acute inflammation of uterus and colon on the bladder via the hypogastric nerve.* Program no. 742.1. 2004, 2004.
191. Winnard, K.P., N. Dmitrieva, and K.J. Berkley, *Cross-organ interactions between reproductive, gastrointestinal, and urinary tracts: modulation by estrous stage and involvement of the hypogastric nerve.* Am J Physiol Regul Integr Comp Physiol, 2006. **291**(6): p. R1592-601.
192. Qin, C., et al., *Cross-organ sensitization of lumbosacral spinal neurons receiving urinary bladder input in rats with inflamed colon.* Gastroenterology, 2005. **129**(6): p. 1967-78.
193. Lamb, K., et al., *Experimental colitis in mice and sensitization of converging visceral and somatic afferent pathways.* Am J Physiol Gastrointest Liver Physiol, 2006. **290**(3): p. G451-7.
194. Dmitrieva, N., O.L. Johnson, and K.J. Berkley, *Bladder inflammation and hypogastric neurectomy influence uterine motility in the rat.* Neurosci Lett, 2001. **313**(1-2): p. 49-52.
195. Berkley, K.J., et al., *Endometriosis-induced vaginal hyperalgesia in the rat: effect of estropause, ovariectomy, and estradiol replacement.* Pain, 2007. **132 Suppl 1**: p. S150-9.
196. Giamberardino, M.A., et al., *Influence of endometriosis on pain behaviors and muscle hyperalgesia induced by a ureteral calculosis in female rats.* Pain, 2002. **95**(3): p. 247-57.
197. Fattori, V., et al., *Nonsurgical mouse model of endometriosis-associated pain that responds to clinically active drugs.* Pain, 2020. **161**(6): p. 1321-1331.
198. Costa, M., S.H. Brookes, and V. Zagorodnyuk, *How many kinds of visceral afferents?* Gut, 2004. **53 Suppl 2**: p. ii1-4.
199. Matalliotakis, M., et al., *Extra pelvic endometriosis: Retrospective analysis on 200 cases in two different countries.* Eur J Obstet Gynecol Reprod Biol, 2017. **217**: p. 34-37.

200. Howard, F.M., A.M. El-Minawi, and R.A. Sanchez, *Conscious pain mapping by laparoscopy in women with chronic pelvic pain.* Obstet Gynecol, 2000. **96**(6): p. 934-9.
201. Demco, L., *Mapping the source and character of pain due to endometriosis by patient-assisted laparoscopy.* The Journal of the American Association of Gynecologic Laparoscopists, 1998. **5**(3): p. 241-245.
202. Demco, L.A., *Pain referral patterns in the pelvis.* J Am Assoc Gynecol Laparosc, 2000. **7**(2): p. 181-3.
203. Jobling, P., et al., *Cervix stimulation evokes predominantly subthreshold synaptic responses in mouse thoracolumbar and lumbosacral superficial dorsal horn neurons.* J Sex Med, 2010. **7**(6): p. 2068-2076.
204. Christianson, J.A., et al., *Convergence of bladder and colon sensory innervation occurs at the primary afferent level.* Pain, 2007. **128**(3): p. 235-43.
205. Chaban, V.V., *Visceral sensory neurons that innervate both uterus and colon express nociceptive TRPv1 and P2X3 receptors in rats.* Ethn Dis, 2008. **18**(2 Suppl 2): p. S2-20-4.
206. Broad, L.M., et al., *TRP channels as emerging targets for pain therapeutics.* Expert Opin Ther Targets, 2009. **13**(1): p. 69-81.
207. Falcone, T. and R. Flyckt, *Clinical Management of Endometriosis.* Obstet Gynecol, 2018. **131**(3): p. 557-571.
208. Howard, F.M., *An evidence-based medicine approach to the treatment of endometriosis-associated chronic pelvic pain: placebo-controlled studies.* J Am Assoc Gynecol Laparosc, 2000. **7**(4): p. 477-88.
209. Guo, S.W., *Recurrence of endometriosis and its control.* Hum Reprod Update, 2009. **15**(4): p. 441-61.
210. Kitawaki, J., et al., *Endometriosis: the pathophysiology as an estrogen-dependent disease.* J Steroid Biochem Mol Biol, 2002. **83**(1-5): p. 149-55.
211. Slopien, R. and B. Meczekalski, *Aromatase inhibitors in the treatment of endometriosis.* Prz Menopauzalny, 2016. **15**(1): p. 43-7.
212. Kim, N.Y., et al., *The efficacy and tolerability of short-term low-dose estrogen-only add-back therapy during post-operative GnRH agonist treatment for endometriosis.* Eur J Obstet Gynecol Reprod Biol, 2011. **154**(1): p. 85-9.
213. Brown, J., et al., *Nonsteroidal anti-inflammatory drugs for pain in women with endometriosis.* Cochrane Database Syst Rev, 2017. **1**: p. Cd004753.
214. Allen, C., S. Hopewell, and A. Prentice, *Non-steroidal anti-inflammatory drugs for pain in women with endometriosis.* Cochrane Database Syst Rev, 2005(4): p. Cd004753.
215. Lamvu, G., et al., *Patterns of Prescription Opioid Use in Women With Endometriosis: Evaluating Prolonged Use, Daily Dose, and Concomitant Use With Benzodiazepines.* Obstet Gynecol, 2019. **133**(6): p. 1120-1130.
216. Kanouse, A.B. and P. Compton, *The epidemic of prescription opioid abuse, the subsequent rising prevalence of heroin use, and the federal response.* J Pain Palliat Care Pharmacother, 2015. **29**(2): p. 102-14.
217. Cheong, Y., et al., *Laparoscopic surgery for endometriosis: How often do we need to re-operate?* J Obstet Gynaecol, 2008. **28**(1): p. 82-5.
218. Wee-Stekly, W.-W., C.C.Y. Kew, and B.S.M. Chern, *Endometriosis: A review of the diagnosis and pain management.* Gynecology and Minimally Invasive Therapy, 2015. **4**(4): p. 106-109.
219. May, K.E., et al., *Peripheral biomarkers of endometriosis: a systematic review.* Hum Reprod Update, 2010. **16**(6): p. 651-74.
220. Castro, J., et al., *Pharmacological modulation of voltage-gated sodium (NaV) channels alters nociception arising from the female reproductive tract.* Pain, 2020.
221. Yoshino, O., et al., *Bradykinin system is involved in endometriosis-related pain through endothelin-1 production. .* European Journal of Pain, 2018. **22(3)**: p. 501-510.
222. Alvarez, P., O. Bogen, and J.D. Levine, *Role of nociceptor estrogen receptor GPR30 in a rat model of endometriosis pain.* Pain, 2014. **155**(12): p. 2680-6.
223. Dmitrieva, N., et al., *Endocannabinoid involvement in endometriosis.* Pain, 2010. **151**(3): p. 703-10.
224. Escudero-Lara, A., et al., *Disease-modifying effects of natural Delta9-tetrahydrocannabinol in endometriosis-associated pain.* Elife, 2020. **9**: p. e50356.

225. Horne, A.W., et al., *Repurposing dichloroacetate for the treatment of women with endometriosis.* Proc Natl Acad Sci U S A, 2019. **116**(51): p. 25389-25391.
226. Quereda, F., et al., *The effect of intraperitoneal interleukin-2 on surgically induced endometriosis in rats.* European Journal of Obstetrics & Gynecology and Reproductive Biology, 2008. **136**(2): p. 243-248.
227. Ingelmo, J.M.R., F. Quereda, and P. Acién, *Intraperitoneal and subcutaneous treatment of experimental endometriosis with recombinant human interferon-α-2b in a murine model.* Fertility and sterility, 1999. **71**(5): p. 907-911.
228. Malvezzi, H., et al., *Endometriosis: current challenges in modeling a multifactorial disease of unknown etiology.* J Transl Med, 2020. **18**(1): p. 311.
229. Nunez-Badinez, P., et al., *Preclinical models of endometriosis and interstitial cystitis/bladder pain syndrome: an Innovative Medicines Initiative-PainCare initiative to improve their value for translational research in pelvic pain.* Pain, 2021. **162**(9): p. 2349-2365.
230. Greaves, E., et al., *Relevant human tissue resources and laboratory models for use in endometriosis research.* Acta Obstet Gynecol Scand, 2017. **96**(6): p. 644-658.
231. Maddern, J., et al., *Pain in Endometriosis.* Frontiers in Cellular Neuroscience, 2020. **14**(335).
232. Braundmeier, A.G. and A.T. Fazleabas, *The non-human primate model of endometriosis: research and implications for fecundity.* Molecular human reproduction, 2009. **15**(10): p. 577-586.
233. Dick, E.J., Jr., et al., *Record review of baboons with histologically confirmed endometriosis in a large established colony.* J Med Primatol, 2003. **32**(1): p. 39-47.
234. D'Hooghe, T.M., et al., *Nonhuman primate models for translational research in endometriosis.* Reprod Sci, 2009. **16**(2): p. 152-61.
235. Langoi, D., et al., *Aromatase inhibitor treatment limits progression of peritoneal endometriosis in baboons.* Fertility and sterility, 2013. **99**(3): p. 656-662.e3.
236. Gashaw, I., et al., *Induced Endometriosis in the Baboon (Papio anubis) Increases the Expression of the Proangiogenic Factor CYR61 (CCN1) in Eutopic and Ectopic Endometria1.* Biology of Reproduction, 2006. **74**(6): p. 1060-1066.
237. D'Hooghe, T.M., et al., *Effect of menstruation and intrapelvic injection of endometrium on inflammatory parameters of peritoneal fluid in the baboon (Papio anubis and Papio cynocephalus).* Am J Obstet Gynecol, 2001. **184**(5): p. 917-25.
238. Pelch, K.E., K.L. Sharpe-Timms, and S.C. Nagel, *Mouse model of surgically-induced endometriosis by auto-transplantation of uterine tissue.* J Vis Exp, 2012(59): p. e3396.
239. Alali, Z., et al., *60S acidic ribosomal protein P1 (RPLP1) is elevated in human endometriotic tissue and in a murine model of endometriosis and is essential for endometriotic epithelial cell survival in vitro.* Mol Hum Reprod, 2020. **26**(1): p. 53-64.
240. Nothnick, W.B., et al., *Inhibition of macrophage migration inhibitory factor reduces endometriotic implant size in mice with experimentally induced disease.* J Endometr, 2011. **3**(3): p. 135-142.
241. Sharpe, K.L., et al., *Spontaneous and steroid-induced recurrence of endometriosis after suppression by a gonadotropin-releasing hormone antagonist in the rat.* American Journal of Obstetrics and Gynecology, 1991. **164**(1, Part 1): p. 187-194.
242. Sharpe, K., M. Bertero, and M. Vernon, *Rapid regression of endometriosis by a new gonadotropin-releasing hormone antagonist in rats with surgically induced disease.* Progress in clinical and biological research, 1990. **323**: p. 449-458.
243. Becker, C.M., et al., *2-methoxyestradiol inhibits hypoxia-inducible factor-1{alpha} and suppresses growth of lesions in a mouse model of endometriosis.* Am J Pathol, 2008. **172**(2): p. 534-44.
244. Birt, J.A., et al., *Developmental exposure of fetal ovaries and fetal germ cells to endometriosis in an endometriosis model causes differential gene expression in the preimplantation embryos of the first-generation and second-generation embryos.* Fertility and Sterility, 2013. **100**(5): p. 1436-1443.
245. Pelch, K.E., et al., *Aberrant gene expression profile in a mouse model of endometriosis mirrors that observed in women.* Fertility and sterility, 2010. **93**(5): p. 1615-1627. e18.

246. Stilley, J.A.W., et al., *Reduced fecundity in female rats with surgically induced endometriosis and in their daughters: a potential role for tissue inhibitors of metalloproteinase 1.* Biology of reproduction, 2009. **80**(4): p. 649-656.
247. Stilley, J.A.W., et al., *Neutralizing TIMP1 Restores Fecundity in a Rat Model of Endometriosis and Treating Control Rats with TIMP1 Causes Anomalies in Ovarian Function and Embryo Development1.* Biology of Reproduction, 2010. **83**(2): p. 185-194.
248. Xu, H., et al., *Green tea epigallocatechin-3-gallate inhibits angiogenesis and suppresses vascular endothelial growth factor C/vascular endothelial growth factor receptor 2 expression and signaling in experimental endometriosis in vivo.* Fertil Steril, 2011. **96**(4): p. 1021-8.
249. Hull, M.L., et al., *Antiangiogenic agents are effective inhibitors of endometriosis.* J Clin Endocrinol Metab, 2003. **88**(6): p. 2889-99.
250. Saunders, P.T.K., *What Have We Learned from Animal Models of Endometriosis and How Can We Use the Knowledge Gained to Improve Treatment of Patients?*, in *Animal Models for Endometriosis: Evolution, Utility and Clinical Relevance*, K.L. Sharpe-Timms, Editor. 2020, Springer International Publishing: Cham. p. 99-111.
251. Vernon, M.W. and E.A. Wilson, *Studies on the surgical induction of endometriosis in the rat.* Fertility and sterility, 1985. **44**(5): p. 684-694.
252. Greaves, E., et al., *A novel mouse model of endometriosis mimics human phenotype and reveals insights into the inflammatory contribution of shed endometrium.* The American journal of pathology, 2014. **184**(7): p. 1930-1939.
253. Hull, M.L., et al., *Host-derived TGFB1 deficiency suppresses lesion development in a mouse model of endometriosis.* Am J Pathol, 2012. **180**(3): p. 880-887.
254. Greaves, E., M. Rosser, and P.T.K. Saunders, *Endometriosis-Associated Pain – Do Preclinical Rodent Models Provide a Good Platform for Translation?*, in *Animal Models for Endometriosis: Evolution, Utility and Clinical Relevance*, K.L. Sharpe-Timms, Editor. 2020, Springer International Publishing: Cham. p. 25-55.
255. Mogil, J.S., *Animal models of pain: progress and challenges.* Nature Reviews Neuroscience, 2009. **10**(4): p. 283-294.
256. Liu, Z., et al., *Fractalkine/CX3CR1 Contributes to Endometriosis-Induced Neuropathic Pain and Mechanical Hypersensitivity in Rats.* Front Cell Neurosci, 2018. **12**: p. 495.
257. Forster, R., et al., *Macrophage-derived insulin-like growth factor-1 is a key neurotrophic and nerve-sensitizing factor in pain associated with endometriosis.* FASEB journal : official publication of the Federation of American Societies for Experimental Biology, 2019. **33**(10): p. 11210-11222.
258. Greaves, E., et al., *EP(2) receptor antagonism reduces peripheral and central hyperalgesia in a preclinical mouse model of endometriosis.* Scientific reports, 2017. **7**: p. 44169-44169.
259. Dmitrieva, N., et al., *Telemetric Assessment of Referred Vaginal Hyperalgesia and the Effect of Indomethacin in a Rat Model of Endometriosis.* Frontiers in Pharmacology, 2012. **3**(158).
260. Chen, Z., et al., *Activation of p38 MAPK in the rostral ventromedial medulla by visceral noxious inputs transmitted via the dorsal columns may contribute to pelvic organ cross-sensitization in rats with endometriosis.* Neuroscience, 2015. **291**: p. 272-8.
261. Liu, M., et al., *Valproic acid and progestin inhibit lesion growth and reduce hyperalgesia in experimentally induced endometriosis in rats.* Reprod Sci, 2012. **19**(4): p. 360-73.
262. Zheng, Y., X. Liu, and S.W. Guo, *Therapeutic potential of andrographolide for treating endometriosis.* Hum Reprod, 2012. **27**(5): p. 1300-13.
263. Mogil, J.S. and S.E. Crager, *What should we be measuring in behavioral studies of chronic pain in animals?* Pain, 2004. **112**(1-2): p. 12-5.
264. Hill, W.G., et al., *Void spot assay: recommendations on the use of a simple micturition assay for mice.* American Journal of Physiology-Renal Physiology, 2018. **315**(5): p. F1422-F1429.
265. Bakacak, M., et al., *The effects of thalidomide in a rat model of surgically-induced endometriosis.* Turk J Obstet Gynecol, 2015. **12**(3): p. 125-131.
266. Yıldırım, G., et al., *The combination of letrozole and melatonin causes regression in size not histopathological scores on endometriosis in an experimental rat model.* J Turk Ger Gynecol Assoc, 2009. **10**(4): p. 199-204.
267. Prodromidou, A., et al., *A Novel Experimental Model of Colorectal Endometriosis.* J Invest Surg, 2018. **31**(4): p. 275-281.

268. McAllister, S.L., et al., *Prostaglandin levels, vaginal innervation, and cyst innervation as peripheral contributors to endometriosis-associated vaginal hyperalgesia in rodents.* Molecular and cellular endocrinology, 2016. **437**: p. 120-129.
269. Zhang, G., et al., *Endometriosis as a neurovascular condition: estrous variations in innervation, vascularization, and growth factor content of ectopic endometrial cysts in the rat.* Am J Physiol Regul Integr Comp Physiol, 2008. **294**(1): p. R162-71.
270. Bruner-Tran, K.L., et al., *Rodent Models of Experimental Endometriosis: Identifying Mechanisms of Disease and Therapeutic Targets.* Current women's health reviews, 2018. **14**(2): p. 173-188.
271. Rogers, P.A.W., et al., *Research Priorities for Endometriosis: Recommendations From a Global Consortium of Investigators in Endometriosis.* Reproductive Sciences, 2016. **24**(2): p. 202-226.
272. Morrison, T.C., et al., *Opposing viscerovisceral effects of surgically induced endometriosis and a control abdominal surgery on the rat bladder.* Fertil Steril, 2006. **86**(4 Suppl): p. 1067-73.
273. Cason, A.M., C.L. Samuelsen, and K.J. Berkley, *Estrous changes in vaginal nociception in a rat model of endometriosis.* Horm Behav, 2003. **44**(2): p. 123-31.
274. Ma, W., Z. Miao, and M.V. Novotny, *Role of the adrenal gland and adrenal-mediated chemosignals in suppression of estrus in the house mouse: the lee-boot effect revisited.* Biol Reprod, 1998. **59**(6): p. 1317-20.
275. Cummings, A.M. and J.L. Metcalf, *Induction of endometriosis in mice: A new model sensitive to estrogen.* Reproductive Toxicology, 1995. **9**(3): p. 233-238.
276. Burns, K.A., et al., *Role of estrogen receptor signaling required for endometriosis-like lesion establishment in a mouse model.* Endocrinology, 2012. **153**(8): p. 3960-3971.
277. Somigliana, E., et al., *Endometrial ability to implant in ectopic sites can be prevented by interleukin-12 in a murine model of endometriosis.* Human Reproduction, 1999. **14**(12): p. 2944-2950.
278. Finnie, G.S., et al., *Characterization of an 'Amyloid Only' Transgenic (B6C3-Tg(APPswe,PSEN1dE9)85Dbo/Mmjax) Mouse Model of Alzheimer's Disease.* J Comp Pathol, 2017. **156**(4): p. 389-399.
279. Jimenez-Vargas, N.N., et al., *Protease-activated receptor-2 in endosomes signals persistent pain of irritable bowel syndrome.* Proc Natl Acad Sci U S A, 2018. **115**(31): p. E7438-E7447.
280. Ness, T.J. and G.F. Gebhart, *Colorectal distension as a noxious visceral stimulus: physiologic and pharmacologic characterization of pseudaffective reflexes in the rat.* Brain Res, 1988. **450**(1-2): p. 153-69.
281. Carstens, B.B., et al., *Structure-Activity Studies of Cysteine-Rich alpha-Conotoxins that Inhibit High-Voltage-Activated Calcium Channels via GABA(B) Receptor Activation Reveal a Minimal Functional Motif.* Angew Chem Int Ed Engl, 2016. **55**(15): p. 4692-6.
282. Berkley, K.J., et al., *Vaginal hyperalgesia in a rat model of endometriosis.* Neurosci Lett, 2001. **306**(3): p. 185-8.
283. Barrot, M., *Tests and models of nociception and pain in rodents.* Neuroscience, 2012. **211**: p. 39-50.
284. Deuis, J.R., L.S. Dvorakova, and I. Vetter, *Methods Used to Evaluate Pain Behaviors in Rodents.* Front Mol Neurosci, 2017. **10**: p. 284.
285. Inserra, M.C., et al., *Multiple sodium channel isoforms mediate the pathological effects of Pacific ciguatoxin-1.* Sci Rep, 2017. **7**: p. 42810.
286. Moen, M.H. and T.B. Halvorsen, *Histologic confirmation of endometriosis in different peritoneal lesions.* Acta Obstet Gynecol Scand, 1992. **71**(5): p. 337-42.
287. Parazzini, F., V. Mais, and S. Cipriani, *Adhesions and pain in women with first diagnosis of endometriosis: results from a cross-sectional study.* J Minim Invasive Gynecol, 2006. **13**(1): p. 49-54.
288. Burns, K.A., et al., *Early Endometriosis in Females Is Directed by Immune-Mediated Estrogen Receptor α and IL-6 Cross-Talk.* Endocrinology, 2017. **159**(1): p. 103-118.
289. Exacoustos, C., L. Manganaro, and E. Zupi, *Imaging for the evaluation of endometriosis and adenomyosis.* Best Practice & Research Clinical Obstetrics & Gynaecology, 2014. **28**(5): p. 655-681.

290. Wieser, F., et al., *Interleukin-1 receptor antagonist polymorphism in women with peritoneal adhesions.* Bjog, 2002. **109**(11): p. 1298-300.
291. Herington, J.L., et al., *Development and prevention of postsurgical adhesions in a chimeric mouse model of experimental endometriosis.* Fertil Steril, 2011. **95**(4): p. 1295-301.e1.
292. Stocks, M.M., et al., *Therapeutically Targeting the Inflammasome Product in a Chimeric Model of Endometriosis-Related Surgical Adhesions.* Reprod Sci, 2017. **24**(8): p. 1121-1128.
293. Braun, K.M. and M.P. Diamond, *The biology of adhesion formation in the peritoneal cavity.* Semin Pediatr Surg, 2014. **23**(6): p. 336-43.
294. Castro, J., et al., *Chronic Oral Administration of Linaclotide Inhibits Nociceptive Signalling in Response to Noxious Colorectal Distension in a Model of Chronic Visceral Hypersensitivity.* Gastroenterology, 2017. **152**(5): p. S204.
295. Jarrell, J., et al., *The Significance of Cutaneous Allodynia in a Woman With Chronic Pelvic Pain.* J Obstet Gynaecol Can, 2015. **37**(7): p. 628-632.
296. Slater, H., et al., *Heightened cold pain and pressure pain sensitivity in young female adults with moderate-to-severe menstrual pain.* Pain, 2015. **156**(12): p. 2468-78.
297. Castro, J., et al., *A mouse model of endometriosis that displays vaginal, colon, cutaneous, and bladder sensory comorbidities.* Faseb j, 2021. **35**(4): p. e21430.
298. Symons, L.K., et al., *Neutrophil recruitment and function in endometriosis patients and a syngeneic murine model.* Faseb j, 2020. **34**(1): p. 1558-1575.
299. Dorning, A., et al., *Bioluminescent imaging in induced mouse models of endometriosis reveals differences in four model variations.* Dis Model Mech, 2021. **14**(8).
300. Brodkin, J., et al., *Validation and implementation of a novel high-throughput behavioral phenotyping instrument for mice.* J Neurosci Methods, 2014. **224**: p. 48-57.
301. Grundy, L., et al., *Histamine induces peripheral and central hypersensitivity to bladder distension via the histamine H1 receptor and TRPV1.* Am J Physiol Renal Physiol, 2020. **318**(2): p. F298-f314.
302. Grundy, L., et al., *NKA enhances bladder-afferent mechanosensitivity via urothelial and detrusor activation.* Am J Physiol Renal Physiol, 2018. **315**(4): p. F1174-f1185.
303. Grundy, L., et al., *Translating peripheral bladder afferent mechanosensitivity to neuronal activation within the lumbosacral spinal cord of mice.* Pain, 2019. **160**(4): p. 793-804.
304. Mills, K.A., et al., *Hypersensitivity of bladder low threshold, wide dynamic range, afferent fibres following treatment with the chemotherapeutic drugs cyclophosphamide and ifosfamide.* Arch Toxicol, 2020. **94**(8): p. 2785-2797.
305. Grundy, L., et al., *Tetrodotoxin-sensitive voltage-gated sodium channels regulate bladder afferent responses to distension.* Pain, 2018. **159**(12): p. 2573-2584.
306. Laganà, A.S., et al., *Anxiety and depression in patients with endometriosis: impact and management challenges.* International journal of women's health, 2017. **9**: p. 323-330.
307. Becker, C.M., et al., *Reevaluating response and failure of medical treatment of endometriosis: a systematic review.* Fertility and Sterility, 2017. **108**(1): p. 125-136.
308. Denny, E. and C.H. Mann, *Endometriosis-associated dyspareunia: the impact on women's lives.* J Fam Plann Reprod Health Care, 2007. **33**(3): p. 189-93.
309. Ferrero, S., et al., *Increased frequency of migraine among women with endometriosis.* Hum Reprod, 2004. **19**(12): p. 2927-32.
310. Ahn, S.H., V. Singh, and C. Tayade, *Biomarkers in endometriosis: challenges and opportunities.* Fertil Steril, 2017. **107**(3): p. 523-532.
311. Llarena, N.C., et al., *Characterizing the endometrial fluid cytokine profile in women with endometriosis.* J Assist Reprod Genet, 2020. **37**(12): p. 2999-3006.
312. Hogg, C., A.W. Horne, and E. Greaves, *Endometriosis-Associated Macrophages: Origin, Phenotype, and Function.* Frontiers in Endocrinology, 2020. **11**(7).
313. Johan, M.Z., et al., *Macrophages infiltrating endometriosis-like lesions exhibit progressive phenotype changes in a heterologous mouse model.* J Reprod Immunol, 2019. **132**: p. 1-8.
314. Simon, P., R. Dupuis, and J. Costentin, *Thigmotaxis as an index of anxiety in mice. Influence of dopaminergic transmissions.* Behav Brain Res, 1994. **61**(1): p. 59-64.
315. Chen, L.C., et al., *Risk of developing major depression and anxiety disorders among women with endometriosis: A longitudinal follow-up study.* J Affect Disord, 2016. **190**: p. 282-285.
316. Bergeron, S., et al., *Vulvodynia.* Nat Rev Dis Primers, 2020. **6**(1): p. 36.

317. Harlow, B.L., L.A. Wise, and E.G. Stewart, *Prevalence and predictors of chronic lower genital tract discomfort.* Am J Obstet Gynecol, 2001. **185**(3): p. 545-50.
318. Pukall, C.F., et al., *Vulvodynia: Definition, Prevalence, Impact, and Pathophysiological Factors.* J Sex Med, 2016. **13**(3): p. 291-304.
319. Tribo, M.J., et al., *Pain, Anxiety, Depression, and Quality of Life in Patients with Vulvodynia.* Dermatology, 2019: p. 1-7.
320. Eisenberg, V.H., et al., *Epidemiology of endometriosis: a large population-based database study from a healthcare provider with 2 million members.* BJOG, 2018. **125**(1): p. 55-62.
321. Torres-Cueco, R. and F. Nohales-Alfonso, *Vulvodynia-It Is Time to Accept a New Understanding from a Neurobiological Perspective.* Int J Environ Res Public Health, 2021. **18**(12).
322. Koninckx, P.R., et al., *Pathogenesis of endometriosis: the genetic/epigenetic theory.* Fertil Steril, 2019. **111**(2): p. 327-340.
323. Thornton, A.M. and C. Drummond, *Current concepts in vulvodynia with a focus on pathogenesis and pain mechanisms.* Australas J Dermatol, 2016. **57**(4): p. 253-263.
324. Goldstein, A.T., et al., *Vulvodynia: Assessment and Treatment.* J Sex Med, 2016. **13**(4): p. 572-90.
325. Zito, G., et al., *Medical treatments for endometriosis-associated pelvic pain.* Biomed Res Int, 2014. **2014**: p. 191967.
326. Berkley, K.J., C.H. Hubscher, and P.D. Wall, *Neuronal responses to stimulation of the cervix, uterus, colon, and skin in the rat spinal cord.* J Neurophysiol, 1993. **69**(2): p. 545-56.
327. Berkley, K.J., A. Robbins, and Y. Sato, *Functional differences between afferent fibers in the hypogastric and pelvic nerves innervating female reproductive organs in the rat.* J Neurophysiol, 1993. **69**(2): p. 533-44.
328. Robbins, A., et al., *Responses of hypogastric nerve afferent fibers to uterine distension in estrous or metestrous rats.* Neurosci Lett, 1990. **110**(1-2): p. 82-5.
329. Berkley, K.J., et al., *Functional properties of afferent fibers supplying reproductive and other pelvic organs in pelvic nerve of female rat.* J Neurophysiol, 1990. **63**(2): p. 256-72.
330. Robbins, A., K.J. Berkley, and Y. Sato, *Estrous cycle variation of afferent fibers supplying reproductive organs in the female rat.* Brain Res, 1992. **596**(1-2): p. 353-6.
331. Liu, B., J.C. Eisenach, and C. Tong, *Chronic estrogen sensitizes a subset of mechanosensitive afferents innervating the uterine cervix.* J Neurophysiol, 2005. **93**(4): p. 2167-73.
332. Liu, B., C. Tong, and J.C. Eisenach, *Pregnancy increases excitability of mechanosensitive afferents innervating the uterine cervix.* Anesthesiology, 2008. **108**(6): p. 1087-92.
333. Israel, M.R., et al., *NaV 1.6 regulates excitability of mechanosensitive sensory neurons.* J Physiol, 2019. **597**(14): p. 3751-3768.
334. Wang, C., et al., *Pirt Contributes to Uterine Contraction-Induced Pain in Mice.* Molecular Pain, 2015. **11**: p. s12990-015-0054-x.
335. Lee, M.C., et al., *Human labour pain is influenced by the voltage-gated potassium channel K_V6.4 subunit.* bioRxiv, 2020: p. 489310.
336. Erickson, A., et al., *Voltage-gated sodium channels: (NaV)igating the field to determine their contribution to visceral nociception.* J Physiol, 2018. **596**(5): p. 785-807.
337. Osteen, J.D., et al., *Selective spider toxins reveal a role for the Nav1.1 channel in mechanical pain.* Nature, 2016. **534**(7608): p. 494-9.
338. Catterall, W.A., *Voltage-gated sodium channels at 60: structure, function and pathophysiology.* J Physiol, 2012. **590**(11): p. 2577-89.
339. Catterall, W.A., A.L. Goldin, and S.G. Waxman, *International Union of Pharmacology. XLVII. Nomenclature and structure-function relationships of voltage-gated sodium channels.* Pharmacol Rev, 2005. **57**(4): p. 397-409.
340. Dib-Hajj, S.D., et al., *Sodium channels in normal and pathological pain.* Annu Rev Neurosci, 2010. **33**: p. 325-47.
341. Waxman, S.G., et al., *Sodium channel genes in pain-related disorders: phenotype-genotype associations and recommendations for clinical use.* Lancet Neurol, 2014. **13**(11): p. 1152-1160.

342. Farrag, K.J., A. Bhattacharjee, and R.J. Docherty, *A comparison of the effects of veratridine on tetrodotoxin-sensitive and tetrodotoxin-resistant sodium channels in isolated rat dorsal root ganglion neurons.* Pflugers Arch, 2008. **455**(5): p. 929-38.
343. Brierley, S.M., et al., *Splanchnic and pelvic mechanosensory afferents signal different qualities of colonic stimuli in mice.* Gastroenterology, 2004. **127**(1): p. 166-78.
344. Bellono, N.W., et al., *Enterochromaffin Cells Are Gut Chemosensors that Couple to Sensory Neural Pathways.* Cell, 2017. **170**(1): p. 185-198 e16.
345. Castro, J., et al., *alpha-Conotoxin Vc1.1 inhibits human dorsal root ganglion neuroexcitability and mouse colonic nociception via GABAB receptors.* Gut, 2017. **66**(6): p. 1083-1094.
346. Brierley, S.M., et al., *TRPA1 contributes to specific mechanically activated currents and sensory neuron mechanical hypersensitivity.* J Physiol, 2011. **589**(Pt 14): p. 3575-93.
347. Lein, E.S., et al., *Genome-wide atlas of gene expression in the adult mouse brain.* Nature, 2007. **445**(7124): p. 168-76.
348. Su, X. and G.F. Gebhart, *Mechanosensitive pelvic nerve afferent fibers innervating the colon of the rat are polymodal in character.* J Neurophysiol, 1998. **80**(5): p. 2632-44.
349. Wesselmann, U. and J. Lai, *Mechanisms of referred visceral pain: uterine inflammation in the adult virgin rat results in neurogenic plasma extravasation in the skin.* Pain, 1997. **73**(3): p. 309-17.
350. Herweijer, G., et al., *Characterization of primary afferent spinal innervation of mouse uterus.* Front Neurosci, 2014. **8**: p. 202.
351. Shafik, A., et al., *Surgical anatomy of the pudendal nerve and its clinical implications.* Clin Anat, 1995. **8**(2): p. 110-5.
352. Yan, T., et al., *Estrogen amplifies pain responses to uterine cervical distension in rats by altering transient receptor potential-1 function.* Anesth Analg, 2007. **104**(5): p. 1246-50, tables of contents.
353. Sandner-Kiesling, A., et al., *Effect of kappa opioid agonists on visceral nociception induced by uterine cervical distension in rats.* Pain, 2002. **96**(1-2): p. 13-22.
354. Schep, L.J., D.M. Schmierer, and J.S. Fountain, *Veratrum poisoning.* Toxicol Rev, 2006. **25**(2): p. 73-8.
355. Stewart, I., et al., *Emerging tropical diseases in Australia. Part 2. Ciguatera fish poisoning.* Ann Trop Med Parasitol, 2010. **104**(7): p. 557-71.
356. Hockley, J.R., et al., *Visceral and somatic pain modalities reveal NaV 1.7-independent visceral nociceptive pathways.* J Physiol, 2017. **595**(8): p. 2661-2679.
357. Hockley, J.R., et al., *Multiple roles for NaV1.9 in the activation of visceral afferents by noxious inflammatory, mechanical, and human disease-derived stimuli.* Pain, 2014. **155**(10): p. 1962-75.
358. Beyak, M.J., et al., *Two TTX-resistant Na+ currents in mouse colonic dorsal root ganglia neurons and their role in colitis-induced hyperexcitability.* Am J Physiol Gastrointest Liver Physiol, 2004. **287**(4): p. G845-55.
359. Sikandar, S., et al., *Sensory processing of deep tissue nociception in the rat spinal cord and thalamic ventrobasal complex.* Physiol Rep, 2017. **5**(14).
360. Todd, A.J., *Neuronal circuitry for pain processing in the dorsal horn.* Nat Rev Neurosci, 2010. **11**(12): p. 823-36.
361. Willis, W.D., et al., *A visceral pain pathway in the dorsal column of the spinal cord.* Proc Natl Acad Sci U S A, 1999. **96**(14): p. 7675-9.
362. Schneider, M.P., et al., *Quality of Life in Adolescent and Young Adult Women With Dyspareunia and Endometriosis.* J Adolesc Health, 2020.
363. Yong, P.J., *Deep Dyspareunia in Endometriosis: A Proposed Framework Based on Pain Mechanisms and Genito-Pelvic Pain Penetration Disorder.* Sex Med Rev, 2017. **5**(4): p. 495-507.
364. Surrey, E.S., et al., *Risk of Developing Comorbidities Among Women with Endometriosis: A Retrospective Matched Cohort Study.* J Womens Health (Larchmt), 2018. **27**(9): p. 1114-1123.
365. Sinaii, N., et al., *Differences in characteristics among 1,000 women with endometriosis based on extent of disease.* Fertil Steril, 2008. **89**(3): p. 538-45.

366. Jiang, Y., et al., *Pharmacological Inhibition of the Voltage-Gated Sodium Channel Na(V)1.7 Alleviates Chronic Visceral Pain in a Rodent Model of Irritable Bowel Syndrome.* ACS Pharmacol Transl Sci, 2021. **4**(4): p. 1362-1378.
367. Bennett, D.L. and C.G. Woods, *Painful and painless channelopathies.* Lancet Neurol, 2014. **13**(6): p. 587-99.
368. Drenth, J.P.H. and S.G. Waxman, *Mutations in sodium-channel gene SCN9A cause a spectrum of human genetic pain disorders.* The Journal of clinical investigation, 2007. **117**(12): p. 3603-3609.
369. Cox, J.J., et al., *An SCN9A channelopathy causes congenital inability to experience pain.* Nature, 2006. **444**(7121): p. 894-898.
370. Drenth, J.P.H., et al., *SCN9A Mutations Define Primary Erythermalgia as a Neuropathic Disorder of Voltage Gated Sodium Channels.* Journal of Investigative Dermatology, 2005. **124**(6): p. 1333-1338.
371. Fertleman, C.R., et al., *SCN9A Mutations in Paroxysmal Extreme Pain Disorder: Allelic Variants Underlie Distinct Channel Defects and Phenotypes.* Neuron, 2006. **52**(5): p. 767-774.
372. Yang, Y., et al., *Mutations in SCN9A, encoding a sodium channel alpha subunit, in patients with primary erythermalgia.* Journal of medical genetics, 2004. **41**(3): p. 171-174.
373. Faber, C.G., et al., *Gain of function Nav1.7 mutations in idiopathic small fiber neuropathy.* Ann Neurol, 2012. **71**(1): p. 26-39.
374. Nassar, M.A., et al., *Nociceptor-specific gene deletion reveals a major role for Nav1.7 (PN1) in acute and inflammatory pain.* Proceedings of the National Academy of Sciences of the United States of America, 2004. **101**(34): p. 12706-12711.
375. Durek, T., et al., *Chemical engineering and structural and pharmacological characterization of the alpha-scorpion toxin OD1.* ACS Chem Biol, 2013. **8**(6): p. 1215-22.
376. Maddern, J., et al., *A syngeneic inoculation mouse model of endometriosis that develops multiple comorbid visceral and cutaneous pain like behaviours.* PAIN, 9000.
377. Maertens, C., et al., *Potent Modulation of the Voltage-Gated Sodium Channel Na_v1.7 by OD1, a Toxin from the Scorpion <em>Odonthobuthus doriae</em&gt.* Molecular Pharmacology, 2006. **70**(1): p. 405.
378. King, G.F. and I. Vetter, *No Gain, No Pain: NaV1.7 as an Analgesic Target.* ACS Chemical Neuroscience, 2014. **5**(9): p. 749-751.
379. Campaniello, M.A., et al., *Activation of colo-rectal high-threshold afferent nerves by Interleukin-2 is tetrodotoxin-sensitive and upregulated in a mouse model of chronic visceral hypersensitivity.* Neurogastroenterol Motil, 2016. **28**(1): p. 54-63.
380. Dib-Hajj, S.D., et al., *The NaV1.7 sodium channel: from molecule to man.* Nature Reviews Neuroscience, 2013. **14**(1): p. 49-62.
381. Siebenga, P., et al., *Lack of Detection of the Analgesic Properties of PF-05089771, a Selective Na(v) 1.7 Inhibitor, Using a Battery of Pain Models in Healthy Subjects.* Clinical and translational science, 2020. **13**(2): p. 318-324.
382. Hameed, S., *Na(v)1.7 and Na(v)1.8: Role in the pathophysiology of pain.* Molecular pain, 2019. **15**: p. 1744806919858801-1744806919858801.
383. King, D.E., R.J. Macleod, and S.J. Vanner, *Trinitrobenzenesulphonic acid colitis alters Na 1.8 channel expression in mouse dorsal root ganglia neurons.* Neurogastroenterol Motil, 2009. **21**(8): p. 880-e64.
384. Hong, S., et al., *Early painful diabetic neuropathy is associated with differential changes in tetrodotoxin-sensitive and -resistant sodium channels in dorsal root ganglion neurons in the rat.* J Biol Chem, 2004. **279**(28): p. 29341-50.
385. Chattopadhyay, M., M. Mata, and D.J. Fink, *Vector-mediated release of GABA attenuates pain-related behaviors and reduces Na(V)1.7 in DRG neurons.* Eur J Pain, 2011. **15**(9): p. 913-20.
386. Klint, J.K., et al., *Spider-venom peptides that target voltage-gated sodium channels: Pharmacological tools and potential therapeutic leads.* Toxicon, 2012. **60**(4): p. 478-491.
387. Cardoso, F.C., et al., *A spider-venom peptide with multitarget activity on sodium and calcium channels alleviates chronic visceral pain in a model of irritable bowel syndrome.* Pain, 2021. **162**(2): p. 569-581.

388. François-Moutal, L., et al., *Inhibition of the Ubc9 E2 SUMO-conjugating enzyme-CRMP2 interaction decreases NaV1.7 currents and reverses experimental neuropathic pain.* Pain, 2018. **159**(10): p. 2115-2127.
389. Li, J., et al., *Small molecule targeting NaV1.7 via inhibition of the CRMP2-Ubc9 interaction reduces pain in chronic constriction injury (CCI) rats.* Channels (Austin, Tex.), 2022. **16**(1): p. 1-8.
390. Yang, S., et al., *Discovery of a selective NaV1.7 inhibitor from centipede venom with analgesic efficacy exceeding morphine in rodent pain models.* Proceedings of the National Academy of Sciences of the United States of America, 2013. **110**(43): p. 17534-17539.
391. Niu, H.-l., et al., *Inhibition of Nav1.7 channel by a novel blocker QLS-81 for alleviation of neuropathic pain.* Acta Pharmacologica Sinica, 2021. **42**(8): p. 1235-1247.
392. Gazvani, R. and A. Templeton, *Peritoneal environment, cytokines and angiogenesis in the pathophysiology of endometriosis.* Reproduction, 2002. **123**(2): p. 217-26.
393. Fauconnier, A., et al., *Relation between pain symptoms and the anatomic location of deep infiltrating endometriosis.* Fertil Steril, 2002. **78**(4): p. 719-26.
394. van Baal, J.O.A.M., et al., *The histophysiology and pathophysiology of the peritoneum.* Tissue and Cell, 2017. **49**(1): p. 95-105.
395. Gibson, D.A., et al., *Pelvic pain correlates with peritoneal macrophage abundance not endometriosis.* Reproduction and Fertility, 2021. **2**(1): p. 47-57.
396. Peeters, P.J., et al., *Molecular profiling of murine sensory neurons in the nodose and dorsal root ganglia labeled from the peritoneal cavity.* Physiol Genomics, 2006. **24**(3): p. 252-63.
397. Struller, F., et al., *Peritoneal innervation: embryology and functional anatomy.* Pleura and peritoneum, 2017. **2**(4): p. 153-161.
398. Tanaka, K., T. Matsugami, and T. Chiba, *The origin of sensory innervation of the peritoneum in the rat.* Anat Embryol (Berl), 2002. **205**(4): p. 307-13.
399. Niu, X., et al., *Mapping of Extrinsic Innervation of the Gastrointestinal Tract in the Mouse Embryo.* J Neurosci, 2020. **40**(35): p. 6691-6708.
400. Gebhart, G.F. and K. Bielefeldt, *Physiology of Visceral Pain.* Compr Physiol, 2016. **6**(4): p. 1609-1633.
401. Robinson, D.R. and G.F. Gebhart, *Inside information: the unique features of visceral sensation.* Molecular interventions, 2008. **8**(5): p. 242-253.
402. Grienberger, C. and A. Konnerth, *Imaging calcium in neurons.* Neuron, 2012. **73**(5): p. 862-85.
403. Renganathan, M., T.R. Cummins, and S.G. Waxman, *Contribution of Na(v)1.8 sodium channels to action potential electrogenesis in DRG neurons.* J Neurophysiol, 2001. **86**(2): p. 629-40.
404. Chen, T.-W., et al., *Ultrasensitive fluorescent proteins for imaging neuronal activity.* Nature, 2013. **499**(7458): p. 295-300.
405. White, J.P., L. Urban, and I. Nagy, *TRPV1 function in health and disease.* Curr Pharm Biotechnol, 2011. **12**(1): p. 130-44.
406. Alawi, K. and J. Keeble, *The paradoxical role of the transient receptor potential vanilloid 1 receptor in inflammation.* Pharmacol Ther, 2010. **125**(2): p. 181-95.
407. Israel, M.R., et al., *Chapter Three - Sodium Channels and Venom Peptide Pharmacology*, in *Advances in Pharmacology*, D.P. Geraghty and L.D. Rash, Editors. 2017, Academic Press. p. 67-116.
408. Berta, T., et al., *Targeting dorsal root ganglia and primary sensory neurons for the treatment of chronic pain.* Expert Opin Ther Targets, 2017. **21**(7): p. 695-703.
409. Christianson, J.A., et al., *Transient receptor potential vanilloid 1-immunopositive neurons in the mouse are more prevalent within colon afferents compared to skin and muscle afferents.* Neuroscience, 2006. **140**(1): p. 247-57.
410. Morales-Lázaro, S.L., S.A. Simon, and T. Rosenbaum, *The role of endogenous molecules in modulating pain through transient receptor potential vanilloid 1 (TRPV1).* J Physiol, 2013. **591**(13): p. 3109-21.
411. Hughes, P.A., et al., *TRPV1-expressing sensory fibres and IBS: links with immune function.* Gut, 2009. **58**(3): p. 465.

412. Jones, R.C.W., 3rd, L. Xu, and G.F. Gebhart, *The mechanosensitivity of mouse colon afferent fibers and their sensitization by inflammatory mediators require transient receptor potential vanilloid 1 and acid-sensing ion channel 3.* The Journal of neuroscience : the official journal of the Society for Neuroscience, 2005. **25**(47): p. 10981-10989.
413. Hockley, J.R.F., et al., *Single-cell RNAseq reveals seven classes of colonic sensory neuron.* Gut, 2019. **68**(4): p. 633.
414. Du, Q., et al., *The Role of Transient Receptor Potential Vanilloid 1 in Common Diseases of the Digestive Tract and the Cardiovascular and Respiratory System.* Frontiers in Physiology, 2019. **10**.
415. Robinson, D.R., et al., *Characterization of the primary spinal afferent innervation of the mouse colon using retrograde labelling.* Neurogastroenterol Motil, 2004. **16**(1): p. 113-24.
416. Chen, Y., et al., *Mechanisms underlying enhanced P2X receptor-mediated responses in the neuropathic pain state.* PAIN, 2005. **119**(1-3).
417. Trapero, C. and M. Martín-Satué, *Purinergic Signaling in Endometriosis-Associated Pain.* International journal of molecular sciences, 2020. **21**(22): p. 8512.
418. Ding, S., et al., *P2X3 receptor involvement in endometriosis pain via ERK signaling pathway.* PloS one, 2017. **12**(9): p. e0184647-e0184647.
419. Yu, J., et al., *The interaction between P2X3 and TRPV1 in the dorsal root ganglia of adult rats with different pathological pains.* Molecular Pain, 2021. **17**: p. 17448069211011315.
420. Horne, A.W., et al., *Surgical removal of superficial peritoneal endometriosis for managing women with chronic pelvic pain: time for a rethink?* Bjog, 2019. **126**(12): p. 1414-1416.
421. Audebert, A., et al., *Anatomic distribution of endometriosis: A reappraisal based on series of 1101 patients.* European Journal of Obstetrics and Gynecology and Reproductive Biology, 2018. **230**: p. 36-40.
422. Dodds, K.N., et al., *Lesion development is modulated by the natural estrous cycle and mouse strain in a minimally invasive model of endometriosis†.* Biology of Reproduction, 2017. **97**(6): p. 810-821.
423. Burns, K.A., et al., *Endometriosis in the Mouse: Challenges and Progress Toward a 'Best Fit' Murine Model.* Frontiers in Physiology, 2022. **12**.
424. Smolarz, B., K. Szyłło, and H. Romanowicz, *Endometriosis: Epidemiology, Classification, Pathogenesis, Treatment and Genetics (Review of Literature).* International journal of molecular sciences, 2021. **22**(19): p. 10554.
425. Borghese, B., et al., *[Definition, description, clinicopathological features, pathogenesis and natural history of endometriosis: CNGOF-HAS Endometriosis Guidelines].* Gynecol Obstet Fertil Senol, 2018. **46**(3): p. 156-167.
426. Khan, K.N., et al., *Pelvic pain in women with ovarian endometrioma is mostly associated with coexisting peritoneal lesions.* Hum Reprod, 2013. **28**(1): p. 109-18.
427. Abd El-Kader, A.I., et al., *Impact of Endometriosis-Related Adhesions on Quality of Life among Infertile Women.* International journal of fertility & sterility, 2019. **13**(1): p. 72-76.
428. Demco, L., *Pain mapping of adhesions.* J Am Assoc Gynecol Laparosc, 2004. **11**(2): p. 181-3.
429. van Goor, H., *Consequences and complications of peritoneal adhesions.* Colorectal Dis, 2007. **9 Suppl 2**: p. 25-34.
430. Wiczyk, H.P., et al., *Pelvic adhesions contain sex steroid receptors and produce angiogenesis growth factors.* Fertility and sterility, 1998. **69**(3): p. 511-516.
431. Fortin, C.N., G.M. Saed, and M.P. Diamond, *Predisposing factors to post-operative adhesion development.* Human Reproduction Update, 2015. **21**(4): p. 536-551.
432. Hao, M., W.H. Zhao, and Y.H. Wang, *[Correlation between pelvic adhesions and pain symptoms of endometriosis].* Zhonghua Fu Chan Ke Za Zhi, 2009. **44**(5): p. 333-6.
433. Herington, J.L., et al., *Immune interactions in endometriosis.* Expert review of clinical immunology, 2011. **7**(5): p. 611-626.
434. Cheong, Y., et al., *Are pelvic adhesions associated with pain, physical, emotional and functional characteristics of women presenting with chronic pelvic pain? A cluster analysis.* BMC women's health, 2018. **18**(1): p. 11-11.
435. Vincent, K. and I. Tracey, *Hormones and their Interaction with the Pain Experience.* Reviews in pain, 2008. **2**(2): p. 20-24.

436. Dodds, K.N., et al., *Spinal Glial Adaptations Occur in a Minimally Invasive Mouse Model of Endometriosis: Potential Implications for Lesion Etiology and Persistent Pelvic Pain.* Reproductive Sciences, 2018. **26**(3): p. 357-369.
437. Iftinca, M., M. Defaye, and C. Altier, *TRPV1-Targeted Drugs in Development for Human Pain Conditions.* Drugs, 2021. **81**(1): p. 7-27.
438. Di Serafino, M., et al., *Pelvic Pain in Reproductive Age: US Findings.* Diagnostics (Basel, Switzerland), 2022. **12**(4): p. 939.
439. Curry, A., T. Williams, and M.L. Penny, *Pelvic Inflammatory Disease: Diagnosis, Management, and Prevention.* Am Fam Physician, 2019. **100**(6): p. 357-364.
440. Mobeen, S. and R. Apostol, *Ovarian Cyst*. 2021: StatPearls Publishing, Treasure Island (FL).
441. Rapisarda, A.M.C., et al., *Benign multicystic mesothelioma and peritoneal inclusion cysts: are they the same clinical and histopathological entities? A systematic review to find an evidence-based management.* Arch Gynecol Obstet, 2018. **297**(6): p. 1353-1375.
442. ten Broek, R.P., et al., *Burden of adhesions in abdominal and pelvic surgery: systematic review and met-analysis.* Bmj, 2013. **347**: p. f5588.
443. Koninckx, P.R., et al., *Anti-TNF-alpha treatment for deep endometriosis-associated pain: a randomized placebo-controlled trial.* Hum Reprod, 2008. **23**(9): p. 2017-23.
444. Amini, L., et al., *The Effect of Combined Vitamin C and Vitamin E Supplementation on Oxidative Stress Markers in Women with Endometriosis: A Randomized, Triple-Blind Placebo-Controlled Clinical Trial.* Pain Res Manag, 2021. **2021**: p. 5529741.